

The role of nitrosative and metabolic stress in vascular cell senescence

Christopher Skene

A thesis submitted to University College London

for the degree of

Doctor of Philosophy

January 2014

Wolfson Institute for Biomedical Research

The Cruciform Building

University College London

Gower Street

London WC1E 6BT

Abstract

Vascular cell senescence has been observed in vascular healing, atheroma and advanced age. Other groups have demonstrated that senescence is a process characterized by metabolic dysfunction. We therefore investigate whether it may occur as a consequence of metabolic stress. Controversy existed as to whether nitric oxide was able to prevent senescence in vascular cells. As nitric oxide is able to inhibit mitochondrial respiration, we investigated its effects both as an oxidant and metabolic stressor.

We observed that cells exposed to nitric oxide donors senesce over a concentration range of DETA-NO 0.5-0.75mM or GSNO 1mM, showing an exponential increase in senescence until succumbing to cell death as concentrations of DETA-NO increase. This was confirmed by cell morphology, senescence-associated β -galactosidase activity, total β -galactosidase activity, cell proliferation assays and expression of p16^{INK4a} and p21^{WAF}. We investigated whether this effect could be reproduced by cells induced to express iNOS *in vitro*.

Using these tools, we investigated the mechanism of NO-induced senescence looking at soluble guanylate cyclase activation, increased generation of ROS, protein transnitrosation and glutathione depletion. We investigated ways in which nitric oxide-induced senescence could be circumvented by using antioxidants (NAC, selenomethionine, uric acid), activating AMP kinase with metformin and AICAR and reducing protein transnitrosation by exposing the cells to cold light. We used pharmacological means to mimic lysosomal dysfunction and to stimulate autophagy.

My findings show that nitric oxide can cause senescence in vascular cells by a mechanism that involves protein transnitrosation. The effect of nitric oxide on senescence is independent of ROS generation, AMP kinase activation, soluble guanylate cyclase activation and glutathione depletion.

My findings may have important implications in vascular disease, particularly in cases of short periods of high nitric oxide production, such as sepsis, but also in the case of low-grade chronic inflammation such as that seen in atherosclerosis. However, their physiological relevance needs to be confirmed. The pathway by which protein transnitrosation induces senescence has yet to be fully elucidated.

Acknowledgements

Without a number of people, this document would not exist.

My wife Sonja has distracted, cajoled, inspired, and provided competition for me to complete this thesis in equal measure. However, her immense patience and understanding, together with her enthusiasm have won through.

My mother and sister have suffered for longer than they should, dreading to enquire over progress.

I am grateful for the great scientific support and detailed analysis from my supervisor, Professor Jorge Erusalimsky.

I would also like to thank Drs. Quintero and Palacios-Callender for their assistance with nitric oxide measurements and tetracycline-inducible iNOS cells.

This work is dedicated to my father.

Table of Contents

1	Introduction.....	19
1.1	Senescence overview	19
1.1.1	Identifying cell senescence.....	21
1.1.2	Senescence-associated β -galactosidase	22
1.1.3	Telomere function and senescence.....	22
1.1.4	Senescence and cell cycle regulation.....	25
1.1.5	Chromatin modification.....	27
1.1.6	Senescence associated secretory phenotype	27
1.2	Nitric oxide and senescence	30
1.2.1	How much nitric oxide is produced <i>in vivo</i> ?.....	31
1.2.2	The protective role of nitric oxide.....	33
1.3	Inflammation, iNOS activity and senescence	36
1.3.1	Deleterious effects of nitric oxide.....	38
1.4	Reactive oxygen and nitrogen species.....	40
1.5	Protein modifications involving nitric oxide.....	41
1.5.1	Metal centre interactions.....	41
1.5.2	Protein transnitrosation.....	42
1.5.3	Tyrosine nitration	42
1.5.4	Transnitrosation as nitric oxide store	43
1.6	Antioxidants.....	43
1.6.1	N-acetyl cysteine	44
1.6.2	Uric acid.....	45
1.6.3	Selenomethionine.....	47
1.7	Bioenergetic crisis and senescence	47
1.7.1	Autophagy and aging.....	47
1.7.2	AMP kinase and cellular senescence	51
1.8	New insights.....	53

1.8.1	Nitrosative stress	53
1.8.2	Transnitrosation effects	54
1.8.3	Transnitrosation without increasing oxidative stress	55
1.8.4	Genetic ablation of senescent cells	55
1.9	Conclusion	55
1.10	Aims	56
2	Methods	57
2.1	Primary cell culture	57
2.1.1	Human umbilical artery smooth muscle cells	57
2.1.2	Human umbilical vein endothelial cells	60
2.1.3	Freezing and thawing cells	61
2.2	Counting cells	61
2.2.1	Trypan blue cell counting	61
2.2.2	Coulter multisizer particle analyzer	62
2.3	Measuring senescence	62
2.3.1	Replicative capacity	62
2.3.2	Senescence associated β galactosidase histochemical staining	63
2.3.3	Fluorimetric assay of β -galactosidase activity	64
2.3.4	Flow cytometric assay of β -galactosidase activity	65
2.3.5	Western blotting for senescence associated proteins	66
2.4	Measuring reactive oxygen species	71
2.4.1	Fluorimetric assay of reactive oxygen species	71
2.4.2	Flow cytometric assay of ROS	72
2.5	Detection of protein nitrosylation by the biotin switch method	72
2.6	Exposure of cells to cold light	74
2.7	BrDU incorporation assay of cell proliferation	75
2.8	Tetracycline-inducible iNOS expression in HEK-293	75
2.9	Measuring nitric oxide generation by nitric oxide electrode	76
3	Assessment of techniques to measure β -galactosidase	77
3.1	Introduction	77

3.2	Hypothesis	78
3.3	Aims	78
3.4	Testing different methodologies for detecting β -galactosidase.....	79
3.4.1	Senescence-associated β -galactosidase.....	79
3.4.2	Methyl-umbelliferyl galactosidase (MUG) assay	81
3.4.3	Measurement of β -galactosidase activity per cell using flow cytometry	83
3.4.4	Detecting senescence and apoptosis using flow cytometry.....	85
3.4.5	Cell proliferation assay	86
3.5	Conclusion	89
4	Reactive oxygen species	91
4.1	Introduction	91
4.2	Effect of nitric oxide donors on cellular reactive oxygen species.	91
4.3	The effect of t-BHP on the H ₂ DCFDA ROS assay by fluorimetry	94
4.3.1	The effect of antioxidants on preventing DETA-NO-induced increases in generation of ROS in HUVEC.....	97
4.4	Conclusion	104
5	The influence of nitric oxide on senescence in human vascular cells.....	107
5.1	Introduction	107
5.2	Aims	108
5.3	The influence of nitric oxide on senescence	109
5.3.1	Effect of DETA-NO on HUVEC senescence.....	109
5.3.2	Assessing nitric oxide-mediated HUVEC and HUASMC senescence by senescence-associated β -galactosidase	114
5.3.3	Senescence vs. apoptosis.....	116
5.3.4	Assessing nitric oxide-mediated HUVEC senescence by cell cycle protein expression	119
5.3.5	Assessing nitric oxide-mediated HUVEC senescence by measuring cell cycle arrest	121
5.3.6	Coculture of HUVEC with tet-iNOS HEK 293	123
5.4	Assessing the potential mechanisms of nitric oxide-mediated HUVEC senescence.....	125

5.4.1	Soluble guanylate cyclase inhibition	125
5.4.2	Antioxidants and DETA-NO	128
5.4.3	DETA-NO and NAC	134
5.4.4	Nitric oxide release from DETA-NO with NAC	135
5.4.5	Cold light with DETA-NO	136
5.4.6	Transnitrosation band analysis	139
5.5	Conclusion	142
6	Metabolic stress and senescence	148
6.1	Introduction	148
6.1.1	Bafilomycin A1	148
6.1.2	Rapamycin.....	148
6.1.3	AMP kinase	149
6.2	Mimicking lysosomal dysfunction	150
6.2.1	Effect of lysosomal proton pump inhibitor, bafilomycin A1 on HUVEC senescence	150
6.2.2	mTOR inhibition.....	157
6.3	AMP kinase activation.....	160
6.3.1	Effect of AMP kinase activator, AICAR on HUVEC senescence and its interaction with DETA-NO.....	160
6.3.2	Assessing the effect of AMP kinase activation on human umbilical artery smooth muscle cells by senescence-associated β -galactosidase staining	168
6.3.3	Effect of metformin on HUVEC proliferation and senescence	169
6.3.4	Effect of metformin on HUASMC senescence	172
6.4	Conclusion	173
7	Conclusions and discussion	173
8	Future work.....	178

Table of figures

Figure 1.2.2-1: Effect of increasing degree of transnitrosation of arginase.	35
Figure 1.2.2-1: Schematic diagram of the interplay between inflammation, aging and nitric oxide generation.	37
Figure 1.3.1-1: Schematic of the pathways by which nitric oxide could signal metabolic stress.	39
Figure 1.7.1-1: Schematic diagram of processes and drugs influencing autophagy.	49
Figure 2.1.1-1: Fluorescence microscopy of explanted smooth muscle cells.	60
Figure 2.2.1-1: Haemocytometer design.	61
Figure 3.4.1-1: Light micrographs of early and late passage HUVEC stained with senescence-associated β -galactosidase.	80
Figure 3.4.2-1: Total β -galactosidase activity by MUG assay: serial passage.	82
Figure 3.4.3-1: Microscopy of total β -galactosidase activity in young HUVEC detected by C_{12} FDG.	84
Figure 3.4.4-1: Flow cytometry of annexin V vs total β -galactosidase.	86
Figure 3.4.5-1: BrDU incorporation and plating density.	88
Figure 4.2-1: UV excited microscopy of endothelial cells treated with H_2 DCFDA for ROS assay.	92
Figure 4.2-2: Light and UV excited microscopy of endothelial cells treated with H_2 DCFDA for ROS assay.	93
Figure 4.2-3: Time-point measurements of ROS and correlation to the standard curve of serial dilutions of t-BHP.	94
Figure 4.3-1: Dose response curve for the effect of t-BHP on the generation of DCF: comparison of different concentrations of fluorogenic probe.	94
Figure 4.3-2: Comparison of concentration of H_2 DCFDA probe and correlation to standard curve of serial dilutions of t-BHP.	95

Figure 4.3-3: Dose response curve for the effect of t-BHP on the generation of DCF.	96
Figure 4.3.1-1: Interaction between DETA-NO and selected antioxidants: ROS generation.	98
Figure 4.3.1-2: Comparison of the effect of nitric oxide donors and NAC on ROS generation.	99
Figure 4.3.1-3: Interaction between GSNO and selected UA: ROS generation.	100
Figure 4.3.1-4: Interaction between t-BHP and NAC: ROS generation.	101
Figure 4.3.1-5: Effect of the calcium ionophore, A23187 on ROS generation by HUVEC.....	102
Figure 4.3.1-6: Assessment for interaction between reagents and fluorogenic probe H ₂ DCFDA in cell-free conditions.	103
Figure 4.3.1-1: Schematic diagram of experimental results investigating the effect of oxidative and nitrosative stressors on generation of ROS.....	105
Figure 5.3.1-1: Effect of DETA-NO on cell diameter.....	109
Figure 5.3.1-2: Dose response for the effect of DETA-NO on β -galactosidase activity.	111
Figure 5.3.1-3: Micrographs of fluorescence post C ₁₂ FDG exposure: DETA-NO...	113
Figure 5.3.2-1: Comparison of the effect of nitric oxide donors on senescence- associated β -galactosidase.	114
Figure 5.3.2-2: Dose-response for the effect of DETA-NO on the induction of senescence in cultures of HUASMC.	116
Figure 5.3.3-1: Effect of DETA-NO on senescence and apoptosis.	118
Figure 5.3.4-1: DETA-NO increases the expression of cyclin-dependent kinase inhibitors.....	120
Figure 5.3.5-1: BrDU incorporation by cells exposed to DETA-NO vs. control.....	122
Figure 5.3.6-1: Confirmation of nitric oxide production after tetracycline-induction of iNOS.....	123

Figure 5.3.6-2: β -galactosidase activity of coculture of HUVEC with iNOS-expressing HEK-293.....	124
Figure 5.4.1-1: Effect of inhibiting soluble guanylate cyclase on the increase in cell diameter measured by particle analyser seen on exposure of HUVEC to DETA-NO.	126
Figure 5.4.1-2: Effect of soluble guanylate cyclase inhibition on the induction of senescence by DETA-NO.	127
Figure 5.4.2-1: Effect of selenomethionine on the induction of senescence by DETA-NO.....	129
Figure 5.4.2-2: Correlation between cell diameter and total β -galactosidase activity in SM treated cells.	130
Figure 5.4.2-3: Effect of uric acid on the induction of senescence by DETA-NO. ...	132
Figure 5.4.3-1: Effect of NAC on the induction of senescence by DETA-NO.	134
Figure 5.4.4-1: Effect of NAC on the generation of nitric oxide from DETA-NO.	135
Figure 5.4.4-2: Comparison between the effects of DETA-NO and GSNO on the induction of senescence: GSNO, DETA-NO and NAC.....	136
Figure 5.4.5-1: Effect of cold light on the induction of senescence by DETA-NO...	137
Figure 5.4.5-2: Identification of transnitrosated proteins by the biotin switch method.	139
Figure 5.4.6-1: Specific band analysis of biotin switch.	141
Figure 5.5-1: Effect of high doses of exogenously added nitric oxide on telomerase activity.	142
Figure 6.2.1-1: Dose response for the effect of bafilomycin A1 on cell diameter of HUVEC.....	150
Figure 6.2.1-2: Effect of bafilomycin A1 or carrier on population doubling per passage HUVEC.....	151
Figure 6.2.1-3: Effect of bafilomycin A1 on cumulative population doubling in HUVEC.....	152

Figure 6.2.1-4: Bafilomycin A1 and DMSO dose response of HUVEC: senescence-associated β -galactosidase.	154
Figure 6.2.1-5: Bafilomycin A1 and DMSO dose response of HUVEC: senescence-associated β -galactosidase.	155
Figure 6.2.1-6: Effect of bafilomycin A1 on HUVEC β -galactosidase activity.	156
Figure 6.2.2-1: Effect of rapamycin on HUVEC cell diameter.....	158
Figure 6.2.2-2: Effect of rapamycin on HUVEC β -galactosidase activity.....	159
Figure 6.3.1-1: Effect of AICAR on HUVEC cell diameter: dose response.....	161
Figure 6.3.1-2: Effect of AICAR on proliferation of HUVEC.....	162
Figure 6.3.1-3: Effect of AICAR on β -galactosidase activity by flow cytometry.	163
Figure 6.3.1-4: Effect of AICAR on side scatter of HUVEC.	164
Figure 6.3.1-5: Interaction between AICAR and DETA-NO on HUVEC β -galactosidase activity.	165
Figure 6.3.1-6: Interaction between DETA-NO and AICAR: flow cytometric analysis of ROS.	166
Figure 6.3.2-1 Effect of AICAR on HUASMC: senescence-associated β -galactosidase.	168
Figure 6.3.3-1: Dose response for the effect of metformin on HUVEC diameter and count.	169
Figure 6.3.3-2: Effect of metformin on HUVEC senescence: senescence-associated β -galactosidase.....	170
Figure 6.3.3-3: HUVEC senescence and metformin: flow cytometric analysis of β -galactosidase activity.	171
Figure 6.3.4-1: Effect of metformin on HUASMC: senescence-associated β -galactosidase.	172
Figure 7-1: Summary of ROS and senescence data.....	175

List of abbreviations

AICAR	5-amino-1- β -D-ribofuranosyl-imidazole-4-carboxamide
AMP	adenosine 5'-monophosphate
AMPK	AMP-activated protein kinase
ANOVA	analysis of variation
ASS1	arginosuccinate synthase 1
AT-1	angiotensin-1
ATM	ataxia telangiectasia mutated
ATP	adenosine triphosphate
AU	arbitrary units
BCA	bicinchoninic acid
Bcl-2	B-cell lymphoma-2
Bcl-xl	B-cell lymphoma-extra large
BEC	boronethyl cysteine
Biotin-HPDP	N-6-(biotinamido) hexyl-3'-(2'-pyridyldithio) propionamide
BrDU	bromodeoxyuridine
BSA	bovine serum albumin
C ₁₂ FDG	dodecanoylaminofluorescein di- β -D-galactopyranoside
CaCl ₂	calcium chloride
CD44	cluster of differentiation 44
cDNA	complementary DNA
cGMP	cyclic guanosine monophosphate
CHAPS	cholamidopropyltrimethylammonio-propanesulfonic acid
CO ₂	carbon dioxide
CO ₃	carbon trioxide
CPD	cumulative population doubling

Cu ²⁺	cupric ion
DAPI	4',6-diamidino-2-phenylindole
DETA-NO	2,2'-(hydroxynitrosohydrazono)bis-ethanimine
DHE	dihydroethidium
DMEM	Dulbecco's modified Eagle medium
DMF	dimethylformamide
DMSO	dimethyl sulfoxide
DNA	deoxyribonucleic acid
EBM	endothelial basal medium
ECL	enhanced chemiluminescence
EDTA	ethylenediaminetetraacetic acid
EGM-2	endothelial growth medium-2
ELISA	enzyme linked immunosorbent assay
eNOS	endothelial nitric oxide synthase
FACS	fluorescence-activated cell sorting
FBS	fetal bovine serum
FDG	fluorescein di-β-galactopyranoside
FRT	Flp-recombination target
FSC-H	forward scatter height
GPS-SNO	group-based prediction system for S-nitrosylation
GSNO	S-nitroso glutathione
H ₂ DCFDA	2,7'-dichlorodihydrofluorescein diacetate
H ₂ O ₂	hydrogen peroxide
H ₂ SO ₄	sulfuric acid
HBSS	Hanks' balanced salt solution
HCl	hydrochloride

hEGF	human epidermal growth factor
HEK-293	human embryonic kidney cell line-293
HEN	HEPES/EDTA/neocuproine
HENS	HEPES/EDTA/neocuproine/SDS
HEPES	N-2-hydroxyethylpiperazine-N'-2-ethanesulfonic acid
hFGF-B	human fibroblast growth factor-basic
HIF-1 α	hypoxia-inducible factor-1 α
HMG-CoA	3-hydroxy-3-methylglutaryl-coenzyme A
HP1	heterochromatin protein 1
HRP	horseradish peroxidase
hTERT	human telomerase reverse transcriptase
HUASMC	human umbilical artery smooth muscle cells
HUVEC	human umbilical vein endothelial cells
IC ₅₀	half maximal inhibitory concentration
IFN- γ	interferon γ
IGF	insulin-like growth factor
IgG	immunoglobulin G
IL-1	interleukin 1
IL-6	interleukin 6
IL-8	interleukin 8
iNOS	inducible nitric oxide synthase
I- κ B	inhibitor of κ B
JNK	C-Jun N-Terminal Kinase
KCl	potassium chloride
KI	potassium iodide
KRH	Krebs/Ringer/HEPES buffer

LKB1	liver kinase B1 (serine/threonine kinase 11)
L-NAME	L-NG-nitroarginine methyl ester
L-NMMA	L-NG-monomethyl arginine citrate
$M^{-1}s^{-1}$	moles per second
MEM	minimal essential medium
$MgCl_2$	magnesium chloride
MMTS	mercaptoethanol methylthiosulfonate
MnSOD	manganese superoxide dismutase
mRNA	messenger ribonucleic acid
mTOR	mammalian target of rapamycin
MUG	methyl-umbelliferyl galactosidase
MW	molecular weight
N_2O_3	dinitrogen trioxide
N_2O_4	dinitrogen tetroxide
Na_2HPO_4	sodium phosphate dibasic
Na_3VO_4	sodium orthovanadate
NAC	N-acetyl cysteine
NaCl	sodium chloride
NADH	reduced nicotinamide adenine dinucleotide
NADPH	reduced nicotinamide adenine dinucleotide phosphate
NaOH	sodium hydroxide
NF- κ B	nuclear factor- κ B
NO	nitric oxide
NOS	nitric oxide synthase
Nox4	NADPH oxidase 4
NP-40	nonyl phenoxyethoxyethanol

NS	non significant
O ₂	oxygen
ODQ	oxodiazolo quinoxalinone
OH ⁻	hydroxyl
p16 ^{INK4a}	kinase 4a inhibitor / cyclin-dependent kinase inhibitor 2a
PAGE	polyacrylamide gel electrophoresis
PAI-1	plasminogen activator inhibitor 1
PBS	phosphate buffered saline
PD	population doubling
PE	phycoerythrin
PFA	paraformaldehyde
PGC-1 α	peroxisome proliferator-activated receptor gamma coactivator 1- α
PI3K	phosphatidylinositol 3-kinase
PICS	PTEN loss-induced cellular senescence
PIKK	phosphatidylinositol 3-kinase-related kinase
PINK1	PTEN-induced kinase
PKC- β	protein kinase C- β
PML bodies	promyelocytic leukemia bodies
PMSF	phenylmethanesulfonyl fluoride
POT1	protection of telomeres 1
PPAR γ	peroxisome proliferators-activated receptor γ
pRB	retinoblastoma protein
PTEN	phosphatase and tensin homolog
PVDF	polyvinylidene difluoride
RAS	rat sarcoma
RhoGAP	Rho GTP(guanosine triphosphate)ase activating protein

RIG-I	retinoic acid-inducible gene-I
RNA	ribonucleic acid
RNS	reactive nitrogen species
ROS	reactive oxygen species
RT	room temperature
SAHF	senescence associated heterochromatin foci
SASP	senescence associated secretory phenotype
SDS	sodium dodecyl sulfate
SEM	standard error of the mean
sGC	soluble guanylate cyclase
shRNA	small hairpin RNA
SIRT1	sirtuin (silent mating type information regulation 2 homolog) 1
SM	selenomethionine
SNAP	S-nitroso-N-acetyl-D,L-penicillamine
SNP	sodium nitroprusside
t-BHP	tert-butyl hydroperoxide
TEMED	tetramethylethylenediamine
TGF- β	transforming growth factor β
TMB	tetramethyl-benzidine
TNF	tumor necrosis factor
TNS	trypsin neutralizing solution
TRF	telomere repeat binding factor
TSC	tuberose sclerosis complex
UA	uric acid
UV	ultraviolet
VEGF	vascular endothelial growth factor

VSMC vascular smooth muscle cell
X-gal 5-bromo-4-chloro-3-indolyl- β -v-galactopyranoside

1 Introduction

1.1 Senescence overview

Cellular senescence, for the purpose of this document, can be defined as an irreversible loss of replicative capacity with the maintenance of cell viability. This state can occur in response to a variety of stimuli, for instance genotoxic and oxidative stress. However, the original description of cellular senescence pertains to what is known as replicative senescence. Hayflick described the observation that normal diploid cells grown in culture and serially passaged, eventually cease replicating – replicative senescence.¹

Replicative senescence describes senescence which occurs as a consequence of repeated cell divisions. It has been thought that replicative senescence could be the biological limit to mortality.

Stress-induced senescence describes the occurrence of irreversible cell cycle arrest after a noxious stimulus.

The influence of both types of senescence on aging in general have been explored but aging is a complex processes and is often accompanied by disease, whether directly as a consequence of age or as a result of more time being available for disease to take hold. This makes the task of assessing the effect of each individual factor associated with initiating senescence difficult.

The hypothesis that older mammals may have an increased number of cells which have undergone senescence and that this may contribute to diseases seen in the elderly population has been encouraged by harvesting cells from elderly humans and establishing their replicative capacity relative to those harvested from younger donors.² However, this may be due to either replicative or stress-induced senescence.

For example, if one applies a noxious stimulus to a cell, such as radiation or an oxidative stressor, the cell may alter its function in order to defend itself and the organism as a whole. The cell may thus be forced to choose between programmed cell death or senescence. The choice of apoptosis limits the potential for the accumulation of cells with genetic damage and therefore avoids the possibility of cell transformation. However, a proportion of cells undergo stress-induced senescence.

Therefore if one harvests cells from older individuals, there may have been a mix of healthy cells able to replicate and stress induced senescent cells. Serial passage of those cells to calculate replicative capacity will not answer the question of mode of senescence. Senescent cells present in the initial sample will not replicate and therefore, normal cells will account for an increasing proportion of the total cells if the cells are serially passaged until ceasing replication altogether. At time of assay, the cells analysed in the population which initially had more stress-induced senescent

cells will actually have none of the original cells which senesced in this manner and a higher proportion of cells which have senesced through more replication cycles.

Either mode of senescence may help to explain the increased incidence of senescent cells seen in vascular disease, which can have its origins in young individuals, manifesting later in life. Vascular smooth muscle cells obtained from atheromatous plaques have been subject to histological analysis. 18% of these cells were observed to be senescent in that they expressed senescence-associated β -galactosidase and p16^{INK4a} and p21^{WAF}, while no such evidence of senescence was found in cells from non-atheromatous arteries.³ Furthermore, vascular smooth muscle cells cultured from atheromatous plaques rapidly accumulated a senescent phenotype with 80.5% demonstrating senescence-associated β -galactosidase on first passage, compared to 5.2% in healthy sections of artery.

Another argument against replicative senescence being the predominant factor in aging is that in many cell types, and for instance endothelial cells, the number of cells replicating at any one point in time *in vivo* is very small. This is because in adult endothelium, cell turnover tends to be by necessity, for instance in the context of growth of new vessels damage and repair of existing vessels. Cells largely tend to be in a quiescent state. *In vitro*, we are often able to see several scores of population doublings before replicative senescence intervenes. Cells grown *in vitro* are grown at a relatively low density to avoid contact inhibition and subsequently increase in number at exponential rates. In contrast, cells analysed *in situ* in the vasculature of rat and pig aortae show a mitotic rate of 0.01% and 0.55% respectively.^{4;5} The standard doubling time of a rat aortic endothelial cell is around 28hrs. If this was a constant rate, rats would produce a new endothelial layer every 32 years and pigs every 7 months. Clearly, if these data are accurate, for rats, endothelial replicative senescence is unlikely to occur but in pigs, there is a possibility it would occur. This assumes that cells in all parts of endothelium are repaired equally. However, disease states are likely to place demands on focal areas and imperfect repair is likely to lead to higher rates of attrition.

Atheroma tends to occur at branch points of arteries.⁶ It has been shown that these cells suffer a higher rate of attrition than cells in straight sections of blood vessels due to changes in shear stress or turbulence and thus may be required to undergo more cell divisions than their neighbouring cells, finally reaching replicative senescence. Alternatively, noxious stimuli such as pro-inflammatory cytokines and the associated rise in oxidative radicals may lead these cells to undergo stress-induced senescence. Regardless of the cause of senescence, it remained to be shown whether senescent cells actively participate in the development of disease, whether they are in fact protective or whether they are simply innocent bystanders.

We became interested in investigating factors involved in the initiation of senescence and the role of stressors likely to be encountered by vascular cells.

Methods to investigate senescence are limited by the source of cells and the artificiality of the system used to grow them. The ideal system would allow the analysis of a subset of young cells of similar replicative age to be analysed in a phenotypically pure population for the early changes associated with the development of senescence and for the subsequent proportion of senescent cells. In this respect, obtaining young healthy human cells limits us to obtaining cells from umbilical cords.

Assessment of senescence by replicative capacity relies on a number of cell manipulations which may introduce error. Standard practice is to keep cells *in vitro* under continual mitogenic stimulus. Cells are not allowed to become confluent in culture as there is contact inhibition between cells and this would make any calculation of cell replication rate inaccurate. Cells which become confluent may also not recover their replicative ability. Thus experiments to assess the effect of stressors on senescence are carried out when cells are at a relatively low density (not in contact). The cells are then repeatedly dissociated using trypsin EDTA, another artificial agent and suffer mechanical stress for a number of passages until replicative senescence. This contrasts with the situation *in vivo* where cells are in contact, forming a layer of quiescent cells. Cells in a confluent monolayer may be better suited to survive any noxious stimulus and also may express their defences in a way more alike to *in vivo*. The ability to assess senescence immediately after any intervention would decrease the chances of culture artefact.

1.1.1 Identifying cell senescence

There appear to be many different ways to senesce. Whether the final senescent phenotype is uniform or variable is also not conclusive. However, cells which senesce tend to display some or all of the following rather descriptive features (abridged from Rodier and Campisi JCB 2011).⁷ These features are discussed after the summary.

- β -galactosidase activity increases.
 - Some of the increase in mass is due to an increase in the size of lysosomes and this can be demonstrated by staining for β -galactosidase.
- Senescent cells tend to increase in mass.
- Irreversible cell cycle arrest.
 - The first essential component point but can sometimes be overcome by interfering with factors required to maintain the cell in growth arrest, resulting in cellular transformation.
- p16^{INK4a}

- Cells which have senesced tend to express the tumour suppressor p16^{INK4a} which in turn activates retinoblastoma protein (pRb).
- DNA-SCARS
 - DNA segments with chromatin alterations reinforcing senescence.
- SASP
 - There is also an altered secretory pattern in senescent cells (senescence associated secretory phenotype).

1.1.2 Senescence-associated β -galactosidase

Senescence-associated β -galactosidase can be visualized by histology and represents an increase in the amount of β -galactosidase activity which is normally active at an acidic pH within lysosomes but, in senescence, can be detected at a relatively alkaline pH of 6.⁸ This correlates well with replicative senescence and has been used to detect the other forms of senescence.⁹ Further analysis of this phenomenon has revealed that the increase in senescence-associated β -galactosidase staining actually represents an increase in the mass and activity of β -galactosidase.¹⁰ Furthermore, the increase is accommodated by an increase in lysosomal mass. It is not known why cells have an increased amount of β -galactosidase enzyme but the subcellular localization of β -galactosidase remains within the lysosomes which tend to enlarge once senescence occurs. One possibility is that senescence is associated with a defect in the function of lysosomes or that they become overwhelmed by an increased demand. This phenomenon has been demonstrated to be non-causal by work on cells unable to manufacture β -galactosidase. In this study, cells continued to replicate until cell cycle arrest was observed.¹¹ However, this did not exclude the possibility that lysosomal dysfunction had occurred and could remain the causative mechanism. I therefore decided to investigate the effect of pharmacological manipulation of lysosomal function on vascular cell senescence.

1.1.3 Telomere function and senescence

The telomere is a complex structure at the ends of chromosomal DNA. It serves as a cap to cover the ends of DNA and thus prevent the loose ends being recognized as strand breaks, which would trigger DNA repair mechanisms or cell death via apoptosis. More than this, DNA replication begins at the telomeric end of DNA and the action of the DNA replication machinery requires a certain minimum length of bases to grip onto the strand of DNA and begin replication. The first bases are thereby not copied in the successive generation and this process leads to progressive shortening of the telomeric DNA, finally rendering it too short to allow the DNA replication machinery to latch on. This makes the cell unable to support replication and leads to senescence.

In more detail, DNA replication by DNA polymerase occurs with the aid of a RNA primer template. DNA synthesis is unidirectional. The DNA polymerase is only able to synthesise nucleotides which start with a 5' base and lead to a 3' base, therefore they start in sequence on a complimentary portion of DNA, closest to the 3' end, proceeding towards the 5' end. This occurs at multiple sites during different stages of S phase. Initially, the double strand is pulled apart, allowing space for RNA primers to recognise the starting point.

The leading strand is that which is using the DNA template generally progressing towards the 5' end and therefore requires only a single starting point and could in theory continue in this direction with minimal DNA strand separation to the end of the molecule, although, in practice, it tends to meet a previously synthesized segment first.

The other strand is referred to as the lagging strand. As the DNA is being separated in the opposing direction to that which DNA polymerase is able to replicate, it uses multiple starting points separated by short gaps to make short segments. Each segment contains an RNA primer, followed by DNA.

After synthesis of DNA, the RNA templates are removed and the gaps in DNA filled by ligase. This is completed in the main portion of DNA where ligase has a preceding DNA segment in order to replace the RNA primer. However, at the end of the chromosome, there is no preceding DNA segment and therefore the final portion of DNA cannot be filled in this manner, leaving a single-strand overhang and relatively shorter DNA.

Thus, the expectation would be that with each replication, DNA would gradually lose length in the region of the telomere. However, the number of base pairs lost in this manner would be minimal and asymmetric (loss occurring only in the lagging end of DNA as the leading end would have no primer to resect). Further loss of the 5' end of DNA is regulated by MRN, a DNA damage response protein and Protection of Telomeres 1 (POT1), one of the capping proteins which seems to regulate a minimum 3' overhang length, perhaps to ensure a t-loop structure suitable for capping.^{12;13}

In this way, without any other mechanism to restore telomeric length, telomeric shortening leads to a predetermined number of cell replications and a maximum organismal age. This is countered in many replicating cell types by restoring telomeric length using the enzyme telomerase. Loss or dysfunction of telomerase, in those cells which express it, eventually occurs with increasing age and this, in turn, allows the telomere to be eroded to a critical length, promoting senescence.

Telomerase assays and telomere length studies showed that cells with high telomerase activity tended to be able to replicate indefinitely and that this was related to maintenance of telomere length.¹⁴⁻¹⁸ Thus cancer cells commonly have a high level

of telomerase and normal cells transfected to constitutively express telomerase are able to circumvent senescence and replicate indefinitely.

Telomerase comprises a catalytic subunit (hTERT) and also contains a RNA template designed to recognise 1½ repeats of TTAGGG and in this way can recognize the telomere and can add more of the 6-base pair units which make up the telomere. It functions as a reverse transcriptase and much of its structure was elucidated by Blackburn et al.¹⁹⁻²² Working in parallel, Szostak developed a non-functioning mutant of telomerase and showed that cells lacking functioning telomerase progressively lost telomere length. The cells were able to replicate up to a certain point but lost this ability earlier than yeasts without the mutation – an alteration to their replicative capacity clearly related to accelerating shortening of telomeres.^{23;24}

Telomere attrition has been demonstrated in cells localised to atherosclerotic plaques. Whilst not conclusive proof of a causal relationship, telomere attrition is not seen in healthy portions of artery and may well play a part in the disease generation, maintenance or even defence. Interestingly, telomere restriction fragment length varied between individuals more than between disease processes when patients undergoing heart transplant were examined to compare atherosclerotic vessels with normal vessels. However, the variation within individuals which was assessed by comparing diseased and healthy portions of vessel from the same patient was more impressive and corresponded to the expected finding of senescence within vascular smooth muscle cells sourced from atherosclerotic plaques. Therefore there is no reliable method of investigating the presence of senescence simply by measuring the current telomere length, rather the telomere shortening compared to the starting length or the process which permits this to occur needs to be assessed.³

However, the telomere's role in the organism may well be less to do with limiting the age it could potentially attain and more to do with maintaining health. The prevention of unlimited cellular replication is an important step to avoiding neoplastic growth. This is amply demonstrated by numerous observations of cancer cell lines being able to circumvent senescence by a variety of mechanisms, including the expression of telomerase.

It is important to differentiate between the Hayflick description of replicometer senescence and other forms of senescence seen *in vivo* or in stress situations *in vitro*. Whether cells which have previously undergone a number of divisions are more susceptible to stress-induced senescence is not known. Cells grown serially in culture have shortened telomeres but lack a DNA damage response at the stage of senescence.²⁵ Factors which are thought to encourage this include tissue culture conditions. Repeated trauma to cells, a lack of shear stress on endothelial cells and a lack of the surrounding connective tissue and other cell types are artifices which make the tissue culture situation different to that seen *in vivo*. Moreover, incubating cells in 21% oxygen is a significantly higher dissolved concentration of oxygen than

cells would generally encounter *in vivo*, although the availability of oxygen *in vivo* is greatly enhanced and regulated by release of oxygen by haemoglobin.

Telomere erosion, as mentioned above, tends to occur in replicative senescence and leads to a senescence characterised by increased expression and activity of p53 and is aided by p21^{WAF}. However, this can be reversed by inactivating p53 or partly reversed by expressing oncogenic RAS, a powerful mitogenic stimulus.²⁶

Therefore cells can senesce in response to DNA damage, telomere attrition due to repeated cell divisions and also in response to tumour suppressor gene loss.

It is always tempting to ascribe an evolutionary purpose to biological phenomena but it seems that senescent cells do afford some protection against tumours, particularly those which may affect life during the childhood and reproductive years. However, the same benevolent process may encourage the development of cancer in later years (antagonistic pleiotropy).

Telomere length is important to maintain telomere function as it serves as the site for telomere capping proteins to cover the end of the DNA molecule. Shortened telomeric DNA leads to an increasing risk that capping proteins will no longer be able to cover the DNA which in turn can be recognized as double-strand DNA breaks and could initiate the DNA damage response mechanism and cell cycle arrest. Alternatively, the exposed DNA could lead to telomeric fusion with other exposed telomeres and cell cycle arrest by this mechanism.²⁷ Telomerase presents a mechanism by which this could be prevented, by adding tails of DNA to their 3' ends.²⁸

Interestingly, telomere length was not the only predictor of proliferative capacity. Cells which are transfected with a fully functional hTERT catalytic subunit of telomerase can elongate their telomeres and become immortal. However, cells expressing a hypomorphic, less functional hTERT exhibit a degree of telomere attrition but after a period of telomeric shortening, stabilise and achieve immortality. Telomerase thus can be assumed to perform more than one anti-replicative senescence function. Telomere protein subunits TRF1 and TRF2 protect the structure of the terminal loop of telomeres and its capping of the bare overhang on the 3' end may prove to be the more important protective function performed by telomerase.^{29;30}

1.1.4 Senescence and cell cycle regulation

Senescence has been ascribed many potential roles in health and disease. In the context of cancer biology, senescence is a barrier to unlimited replication and as such may be a barrier to neoplasia which must be overcome by successful tumours.³¹⁻³⁶

On the other hand, in aging, senescence is purported to be one of the mechanisms of tissue decay by which organisms are limited to a certain lifespan. Therefore in

this context, circumventing the mechanisms behind senescence may offer a means of promoting healthy ageing and extending lifespan.^{33;34}

Perhaps more importantly, senescence could play a part in age-related diseases such as atherosclerosis.^{35;37;38} This could offer an answer to the question of why cardiovascular disease is so common in the elderly, even when other, known risk factors have been treated or were previously normal.

Within these broad questions lies an intrinsic problem. If senescence acts as a barrier to neoplastic growth but plays a causative role in cardiovascular disease, treatment to prevent cancer which encourages senescence and to prevent atherosclerosis which retards senescence will rely on there being intrinsic differences in the mechanisms of senescence between cell types. Fortunately, there does seem to be a degree of heterogeneity between cell types in the mechanism by which they undergo this change.³⁹⁻⁴¹

As one may expect, the irreversible cell cycle arrest seen in senescence involves the cell cycle regulatory molecules. An early signal of senescence, specific for endothelial cells and vascular smooth muscle cells, has not been identified but investigation of the cell cycle regulatory proteins could provide a signature of the initial signal, the initial response and finally, senescence.

The tumour suppressor, p16^{INK4a} has been implicated in the development of cell cycle arrest in the context of senescence and when it is overcome, cells may be transformed and immortalized and no longer show any features of senescence.³² Moreover, cells in senescent vascular cells express p16^{INK4a}.³⁷

Ectopic expression of p21^{WAF} and p16^{INK4a}, which are cyclin dependent kinase inhibitors induces senescence without needing to initiate a DNA damage response and again suggests an independent pathway to senescence.

In cells which have senesced and where p16^{INK4a} is not part of their expression repertoire (eg the BJ fibroblast cell line from human foreskin), inactivation of p53 is able to reverse the growth arrest and allow cell proliferation to resume.⁴² Therefore p53-led senescence is reversible when the brake is released. However when p16^{INK4a} is able to be expressed by a cell type, p53 senescence is not reversible. p16^{INK4a} therefore acts as an additional and more definite growth arrest signal. Suppressing continued expression of p16^{INK4a} by using shRNA does not reverse senescence any further than the DNA S-phase. This also suggests p16/pRb pathway acts in more than one phase of cell replication, preventing entry to S phase and then later in the cycle. Senescence associated with intrinsic expression of p16^{INK4a} is therefore more secure against inactivation.

Ectopic expression of p16^{INK4a} does not proffer the same secure growth arrest when expressed after the onset of senescence as it can be reversed by shRNA against p16^{INK4a}. This suggests p16^{INK4a} acts not so much as a brake to cell proliferation and

more akin to a decommissioning agent which requires the cell cycle machinery to be running and at a certain stage of replication to act, perhaps by altering chromatin such that DNA replication becomes impossible.^{42;43}

1.1.5 Chromatin modification

Chromatin is a structure combining DNA and histones. Histones aid the wrapping of the DNA molecule into ever-tighter loops around the histone proteins which serve to compact the molecule in an ordered structure and conceal genes from transcriptional machinery until it is required, when it unwraps to reveal the DNA.

Senescence associated heterochromatin foci (SAHF) are densely DAPI-staining foci seen in senescent cell nuclei. Initially merely an interesting observation useful in identifying senescent cells, this morphological change appears to have a functional significance. Alterations to the histone proteins have been widely observed, but other proteins have also been seen to enter the chromatin structure and may represent a means of blocking DNA replication in senescence. Narita et al⁴⁴ describe the involvement of high-mobility group A proteins (HMGA) in senescent cells. HMGA proteins localize to the chromatin structure and act to hinder DNA replication, an effect which was amplified by the presence of p16^{INK4a}. They also inhibit proliferative signals and help with senescence maintenance.

Replicative genes such as cyclin A are hidden into SAHF complexes, facilitated by pRb.⁴³ The formation of SAHF in senescent cells takes place on a chromosome by chromosome basis, rather than collecting related genes across chromosomes.⁴⁵ One of the major groups of histone proteins, the HP1 proteins, demonstrate changes in cellular location (in PML bodies) followed by selective phosphorylation leading up to the development of senescence. On senescence, HP1 relocates to the chromatin structure and to what become SAHF. The phosphorylation appears to improve efficiency of transport of HP1 which accumulates in high levels within SAHF.⁴⁵ Interestingly, these high levels of HP1 are not necessarily required for senescence-associated β -galactosidase expression, although this may not necessarily mean that it is not essential at low levels.

Therefore SAHF block replicative genes from replicative machinery, a process which is aided by the presence of cell cycle proteins known to be associated with the senescent phenotype, but at a stage earlier than the increased activity of β -galactosidase seen in more mature senescence. Thus it made sense for us to confirm senescence in our investigations by detection of p16^{INK4a} and p21^{WAF}.

1.1.6 Senescence associated secretory phenotype

Senescent cells may occur in disease environments and may be a phenomenon of aging but are they of any functional significance?

Evidence suggests they alter their secretory profile and play an active role in the pathogenesis of disease.

Frippiat et al⁴⁶ described the effects of both oxidative stress in the form of hydrogen peroxide and TGF- β 1 on the expression of several protein markers of senescence. While both hydrogen peroxide and TGF- β 1 increased the numbers of senescent cells when measured by senescence-associated β -galactosidase, other proteins were also called upon with increased levels of mRNA for fibronectin, osteonectin, SM22 and apolipoprotein J. In fact, the effect of hydrogen peroxide was mediated by TGF- β 1 and required hypophosphorylation of pRb. This was demonstrated by antibodies to TGF- β 1 or its receptor circumventing the effect. pRb's role was elucidated by knocking it down and the observed increase in TGF- β 1 was no longer seen.

Blanco et al⁴⁷ describe an alteration of TGF- β auxiliary receptors in senescent endothelial cells of mice, endoglin. Mice which were induced to express S-endoglin (the senescent form of endoglin) also display a hypertensive, pro-thrombotic state with increases in PAI-1, extracellular matrix production and decreases in eNOS. While the mice expressing S-endoglin maintain the ability to vasodilate in response to nitric oxide donors, inhibition of nitric oxide synthases by L-NAME results in a lesser hypertensive response in the mice induced to express S-endoglin. These mice then have impaired endothelial dilation in response to acetyl-choline, an effect normally mediated by increasing production of nitric oxide via eNOS. The S-endoglin form of this receptor was observed in human coronary artery endothelium and in HUVEC grown to replicative senescence in culture.

Cells expressing p16^{INK4a} have been demonstrated to secrete pro-inflammatory cytokines such as interleukin-6 (IL-6).^{48;49} This was observed in HUVEC subjected to replicative senescence and radiation-induced senescence. IL-6 and IL-8 were demonstrated to play a part in maintenance of senescence and this could be circumvented by replacing depleted levels of Klotho protein. Klotho deficient mice had previously been shown to have a premature aging phenotype which included atherosclerosis and endothelial dysfunction. The way in which Klotho led to increases in interleukin-6 was further elucidated by the group. They demonstrated in murine brain and kidney that interfering with expression of the ataxia telangiectasia mutant (ATM) protein prevented the pro-inflammatory phenotype and that further upstream, the pathway also used retinoic acid-inducible gene-I (RIG-I) as demonstrated by knocking down expression of RIG-I in senescent HUVEC. NF- κ B was also implicated in the pathway and increased expression of NF- κ B was demonstrated in senescent cells. Knock down or expression of RIG-I by Klotho managed to increase the proliferative capacity of pre-senescent cells. Klotho has been implicated in suppression of the Wnt pathway, interacts with insulin-like growth factor and is protective against some forms of cellular oxidative stress.⁵⁰ Thus the pro-inflammatory secretory phenotype of HUVEC is seen both in replicative and stress-induced senescence. The process is regulated by Klotho and RIG-I in an inverse manner with Klotho maintaining the younger non-inflammatory phenotype and giving way to RIG-I in aging cells, a process which can be reversed by

reintroducing Klotho into the system. Not only does suppression of RIG-I by Klotho lead to reduced cytokine expression, but it also restores replicative capacity.

The role of NF- κ B as a promoter of senescence was investigated by Hasegawa et al.³² They demonstrated that, in mice transgenically bred to have deficient endothelial responses to NF- κ B, there was a lower incidence of insulin resistance and preserved eNOS expression in response to high fat diets, and their lifespans were increased. Analysis of adipose tissue in genetically obese mice with deficient NF- κ B responses revealed a reduction of macrophage recruitment and decreased iNOS expression. The expression of MnSOD and glutathione peroxidase was also decreased in the aorta, suggesting lower degrees of oxidative stress. Moreover, NF- κ B suppression in the obese mice reduced age-related vascular senescence, measured by senescence-associated β -galactosidase which was consistent with the increase in lifespan.

NF- κ B is constitutively inactive in the cytosol, bound to an inhibitor protein I- κ B. Phosphorylation of I- κ B leads to disassociation from NF- κ B allowing it to relocate to the nucleus and to become active. Factors associated with I- κ B phosphorylation include TNF- α , lipopolysaccharide and inflammatory cytokines.

ATM protein, in common with mammalian target of rapamycin (mTOR), is a member of the PIKK family of kinases. The role of ATM as a central coordinator of the DNA damage response to oxidative stress was explored by Zhan et al.⁵¹ Using HUVEC with H₂O₂ 100 μ M as an oxidative agent, they demonstrate that ATM protein is associated with oxidative stress-induced senescence. ATM levels increase in response to oxidative stress, being shown in other studies to be localised to foci on DNA of senescent cells exposed to genotoxic stress which results in double-strand DNA breaks.⁵² As a consequence of auto-phosphorylation of ATM in response to this stress, ATM phosphorylates Akt and p53 and increased levels of p21^{WAF} follow. Inhibitors of ATM, including caffeine, were seen to prevent this response and knock down of ATM was also able to prevent senescence induced by H₂O₂. This was confirmed in vitro and further supported by ATM knock-out mice with streptozosin-induced diabetes (streptozosin is a drug which is toxic to pancreatic islet cells, the source of insulin). Diabetic mice showed senescence-associated β -galactosidase positive cells which also expressed p16^{INK4a} and p21^{WAF}. This phenomenon was not observed in the ATM negative mice.

Furthermore, ATM also autophosphorylates in response to cellular hypoxia. Bencokova et al.⁵³ report that extreme hypoxia (0.02%) caused ATM to autophosphorylate and that this was independent of mitochondrial signalling or other PIKK family members. This also occurred in response to DNA strand breaks and was unaffected by the hypoxia-inducible factor (HIF-1 α)-inducing agent cobalt chloride, even at higher oxygen concentrations. Furthermore, phosphorylation of ATM occurred in hypoxia in HIF-1 α knock-out cell lines. However, ATM does not

relocate to DNA strand breaks in hypoxia but remains distributed throughout the nucleus.

Microarray studies have shown an increase in the expression of monocyte adhesion molecules in senescent endothelial cells. Mun et al⁵⁴ demonstrated in HUVEC grown to replicative senescence either with or without laminar shear stress that there was an increased expression of the CD44 gene. This led to an increase in mRNA and protein levels. Furthermore, this increased the ability of monocytes to attach to the senescent cells. They also demonstrated that cells from older rats express increased CD44 in their aortae.

However, in contrast to other groups, Coleman et al⁵⁵ report that cells subjected to oxidative stress-induced senescence display an anti-inflammatory phenotype, being resistant to the effects of TNF- α and lacking correct localization of cell adhesion molecules for recruiting pro-inflammatory leukocytes. By investigating the influence of SENEX, a RhoGAP protein, which may be involved in the DNA damage response, they noted that increased expression of SENEX promoted senescence and down-regulation led to apoptosis. SENEX was increased in response to moderate doses of H₂O₂ and this led to cell senescence.

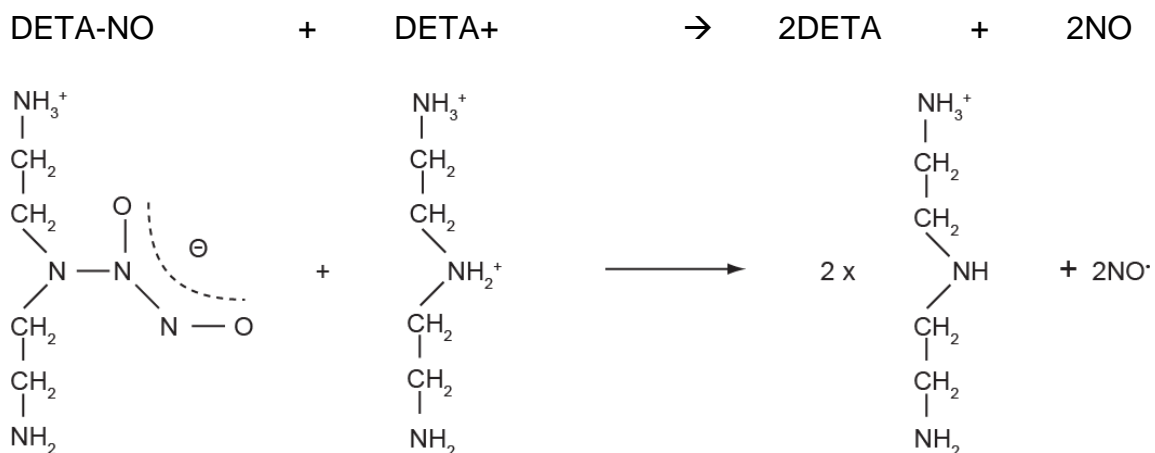
Therefore, senescent cells have an altered secretory phenotype and mostly, this appears to lead to both a constitutive preference for a pro-inflammatory state and to an enhanced ability to respond to pro-inflammatory stimuli. Senescence also appears to be accelerated in response to these pro-inflammatory stimuli. However, in certain conditions, there may also be cells which are senescent but anti-inflammatory and may remain at sites subjected to a stressful stimulus perhaps to support the structural integrity of the endothelial layer.

As nitric oxide-related reactive nitrogen species are increased by inflammation, we decided to investigate this further.

1.2 Nitric oxide and senescence

Nitric oxide is a cell signalling molecule, a reactive oxygen species, able to inhibit cell respiration and produced in higher quantities in the inflammatory response. Nitric oxide is produced in many cell types involved in health and disease of the vasculature, endothelial cells, vascular smooth muscle cells and monocytes/macrophages. Therefore its effect on vascular senescence is of interest. However, nitric oxide at a wide range of doses exerts a powerful anti-proliferative action on growing cells.^{56;57} This effect has been observed in endothelial and vascular smooth muscle cells. This creates problems for the *in vitro* model of growing cells continually in the log-phase, particularly if one wishes to investigate the effect of nitric oxide on replicative senescence. Thus I developed a method of investigating senescence after cells have become confluent. Studies have previously shown that confluent cells express a greater basal amount of senescence-associated β -gal irrespective of replicative age.⁵⁸ I overcame this by

The levels of nitric oxide encountered by cells varies widely and presents many technical problems in relation to measurement and reproducing these conditions *in vitro*. As nitric oxide has a short half-life both *in vivo* and *in vitro*, concentrations encountered within cells, between cells in the interstitium and between cells in contact in culture may be much higher than that measured a short distance away in serum or in medium. The peak concentration of nitric oxide may therefore be higher at the cell surface and in endothelium, a thin layer of high concentration nitric oxide bathes cell surfaces. Experiments designed to investigate this have used fine tip electrodes and discovered concentrations of 500-600nM nitric oxide measured in rat and mouse renal tubules and in human *in vivo* studies have suggested a peak bioavailable nitric oxide concentration as high as 800nM.^{64;65} These peaks of nitric oxide are followed by a relatively quick decrease and therefore the choice of an exogenous nitric oxide donor would ideally mimic repeated bursts of nitric oxide release followed by a decrease. The nitric oxide donor diethylenetriamine NONOate (DETA-NO) provides a stable level of nitric oxide release with a half-life of 20 hours at room temperature in PBS and normal medium at 20°C. The half-life of DETA-NO is shorter at higher temperatures.⁶⁶



Laminar shear stress affects the endothelial cell monolayer, with increasing levels of stress leading to enhanced nitric oxide production and expression of nitric oxide synthase and other permissive enzymes, for example arginosuccinate synthase (ASS1)⁶⁷ and is largely held to be protective against atheroma formation and senescence. Atheroma and senescence tend to occur more readily at arterial branch points, where laminar shear stress is instead replaced by oscillatory shear stress.⁶⁸ Giant endothelial cells were observed in human atheromatous plaques by scanning electron microscopy, presumed by the authors to be senescent cells, in the absence of techniques to verify this at the time.⁶⁹ The oscillatory stress occurs at relatively low tensions when compared to laminar shear stress areas and fails to generate the favourable phenotypic adaptation seen in endothelial cells exposed to laminar shear stress which express NOS, permitting generation of nitric oxide, which

in turn regulates vascular tone and is one factor associated with reducing the pro-thrombotic state.

1.2.2 The protective role of nitric oxide

The presence of eNOS generally declines with advancing replicative and organismal age. In addition, some models of senescence show an increase in eNOS protein but a reduction in eNOS function and thus this is postulated to be a mechanism behind reducing endothelial function with age.^{70;71} eNOS-related nitric oxide formation varies widely *in vivo* in response to a variety of stimuli. However, young endothelial cells are thought to release a basal amount of nitric oxide.^{72;73} The amount of nitric oxide produced basally has been reproduced *in vitro* by using nitric oxide donors and this has been shown to retard the development of replicative senescence in HUVEC grown in culture. This effect was thought to be telomerase-mediated as telomerase activity was increased by nitric oxide donors.^{62;63} A lack of nitric oxide increases the rate of apoptosis in endothelial cells exposed to a variety of stresses and this has been shown to be reversible with the addition of exogenous nitric oxide donors.⁷⁴⁻⁷⁷

Analysis of endothelial cells *in vivo* have confirmed the concentration and activity of nitric oxide synthase varies. Cells from younger animals tend to have a higher amount of endothelial nitric oxide synthase and this has been shown by some groups to be progressively lost with advancing age.⁷⁸ eNOS re-expression by gene transfer was shown to encourage a regression of atherosclerosis in rabbits.⁷⁹ eNOS expression can also be increased by the presence of shear stress and this effect is attenuated with advanced age. In turn, the effect of advanced age may be reversed by exercise training in rats, increasing eNOS expression.^{61;80-82} Thus it is assumed a basal level of nitric oxide is synthesized in young, healthy arteries and this can be physiologically modulated to accommodate varying amounts of shear stress.^{60;61;83} There is a question as to whether a certain level of nitric oxide may be required at a maintenance level for signalling or to prevent aging. For instance, nitric oxide may maintain a healthy relaxed state of artery which is able to accommodate increases in vessel flow without unduly increasing vessel pressure and conversely, to be able to constrict to increase pressure in cases of reduced flow. Thus it is essential that a vessel remains in a mid-state, capable of changing in both directions.

Nitric oxide also aids signalling by S-nitrosylation and transnitrosation of proteins such as NF- κ B, p21^{ras} and eNOS to modulate their function and may potentially compete with oxidative species in this respect. Transnitrosation produces a more readily-modifiable alteration than the corresponding oxidation reaction.⁸⁴⁻⁸⁹

As a further example, transnitrosation of arginase has been shown to have an important regulatory role in the activity of iNOS. Arginine is a substrate in the urea cycle and is the source of nitric oxide for iNOS. While the Km for each enzyme is of a different order of magnitude (much higher in the case of arginase), increasing arginase activity could potentially rob iNOS of substrate and lead to a reduction in its

ability to generate nitric oxide. Santhanam et al⁹⁰ report that transnitrosation of two distinct cysteine residues of arginase lead to an increase in enzyme activity. This can be achieved either by the addition of GSNO 50µM or by inducing iNOS. Aged rats have a higher concentration of cysteine-nitric oxide (cys-SNO) residues than young rats and have a reduced level of nitric oxide production, a deficiency which can be reversed by inhibiting arginase with boronethyl cysteine (BEC). Using the fact that aged rats also express higher levels of iNOS enzyme, the group went on to demonstrate that this was associated with increased transnitrosation of arginase. Furthermore, inhibiting iNOS with 1400W successfully prevented the increased transnitrosation of arginase. Inhibiting iNOS thereby effectively decreased arginase activity, which in turn increased arginine concentrations which would then be available as a substrate for NOS to resume nitric oxide production. Higher concentrations of exogenous nitric oxide were also investigated and were found to begin to inactivate arginase at GSNO concentrations of 100µM. This may reflect that one of the cysteine residues (C303) is more readily transnitrosated at lower concentrations and this increases the activity of arginase, whereas a second residue becomes transnitrosated at higher concentrations and inactivates the enzyme (C168).

Therefore the action of iNOS may be buffered by its effect on arginase activity and the corresponding change in substrate availability. Substrate availability reduces iNOS activity at increasing concentrations of nitric oxide until this is overcome and arginase activity begins to be inhibited and substrate availability is restored. The latter effect may be part of the host defence against sepsis, able to allow much higher concentrations of nitric oxide in order to be cytotoxic to local pathogens.

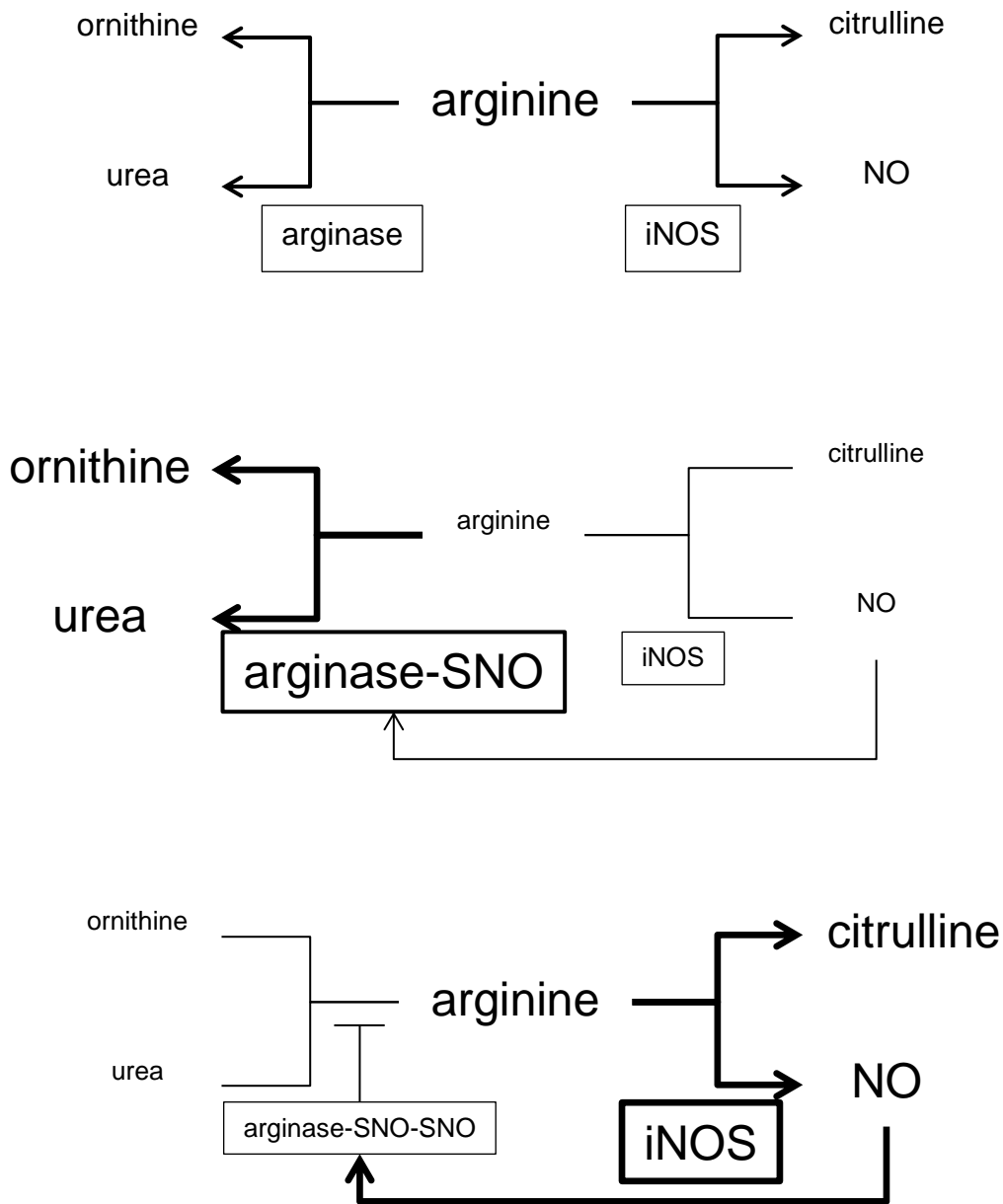


Figure 1.2.2-1: Effect of increasing degree of transnitrosation of arginase.

Top panel is a schematic of the effect of arginase on the balance of arginine as a substrate of both arginase and iNOS. After a single transnitrosation (middle panel), the activity of arginase increases and therefore the balance shifts towards the formation of ornithine at the expense of substrate availability of arginine for iNOS to convert to nitric oxide and citrulline. At higher concentrations of nitric oxide (lower panel), such as that seen in sepsis, where there may also be the addition of nitric oxide from surrounding inflammatory cells, arginase is transnitrosated on a second cysteine residue. This reduces its activity and arginine is therefore once again available to iNOS for the formation of nitric oxide.

1.3 Inflammation, iNOS activity and senescence

Kim et al⁹¹ demonstrate a simple correlation between the addition of bacterial lipopolysaccharide to a cell culture in a pulmonary epithelial cell line and the generation of hydrogen peroxide. This dose-dependent increase in hydrogen peroxide was eventually associated with a dose which induced apoptosis. A sub-lethal dose was however, associated with an increase in cell diameter, lysosomal content and senescence-associated β -galactosidase percentage. This effect was inhibited by the addition of glutathione as an antioxidant. The implication of this is that hydrogen peroxide may have been a marker of oxidative stress induced by nitric oxide and that nitric oxide had increased superoxide production by inhibiting mitochondrial respiration. The addition of glutathione would effectively counter the oxidative stress by removing the source, nitric oxide. The senescence induced in this model was not associated with a loss of telomere length.

Vascular iNOS and eNOS mRNA has been observed to increase in old, or at least middle-aged rats. This occurs in the absence of inflammation or hypertension.⁹² Older rats' vascular smooth muscle cells also have an enhanced response to high glucose-mediated increases in iNOS mRNA expression.⁹³

Elderly (non-transformed) human embryonic fibroblast cells from the line WI38 exposed to inflammatory cytokines exhibit a reduced proliferation rate and increased rate of apoptosis. This effect was reduced when the NOS inhibitor L-NMMA was added, suggesting it is at least in part mediated by a nitric oxide synthase. Moderate levels of exogenous nitric oxide released by SNP and SNAP donors improved proliferation rates in pre-senescent cells but higher levels produced a non-significant decrease in proliferation. These older rat fibroblasts reacted more readily to inflammatory and anti-cancer cytokines than younger cells. iNOS expression was found to be readily increased by TNF- α and IFN- γ . This effect was much more pronounced in cells which had undergone several passages as opposed to younger cells. This resulted in increased levels of nitric oxide production in the region of 14-15-fold when compared to younger cells.⁹⁴ A similar response has been seen in mouse macrophages.⁹⁵

Other rat studies have shown increased levels of nitric oxide production in elderly animals as measured by nitrite and nitrate assays. While both eNOS and iNOS protein levels increased, the activity of eNOS was decreased and this was associated with decreased vasorelaxation, suggesting that the nitric oxide produced by iNOS was reducing the ability of eNOS to regulate vascular tone.⁹⁶

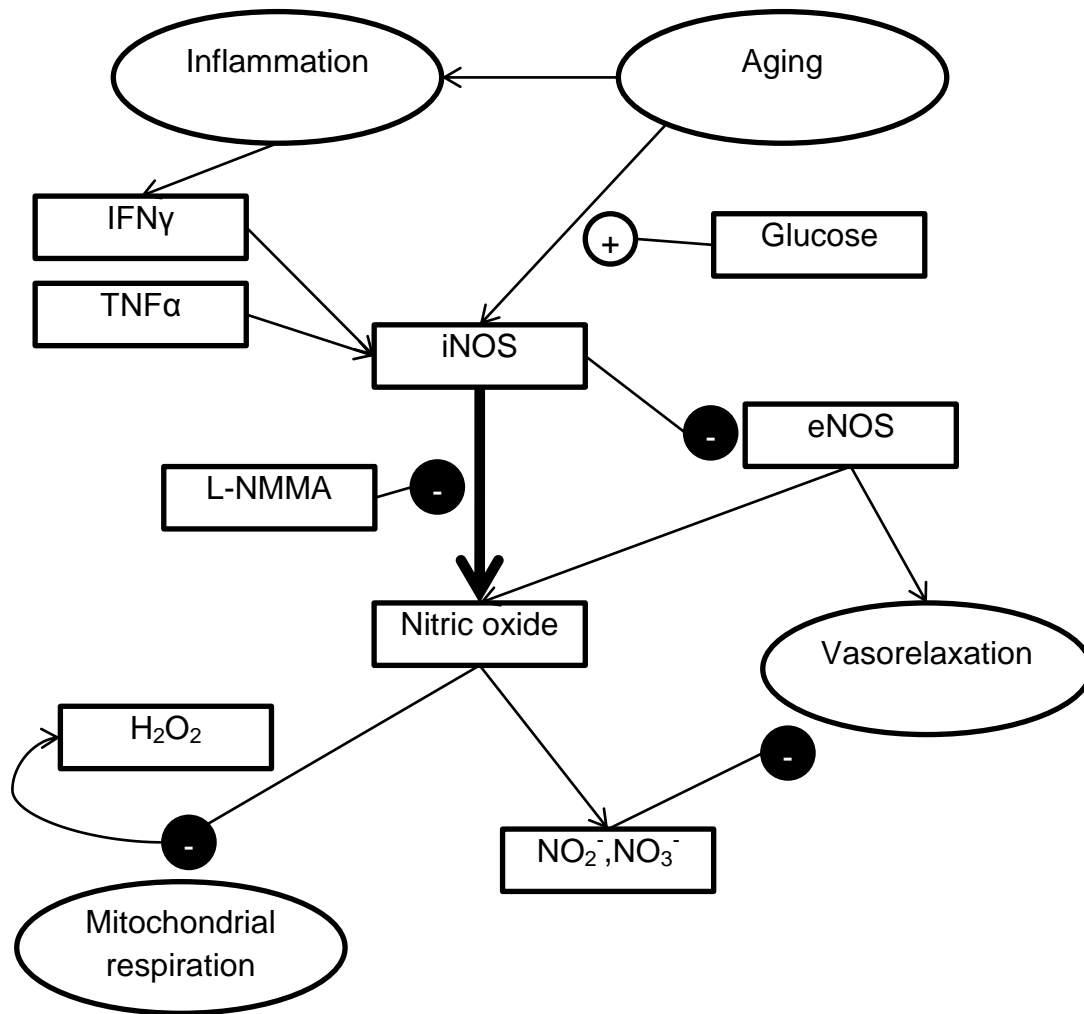


Figure 1.2.2-1: Schematic diagram of the interplay between inflammation, aging and nitric oxide generation.

Arrows and white circles with plus signs demonstrate increasing activity, filled circles with minus sign, inhibition.

Further associations between aging and iNOS have been elucidated. The p66^{shc} protein recognizes phosphorylated protein tyrosine residues and appears to aid in a PKC-β-mediated signalling cascade leading to apoptosis. PKC-β phosphorylates p66^{shc}, allowing it to enter mitochondriae. Pro-apoptotic signals then allow p66^{shc} to disassociate from a protein complex to become active. Active p66^{shc} causes a reduction in mitochondrial membrane potential, an increase in hydrogen peroxide production, opening of mitochondrial membrane pores and the release of pro-apoptotic proteins and finally apoptosis. Knock out of p66^{shc} leads to a reduction in iNOS expression in older mice, is associated with reduced ROS production and results in increases in longevity.⁹⁷ Moreover, p66^{shc} expression appears to be inversely related to SIRT1 expression.⁹⁸

p66^{shc} has been seen to have increased expression in elderly human subjects. The levels continue to increase, even in centenarians, suggesting a compensatory mechanism may have developed in humans capable of extremely advanced age.⁹⁹

Increased iNOS expression and activity has been shown to contribute to cardiac dysfunction and damage in the context of adrenergic stimulation in a model of cardiac ischaemia in aged versus young rats, an effect which was associated with increased nitric oxide and ONOO⁻ production.¹⁰⁰ The effect was avoided if the iNOS inhibitor 1400W was given prior to ischaemia. Similar effects have been observed in dogs.¹⁰¹

Wnt signalling is primarily involved in development and polarity in animal tissues. However, the Wnt pathway is also activated in tissues obtained from elderly animals. Microarray analysis of mammary arteries obtained from human subjects who were undergoing coronary artery bypass grafting revealed that Wnt signalling was more active in elderly subjects, compared to a middle-aged group. Vascular smooth muscle cells obtained from the more aged group showed increases in senescence-associated- β -galactosidase activity and were unable to proliferate in culture.¹⁰²

C1q (the initiating component of the classical complement pathway) and C3 (a key component of the alternative complement pathway) have long been known to increase in response to advancing age in humans.¹⁰³

More recently, Naito et al¹⁰⁴ describe a link between the Wnt signalling pathway, inflammation and aging. They elucidated a pathway involving Wnt activation by the complement component C1q. Activation of the Wnt pathway by C1 in their mouse model prevented regeneration of skeletal muscle.

Thus key elements of the inflammatory cascade interact with elements of developmental pathways, conspiring to bring about senescence.

The relevance of inflammation in our investigation is that it is a process likely to generate high concentrations of nitric oxide, potentially rendering the organism more susceptible to age-related phenotypes in recovering from severe sepsis. Alternatively, in the case of chronic inflammatory diseases, multiple pulses of higher nitric oxide concentrations could both reduce vascular reactivity and could lead to accumulated damage and senescence.

1.3.1 Deleterious effects of nitric oxide

Nitric oxide has a number of potential targets within cells. Soluble guanylate cyclase acts as a receptor for nitric oxide and mediates its action on smooth muscle relaxation in smooth muscle cells and many of the physiological actions of nitric oxide. Nitric oxide competes with O₂ in the electron transport chain and thereby inhibits respiration.^{105;106} The reduction in respiratory capacity may lead to an increased AMP:ATP ratio and thereby activate AMPK. The inhibition of mitochondrial respiration leads to an increase in superoxide generation and this in turn may cause toxic effects or activate defence mechanisms which may lead to senescence. Nitric oxide also acts via the Akt pathway and this may mediate some of its toxic effects and facilitate activation of constitutive eNOS to further increase

nitric oxide production in response to pathophysiological conditions such as anaphylaxis.⁸³ Nitric oxide has been shown to cause apoptosis via the MEK/HIF-1 α pathway.¹⁰⁷

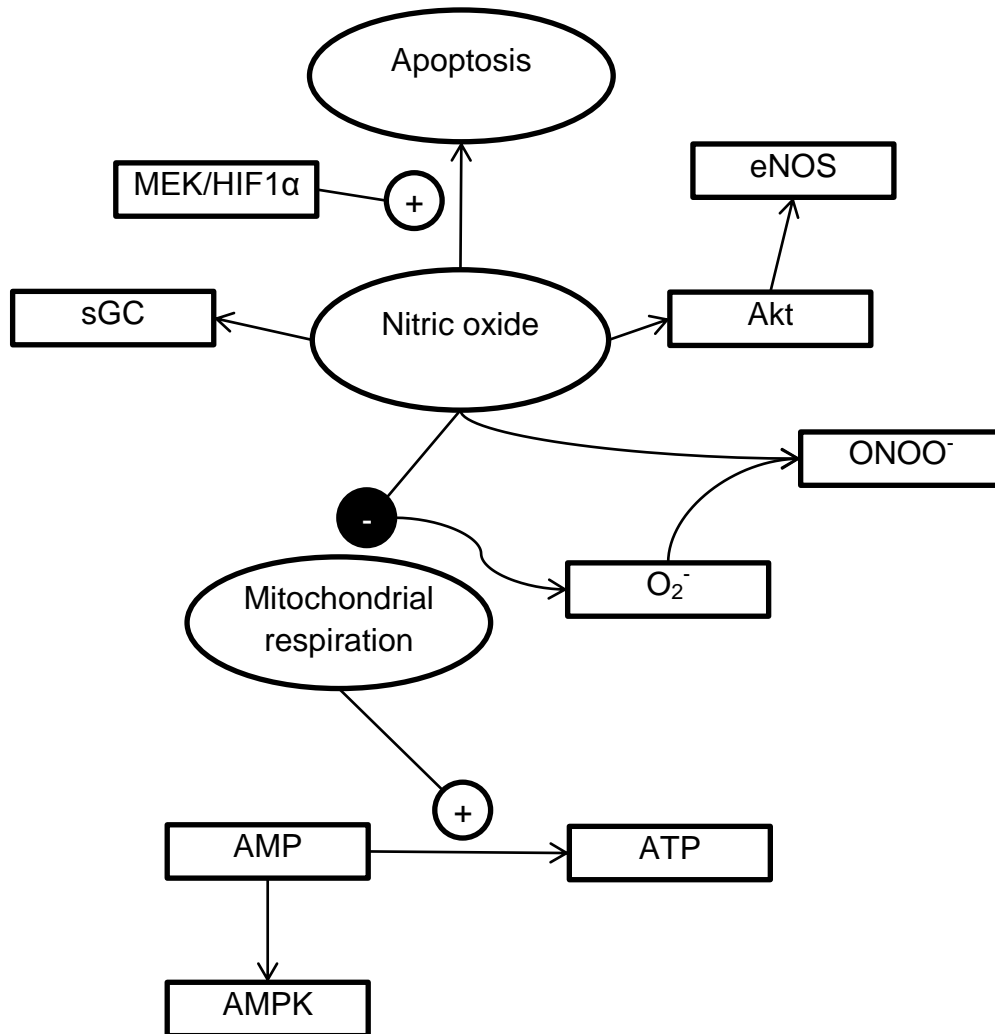


Figure 1.3.1-1: Schematic of the pathways by which nitric oxide could signal metabolic stress.

Investigating each of these potential pathways as a means to assessing the mechanism of potential roles of nitric oxide – as a protector and as a protagonist to senescence – could start with blocking the action of sGC using the synthetic compound ODQ. Heller et al¹⁰⁸ describe the observation that a number of exogenous sources of nitric oxide caused cell cycle arrest when nitric oxide was generated by the nitric oxide donors GSNO, SNAP and sodium nitroprusside at 1mM concentrations. However, cells recovered their replicative capacity as soon as the source of nitric oxide was removed. Investigating the mechanism of this phenomenon led them to investigate sGC as a potential target of the anti-mitogenic properties of nitric oxide. However, application of the specific sGC inhibitor, ODQ failed to prevent the anti-proliferative effect of nitric oxide. This was despite a clear

abolition of sGC activity at a concentration of 1 μ M. cGMP levels were measured to ensure ODQ had performed the desired inhibition of sGC and the ten-fold increase of cGMP seen in nitric oxide donor-exposed cells was completely abolished when cells were exposed to ODQ.

As stated above, eNOS is associated with a young phenotype and may play a role in maintenance of this phase. However, Erwin et al¹⁰⁹ have demonstrated that eNOS tends to be S-nitrosylated in vascular endothelial cells and that the nitrosylation determines its subcellular location in caveolae. Once released from this location, eNOS is exposed to a more reducing environment with glutathione able to denitrosylate the enzyme which in turn is thought to be able to increase its activity. Thus high local concentrations of nitric oxide could be used to negatively feedback on enzyme activity.

Van der Loo et al¹¹⁰ demonstrated an association between advancing age and protein transnitrosation in aging rats. They demonstrated that there is a high concentration of transnitrosated proteins, particularly in the vascular endothelium and the highest concentrations were seen in endothelial cell mitochondriae.

Therefore direct effects of nitric oxide on cells can be assessed by looking at soluble guanylate cyclase inhibition and protein transnitrosation.

1.4 Reactive oxygen and nitrogen species

Reactive nitrogen species can be generated from a variety of sources including many nitrites and nitrates – both dietary and pharmacological - but the most important source I consider here is nitric oxide via nitric oxide synthases. Nitric oxide is a highly reactive free radical which readily reacts with superoxide to form peroxynitrite. The source of superoxide is generally the mitochondrial production of O₂⁻ during oxidative phosphorylation. At low concentrations of nitric oxide and O₂⁻, nitric oxide may quench O₂⁻ but at higher concentrations, nitric oxide reacts with ubiquinol which receives the unpaired electron and readily donates it to oxygen to form the superoxide radical. Nitric oxide inhibits cytochrome c oxidase and also mitochondrial electron transport chain complex I causing an electron leak which increases superoxide formation. Superoxide readily reacts with nitric oxide to form peroxynitrite and this in turn, increases the electron leak to form the superoxide radical, thus increasing both substrates' concentration to form more peroxynitrite.¹¹¹

The relationship between ROS exposure and chronic oxidative stress was examined in healthy and atherosclerotic plaque vascular smooth muscle cells by the pulsed administration of 18-80mmol/L tert-butyl hydrogen peroxide by Matthews et al.³ They demonstrated a marked increase in vascular smooth muscle reactive oxygen species and consequently, an increase in senescence-associated β -galactosidase positive cells (11.9%, increasing to 55.5%). This increased p21^{WAF} but not p16^{INK4a} and had a negative effect on the activity of telomerase without decreasing telomere length.

Lener et al¹¹² describe the effect of knocking down expression of the NADPH oxidase 4 (Nox4), which they first determined was the dominant isoform in HUVEC. This led to a decrease in ROS production and reductions in oxidative DNA damage. This was also associated with increased cell proliferation rates and proliferative capacity, although the latter may have been due to transformation in one of the donor cell populations. There was continuing telomere erosion in both control cells and cells unable to express Nox4, appropriate to replicative age. As such, cells which did not express Nox4 were seen to replicate through more cell divisions and therefore had shorter telomeres.

Nitric oxide donors were used by Boriquel et al¹¹³ to investigate the effect of nitric oxide on cellular oxidative defences. A range of concentrations of DETA-NO were used to investigate their effect, up to 1mM. They settled on a concentration of 61µM. They observed that short term exposure to those concentrations of nitric oxide led to a reduction in expression of peroxisome proliferators-activated receptor γ (PPAR γ) cofactor 1- α (PGC-1 α) which in turn down-regulated the expression of many antioxidant defences, suggesting that nitric oxide initially acts as an antioxidant, or removes the signals to generate the antioxidant defence. However, as exposure times increased beyond 24hrs, the reverse became true and antioxidant defences were activated with increased expression of mRNA for MnSOD, catalase, thioredoxin, thioredoxin reductase and uncoupling protein-2. Downward regulation on short exposures was mediated via soluble guanylate cyclase as shown by inhibiting the effect using ODQ 1µM. However, no effect was seen on cell respiration despite a relatively high concentration of nitric oxide. The opposite effects were observed by using L-NAME to inhibit eNOS – short exposures led to upregulation of antioxidant defences and long exposures led to downregulation. In contrast, ectopic PGC-1 α expression was seen to up-regulate eNOS expression and to increase nitric oxide production. Whether this dual time-dependent effect of nitric oxide donors is of physiological relevance is uncertain as concentrations of nitric oxide were high. However, the effect was explained as a means of preconditioning the cell to an oxidative insult. Stage one involves a burst of nitric oxide which in turn reduces antioxidant capacity, allowing other reactive oxidant species to escape mitochondria and begin to generate a damage response. Thereafter, stage two leads to an increase in PGC-1 α and all that this entails – increased mitochondrial biogenesis and improved antioxidant defences, finally leading to increased expression of the protective eNOS.

1.5 Protein modifications involving nitric oxide

1.5.1 Metal centre interactions

Soluble guanylate cyclase and cytochrome c oxidase contain a haem moiety which acts as the target for nitric oxide's action. Nitric oxide is thought to activate soluble guanylate cyclase via inducing conformational change after binding to the haem site, allowing an increase in cGMP production and the resultant vasodilation in vascular

cells. In contrast, an inhibiting interaction occurs when nitric oxide induces conformation change by binding in the haem moiety of cytochrome c oxidase, the terminal enzyme in the electron transport chain.

1.5.2 Protein transnitrosation

This process describes the nitrosative modification of thiol residues in cysteine within proteins. Reviewed in Gödecke et al¹¹⁴ and Gow et al,¹¹⁵ protein transnitrosation is postulated as most likely to occur between nitrosylated proteins or via the nitrosonium ion (NO^+) reacting with reduced thiol residues rather than spontaneous interactions with nitric oxide itself. Nitrosonium ions are formed via nitric oxide reacting with itself or oxygen to form N_2O_3 and N_2O_4 which is a slow reaction in physiological ranges of nitric oxide concentration.

The reaction can be catalysed by iron or copper ions (Cu(I)), although the most available source of the former is haemoglobin and the latter, caeruloplasmin, neither of which are present in vascular cells. Reduced glutathione and cytochrome c oxidase do however, bind copper ions. Copper zinc superoxide dismutase has a higher affinity for copper ions than glutathione or cytochrome c oxidase and this is the likely site for most intracellular Cu(I) -catalysed reactions with glutathione acting as a store.¹¹⁶ Conditions which make transnitrosation of proteins more likely include the sequence of amino acids before and after the cysteine residue and the 3-D structure of the protein where the cysteine lies, in particular whether the cysteine is in an exposed part of the molecule. This is discussed later in chapter 5.¹¹⁷

1.5.3 Tyrosine nitration

Protein and peptide tyrosine residues are vulnerable to a number of modifications including targeted phosphorylation and also nitration. The nitration of tyrosine residues has been shown to have both an enzymatic dependent and a simpler, chemical mechanism. Myeloperoxidase, myoglobin, manganese superoxide dismutase and cytochrome P-450 are capable catalysts which promote the formation of tyrosine nitrate residues in the presence of nitrates or nitrites. One of the products of the reaction of carbon dioxide and peroxynitrite, nitroso-peroxocarbonate, also readily leads to tyrosine nitration. Nitration of a tyrosine which forms part of MnSOD is associated with a reduction in function and has been observed in the mitochondria of aging rat vasculature.^{118,119}

Tyrosine nitration has also been shown to behave as a biomarker for atherosclerosis. Shishehbor et al¹²⁰ report that circulating protein tyrosine nitration is an independent risk marker for the presence of atherosclerotic disease. They also demonstrated decreased levels of protein nitration when subjects were treated with an HMG Co-A reductase inhibitor (atorvastatin), postulating that this may account for some of the beneficial effects of statin therapy.

1.5.4 Transnitrosation as nitric oxide store

The pre-addition of low doses of GSNO (1 μ M) has been shown to cause persistent hyporeactivity to phenylephrine-induced contraction of angiotensin-stressed rat aortic rings without endothelium. The authors demonstrate that this is likely to be due to nitric oxide release from transnitrosated proteins which act as a store of nitric oxide, perhaps in the form of a nitrosated carrier, such as glutathione. In aortic rings with endothelium, the hyporeactive effect was less pronounced where there was endogenous nitric oxide generation as proven by subsequent nitric oxide synthase inhibition.

Authors Sarr et al¹²¹ describe the above phenomenon and demonstrate that aortic rings in these conditions have increased cysteine-nitric oxide residue formation and that NAC 1mM is able to cause relaxation in these rings. They postulate that NAC is able to release the nitric oxide stored in cysteine-nitric oxide residues and thereby nitric oxide is free to act as a vasorelaxor. Cells pre-exposed to GSNO also showed a decrease in angiotensin-induced superoxide staining, measured by DHE fluorescence. Thus, low concentrations of exogenously-supplied nitric oxide led to the formation of a sink of nitric oxide in cells which could be mobilised to protect against vasoconstriction and potentially acted to decrease oxidative stress. The difference was not seen in cells which had functioning endothelial nitric oxide synthase, suggesting that basal eNOS regulates nitric oxide levels both by nitric oxide formation and by influencing the rate of release from stores.

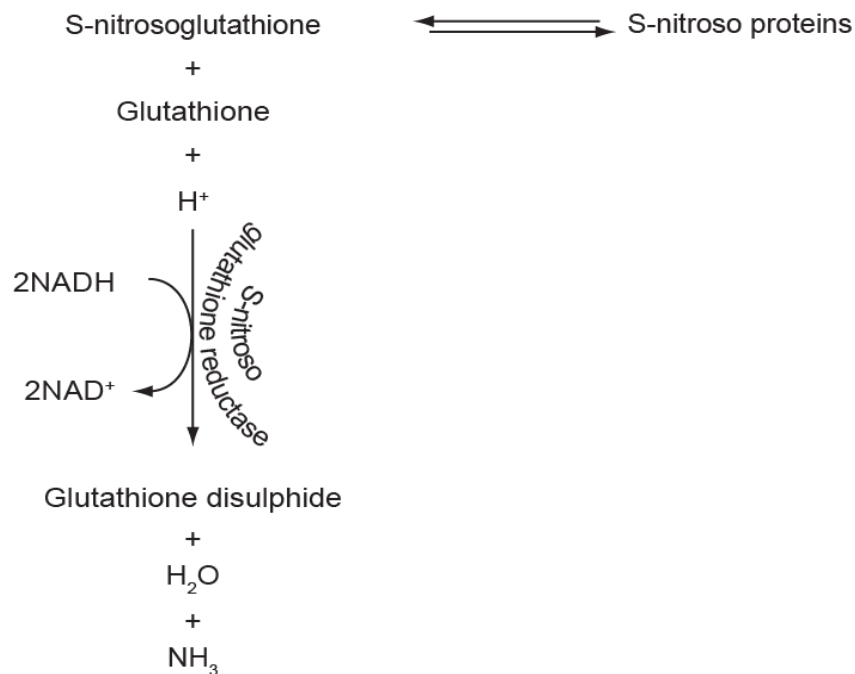
1.6 Antioxidants

A number of vitamins and other chemicals have been assessed for their beneficial effects in disease and *in vitro*. The free radical theory of ageing supports the idea that antioxidants ought to prevent or delay the deleterious effects of accumulating oxidative damage. However, attempts to confirm that this effect could be translated to the *in vivo* situation, particularly in cardiovascular disease have proved unsuccessful. This blunt observation would seem to suggest that the free radical hypothesis may not be valid but there are a number of reasons to retain the theory. Firstly, as we have already discussed, nitric oxide is required as a part of normal signalling and this includes the increased production of other reactive oxygen and nitrogen species; thus interference with this may promote disease in healthy systems. Secondly, the antioxidants used may not be active against the molecules causing the most damage and therefore it is important to investigate the effect of antioxidants at a cellular level and against the different reactive species. Thirdly, ensuring an adequate concentration of antioxidant where it is needed may not be possible via systemic non-targeted administration. Loss of the reducing potential of antioxidants could result from oxidation by oxidants involved in tissues and blood during normal signalling and function well before they were able to reach areas of high oxidative stress.

1.6.1 N-acetyl cysteine

N-acetyl cysteine (NAC) is a glutathione precursor which adds to the glutathione pool. The action of NAC on hepatocytes has been widely investigated as it is an effective treatment for paracetamol overdose which depletes the glutathione pool and can lead to fulminant hepatic failure. The damage caused by glutathione depletion is thought to be free radical mediated.¹²²

Glutathione is used to regulate the amount of bioavailable nitric oxide and as a pool of S-nitroso groups by forming S-nitrosoglutathione. This pool is dependent on the amount of glutathione and the activity of the enzyme S-nitrosoglutathione reductase and is in equilibrium with the amount of transnitrosated protein. Thus glutathione depletion could result as a consequence of an increase in the amount of S-nitrosoglutathione and therefore S-nitroso-proteins.



NAC also directly reduces the production of nitric oxide and also the amount of iNOS produced in cells in response to the inflammatory cytokines IL1- β and TNF α .¹²³ This effect can be reversed by thioredoxin which acts via denitrosylating iNOS and has anti-apoptotic effects. Thioredoxin itself is modified by two transnitrosations, one activating and the second, blocking its activity.

The reduction in nitric oxide concentration and synthesis by glutathione may therefore be important in reducing the toxic effect of paracetamol. Glutathione will reduce superoxide production by nitric oxide and decrease the availability of nitric oxide to form reactive nitrogen species and protein transnitrosation. However, the opposite effect has been seen in vascular smooth muscle cells with an increase in iNOS expression and nitric oxide generation in cells treated with IL-1 β and NAC compared to IL-1 β alone.¹²⁴

Nitric oxide has also been reported to reduce IL-1 β activity. There appear to be two steps in the effect - first there is an increase in ROS production, then this causes protein oxidation of downstream phosphatases. If NAC reduces nitric oxide levels, this mechanism would increase IL-1 β activity which could further induce iNOS synthesis and further increase the rate of nitric oxide production.

This complex picture may help to provide an explanation of one of the central inconsistencies with the research into nitric oxide and senescence. The beneficial effects of nitric oxide reported by Vasa et al¹²⁵ and Hayashi et al⁶³ was observed in healthy and relatively young cells whereas the high levels of nitric oxide which may be induced by a cytokine mix and iNOS may help to explain the expected deleterious effects of nitric oxide at a higher concentration. Other groups have contradicted or been unable to reproduce these findings. Members of the same group could not replicate the decrease in telomerase activity postulated to be due to nitric oxide synthase inhibition, nor could they demonstrate the effect of nitric oxide donor-induced decreases in telomerase in endothelial progenitor cells.^{126;127} This was stated in the Vasa et al paper to be a possible mechanism behind nitric oxide protection against senescence. Moreover, data from our group (Trivier unpublished) suggests a dose-dependent nitric oxide-mediated decrease in telomerase activity.

If we assumed the primary task of an inflammatory response was to combat infection, the cytotoxic effects of high dose nitric oxide are desirable to aid clearing infection and a senescent response in neighbouring cells in preference to apoptosis may allow structures to maintain their integrity while perhaps lacking some of their more refined functions.

1.6.2 Uric acid

Uric acid is present in serum of normal adults at a concentration range of 120-420 μ M and higher than normal levels have been linked to an increased risk of cardiovascular disease. However, the mechanism of increasing risk is uncertain and it is surprising given the potential benefits of uric acid with respect to lowering oxidative and nitrosative stress. Despite this, uric acid levels are increased in severe septic illnesses and higher levels are associated with an increase in mortality in patients with severe sepsis.¹²⁸ Uric acid accounts for an overall increase in serum antioxidant capacity when measured in patients with sepsis, a phenomenon which may represent a response to the increased oxidative stress of such illnesses or may be a bystander effect more indicative of renal dysfunction or increased cell turnover.

In cell-free assays, uric acid acts as a peroxynitrite scavenger at concentrations well below those seen in serum at an IC₅₀ of 13 μ M but also acts as a hydroxyl scavenger at a higher IC₅₀ of 134 μ M.¹²⁹ In this higher concentration range, uric acid has been observed to prevent apoptosis induced by nitric oxide released by DETA-NO at a concentration of 1mM in hypoxic endothelial cells.¹³⁰ Thus the hydroxyl effect may be more *important in vivo* than the peroxynitrite scavenging ability. Uric acid, at an *in*

in vitro concentration of 100µM, also acts on anti-proliferative pathways in renal tubular cells on NF-κB and p38MAPK.¹³¹ Uric acid at a concentration of 50µM was found to be a potent antagonist to the formation of S-nitrosyl tyrosine in response to endothelial cell shear stress, a stimulant to eNOS-mediated nitric oxide production. This effect was obviated by the addition of L-NMMA, a non-specific antagonist to nitric oxide formation by nitric oxide synthases.⁶⁰

The chemical interactions between nitric oxide and uric acid are complex. Uric acid been thought of as an antioxidant as it is able to react with superoxide, peroxyntirite, hydrogen peroxide and the hydroxyl radical.^{132;133} However, in anaerobic cell-free systems, the reaction of uric acid with nitric oxide leads to decomposition and formation of free radicals such as the aminocarbonyl radical.¹³⁴ The formation of aminocarbonyl was unhindered by adding substances thought to cause oxidative stress, peroxyntirite and hydrogen peroxide. The reaction could be partially prevented by the addition of antioxidants, especially glutathione.

In the presence of oxygen, the reaction between uric acid and nitric oxide leads to a nitrosated form of uric acid, designated UA-NO. This in turn is capable of reacting with glutathione to form GSNO and restores uric acid to its original form.¹³⁵ Thus the theory is advanced that UA is able to act as a carrier molecule for nitric oxide, which can then nitrosate other target molecules at a site distant to its manufacture. Suzuki, who investigated the formation of UA-NO from the mixture of UA and nitric oxide in a cell-free *in vitro* experiment, later repeated the experiment in the presence of human serum and urine with similar consequences, albeit at less efficient levels due to the presence of ascorbic acid and glutathione in those fluids. Uric acid was consumed by peroxyntirite, but the product of the reaction was not UA-NO. Previous investigations had revealed that the products of the reaction between UA and peroxyntirite were rather allantoin and other oxidation products including triuret. Skinner et al¹³⁶ described the readiness with which uric acid both oxidized and nitrosated peroxyntirite. The nitrosated product was able to act as a vasodilator in endothelium-denuded arteries and this was shown to be due to the spontaneous release of nitric oxide. Cysteine and glutathione were ineffective in increasing the release of nitric oxide, but light significantly decreased the half-life of the nitrosated uric acid.

Uric acid acts as a scavenger of peroxyntirite but this is not in a direct way owing to substrate competition with carbon dioxide. However, some of the products of the reactions between peroxyntirite and carbon dioxide are amenable to scavenging and in particular, uric acid seems to be able to scavenge the most potentially damaging products, the CO_3^- and nitrogen dioxide radicals.¹³⁷

Transnitrosation of cysteine residues is readily reversed with liberation of nitric oxide but tyrosine residues are readily nitrated by peroxyntirite and there are a number of potential protein targets which may be regulated in this way. For instance, manganese superoxide dismutase is inactivated in this way in transplant-rejected kidney. *In vivo*, peroxyntirite reacts readily with carbon dioxide to form the carbonate

and nitrogen dioxide radicals and these can nitrate tyrosine. The reaction of tyrosine nitration by peroxynitrite is more efficient than nitration by nitric oxide, where nitric oxide is relatively inefficient. Teng et al¹³⁸ investigated this phenomenon in brain and heart homogenates from rats. Investigating under anaerobic conditions, they found tyrosine nitration by the addition of peroxynitrite was significantly reduced in the heart homogenates. They demonstrated that this was due to the presence of uric acid by using uricase to remove uric acid from the heart homogenate. The addition of uricase, which allows conversion of uric acid to allantoin, allowed tyrosine nitration to take place.

The increases in such radicals may help explain why high serum urate levels are associated with many age and inflammatory-related conditions.^{139;140;140} Uric acid interacts with vascular smooth muscle cells *in vitro* by acting to promote replication and by increasing oxidative stress.¹⁴¹ Furthermore, reduction in serum urate levels by the xanthine oxidase inhibitor allopurinol is a useful vasodilator treatment for coronary artery disease induced angina, perhaps by preventing the interaction between nitric oxide and uric acid and by reducing the generation of O_2^- .¹⁴²

1.6.3 Selenomethionine

Selenomethionine is a potent peroxynitrite scavenger and also prevents protein nitration at higher concentrations. It is more effective than methionine and acts in concert with glutathione which aids its cycling between its reduced and oxidized forms, a reaction catalysed by glutathione peroxidase. Serum levels have been observed in the range of 0.3 μ M but higher concentrations have been shown to be more effective antioxidants in chemical studies. We chose to investigate the effect of a 30 μ M concentration as this afforded most of the effect on peroxynitrite scavenging and approached the IC_{50} for prevention of protein nitration (50 μ M).^{143;144}

1.7 Bioenergetic crisis and senescence

1.7.1 Autophagy and aging

Autophagy plays an important role in normal cellular metabolism and its dysfunction leads to some of the features seen in ageing cells. Autophagy describes the process of cellular removal of cytoplasmic waste products. The first step in the autophagy process is the formation of a membrane followed by engulfment of the waste product within this membrane (the membranous *phagophore* becomes an *autophagosome* when it engulfs its targeted waste substance). Later there is presentation to the lysosome which then becomes an *autophagolysosome* for final degradation of the waste product. This digestive process is cyclical and release of the end products can be a means of recycling dysfunctional molecules and also can be useful if the cell lacks external energy sources and is forced to enter a catabolic state.¹⁴⁵

The autophagy response to energy depletion is mediated by multiple pathways, suggesting this is an important function. Mammalian target of rapamycin (mTOR) is

the main autophagy-preventing molecule in humans. As one may expect, to allow catabolic conditions to make use of autophagy as an energy source, mTOR is effectively inhibited in starvation. The converse happens when insulin-like growth factor (IGF) is secreted in times of energy availability. IGF acts via insulin-like growth factor receptors which activate Akt which indirectly inhibits autophagy via activating mTOR.

Many drugs are known to affect the autophagy process. Hundeshagen et al¹⁴⁶ performed a screen of many drugs commonly used in cardiology and oncology to assess the effect on autophagy. In addition to using rapamycin as a known autophagy inducer and bafilomycin as its antithesis, they discovered that cardiac glycosides (e.g. digoxin) are potent autophagy inducers. They are joined in the group by other beneficial cardiac drugs, such as the aldosterone antagonist, spironolactone and the antiplatelet drug, ticlopidine. Flavonoids such as resveratrol were inducers. However, many cardiotoxic drugs used in oncology such as doxorubicin were also seen to induce autophagy, although this may have been a secondary effect due to cytotoxicity increasing the demand for autophagy.

Drugs which inhibit autophagy included the corticosteroids and the anti-inflammatory drug colchicine. During nutrition deprivation, cells inhibit mTOR and autophagy increases via phospho-inositol 3 kinases. The PI3K inhibitor, wortmannin was observed only to inhibit autophagy in conditions of nutrition deprivation, in contrast to bafilomycin which was capable of autophagy inhibition in all conditions.

AMPK plays a direct role in stimulating autophagy when energy depletion (which activates AMPK by increasing AMP:ATP ratios) results in its activation.¹⁴⁷ Sirtuin 1 (SIRT1) encourages autophagy and levels fall in metabolic syndrome, with a corresponding reduction in autophagy.¹⁴⁸

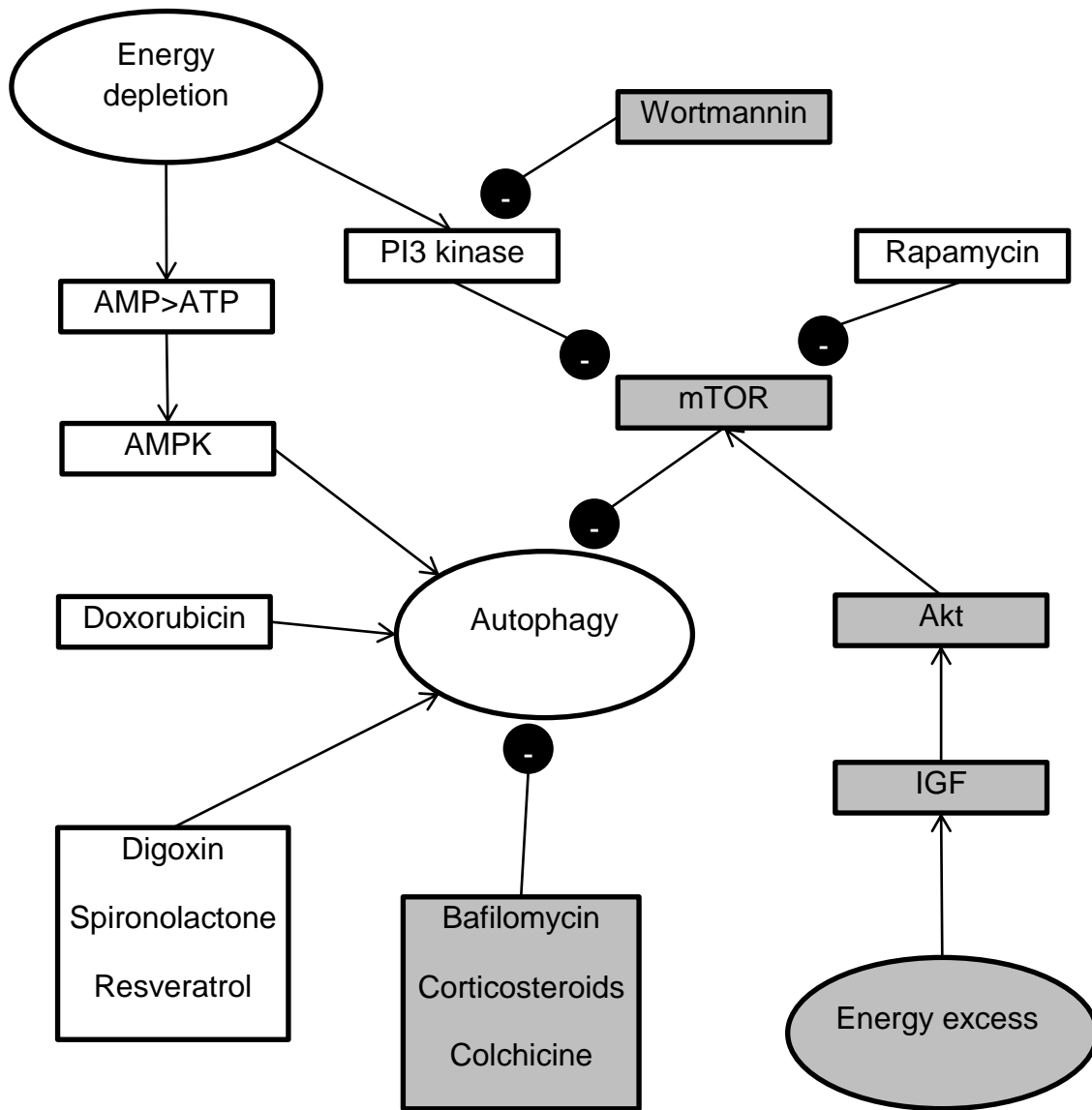


Figure 1.7.1-1: Schematic diagram of processes and drugs influencing autophagy.

Shaded objects represent a net negative effect on autophagy. Arrows demonstrate increasing activity, filled circles with minus sign, inhibition.

The importance of autophagy in clearing potential toxins and thus avoiding cellular transformation is suggested by the complex interactions with tumour suppressor, p53. Extremes of p53 function modify autophagy - increasing p53 activity is able to both increase and decrease autophagy. Increasing p53 activity increases mTOR activity via AMPK activation by increasing Akt. However, p53 increases are also able to decrease autophagy by activating *phosphatase and tensin homology* (PTEN) which decreases Akt activity and TSC. Inhibition of p53 activity also increases autophagy.^{149;150}

Mutations in genes which encode other proteins involved in permitting autophagy seen in yeasts are associated with premature aging phenotypes.¹⁵¹

Autophagy has therefore been associated with increases in longevity, which may occur via a number of potential processes, including an improvement in cell hormesis (for example as seen in ischaemic preconditioning), this describes a process whereby cells survive a sub-lethal insult, triggering an autophagy-led clear up of damaged proteins and organelles, such that the remaining organelles have an aggregated improved efficiency and the cell as a whole is able to survive greater insults in the near future.¹⁵² However, it has also been implicated in the avoidance of cellular senescence. PTEN loss-induced cellular senescence (PICS) requires mTOR activation to exert its effect. This will lead to a reduction in autophagy which suggests a role for autophagy in the maintenance of a young cellular phenotype.^{153;154} In addition, inducible p21-induced cellular senescence can be avoided by exposing cells to rapamycin, the mTOR inhibitor which could be expected to aid the autophagic process.¹⁵⁵

Senescence without a DNA damage response can occur when the tumour suppressor phosphatase and tensin homologue (PTEN) is lost. PTEN is a protein tyrosine phosphatase which itself acts via pro-growth and pro-survival kinases. Loss-of-function mutations in PTEN can cause multiple benign tumours (hamartomas). Cells within hamartomas tend to display a high degree of senescence. In a PTEN knock down model, increased senescence was seen and this could be overcome by inhibiting the action of the mammalian target of rapamycin (mTOR) with rapamycin.^{42;153}

PTEN also indirectly affects the ability of p66^{shc} to increase ROS and to trigger apoptosis. By acting via PINK1 (PTEN-induced kinase), PTEN prevents the activation (phosphorylation) of p66^{shc}. Fibroblasts from a patient suffering from the hamartoma-associated loss-of-function PTEN mutation showed an increase in phosphorylated p66^{shc}.¹⁵⁶

Caloric restriction promotes longevity and autophagy. There is some evidence that the two are correlated in a causal manner as inhibition of autophagy-associated proteins is able to prevent the gain in longevity normally associated with caloric restriction. Caloric restriction acts via AMPK or SIRT1 which are able to detect the relative lack of available energy.¹⁵⁷⁻¹⁵⁹ As mentioned above, IGF inhibits autophagy. The effect of IGF was investigated in *C. elegans* and it was seen that inhibiting the IGF pathway was able to cause an increase in longevity. This effect appeared to be due to autophagy as reduced expression of autophagy associated proteins was associated with a loss of the effect on longevity.¹⁶⁰ This effect was seen in mammalian species and human cells.

While measurement of the degree of autophagy taking place and its activity relative to what is required for a given situation is not directly available, modification of the process is possible pharmacologically. One is able to increase autophagic activity using either rapamycin to inhibit mTOR or AICAR to activate AMP kinase. Subsequent effects on the degree of cellular senescence in response to a given

stressors allow some estimation of the degree of senescence which can be avoided by improving the autophagic response.

1.7.2 AMP kinase and cellular senescence

AMP kinase is a central co-ordinator of the cellular response to metabolic stress and acts as a switch from synthetic processes to energy production in times of increased demand for fuel. The main signal for AMP kinase activation is a fall in ATP levels in comparison to AMP. AMP kinase is a heterotrimer which requires phosphorylation for activation. AMP is able to bind to AMP kinase locking it in a shape which is unfavourable for de-phosphorylation and inducing a favourable change in the arrangement of the 3 subunits; α , β and γ , increasing the activity of the kinase.

Phosphorylation of AMP kinase is mediated by LKB1 and the calmodulin-dependent kinase kinases (and therefore by increasing intracellular calcium).^{161;162} Hardie et al demonstrated that many drugs and toxins which activate AMP kinase depend on inhibition of the electron transport chain and synthesis of ATP. The consequential increase in AMP:ATP ratio which activates AMP kinase requires the γ subunit of AMP kinase to have an AMP binding site. When AMP binds to the AMP binding site, it encourages the γ subunit to reveal the catalytic (α) subunit to the targets for phosphorylation. Examples of drugs able to act in this manner include metformin and troglitazone (oral hypoglycaemic drugs) and resveratrol. AICAR also requires the AMP binding site, but did not require inhibition of the electron transport chain as its metabolite is an AMP mimetic, able to bind to the AMP site. Hydrogen peroxide was also only able to activate AMP kinase when the AMP binding site was available, also by inhibiting the electron transport chain. However, CaMKK-dependent activation of AMP kinase did not require the AMP binding site, as demonstrated by the action of the calcium ionophore A23187.¹⁶³

AMPK activity has been shown to increase with advancing organismal age in response to hypoxic stress.¹⁶⁴ AMPK is activated by the tumour suppressor gene LKB1 and this is also responsive to the effects of AICAR. LKB1 activation confers an anti-apoptotic effect and we postulated this could in turn allow cells posed with excessive bioenergetic or oxidative stress to be able to choose senescence instead of apoptosis.¹⁶⁵

Zu et al link senescence, SIRT1, LKB1 and AMP kinase activation. By using porcine aortic endothelial cells and culturing them to a pre-senescent state, they analysed old versus young cells and separately, the effect that constitutive expression or knock down of SIRT1 would have on levels and activity of LKB1 and phosphorylation of AMP kinase. As before, up-regulation of SIRT1 was able to prevent senescence and promote proliferation. This was accompanied by an inverse correlation in the activities of LKB1 and AMP kinase. However, expression of a SIRT1 mutant protein which had loss-of-function led to increased levels of phosphorylated AMP kinase and LKB1, leading to senescence. Interestingly, they postulate that the pro-senescent

effect of LKB1 is mediated by increasing AMP kinase activity and they supported this using AICAR, the AMP analogue to demonstrate a marked increase in senescence-associated β -galactosidase staining (approx. 5-fold increase in percentage of senescent cells).¹⁶⁶

However, these findings were to a certain extent contraindicated by the following work.

AMP kinase was shown to activate eNOS by phosphorylation by Morrow et al. It was also found to act as a protector against oxidative stress and prevents vascular smooth muscle cell proliferation.¹⁶⁷⁻¹⁶⁹ eNOS phosphorylation by AMP kinase activation was demonstrated by exposing human aortic endothelial cells to the AMP analogue, AICAR. The increase in eNOS phosphorylation led to increased nitric oxide generation. The effect was associated with phosphorylation of protein kinase B but, crucially, was not seen in cells without the ability to express the α 1 catalytic subunit of AMP kinase. The effect of AMP kinase on protection against oxidative stress-induced cell death required prolonged (20h) AMP kinase activation prior to the oxidant; in this case, hydrogen peroxide *in vitro* and angiotensin II or lipopolysaccharide *in vivo*. This was seen with either AICAR or metformin-induced AMP kinase activation. In this model, H₂O₂ reduced mitochondrial membrane potential and this was prevented by both metformin and AICAR. The metformin effect seen is in contrast to papers published by Hawley et al¹⁶³ and El-Mir et al¹⁷⁰ whereby in the absence of an oxidative stressor, metformin is seen to inhibit the activity of complex I of the electron transport chain, an action observed to reduce the mitochondrial membrane potential. However, in the context of an insult mediated by hydrogen peroxide, AMP kinase activation was observed to prevent the cell death signal mediated by c-Jun N-terminal kinase (JNK) activation. Chronic AMP kinase activation allowed signalling to result in increased mitochondrial synthesis and this led to resistance of cells to the oxidative stressor.¹⁶⁸

Krölller-Schön et al¹⁷¹ describe the effect of AMP kinase α 1 subunit knock out in mice and their response to exercise. Knocking out the α subunit renders the AMP kinase unresponsive to phosphorylative activation. Mice without a functional AMP kinase failed to demonstrate the benefits of exercise with respect to exercise-induced improvements in endothelial function. This effect was due to a lack of up-regulation and phosphorylation of eNOS seen in cells with functioning AMP kinase in response to exercise. In fact, this seemed to be consistent with a younger phenotype of endothelial cell in mice with functioning AMP kinase in response to exercise. Other effects seen were an increase in the activity of telomerase and reduced oxidative stress due to better antioxidant defences (haem oxygenase-1). In line with the younger phenotype, there were reductions in the expression of p53 and p16^{INK4a} and a reduced endothelial progenitor cell count and capacity for endothelial repair. The authors suggested that the effect of exercise on vascular function and vascular senescence were parallel mechanisms but a linear mechanism starting with decreased antioxidant defence, reduced telomerase activity and falling nitric oxide

bioavailability could equally give rise to a linear progression from failed AMP kinase response to cell stress and finally arriving at senescence.

AMP kinase is not uniform in all cell types. The $\alpha 1$ subunit is expressed in endothelial cells and both $\alpha 1$ and $\alpha 2$ subunits are expressed in liver, cardiomyocytes, and skeletal muscle. The $\alpha 2$ subunit is more responsive to bioenergetic stress than the $\alpha 1$ subunit.¹⁷²

Therefore we see a dichotomous response to AICAR with respect to senescence research between groups with the majority suggesting that AMP kinase activation by AICAR helps to maintain a young phenotype by protecting against oxidative stress, perhaps by increasing mitochondrial synthesis and mimicking energy crisis, activating a protective response and helping circumvent some aspects of the apoptotic response.

We therefore decided to investigate the influence of AMPK and autophagy on vascular cell senescence in general and in particular, its effect on cells exposed to oxidative and nitrosative stress.

1.8 New insights

1.8.1 Nitrosative stress

Chronic nitrosative stress has been observed in patients suffering from inflammatory bowel disease. Using tissue samples from human subjects, Sohn et al¹⁷³ found that nitrosative stress and a DNA-damage response-type senescence was due to macrophage accumulation. The degree of macrophage infiltration was then graded. Greater infiltration correlated with greater senescence markers. Coculture of fibroblasts with macrophages also induced senescence and this could be prevented by the addition of nitric oxide synthase inhibitors. Furthermore, in the absence of macrophages, fibroblast senescence could be induced using an exogenously-added nitric oxide donor.

There was a greater degree of senescence in patients who suffered one type of inflammatory bowel disease (Crohn's disease) versus the other (ulcerative colitis) and this appeared to correlate to an enhanced degree of iNOS in the colonic epithelium. A microRNA microarray analysis revealed that MiRNA-21 was associated with the development of senescence in both types of inflammatory bowel disease. Targets for MiRNA-21 include PTEN and TGF β 2 receptors, both of which are tumour suppressor genes and are mentioned previously.

MiRNA-21 has also been found to be up-regulated in a mice sepsis model. However, the expression of MiRNA-21 was unaffected in mice unable to express iNOS.¹⁷⁴ The effect could, however, be prevented by the addition of NAC. It may be that mice failing to express iNOS up-regulate other NOS isoforms in the context of sepsis. In this study, nitric oxide generation was not measured. In addition, MiRNA-29b was

up-regulated and MiRNA-29c down-regulated in wild type mice exposed to the septic stress and these changes were not observed in the iNOS knock-out mice. These MiRNA interact with tumour suppressors (preventing lung tumours and promoting acute myeloid leukaemia) and the pro-apoptotic factor VDAC (voltage-dependent anion channel) which is associated with increasing mitochondrial membrane permeability for cytochrome c, which is pro-apoptotic when released from mitochondriae.¹⁷⁵

The role of nitrosative stress in age-related diabetes was investigated after the observation that older mice have both a tendency to insulin resistance and increasing iNOS.¹⁷⁶ Using a model based on iNOS knock down and also the exposure of wild-type mice to increasing doses of GSNO as a nitric oxide donor, the authors demonstrated increasing insulin resistance was related to the ability to synthesise nitric oxide with iNOS, which increased with age in wild type mice. The effect could also be mimicked in younger wild type mice using the exogenous nitric oxide donor. Using the biotin switch method to detect protein transnitrosation, they demonstrated that the effect was associated with transnitrosation of several insulin signalling proteins (insulin receptor β , insulin receptor substrate S-1 and Akt).

1.8.2 Transnitrosation effects

Recent data have shown that glutathione-S-transferase can be subject to transnitrosation by GSNO at two cysteine sites. This impairs the function of the enzyme which acts as a significant detoxification enzyme and can prevent the pro-apoptotic action of c-Jun N-terminal kinase (JNK). One site, Cys⁴⁷ has a larger effect on enzymatic activity but more readily dissociates. The other, Cys¹⁰¹, is very stable and may therefore have an additional function as a means of storing or transferring nitric oxide.¹⁷⁷

The role of soluble guanylate cyclase (sGC) as a mediator of nitric oxide's action has been discussed but mainly as a means of a classical ligand-receptor model. Crassous et al¹⁷⁸ explored the effect of nitrosative stress on the enzyme and observed that not only is sGC susceptible to activation by S-nitrosylation by nitric oxide, it is also susceptible to transnitrosation and loss of activity by nitrosative stress. They provide evidence that this mechanism may play a part in the observed loss of vasorelaxation response to nitric oxide in angiotensin II-induced stress.

Another mechanism for transnitrosation-dependent control of enzymatic function has been described by Jandu et al.¹⁷⁹ Tissue transglutaminase is a predominantly cytosolic protein and appears to localise within cell walls when it is nitrosated. However, in the presence of nitric oxide synthase inhibitors, the enzyme is denitrosated and is able to translocate out of cells and assumes its active state. Conversely, any extracellular enzyme is depleted in the presence of increasing nitric oxide concentration, either with laminar shear stress on endothelial cells, the addition

of GSNO or coculture of smooth muscle cells with endothelial cells expressing eNOS.

1.8.3 Transnitrosation without increasing oxidative stress

S-nitrosated N-acetyl cysteine has been investigated as an agent with both antioxidant and pro-nitrosating agent.¹⁸⁰ In a murine model of left ventricular hypertrophy, S-nitrosated N-acetyl cysteine was found decrease superoxide and hydrogen peroxide generation and increase Gi-coupling and transnitrosation of the β -adrenoreceptor, making cells less responsive to catecholaminergic stimulation (a key driver to cardiac rhythm disturbance and heart failure). This had the combined effect of reducing apoptosis.

1.8.4 Genetic ablation of senescent cells

The evidence for a role of senescent cells in disease has been strengthened in a pro-geroid mouse model by selective ablation of cells which express p16^{INK4a}.¹⁸¹ In these mice, adipose, skeletal, muscular and cataract changes could be prevented if cells which attempted to express p16^{INK4a} were subjected to selective apoptosis by using a gene construct on the p16^{INK4a} promoter which allowed drug-induced apoptosis. There were no adverse effects from this loss of cells expressing p16^{INK4a} but equally, loss of vascular stiffness could not be prevented.

1.9 Conclusion

There are many phenotypical changes seen in cells which senesce and the significance of senescent cells in health and disease remains to be fully elucidated. Whilst senescent cells are clearly found in vascular cells of older individuals or in cases of repeated vascular injury, this may be a protective response to injury. However, the accumulation of senescent cells appears more likely to have a deleterious effect on vascular health as the secretory profile of senescent cells infers that they are active participants in disease states.

Controversy also existed as to the significance of culture-based replicative senescence, which is either identical to or at least very closely resembles the phenotype of cells found to senesce *in vivo*. The link between β -galactosidase and senescence is curious as it hadn't been shown to be a causal relationship.

Further conflicts as to the role of nitric oxide in protecting cells from senescence were prevalent in the literature when we embarked on this path of investigation. There were claims that some concentrations of nitric oxide were protective and a lack of nitric oxide encouraged cells to senesce. This finding was consistent with the hypothesis that endothelial cells which were younger possessed more functional eNOS than older vascular cells. This was a finding that other groups were unable to replicate.

If this could be replicated, what was the underlying pathway by which nitric oxide conferred protection against senescence and could nitric oxide also have deleterious effects?

1.10 Aims

1. Vascular cell senescence plays a role in health and disease. I will attempt to identify a means to readily identify senescent cells in culture.
2. Using a successful test, I will assess whether exogenously supplied and endogenously-produced nitric oxide exerts an effect on senescence.
 - a. I will investigate the features of cells which senesce, including its relation to autophagy and apoptosis.
3. If a nitric oxide-induced effect is observed, I will investigate the mechanism.
 - a. Does it relate to the generation or prevention of the formation of reactive oxygen species?
 - b. Is the effect mediated by soluble guanylate cyclase?
 - c. Is the effect due to metabolic stress?
 - d. Is the effect due to general toxicity and transnitrosation?
4. I will investigate the influence of metabolic stress on vascular cell senescence.

2 Methods

2.1 Primary cell culture

2.1.1 Human umbilical artery smooth muscle cells

2.1.1.1 Cell isolation

Equipment

Scalpel

2x tissue forceps

Fine scissors

McIlwain tissue chopper

Razor blade

1x 100mm tissue culture plate

50mL falcon tube

T-25 tissue culture flasks

Reagents

HBSS with no calcium, no magnesium, no phenol red (Gibco 14175-053).

Dissecting medium

DMEM (Invitrogen 41966-029)

10% foetal calf serum

20mM HEPES buffer

1% penicillin / streptomycin / amphotericin

Culture medium

DMEM (Invitrogen 41966-029)

20% foetal calf serum

1% penicillin / streptomycin / amphotericin

1% MEM Non-essential Amino Acids (100x) (Gibco 11140-035)

Trypsin/EDTA 0.05%, phenol red (Gibco 25300)

Trypsin neutralizing solution (Promocell TNS C-41100) (0.05 % trypsin inhibitor, 0.1% BSA)

Umbilical arteries were obtained after appropriate ethical approval and informed consent from mothers undergoing elective caesarean section at the Elizabeth Garrett Anderson Hospital, University College London Hospitals NHS Trust. Umbilical cords were collected after birth and placed in 50mL Falcon tubes with an amount of sterile Phosphate Buffered Saline (PBS) solution sufficient to submerge the cord. The cord was then taken to the laboratory for dissection.

Dissection was carried out using aseptic technique under sterile conditions in a laminar flow hood using standard vascular surgical instruments. Human umbilical arteries are present in pairs within the Wharton's jelly of the umbilical cord. Careful stripping of the jelly from the underlying vessels could almost always give a length of 5-10cm undamaged artery. This was then placed in dissecting medium until using the tissue chopper to create rings of vessel of around 1mm long. Rings of vessel were then placed in growth medium and plated on either T-25 flasks at 40 rings per flask, 6-well plates at 3 rings per well or 12 well plates with 1 ring per plate.

Outgrowth was seen after 1 week but it took at least 3 weeks to observe significant numbers of cells explanting from the rings. Medium was changed carefully at weekly intervals in order to avoid displacing adhered rings of artery. Cells were harvested by removing the ring of tissue and then washing twice in HBSS and adding trypsin/EDTA dissociation solution for 5-7 minutes. Flasks or plates were tapped gently to assist the cell detachment and cells were then aspirated with a 5mL pipette into a Falcon tube. Trypsin was neutralised using trypsin neutralizing solution, and cells were then counted using a variety of methods (see below section). Cells were replated at passage at 3500 cells/cm² and thereafter fed three times weekly until 80% confluent, when they were passaged again.

2.1.1.2 Confirming phenotype

Phenotype was confirmed primarily by morphology. Cells were fusiform and formed hill and valley whorls when approaching confluence.

Further confirmation was obtained using fluorescence microscopic visualization of cells grown on coverslips and stained with an antibody to smooth muscle actin or α -tubulin followed by a fluorescein or TRITC-conjugated secondary antibody as follows.

Equipment:

18mm glass coverslips

Standard 12-well tissue culture plates

Confocal microscope

Reagents:

Primary antibodies

Mouse monoclonal anti-smooth muscle actin antibody CGA7 (Santa Cruz sc-53015)

Rat monoclonal anti- α -tubulin antibody 3H3087 (Santa Cruz sc-69971)

Secondary antibodies

TRITC-conjugated goat anti-mouse antibody (Santa Cruz sc-3796)

FITC-conjugated goat anti-rat antibody (Santa Cruz sc-2011)

DAPI (Molecular Probes)

PBS (Invitrogen)

Paraformaldehyde prepared as described below (Sigma)

0.1% Tween-20

1% bovine serum albumin (Sigma)

All steps were carried out in 12 well tissue culture plates but with coverslips in the base of each well. Cells were not allowed to dry between steps. Culture medium was aspirated and coverslips were washed with 3 changes of 2 mL PBS at room temperature. Cells were fixed for 10 min at room temperature with 2 mL 4% paraformaldehyde (PFA) in PBS. Fixative was aspirated and coverslips were washed with 2 changes of 2 mL PBS at RT. Cells were post-fixed with 2 mL methanol (-20 °C) for 1 min at 4 °C. Methanol was aspirated and coverslips were washed with 2 changes of 2mL PBS / 0.1% Tween-20 at RT.

Coverslips were blocked overnight at 4°C with 1% BSA in PBS / 0.1 % Tween-20 (or blocked for 1hr at RT). Following blocking, slides were incubated with 0.25mL primary antibody at the appropriate dilution in PBS / 1%BSA / 0.1% Tween-20 for 1hr at RT in a humidified chamber. A parallel sample was incubated with diluent alone (blank sample). Primary antibodies were aspirated and coverslips were washed with 3 changes of 2 mL PBS / 0.1% Tween-20 at room temperature over 5 min. Slides were incubated with 0.25mL secondary fluorescent antibodies at the appropriate dilution in PBS / 1% BSA / 0.1% Tween-20 for 1hr at room temperature in the humidified chamber and in a dark room (or overnight at 4°C). Secondary antibody was aspirated and coverslips were washed at room temperature over 5 min with two changes of 2mL PBS / 0.1% Tween-20 and once with PBS. Coverslips were removed from the wells, wiped dry, and mounted onto a microscope slide with 20 μ l DAPI/Vectashield and sealed with nail varnish.

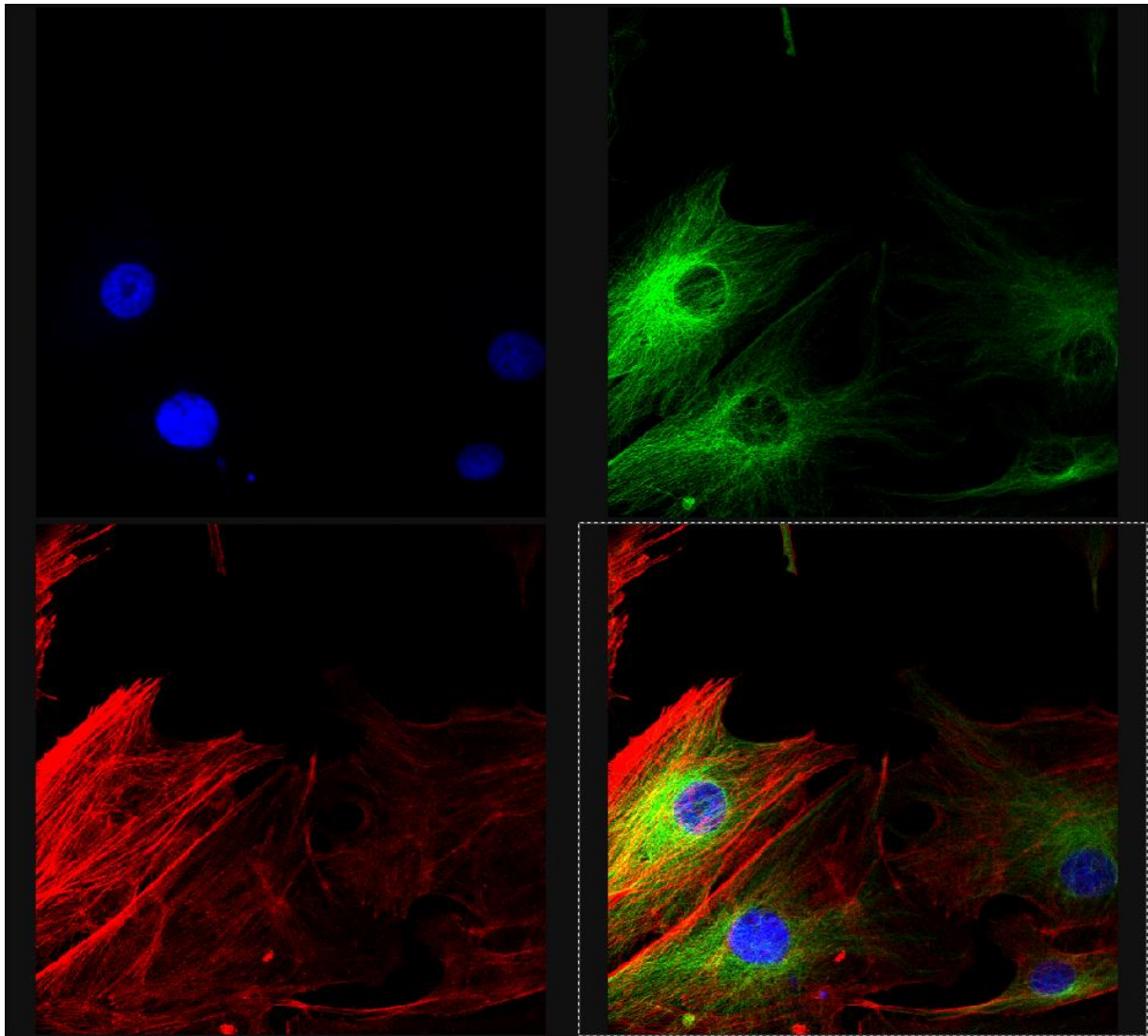


Figure 2.1.1-1: Fluorescence microscopy of explanted smooth muscle cells.

The above figure shows DAPI nuclear staining (top left panel), FITC-conjugated α -tubulin staining (top right panel), TRITC-conjugated smooth muscle actin staining (bottom left panel) and a composite image in the bottom right panel. Performed with assistance from Neale Foxwell, Wolfson Institute of Biomedical Research (UCL).

2.1.2 Human umbilical vein endothelial cells

First passage single donor endothelial cells were purchased from Promocell and cultured in EGM-2 (Cambrex or Promocell) made with EBM containing 2% FBS and EGM-2 BulletKit (CC-3162) consisting of hEGF, hydrocortisone, GA-1000 (Gentamicin and Amphotericin-B), VEGF, hFGF-B, R3 -IGF-1, ascorbic acid and heparin as supplied by the manufacturer.

At passage, cells were washed twice in PBS and trypsin / EDTA 0.05% was used to dissociate the cells from the bottom of the tissue culture plate. 0.5mL was used in the case of 6-well plates and the amount was adjusted per growth surface area if using alternatively-sized plates or flasks. An equal volume of trypsin neutralizing

solution was used at the end of dissociation before counting cells by haemocytometer or Coulter particle analyser. Cells were reseeded at 3500 cells/cm².

2.1.3 Freezing and thawing cells

For freezing, VSMC or HUVEC from one 75 cm² flask were trypsinised, spun down and resuspended in ice-cold freezing medium (1.1 mL DMSO, 8 mL DMEM, 2 mL foetal calf serum). 1 mL aliquots were frozen in cryovials first at -20°C for one day, then at -80°C overnight before long term storage at -196°C in liquid nitrogen. For thawing, cells were warmed to 37°C and immediately dissolved in pre-warmed culture medium. After resuspension, cells were placed in culture medium and placed in a 75 cm² flask.

2.2 Counting cells

Cells were counted by two separate methods.

2.2.1 Trypan blue cell counting

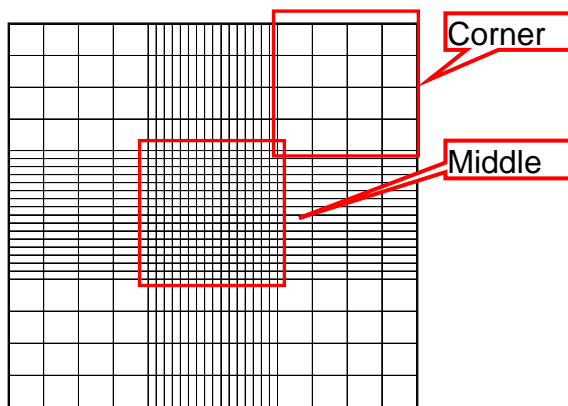


Figure 2.2.1-1: Haemocytometer design.

Representation of a haemocytometer with differing sizes of squares to allow counting of particles of different sizes and number.

Trypan blue is taken up by dead cells but not viable cells. Cells exposed to Trypan blue for extended periods of time, may begin to take up dye, even if they are viable.

Reagents

Trypan blue solution 0.4% (Gibco 15250-061)

Hanks' balanced salt solution, no phenol red (HBSS) (Gibco 14025-050)

0.5mL trypan blue solution was transferred to a 12x75mm test tube and 0.3mL HBSS was added to 0.2mL cell suspension (dilution factor of 5) and mixed thoroughly. The suspension was allowed to stand for 5-15 minutes. With a coverslip in place, a small amount of cell suspension (about 10 microliter) was transferred to both chambers of the haemocytometer.

The total number of cells was counted in the 4 corner squares first, then the stained (non-viable) cells. This was repeated in the opposite chamber. If over 10% of the cells were clustered, the procedure was repeated after further dispersal by pipetting. If less than 200 or more than 500 cells were observed in 8 squares, the count was repeated adjusting to an appropriate dilution factor. The cell density and viability of the suspension was calculated as follows:

Cells per mL = average count per square x dilution factor x 10^4 .

Cell viability = viable cells / total cell count.

2.2.2 Coulter multisizer particle analyzer

This semi-automated cell counter gives information about the cell density in suspension and a measure of the cells' diameter or volume. The instrument works on the principle of an aspirated stream of solution through a 100 μ m aperture with an electrode inside and outside the collecting chamber. The change in impedance is used to assess the cell size and the number of discrete disturbances is used to calculate the cell count. Furthermore, where cells are adherent to each other, the analysis software was able to discriminate to a certain degree and take this into account when delivering the final analysis.

2.3 Measuring senescence

2.3.1 Replicative capacity

Calculating population doublings

The number of population doublings that the culture attains between passage $x-1$ and x is calculated by $PD = \log_2(N_x/N_{x-1})$. N_{x-1} is calculated using the original plating density of the cell suspension adjusted to seeding efficiency and N_x is the cell count at passage.

The replicative capacity is a calculation of the cumulative population doublings achieved by a cell population. The cells were counted and replated at each passage with a known cell density per plate or well. This allowed a calculation of the population doubling, population doubling time (population doubling/days between passages) and cumulative population doublings (the sum of each passage's population doubling). It is vital when calculating doubling time that cells do not become confluent to avoid contact inhibition of growth. However, the initial doubling time may be longer than the subsequent middle phase as cells show a slower proliferative rate at very low cell densities.

2.3.2 Senescence associated β galactosidase histochemical staining

2.1.1.1 Reagents

PBS

3% paraformaldehyde preparation (always made fresh).

3g paraformaldehyde was placed in a 200mL flask to which 60mL PBS was added. The mixture was warmed to 60°C in a fume hood and mixed with a magnetic stirrer. 0.5M NaOH was added drop-wise, until a clear solution was produced. The solution was allowed to cool and pH was checked. Further NaOH was added to titrate to pH 7.4. The volume was made up to 100mL with PBS.

X-Gal Staining solution :

Potassium ferrocyanide 5mM, potassium ferricyanide 5mM, sodium chloride 150mM, magnesium chloride 2mM, citric acid 40mM / sodium phosphate 50mM, (all Sigma) titrated to pH 6.0. Store at 4°C for up to 3 months.

Ethanol (70%, 95%, 99.7%)

5-bromo-4-chloro-3-indolyl- β -v-galactopyranoside (X-gal) was kept as a stock solution of 48.95mM (20mg/mL) in DMF at -20°C in the dark and in a glass bottle. X-gal was added to the above buffer immediately before the staining procedure at a concentration of 2.45mM (1mg/mL) and the resulting solution was filtered using a 0.22 μ m filter.

2.3.2.1 Method

Medium was removed from wells and cells were washed twice in PBS (2mL) at room temperature. PBS was removed and cells were fixed for 3min with 1.5mL 3% paraformaldehyde per well of a 6 well plate at room temperature. Cells were washed once more with PBS at room temperature.

Cells were then exposed to the prepared X-gal staining solution (1.5mL per well of a 6 well plate) and samples were incubated overnight (20 hours) at 37°C. Plates were wrapped in Parafilm to prevent evaporation and, if kept in 5% CO₂ incubator, to prevent alteration of pH by CO₂. Staining solution was then removed and the plates were washed once with double distilled water at room temperature. Cells were then washed through grading ethanol solutions of 75%, 95%, and 99.7% using 1mL per 6-well plate well for 1min each. Plates were allowed to air dry after the last ethanol passage and were then ready for counting or photography.

2.3.3 Fluorimetric assay of β -galactosidase activity

Quantitative assay of senescence-associated β -galactosidase using cell extracts

Senescence-associated β -galactosidase was measured by the rate of conversion of 4-methylumbelliferyl- β -D-galactopyranoside (MUG) to the fluorescent hydrolysis product 4-methylumbelliferone (4-MU) at pH 6.0.

2.3.3.1 Materials

4-methylumbelliferyl- β -D-galactopyranoside (MUG)

400mM sodium carbonate

PBS

Lysis buffer pH 6.0

5mM 3-[(3-cholamidopropyl) dimethylammonio]-1-propanesulfonate (CHAPS)

40mM citric acid

40mM sodium phosphate

0.5mM benzamidine

0.25mM phenylmethanesulfonyl fluoride [PMSF]

Reaction buffer

40mM citric acid

40mM sodium phosphate

300mM NaCl

10mM β -mercaptoethanol

4mM $MgCl_2$ (pH 6.0) with 1.7mM of MUG added immediately prior to use from a 34mM stock in DMSO.

2.3.3.2 Method

Plates were washed six times with PBS after which 75 μ L lysis buffer was added at room temperature. Cells were scraped and transferred to a 1.5-mL tube. The lysate was vortexed vigorously and then centrifuged for 5min at 12000g and kept on ice until use. Reaction buffer was kept at room temperature to prevent precipitation.

Reaction buffer (150 μ l) was added to 150 μ l of clarified lysate (100 μ l of lysate diluted with 50 μ l of lysis solution) and the reaction mixture was incubated at 37°C for 1 hour.

50µl of the reaction mixture was added to 500µl of 400mM sodium carbonate stop solution and kept at 4°C until measurement of fluorescence. 150µL of the final sample mix was transferred into a 96-well plate and was read at 465nm using a Victor automated plate reader with excitation at 360nm, .

2.3.4 Flow cytometric assay of β -galactosidase activity

2.3.4.1 Materials

5-dodecanoylamino fluorescein di- β -D-galactopyranoside (C_{12} FDG) (Molecular Probes Catalog Number - D2893) MW 853.92.

Dissolve in DMSO to give stock solution of 20mM.

PBS

2.3.4.2 Method

Plates were washed twice with PBS at room temperature. Cells were incubated with 25µM C_{12} FDG in medium for 4hrs at 37°C in 5% CO₂ humidified incubator.

After incubation, cells were washed twice with PBS. Cells were disassociated from the plate using trypsin / EDTA 0.05% and tapping gently until cells detached. Cell suspensions were transferred to 5mL tubes suitable for FACS machine containing an equal volume of full medium and placed on ice until analysis.

When hydrolyzed by β -galactosidase, C_{12} FDG gives rise to the fluorescent product fluorescein by β -galactosidase which when excited at 488 nm emits fluorescence at 518nm. Cells were therefore analysed by forward and side scatter and fluorescence intensity. The flow cytometer was set to acquire 10000 events.

As part of the optimisation of the model, cells were subjected to different drug treatments while they were actively replicating (i.e. pre-confluent). However, some treatments - most notably those involving incubation with a nitric oxide donor - caused both inhibition of cell replication and cell death in this situation. However, since I wished to analyse the effect of these drugs on the potential to cause a stress-related senescence in subsequent experiments, I tried exposing the cells to the drug in a confluent state. I found that confluent cultures were more able to tolerate and recover after the drug treatment. This may nevertheless be more similar to the *in vivo* situation where endothelial cells are rarely out of contact with other cells.

In the first series of experiments, cells were analysed immediately after their treatment. However, changes in β -galactosidase activity appeared to require at least 48 hours of exponential growth post trypsinization. Partly, this allowed cells to recover so that they were able to survive the following stage of analysis but also, the increase of β -galactosidase activity appeared to need cells which were not subject to cell contact inhibition.

This was demonstrated in optimisation experiments which show a sufficient number of cells to be analysed at the time of harvest, without large numbers of cellular fragments which would be a sign of cell death at the time of analysis. However, greater differences in β -galactosidase activity were seen between cell populations when cells were harvested after a period of non-confluence.

2.3.5 Western blotting for senescence associated proteins

2.3.5.1 Cell lysis

Reagents

Lysis buffer

50mM Tris-HCl pH8

150mM HCl

1mM EDTA

1mM Na₃VO₄

1% NP-40 (Sigma)

Cells were washed twice in PBS and scraped using a cell scraper in 100-150 μ L lysis buffer per 6-well plate well on ice. The lysate was then collected in Eppendorf tubes and kept on ice. Samples were then frozen to -20°C and stored until use.

Samples were then thawed and sonicated on ice using a sonicator for 3 x 5 second bursts. Samples were centrifuged at 200g for 5 minutes and 30 or 50 μ L supernatant was collected in Eppendorf tubes.

2.3.5.2 Protein estimation

Two protein assays were used as the BCA method contained cupric sulphate and this would have interfered with the biotin switch method of measuring protein transnitrosation.

2.3.5.2.1 BCA Protein assay kit (Pierce)

Reagents

Sample A

Sodium carbonate, sodium bicarbonate, bicinchoninic acid and sodium tartrate in 0.1M sodium hydroxide.

Sample B

4% Cupric sulphate.

Standard

Bovine serum albumin (Sigma).

The assay is based on detection of reduction of Cu^{2+} to Cu^+ by protein in an alkaline medium (the biuret reaction) with colorimetric detection of the cuprous cation (Cu^+) using a unique reagent containing bicinchoninic acid. It was first described by Smith et al in 1985.¹⁸² A purple reaction product is formed by the chelation of two molecules of BCA with one cuprous ion. This water-soluble complex exhibits a strong absorbance at 562 nm that is nearly linear with increasing protein concentration.

Protein standards were prepared using bovine serum albumin serial dilutions in lysis buffer at concentrations of 2mg/mL, 1.5, 1, 0.75, 0.5, 0.25, 0.125 and 0 mg/mL.

The reaction mix was prepared immediately prior to the assay by mixing samples A and B at the recommended dilution and 200 μL solution was added to the corresponding number of wells using a multichannel pipettor. 10 or 15 μL aliquots of samples and standards were then added to the wells using a single channel electronic multi-pipettor and incubated for 30 min at 37C in a humidified incubator with 5% CO_2 .

Samples were then analyzed in a Spectramax colourimeter at 562nm and values plotted on the standard curve generated from the BSA standards.

2.3.5.2.2 Bradford protein assay kit (Bio-rad)

This assay is based on an assay first described by Bradford in 1976.¹⁸³ Briefly, an acidic solution containing Coomassie Brilliant blue dye demonstrates a change in light absorbance becoming blue with a maximum light absorbance at 595 nm when bound to protein. This is especially true for arginine and aromatic amino acid residues.

Reagents (all Bio-Rad):

Protein assay dye reagent (Bio-Rad)

Coomassie blue dye, phosphoric acid, methanol

Distilled de-ionized water

Standard

Bovine serum albumin (Sigma)

Method

Standard solutions of BSA were prepared by reconstituting a stock solution of BSA 10mg/mL in filtered, deionized water. Serial dilutions in lysis buffer gave concentrations of 2mg/mL, 1.5, 1, 0.75, 0.5, 0.25, 0.125 and 0 mg/mL.

The dye reagent was diluted in water with a 1:4 dye:water ratio. Using a standard 96 well plate, 10 μ L per well of standard and sample solutions were loaded and 200 μ L diluted dye solution were added using a multi-channel pipettor, discarding tips after mixing each well. The sample was placed in the plate-reading colorimeter and incubated at room temperature for 5 minutes before reading absorbance at 595 nm.

Samples were then analysed in a Spectramax colorimeter at 562nm and values plotted on the standard curve generated from the BSA standards.

2.3.5.3 Sample preparation for SDS PAGE

Reagents

Sample buffer

5mM Tris HCl pH 6.8

0.5mM EDTA

0.5% SDS

5% Glycerol

5% Mercaptoethanol (Add on day of use)

Bromophenol blue (Small amount on day of use)

1:1 dilution with sample

Lysates were aliquotted in Eppendorf tubes and made up to an equal concentration and volume with lysis buffer. Sample buffer was added and samples were mixed thoroughly and then boiled at 100°C for 5 minutes before loading into wells of a 15% SDS polyacrylamide gel. 40 μ g of protein diluted to 40 μ L total volume in sample buffer was loaded per sample.

2.3.5.4 SDS PAGE

Reagents

Stacking gel

5% acrylamide/bisacrylamide mix

125mM Tris (pH6.8)

1% SDS

4.38mM ammonium persulfate

6.63mM Tetramethylethylenediamine (TEMED)

Separation gel

15% acrylamide/bisacrylamide mix

375mM Tris (pH8.8)

0.1% SDS

4.38mM ammonium persulfate

2.65mM TEMED

Running buffer

25mM Tris base

192mM glycine

0.1% SDS

Transfer buffer

25mM Tris base

200mM glycine

20% methanol

In the case of experiments to detect p16^{INK4a} and p21^{WAF}, I used a 1.5mm thick, 15% polyacrylamide gel to allow sufficient resolution of these low molecular weight proteins (selected to offer the optimal resolution for proteins <30kDa). This was poured between glass plates cleaned first with water, then acetone and left to dry. 10mL of the 15% acrylamide separation gel was poured per set of glass plates and covered with isopropanol and allowed to polymerise for an hour.

In order to allow for loading of separate samples, a stacking gel was added with a comb to create empty spaces for the samples to be loaded. The stacking gel was made of a 5% acrylamide gel.

Gels were run, in running buffer, at 120V for 1-1.5 hours, using a coloured molecular weight marker to assess gel progress. Gels were then carefully removed and placed in a bath of transfer buffer.

2.3.5.5 Protein transfer

A PVDF transfer membrane was cut to the size of the gel, bathed in methanol then put it in the transfer buffer bath together with a sponge and 6 x whatman paper sheets

The membrane and gel were then placed in between three layers of soaked whatman paper on either side and transfer was performed from gel to membrane at 150V for 45 minutes using a trans-blot cell.

2.3.5.6 Western blotting and ECL protein detection

Reagents

Membrane

Blocking buffer

PBS-0.1% Tween-20

6% fat-free skimmed milk

Antibodies

Rabbit anti-p21^{WAF1} C-19 polyclonal antibody (Santa Cruz sc-397)

Rabbit anti-actin I-19 antibody (Santa Cruz sc-1616)

Mouse anti-p16 F-12 polyclonal antibody (Santa Cruz sc-1661)

HRP-conjugated goat anti-mouse IgG antibody (Santa Cruz sc-2005)

HRP-conjugated goat anti-rabbit IgG antibody (Santa Cruz sc-2004)

ECL detection kit (Amersham RPN2109), containing reagents 1 and 2, contents not published.

After transfer, the membrane was incubated in blocking buffer for 1hr at 37°C under shaking or overnight, at 4°C. The primary antibody was incubated for 1h at 37°C in the blocking buffer under a paraffin paper (2 mL/membrane) at 1:1000 dilution, 1:2000 in the case of anti-actin. After incubation, the membrane was cleaned with five washes in PBS - 0.1% Tween 20 under shaking at room temperature. Thereafter, I incubated the membrane for an hour at 37°C with the secondary antibody-horseradish peroxidase conjugate (HRP) (anti-rabbit or anti-mouse- in function of the first Ab in the blocking buffer at 1:2000 dilution). After this, the membrane was washed five more times in PBS - 0.1% Tween 20 under shaking at room temperature.

Bound, HRP-conjugated antibodies were detected using the ECL system. The ECL system relies on the chemiluminescence of luminol when it is oxidized with the

assistance of the catalysts HRP/H₂O₂, a reaction which is greatly enhanced in the presence of phenols in an alkaline buffer. After mixing the two ECL reagents, 2mL of the solution was pipetted onto the membrane and left for 5 minutes before analysis.

After draining the membrane over a tissue, the membrane was wrapped in Saran film and exposed to an X-ray film. The strength of the signal obtained after an initial exposure of 15s permitted estimation of subsequent exposure times to obtain optimal signals.

2.3.5.7 Optical density analysis

After film processing, films were subjected to optical density analysis as a means of avoiding subjective interpretation of the results. Using Alphaease software, a light box and a digital camera, bands of interest were quantified and compared and adjusted to their loading controls.

2.4 Measuring reactive oxygen species

2.4.1 Fluorimetric assay of reactive oxygen species

In order to determine the levels of reactive oxygen species seen in cells, we used H₂DCF-DA as a probe. H₂DCF-DA is a diacetate derivative of another ROS probe, dichlorodihydrofluorescein. The diacetate moiety enhances membrane permeability and thereby permits better diffusion of the molecule throughout cells. H₂DCF-DA is deacetylated within cells to a non-fluorescent and membrane impermeable carboxy-dichloro-dihydro-fluorescein. Carboxy-dichloro-dihydro-fluorescein is converted to the fluorescent carboxy-dichloro-fluorescein by reactive oxygen species. This reaction detects ROS and RNS by direct reaction or by reaction with a reaction product of the originator reactive species and thus can only be regarded as a rough measure of total oxidant levels.

The substrate reacts predominantly with hydroxyl radicals, H₂O₂ and peroxynitrite but also detects superoxide indirectly via the production of peroxynitrite; or either the hydroxyl radical or H₂O₂. Superoxide is dismutated by superoxide dismutase to form H₂O₂ and then may be further converted to the OH radical via the Fenton reaction. The probe also reacts to a far lesser extent directly with nitric oxide.¹⁸⁴⁻¹⁸⁷

Reagents

H₂DCF-DA (Fluka 35845, dissolved in DMSO (Sigma))

KRH buffer (all Sigma and corrected to pH 7.4):

1.8mM CaCl₂, 1mM MgCl₂, 5.5mM KCl, 145mM NaCl, 0.8mM Na₂HPO₄, 5mM glucose, 20mM HEPES.

EGM-2 (Promocell)

Method

HUVEC were seeded onto 96 well plates at 10000cells/well and grown in EGM-2 for 2 days. Cells were then washed in KRH buffer 100 μ L per well. Cells were then incubated with 25 μ M H₂DCF-DA at 37°C for 30 minutes except the non-staining wells. This allowed the fluorogenic progenitor to enter the cells. Cells were washed with 70 μ L KRH buffer and incubated at 37°C with the relevant compound for 60 minutes with fluorescence readings every 10 minutes to provide kinetic data. A VICTOR™ X light luminescence plate reader (Perkin Elmer) was set to excite at 485 \pm 10nm, and to read at 520 \pm 25nm.

This experiment, being conducted in the presence of the active reagents, was prone to extracellular bias. In order to assess the possible effects of fluorescence being generated by an extracellular reaction between H₂DCF-DA and the drugs used to treat the cells, I repeated the experiment using the drugs and the fluorescent probe alone.

2.4.2 Flow cytometric assay of ROS

Another way to reduce the chance of extracellular reactions being incorrectly thought of as intracellular, I also repeated the experiment using flow cytometry. This gave the added advantage of being able to quantify fluorescence per cell and to use gating to remove cell debris from the analysis.

Cells were incubated with H₂DCF-DA for 30 mins at 37°C in a T-25 flask, harvested with trypsin/EDTA followed by neutralization with phenol-free EGM-2. Cell suspensions were then incubated at 37C with the relevant compounds for 30 minutes on ice and analysed using a Beckman FACSCalibur flow cytometer without further processing.

2.5 Detection of protein nitrosylation by the biotin switch method

Protein nitrosylation as a consequence of exposure to nitric oxide was assessed using the biotin switch method. The principle behind this technique is that protein nitrosylation occurs on thiol residues. However, direct measurement of protein nitrosylation was not possible. The biotin switch method first blocks free cysteine residues, before switching nitrosyl residues for a labelled, irreversibly bound reagent (HPDP). The removal of nitrosyl residues is achieved by reduction by ascorbic acid prior to the labelling step. In this case, labelling was performed using a Biotin-labelled hexyl pyridyl dithiopropionamide (HPDP) which could itself be labelled with Avidin labelled with horse-radish peroxidase. Subsequent analysis was made using the ECL detection kit as previously described.

2.5.1.1 Materials

Blocking buffer

9 volumes of HEN buffer (HEPES 250mM, pH 7.7 (Sigma); EDTA 1mM (Sigma), neocuproine 0.1mM (Sigma)) to 1 volume of 25% SDS (Sigma)

Mercaptoethanol methylthiosulfonate (MMTS) 20mM made from a stock 2M solution in dimethyl formamide (DMF) (both Sigma)

Acetone (Sigma)

HENS buffer

HEPES 25mM, pH 7.7; EDTA 0.1mM, neocuproine 10mM, 1% SDS

Reducing agent

Sodium ascorbate 50mM (Sigma)

Biotin-hexyl pyridyl dithio propionamide (Biotin-HPDP) (Pierce)

Avidin-horseradish peroxidase (Avidin-HRP) (Sigma)

ECL plus kit

2.5.1.2 Method

The precise method was taken from Jaffrey et al but was performed with modification.¹⁸⁸ The most important difference was the use of the Bradford protein assay in preference to the BCA (Biuret assay) as this assay can be performed in samples which may contain reducing agents including ascorbic acid and also copper chelators, including neocuproine, unlike the BCA (Biuret) protein assay.

Cells were washed in PBS buffer after being grown in 6-well standard tissue culture plates. The plates were then transferred to an ice bucket where they were washed in PBS and harvested by scraping. The resulting suspension was transferred to a 1.5mL Eppendorf tube. After centrifuging at 500g for 5 minutes, the supernatant was removed by suction. The pellet was then re-suspended in blocking buffer and either stored in -20°C for future analysis or I directly proceeded to perform the assay.

Free thiol blockade was achieved using blocking buffer which contained the active blocker, methyl methane thiosulfonate (MMTS), by gently shaking the re-suspended pellet in 0.5mL blocking buffer at 50°C for 20 minutes. The mixture was then centrifuged again at 500g for 5 minutes and the supernatant was split into 3 aliquots of 0.15mL for separate analysis to compare a negative non-labelled sample, a biotin-labelled sample and a labelled and ascorbic acid-reduced plus biotin-labelled sample. MMTS was then removed by the addition of 0.8mL ice-cold acetone for 30 minutes in a -20°C freezer. Samples were then centrifuged at 5000g for 5 minutes at 4°C and the supernatant was discarded. The pellet was then re-suspended in 0.1mL PBS .

Protein concentration was determined using the Bradford assay. After determining protein concentration, equal amounts of protein were loaded per condition onto a 15% acrylamide gel which was made as previously described. The loading buffer could not contain β -mercaptoethanol as this interfered with the labelling process. In addition, protein samples were not heated as they could not be boiled for maximal protein denaturation for the same reason.

After running the samples through the gel at 150V for 90 minutes, monitoring the progress using dyed protein molecular weight markers, a wet transfer of the gel onto PVDF membrane was performed for 1 hour at 100V. Milk blocking was not used as it contains biotin, therefore 3% bovine serum albumin was used as an alternative. Blocking was performed over 1 hour at room temperature or overnight at 4°C. The membrane was then exposed to a 1:1000 dilution of Avidin-HRP conjugate for 1 hour at room temperature in the 3% BSA/PBS buffer and washed before analysis with ECL plus detection reagent as previously described.

2.6 Exposure of cells to cold light

The light source was a KL1500 Schott (Mainz, Germany) which delivers cold light from a 150W bulb via a fibre optic arm. In order to standardise the experiment, a number of adjustments were made to our standard cell incubation practice. In order to intensify the light to cells, all flasks were placed in the same incubator within a polystyrene ice box with the lid removed and positioned to face the inner glass door of the incubator. The box was in turn lined with reflective aluminium foil, as was the inner glass door of the incubator, except for a window left to allow light from the light source to enter. The need to leave the outer door of the incubator open compromised its insulation but as this was thermostatically-controlled, the main difficulty was that water condensed on the inner surface of the inner glass door and necessitated careful observation to ensure the water tray at the bottom of the incubator was replenished in order to maintain the humidity of the incubator and that excess water on the floor was removed.

Cells were grown in T-25 flasks with the cells which were not to be exposed to light being wrapped in aluminium foil covered in black ink on the inner surface. The rationale for this was that any leakage of light into the flask would be readily absorbed by the black ink. However, a temporary covering was necessary to allow careful cell harvest at the end of the experiment and to permit any necessary photography of the cells. The aluminium foil on the outer of the flask also prevented absorption of the light by any pigment used to opacify the tissue culture plastic and the likely conversion of this to heat.

Finally, the light source could not be left in operation for the length of the experiment and continuous light exposure could have exerted an effect on the reagents as much as on the cells. Therefore, timed light exposures were managed by a generic mains electricity power timer used for domestic light timing. This was programmed to cycle with 1 hour of light followed by 5 hours of ambient light only.

2.7 BrDU incorporation assay of cell proliferation

Reagents (all Roche):

BrDU labelling agent (10mM 5-bromo-2'-deoxyuridine in PBS, pH 7.4).

FixDenat solution.

Peroxidase-linked anti-BrDU antibody (monoclonal antibody from mouse-mouse hybrid cells, clone BMG 6H8, conjugated with peroxidase).

Antibody dilution solution.

Washing buffer (PBS 10x solution).

Substrate solution (TMB, tetramethyl-benzidine)

A colorimetric cell proliferation ELISA was obtained from Roche (Cell Proliferation ELISA, product number 11 647 229 001). The assay exploits the thymidine analogue 5-bromo-2'-deoxyuridine (BrDU) which is incorporated into DNA during synthesis and can then be detected by immunoassay with a peroxidase-linked antibody. Details of concentrations and dilutions and some ingredients were not all supplied by Roche. Cells were plated at a range of cell concentrations for the assay on 96-well plates and the assay was performed 16 hours later. Attempts to assay at a later stage were less successful due to the degree of proliferation during the period between plating and assay (data not shown). Cells were incubated with BrDU in normal medium as per the supplied protocol from Roche for 2hr at 37C. After washing, cells were fixed, washed and labelled with anti-BrDU-peroxidase conjugated antibody for 90min at room temperature. Peroxidase-labelled cells were detected with a chromogenic substrate of peroxidase, tetramethyl-benzidine (TMB) and this was detected in a Spectramax plate reader at 370nm every 5min for 30min and the area under the curve was calculated.

2.8 Tetracycline-inducible iNOS expression in HEK-293

Tetracycline-inducible iNOS expressing cells from a human embryonic kidney cell line (HEK-293) were a kind gift from Dr Palacios-Callender. They were manufactured using a previously-described method by Mateo et al.¹⁸⁹

In order to achieve a cell line which could stably and predictably express our gene of interest, cells had been transfected with a tetracycline-inducible expression vector which contained cDNA for the complete iNOS gene found in human chondrocytes, flanked by an antibiotic resistance gene for cell selection, a cytomegalovirus gene promoter and Flp-recombination target (FRT). This is then transfected into the cell line which already contains its own FRT site which has been selected to be in an area of the genome which is able to tolerate gene insertions without destabilising the cell line.

Using a plasmid to express Flp recombinase, the host genome FRT site is cleaved and the new sequence is inserted into this pre-selected site. Successfully transfected cells are then selected using the antibiotic to which those cells are now resistant and therefore a stable, pure population of cells is obtained.

2.9 Measuring nitric oxide generation by nitric oxide electrode

Using an Innovative Instrument 700 micrometre tip nitric oxide sensor, I measured the concentration of nitric oxide in medium. The sensor has a series of gas-permeable membranes surrounding an electrode plate. The membranes present a series of obstacles to gaseous diffusion until nitric oxide is the only gas which can reach the electrode surface and once there, the nitric oxide reacts with the electrode plate, generating an electrical current which is directly proportional to the concentration of nitric oxide.

The sensor is immersed in an aqueous solution for at least 18 hours in order to allow membrane equilibration. The electrode measurements were calibrated using a standard solution to generate known concentrations of nitric oxide. Sodium nitrite is used as the donor and is added to a solution of sulphuric acid, in the presence of a reducing agent, in this case, potassium iodide.

Potassium iodide 20mM and sulphuric acid 200mM solutions were mixed at a 1:1 ratio to make up 1mL of the calibration solution (final concentration KI 10mM and H₂SO₄ 100mM) immediately before starting the experiment and were then warmed to 37°C. After adding the calibration solution to the thermostatic measuring chamber, the electrode was immersed in the solution and a mechanical stirrer was used to achieve an even temperature and concentration of the solution. The Tarragona recording software was initiated to allow a stable reading to be achieved before adding the standard concentration of sodium nitrite. After the reading achieved the maximum current, the experiment was terminated, the probe is washed and the experiment was repeated in triplicate to ensure reproducibility. From the standard concentrations of sodium nitrite, a calibration factor was calculated and therefore a concentration of nitric oxide could be measured using different solutions of media and nitric oxide donor. The sensitivity of the electrode is 150 to 250 pA/nM and this makes it able to measure concentrations of less than 50nM nitric oxide with an accuracy of as little as +/- 1nM. (Manufacturer's data <http://2in.com/products/no-sensors/compare-select.html>). Experiments were performed with the assistance of Dr Miriam Palacios-Callender, UCL.

3 Assessment of techniques to measure β -galactosidase

3.1 Introduction

There are many features of senescent cells which help to differentiate them from other cell states.

In the presence of a mitogenic stimulus and the absence of any other impediment, senescent cells will not replicate. Thus the first distinguishing feature of senescent cells when compared to normal cells would be evidence of irreversible cell cycle arrest.

In Hayflick and Moorhead's description of replicative senescence,¹ foetal fibroblasts were grown *in vitro* until the growth rate subsided and finally ceased at a predictable 50 population doublings. This limit (later called the Hayflick limit or proliferative capacity) was thought to have been the consequence of a pre-programmed event which occurred within the cell and would occur in the same population of cells at the same number of population doublings, even when the investigators sent their samples to other labs for verification.

One of the burning questions in this field of research is whether growing cells *in vitro* to a state of irreversible cell cycle arrest actually mimics any condition which could occur *in vivo*. To this end, many groups have attempted to identify markers which could identify senescence in another way and to describe the occurrence of senescence *in vivo*.

Methods to investigate senescence are limited by the source of cells and the artificiality of the system used to grow them. The ideal system would allow the analysis of a subset of young cells of similar replicative age to be analysed in a phenotypically pure population for the early changes associated with the development of senescence and for the subsequent proportion of senescent cells. In this respect, obtaining young healthy human cells limits us to obtaining cells from umbilical cords. Assessment of senescence by replicative capacity relies on a number of cell manipulations which may introduce error. Standard practice is to keep cells *in vitro* under continual mitogenic stimulus. Cells are not allowed to become confluent in culture as there is contact inhibition between cells and this would make any calculation of cell replication rate inaccurate. There is also widespread advice that cells which become confluent may lose some of their replicative ability. Thus experiments to assess the effect of stressors on senescence are carried out when cells are at a relatively low density and are not in contact. The cells are then repeatedly dissociated using ion chelators or proteolytic enzymes and suffer mechanical stress for a number of passages until replicative senescence. This contrasts with the situation *in vivo* where cells are in contact, forming a layer of quiescent cells. Cells in a confluent monolayer may be better suited to survive any noxious stimulus and also may express their defences in a way more alike to *in vivo*.

The ability to assess senescence immediately after any intervention would decrease the chances of culture artefact.

3.2 Hypothesis

The presence of β -galactosidase confirms and corresponds to cellular senescence. This will be consistent with other methods to measure senescence.

3.3 Aims

To assess some of the various methods of detecting senescence, aiming to produce a reliable, sensitive and incontrovertible means of detecting senescent cells.

Find an *in vitro* method which remains as close as possible to likely *in vivo* conditions, keeping the number of *in vitro* interventions to a minimum.

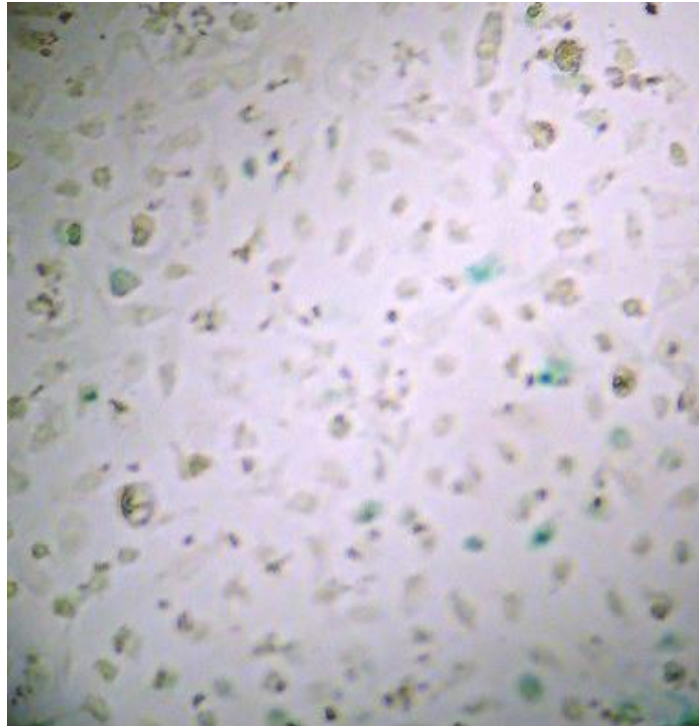
3.4 Testing different methodologies for detecting β -galactosidase

3.4.1 Senescence-associated β -galactosidase

Human umbilical vein endothelial cells were grown in normal EGM-2 and passaged at 80% confluence until cessation of growth. A subset of HUVEC were stained for senescence-associated β -galactosidase using the method described. Late passage HUVEC were also stained in this manner. The percentage of senescence-associated β -galactosidase positive cells are counted first by using phase contrast light microscopy and later by using unfiltered light to count stained cells in the same light field and a percentage can be attributed to the proportion of senescent cells.

This measure has been used to a great extent since first described by Dimri et al in 1995.⁸ As every cell has a certain amount of β -galactosidase activity, the method relies on a threshold of enzyme activity beyond which there is an overspill of galactosidase activity which can be detected at pH 6.0. This overspill represents a general increase in enzyme amount and activity and is associated with senescence rather being causative.

A



B

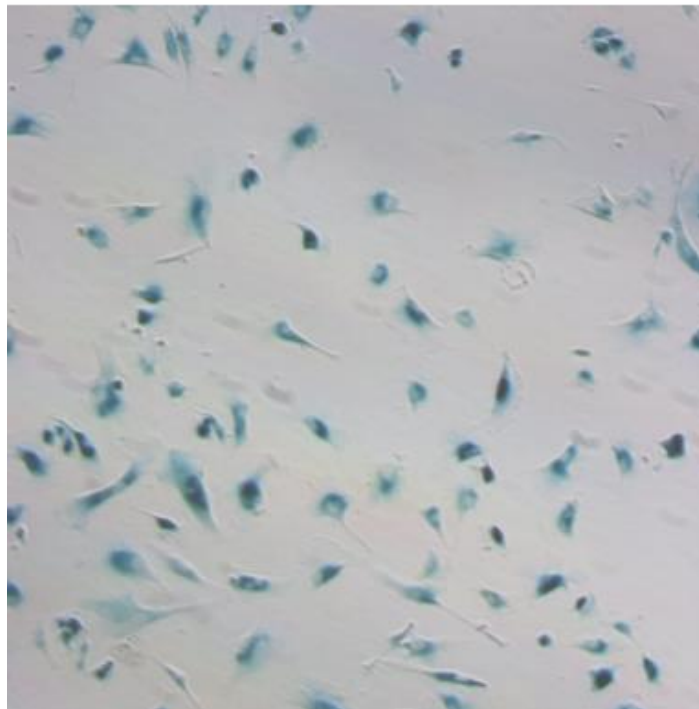


Figure 3.4.1-1: Light micrographs of early and late passage HUVEC stained with senescence-associated β -galactosidase.

Representative light micrographs of endothelial cells stained for senescence-associated β -galactosidase (blue colour). Upper panel (A) shows early passage cells, lower panel (B) late passage cells. Upper panel cells show a majority of cells negative for senescence-associated β -galactosidase and sporadic staining of some cells. Lower cells appear flatter and larger and are universally densely stained with blue colour. Despite plating at same density, the density of cells in the lower panel is reduced due to reduced proliferation.

3.4.2 Methyl-umbelliferyl galactosidase (MUG) assay

In an effort to find a more objective and quantitative alternative to the determination of senescence-associated β -galactosidase, we investigated a biochemical method to measure total β -galactosidase activity in cell lysates. One concern over the Dimri method of detecting threshold levels of galactosidase is that cells may be lost during fixation and there is no way of measuring whether these were senescent, healthy or both. Measuring the total β -galactosidase activity of cell cultures using lysates has the advantage of avoiding this but the disadvantage of having to decide what merits the term senescent, and has a dilutional effect when considering small numbers of senescent cells in a healthy culture. Whilst not definitively proven, it seems that cells operate a binary mode of senescent or non-senescent phenotype, rather than normal, pre-senescent and finally senescent.

Furthermore, this method allows a more objective measurement, less prone to observer bias when counting cells which are blue or faintly blue.

Experiments were designed according to the protocols mentioned in the methods section (2.3.3). Cells were grown in the standard fashion on 6-well plates using EGM-2 medium. When the assay was to be performed, plates were washed, and cells were scraped from the dish in lysis buffer. The resulting mix was transferred into 1.5ml Eppendorf tubes, vortexed and kept on ice until ready to perform the assay with reaction buffer which contained 4-methylumbelliferyl- β -D-galactopyranoside (MUG). MUG is the β -galactosidase substrate which is hydrolysed by β -galactosidase giving 4-methylumbelliferone (4-MU), the fluorescent product detected in the assay by a fluorescent plate reader.

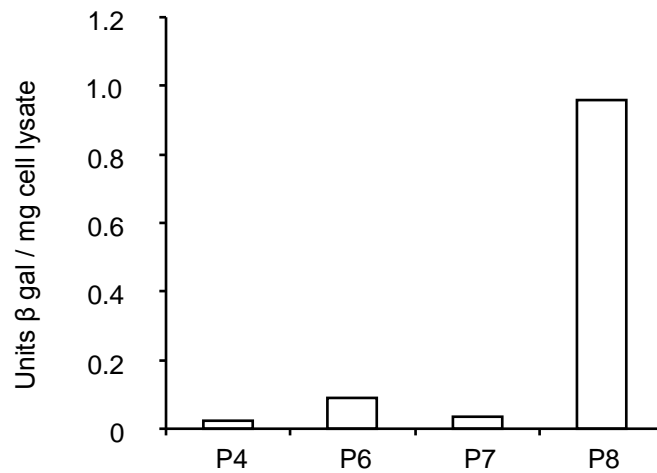
The system was validated using the HUVEC cultures from several serial passages of the same initial population as a positive control for senescence. Attempts to quantify the amount of cells proved difficult when using standard protein assay methods as the lysis solution interacted with protein assays and the total protein was not representative of the total number of cells which vary in size according to replicative age and increase their production of other proteins, including extracellular matrix and senescence-associated proteins as discussed in the introduction.

Bacterial β -galactosidase was used as a standard to compare the activity of cell lysates by using known dilutions of the enzyme.

This method proved effective but too insensitive to measure small differences in the proportion of senescent cells in a given population.

Furthermore, the need for storage of cells or cell lysate in order to perform an assay on several passages of cells on the same occasion or to perform several assays on the occasion of each passage introduced further uncertainty.

Experiment 1



Experiment 2

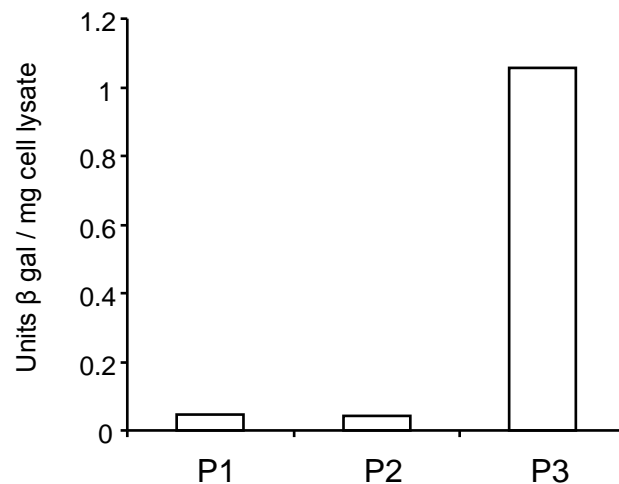


Figure 3.4.2-1: Total β-galactosidase activity by MUG assay: serial passage.

Results of 2 separate experiments carried out using the MUG β-galactosidase assay are shown. Cells were grown by serial passage, and lysed at the indicated passages. Lysates were stored at -80°C until the time of analysis.

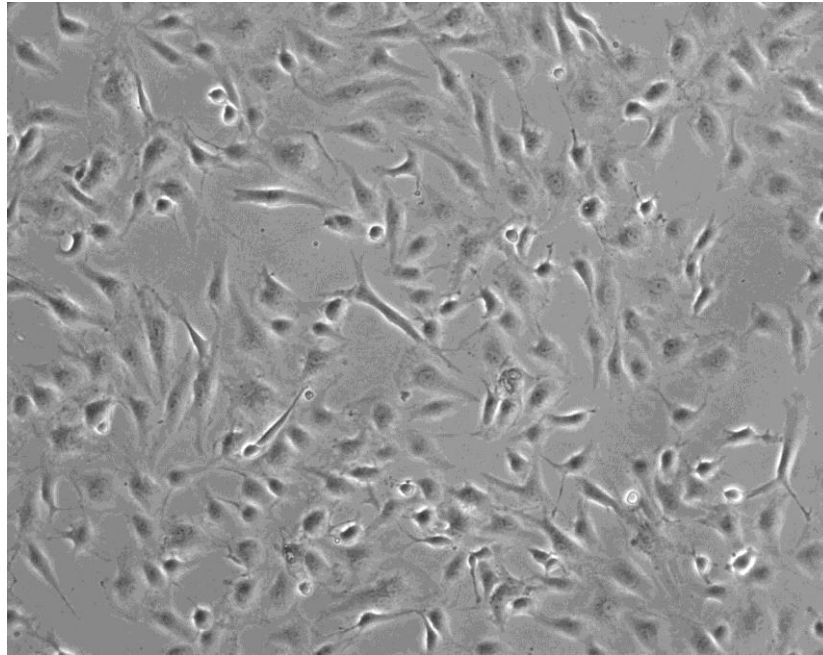
Serial dilutions of bacterial β-galactosidase were used to normalise the results and thus compare between experiments. There is a background variability of β-galactosidase activity which led us to believe that the method could be useful for detecting large differences in β-galactosidase activity but may not be sensitive enough to allow interventions at lower passages to be assessed. In the two experiments above, I saw a large increase in β-galactosidase between passages. The increase with experiment 2 occurred at 3rd passage, which is unlikely to represent senescence given the usual replicative lifespan of HUVEC.

3.4.3 Measurement of β -galactosidase activity per cell using flow cytometry

Cells were grown in the standard fashion on 6-well plates in EGM-2 until the time of analysis. The β -galactosidase substrate, 5-dodecanoylaminofluorescein di- β -D-galactopyranoside (C₁₂FDG) was then incubated with the cells in medium and cells were harvested by washing and trypsinization, being stored on ice until analysis by flow cytometry.

The limitation of this technique for our purposes was that cells from different serial passages could not be analysed all at the same time as in this method cells ought to be analysed directly from live culture and could not be stored without freezing live cells, a major problem when cells reach advanced replicative age. There was variability in control fluorescence on each assay according to atmospheric conditions, light and FACS machine settings without a way to standardise this. Thus we were unable to analyse cells treated over several passages to compare this method to the standard of replicative senescence. As an advantage, staining techniques and analysis using more than one laser wavelength also allow the investigation of co-phenomena such as apoptosis.

A



B

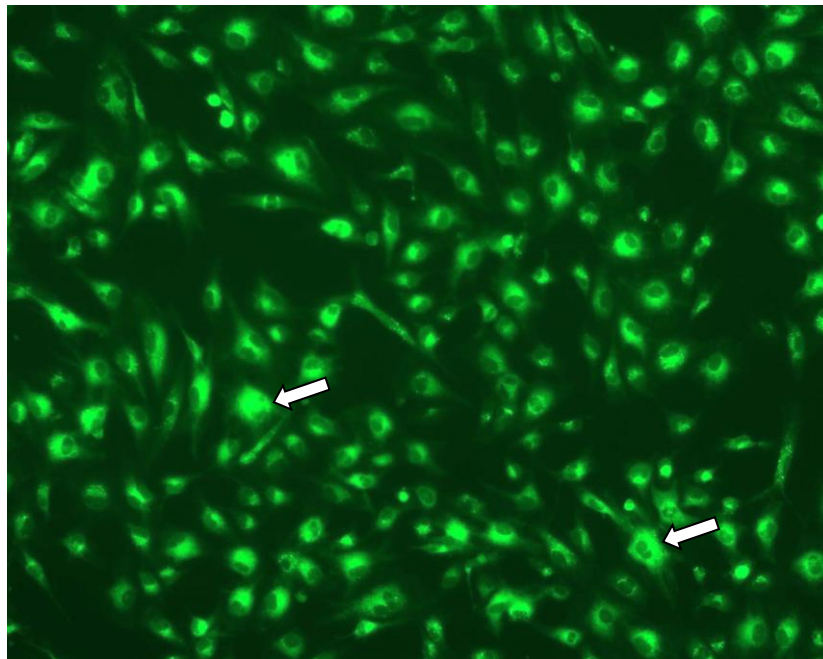


Figure 3.4.3-1: Microscopy of total β -galactosidase activity in young HUVEC detected by C_{12} FDG.

Phase contrast and fluorescence microscopy images of HUVEC following incubation with C_{12} FDG. Photographs were acquired immediately prior to flow cytometric analysis. The cells pictured are 2nd passage HUVEC. The top picture (A) is a phase contrast light micrograph (40x magnification) viewed under an inverted light microscope (Zeiss). The lower picture (B) is from the same field of cells at the same magnification. The fluorescent substrate of C_{12} FDG has been excited using the UV light via the inverted microscope.

The above photographs demonstrate cells treated with C_{12} FDG prior to quantitative assessment by flow cytometry. Cells have not yet been dissociated from the culture plate but they appear healthy and are not completely confluent. Despite being relatively young HUVEC, they demonstrate lysosomal β -galactosidase activity.¹⁰ Imaging in this fashion tended to quench the fluorescent probe in the field of view

after a few seconds and so was not performed routinely before analysing cells in flow cytometry. Arrows point to very bright cells which may represent sporadic occurrences of senescence, which was present even in this young population and is consistent with the histological senescence-associated β -galactosidase staining above (3.4.1) which also showed some cells which were more densely-stained.

3.4.4 Detecting senescence and apoptosis using flow cytometry

Senescence and apoptosis occur in similar environments and with similar stimuli.^{190;191} Cells which irreversibly cease to replicate may in fact be slowly undergoing apoptosis. We wished to use flow cytometry to assess whether cells which have high levels of β -galactosidase activity were also showing evidence apoptosis. It was possible with flow cytometry to assess populations of cells for the coexistence of these phenomena, exploiting the abnormal expression of phosphatidyl serine which can be detected by fluorochrome-conjugated Annexin V. Phosphatidyl serine, while normally expressed on cell membranes, is located on the inner surface of the cell membrane and not exposed to the extracellular surface until membrane function is lost as in apoptosis. At this stage, the membrane allows phosphatidyl serine to flip over to the outer surface of the membrane and it can thus be detected using Annexin-V with attached fluorescent probes. By staining with two fluorescent probes, one to assess β -galactosidase activity and the other to label extracellular cell membrane surface Annexin-V, we were able to investigate if cells which have some of the features of senescence are actually undergoing an early stage of apoptosis.

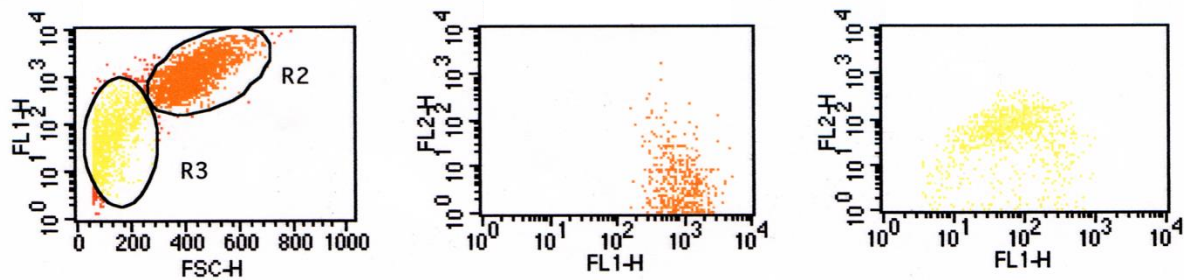


Figure 3.4.4-1: Flow cytometry of annexin V vs total β -galactosidase.

3 dot plot histograms of a flow cytometry experiment of 4th passage HUVEC. FL1-H is fluorescence from fluorescein and in this case is a measure of β -galactosidase activity. FL2-H is a marker of PE fluorescence which is the fluorochrome used to label Annexin V and is a measure of membrane dysfunction in apoptosis. FSC-H is forward scatter height, a measure of cell size. Events from the R2 region in the graph on the left are shown in the middle graph. Events from the R3 region in the graph on the left are shown in the right-hand graph.

The above figure demonstrates that cells show an inverse relationship between β -galactosidase activity and annexin V labelling. R2 is gated to what were thought to be healthy cells and sporadically senescent cells (normal-to-high β -galactosidase activity) and the gated events are shown in the middle graph. R3 is gated to what were thought to be a mixture of cell fragments and apoptotic cells by virtue of fragment size.

3.4.5 Cell proliferation assay

As mentioned previously, the original description of cell senescence was based on the observation of a limited replicative capacity by Hayflick. Thus establishing the replicative limit of a population of cells will tell us the starting replicative age or replicative potential if one is able to count the number of times a population of cells is able to divide. This relies on long-term cell culture with seeding, counting and reseeded followed by a calculation of population doublings to give a final number of cumulative population doublings or replicative capacity. Unfortunately, the method also requires that any intervention to test for an effect on replicative capacity also has to be made for a prolonged period as cells which senesce will be diluted by serial passaging until the whole population senesces. For example, if half a population of cells senesce during an intervention on cells which are in their second passage, replating them at one tenth of their density several times until replicative senescence will cause a dilutional effect as the cells which are not senescent will continue to replicate while the senescent cells will constitute 5% of the subsequent passage, 0.5% the next and so on. Finally, a population of cells which reach senescence after doubling their population fifty times will only be able to do so 49 times if an intervention which causes 50% to senesce on their first passage is not repeated. This would not be problematic if all cells responded in the same fashion on each occasion. However, the subpopulation of cells which survive the intervention may be a select population which are inherently more resistant or may undergo adaptive changes so that prolonged intervention may not be representative

of the initial effect on first intervention. Unfortunately, this is also the gold standard assessment of senescence – demonstrating replicative senescence.

In order to avoid this experimental artefact, we used methods to detect cell proliferation immediately after or shortly after an intervention. This would provide greater power to detect immediate effects and reduce error from repeated counting and replating. This would not necessarily be able to distinguish if a proportion of cells were stunned into quiescence but, by comparing two populations of cells, we would hope to be able to identify if more cells within a given population had undergone senescence.

Bromo-deoxyuridine (BrDU) is a thymidine analogue and is incorporated into genomic DNA during DNA synthesis. The labelled nucleoside analogue can be detected after cell fixation and permeabilisation by enzyme-linked antibodies which catalyse a colorimetric reaction which can be detected on a Spectramax plate reader. Using cells which were in a confluent monolayer, we were able to subject them to various interventions, allow a washout period and replate. In this way, we performed our analysis distant to the initial insult after a recovery period had passed of approximately one cell doubling time and cells were then replated at a variety of cell densities to provide a statistically-robust means of differentiating populations of cells.

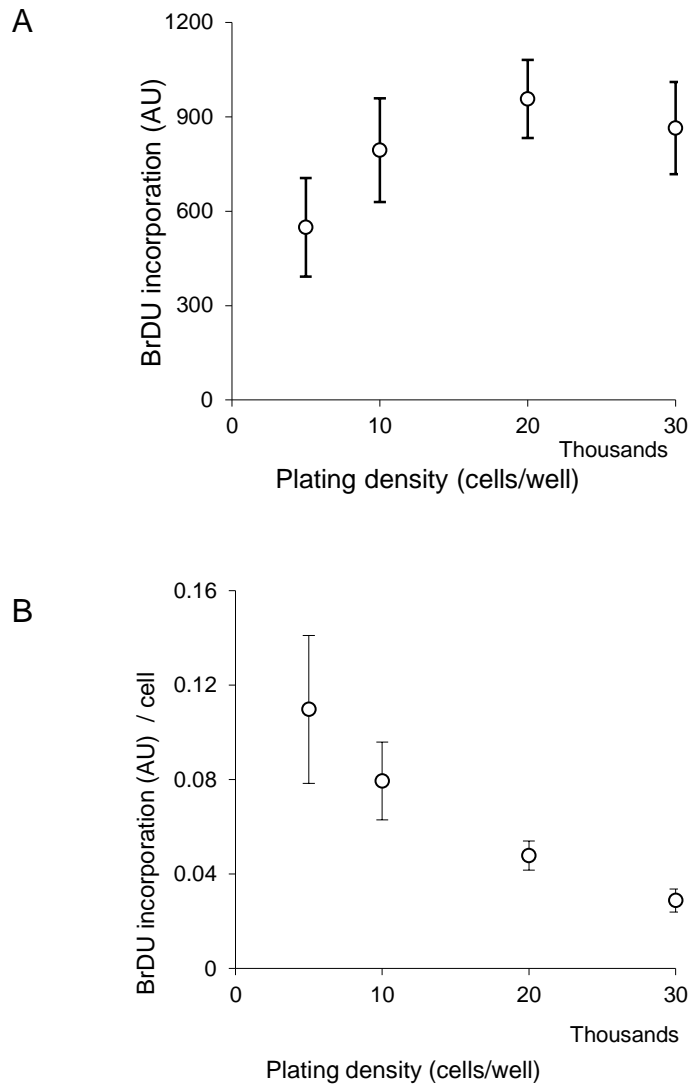


Figure 3.4.5-1: BrDU incorporation and plating density.

The above graphs demonstrate the effect of replating 3 separate donor cultures of HUVEC at varying cell densities and assessing BrDU incorporation. All cells were analysed after 3 passages. The upper graph (A) demonstrates total BrDU incorporation which is expressed as arbitrary units and error bars indicate standard error of the mean. The lower graph (B) demonstrates BrDU incorporation per cell plated.

The above graph demonstrates the effect of replating 3 separate donor cultures of HUVEC at varying cell densities and assessing BrDU incorporation. Cells were replated after 3rd passage and assays were performed 16 hours after plating. Cells in the higher densities were confluent, exhibiting contact inhibition quiescence, both by visual inspection on the tissue culture plate and also by the amount of BrDU incorporation per cell. This way, even if there is doubt about the number of viable cells plated, provided serial dilutions are used, a maximum estimation of BrDU incorporation can be made. Thus titrating the well with increasing seeding densities

until the effect of contact inhibition was observed had the advantage of assessing the maximum potential proliferation and reduced the chance that an observed difference in cell proliferation may be due to an error in counting or a differing ability to adhere to the tissue plate after replating.

Senescence typically causes growth arrest in the G1 phase of cell replication, prior to the DNA synthesis phase and as a marker of cellular proliferation, the BrDU ELISA is thus suited to our model.¹⁹²⁻¹⁹⁴ As previously described, senescent cells typically increase in mass, while remaining incapable of replication. Measurements of increases of cellular protein as a measure of proliferation are therefore less helpful.

We were concerned that many of our stressors could cause a stunning effect with an insult leading to delayed recovery of cellular function. To avoid this, we tested the effect on proliferation after a period of washout and recovery.

3.5 Conclusion

Methods used to detect senescence are imperfect and are prone to culture artefact. The use of serial passage to detect the proliferation potential of a population of cells is inherently unattractive as a means to detect all but the largest differences in cell populations and can do little to detect differences in individual cells. Furthermore, there is a conceptual difficulty with this continual exponential growth in that there is little to suggest this is a phenomenon which occurs in life.

The inability to measure how many population doublings an individual cell has undergone in a lifetime is only partly circumvented by experiments where serial passage of cells taken from young and old animals undergo fewer population doublings when taken from older animals because these cells may have an impaired ability to replicate due to a loss of ability to protect themselves against insults which younger animals would be able to withstand.

It is not known why senescent cells have an increased amount of β -galactosidase enzyme but the subcellular localization remains within the lysosomes which tend to enlarge once senescence occurs. One possibility is that senescence is associated with a defect in the function of lysosomes or that they become overwhelmed by an increased demand. This phenomenon is probably a consequence rather than a cause of senescence as suggested by recent work on cells unable to manufacture β -galactosidase. In this study, cells continued to replicate until cell cycle arrest was observed. However, no β -galactosidase expression was seen.¹¹

Using the progressive accumulation of senescence-associated β -galactosidase in senescent cells as a marker may have limitations in that cells may senesce first, then begin accumulating senescence-associated products. Alternatively, the accumulation of senescence-associated- β -galactosidase may be a reversible sign of a cell in distress. However, in order to get the most of this marker of senescence,

we combined the histochemical method, a biochemical assay and flow cytometry to measure cells and populations of cells as accurately as possible.

Failure to show an increase in population number in a cell culture model may be due to cell death or growth arrest and a measure of cell proliferation was therefore used to complement our other methods to confirm our findings. This cannot distinguish between causes of cell growth arrest, in that it is unable to differentiate between quiescence and senescence but given appropriate stimuli, cells which ought to be proliferating can be assayed to assess if growth arrest is at least persistent, if one cannot be certain that it is permanent.

We aimed to use a comprehensive array of methods to detect senescence and to adapt them to a model which was intended to reduce artefact.

Measuring enzyme activity in a cell suspension by flow cytometry has certain advantages over the other methods. The automated counting of single cells is preferable to analysing cell lysates as one can identify subpopulations within the greater population. Unfortunately, we lacked a standard of senescence which could be measured in this way. One can also distinguish degrees of enzymatic activity within subsets of cells.

The use of a combination of quantitative methods to analyse a population of cells and comparative methods to delineate single cells' characteristics will be used to assess whether cells are affected equally in a gradual shift to senescence or if there was a binary switch to senescence in some cells with others remaining unaffected.

Regardless of the cause of senescence, it remains to be shown whether senescent cells actively participate in the development of disease, whether they are in fact protective or whether they are simply innocent bystanders.

4 Reactive oxygen species

4.1 Introduction

The free radical theory of ageing suggests that nitric oxide could play an important part in senescence. Thus I investigated whether nitric oxide donors were able to increase ROS generation in HUVEC. Furthermore, I wanted to investigate whether antioxidants were able to prevent this effect. This was intended to show a means by which nitric oxide could cause senescence and whether senescence could be prevented by antioxidants by reducing ROS.

Endothelial cells are able to generate nitric oxide via activation of eNOS by shear stress and yet loss of functioning eNOS is associated with advancing age in cell culture and whole organisms. Thus I wanted to investigate the net effect of eNOS activation in a relatively young population of HUVEC on the production of ROS.

4.2 Effect of nitric oxide donors on cellular reactive oxygen species.

HUVEC were seeded onto 96 well plates at 5000-10000 cells/well and grown in EGM-2 for 2 days. They were washed and then incubated with 2,7 - dichlorodihydrofluorescein diacetate at 37°C for 30 minutes. Following this, cells were washed and placed in phenol-free EGM-2 with the nitric oxide donors, DETA-NO or GSNO; or antioxidants, N-acetyl cysteine, uric acid and selenomethionine. We also assessed the effect of the guanylate cyclase inhibitor, ODQ; the eNOS inhibitor, L-NMMA; and the calcium ionophore, (eNOS activator) A23187. This had previously been shown to generate a burst of nitric oxide generation, followed by a more sustained increase in superoxide production.¹⁹⁵⁻¹⁹⁷ Concentrations of each reactant were chosen according to likely *in vivo* concentrations and known effective doses as discussed above. Treatments were assessed for their ability to generate reactive oxygen species within cells using a plate reader at excitation 485±10nm, emission 520±25nm for 60 minutes at 37°C. Serial dilutions of tert-butyl hydrogen peroxide was used as a positive control.

Experiments using phenol-containing medium caused universal cell death as shown in light and fluorescent micrographs below. Thus all subsequent experiments were carried out using phenol-free medium. The reason for the interaction between phenol red-containing media and the ROS probe was not investigated as it was easily circumvented and not central to our investigation.

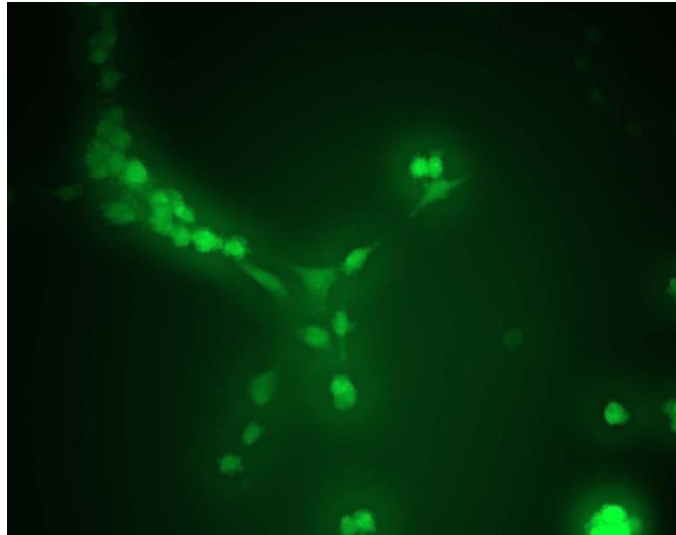


Figure 4.2-1: UV excited microscopy of endothelial cells treated with H₂DCFDA for ROS assay.

40x magnification of HUVEC with UV light excitation which had previously been incubated with 100 μ M H₂DCFDA in phenol red-containing medium. Pictures taken using Zeiss inverted UV microscope using digital camera.

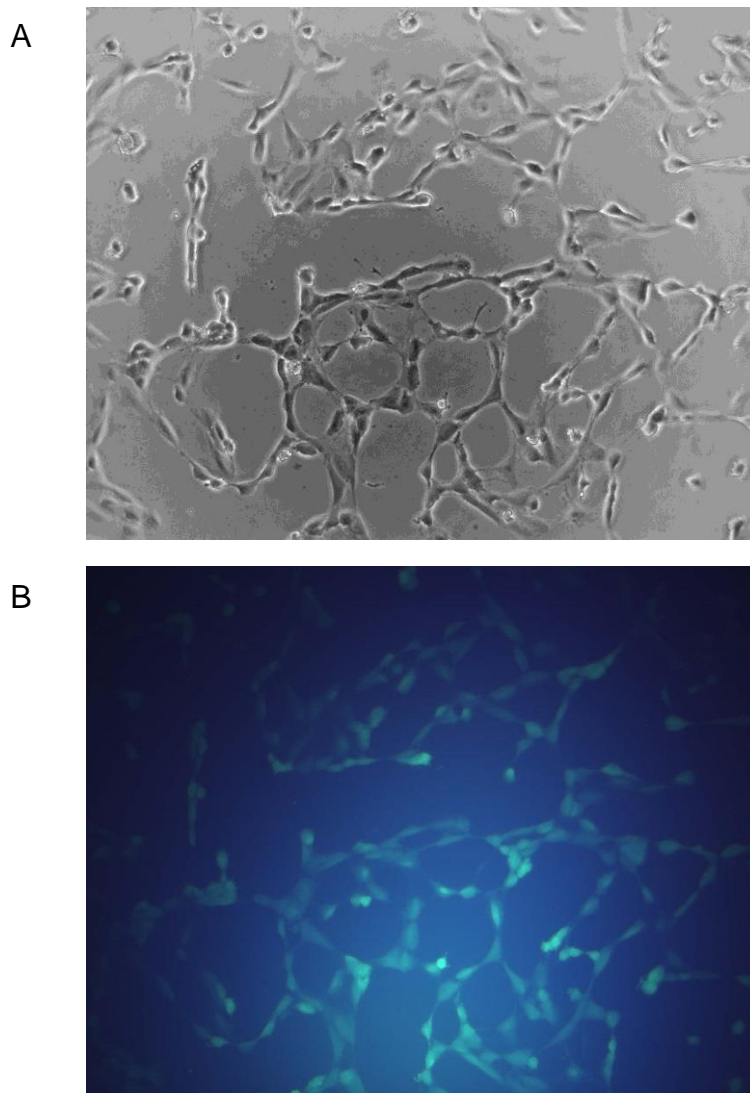


Figure 4.2-2: Light and UV excited microscopy of endothelial cells treated with H₂DCFDA for ROS assay.

Upper panel (A): 40x magnification phased light microscopy of HUVEC in a tissue culture well. Lower panel (B): 40x magnification of same HUVEC with UV light excitation which had previously been incubated with 100 μ M H₂DCFDA. Pictures taken using Zeiss inverted white light and UV microscope using digital camera.

Measurements of fluorescence were assessed at 60 minutes as this time-point had the greatest correlation when tested on the standard curve of dilutions of t-BHP. The single time-point data showed greater correlation with the standard curve of dilutions of t-BHP than measurements of maximum slope of measurements taken at 10 minute intervals.

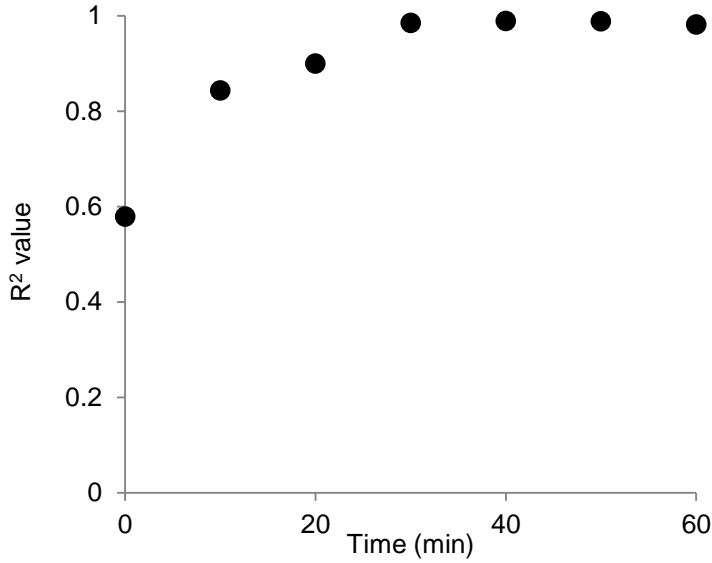


Figure 4.2-3: Time-point measurements of ROS and correlation to the standard curve of serial dilutions of t-BHP.

Graph shows the result of a single experiment to assess the effect of analysing ROS generation by HUVEC using the probe, H₂DCFDA.

4.3 The effect of t-BHP on the H₂DCFDA ROS assay by fluorimetry

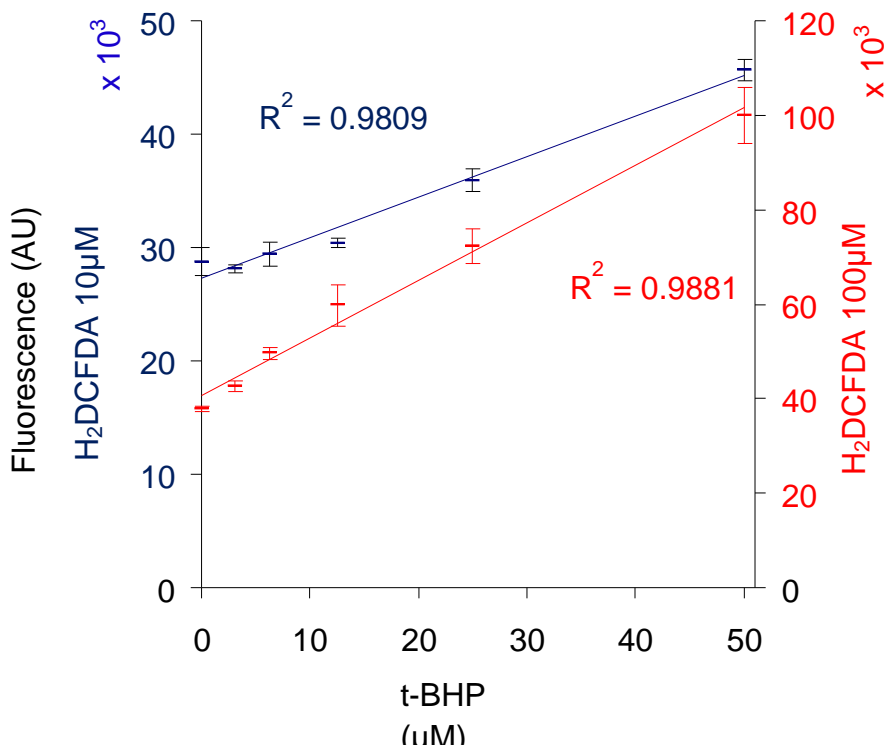


Figure 4.3-1: Dose response curve for the effect of t-BHP on the generation of DCF: comparison of different concentrations of fluorogenic probe.

Cells were incubated with either 10µM (blue line) or 100µM (red line) H₂DCFDA for 60 min and then fluorescence was recorded. R² values for correlation to the linear trendline are shown. Results represent the average of quadruplicate determinations. Error bars indicate SEM.

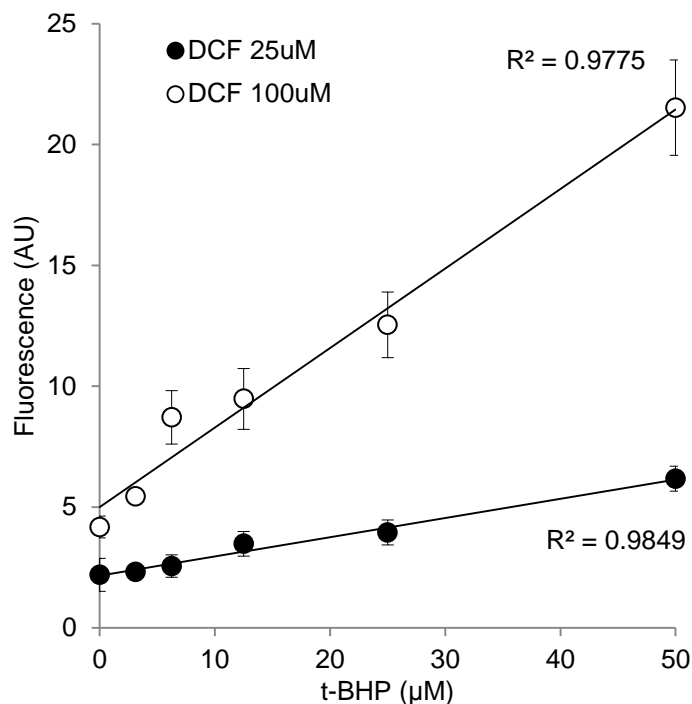


Figure 4.3-2: Comparison of concentration of H₂DCFDA probe and correlation to standard curve of serial dilutions of t-BHP.

Cells were incubated with either 25µM (black circles) or 100µM (white circles) H₂DCFDA for 60 min and then fluorescence was recorded. R² values for correlation to the linear trendline are shown. Results represent the average of quadruplicate determinations. Error bars indicate SEM.

Several concentrations of probe were used to assess whether there was a difference in accuracy according to concentration of the probe. There appeared to be good correlation between the concentration of t-BHP added to the system and fluorescence with either concentration of probe. The dynamic range at the lower concentration was however reduced (difference between no t-BHP and 50µM t-BHP was approximately a 50% increase in the lower concentration, compared with more than 100% in the higher concentration).

H₂DCFDA was used at 25µM, rather than previously-published 100µM in order to reduce the potential effect of the solvent, ethanol, on results and was equally effective as the higher dose.

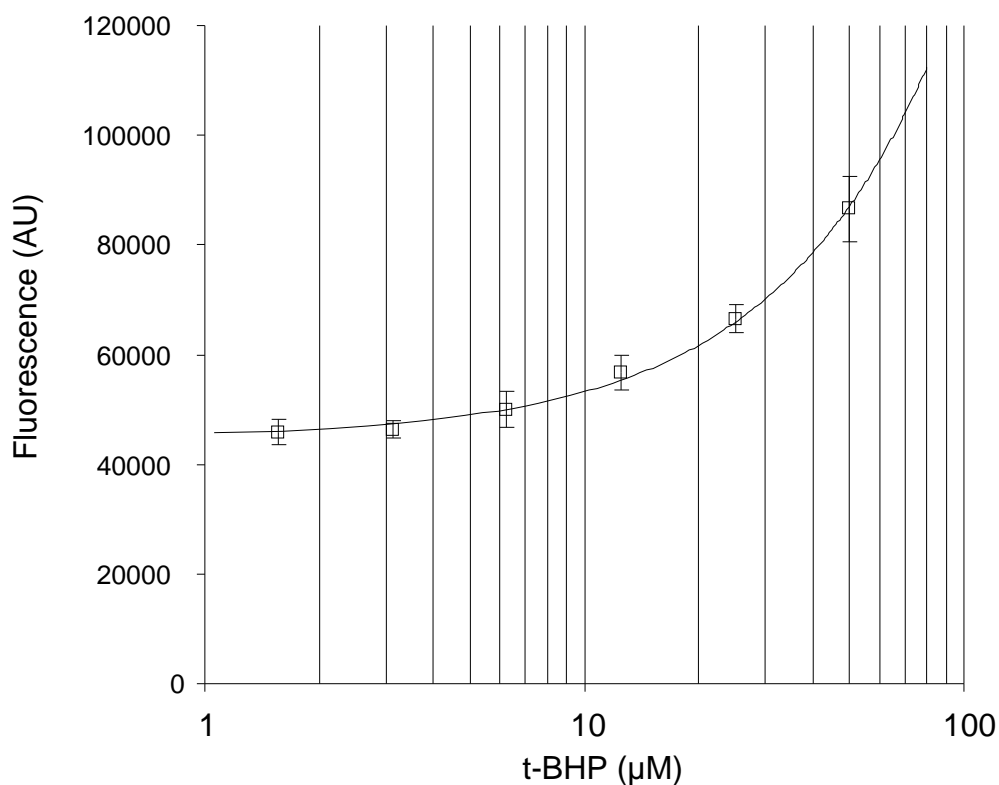


Figure 4.3-3: Dose response curve for the effect of t-BHP on the generation of DCF.

Graph shows a dose response curve of HUVEC exposed to 25µM H₂DCFDA and then t-BHP. X-axis is logarithmic. R² values for correlation to the linear trendline = 0.9968. Error bars indicate standard error of the mean.

Assays of the effect of t-BHP on ROS production in HUVEC revealed a linear dose response within the ranges of 1.5625-50µM t-BHP as shown above. This experiment was performed using 3 separate cell populations. Averages of 3 wells were used to generate SEM. Using Microsoft Excel, calculated trendline formula is $y = 846.64x + 44.7 \times 10^3$ with a correlation R² value of 0.9968. The baseline fluorescence of greater than 40×10^3 arbitrary units may represent baseline cellular production of oxidative species.

The use of a standard curve in this manner would help to compare between replicates and allow the use of equivalent amounts of oxidative stress to be induced by different pharmacological agents.

4.3.1 The effect of antioxidants on preventing DETA-NO-induced increases in generation of ROS in HUVEC

The effect of DETA-NO on ROS generation was tested against the various antioxidants. Experimental design was identical, using 3 separate cultures of early passage HUVEC and measuring peak fluorescence at 60 minutes.

Using the calculated trendline from the dose response curve from t-BHP, the addition of DETA-NO 0.5mM increased ROS production to an equivalent of t-BHP 19.4 μ M. The addition of N-acetyl cysteine 4mM or uric acid 150 μ M significantly reduced measured ROS generation in control cells (Control vs NAC p=0.003, Control vs UA p=0.01, by two sample t-test) and in cells exposed to DETA-NO (DETA-NO vs DETA-NO + NAC p=0.03, DETA-NO vs DETA-NO + UA p=0.04). No significant difference in ROS generation was observed in the panel of cells treated with selenomethionine 30 μ M.

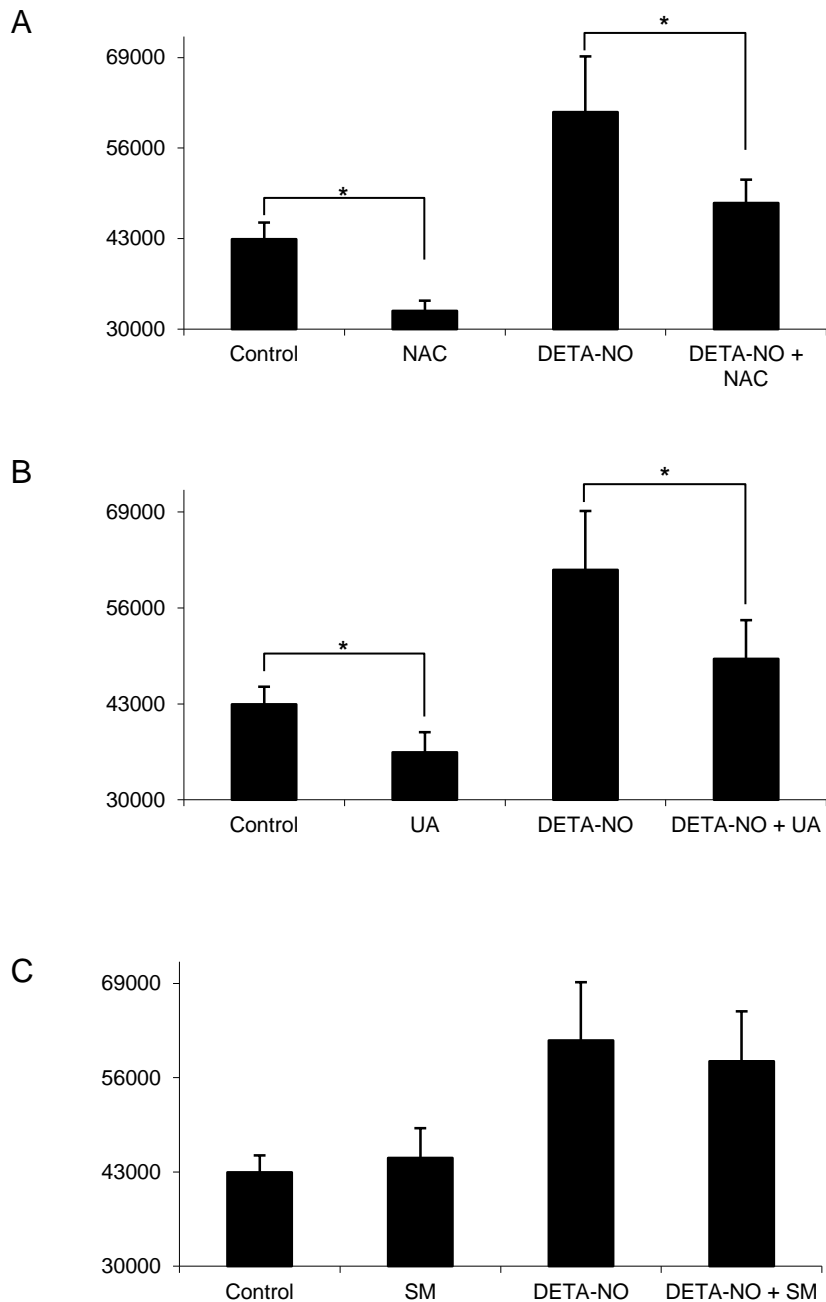


Figure 4.3.1-1: Interaction between DETA-NO and selected antioxidants: ROS generation.

Fluorescence after exposing the cultures to H_2DCFDA . A: Interaction between DETA-NO and NAC. B: Interaction between DETA-NO and uric acid. C: Interaction between DETA-NO and selenomethionine. Error bars indicate standard error of the mean and callipers with asterisks indicate significant differences between conditions as analysed by t-test. Results of 3 separate populations of HUVEC exposed to DETA-NO and antioxidants.

In order to ascertain if the effect was due to nitric oxide, rather than an effect of another product of the breakdown of DETA-NO, the experiment was repeated with GSNO. GSNO was able to increase measured ROS production in a similar manner to DETA-NO. The effect of NAC on the observed increase in ROS production was

also assessed. This experiment was carried out using two separate cultures and 4 wells per condition. GSNO 1mM exerted a similar effect on the fluorogenic probe, suggesting equivalence with DETA-NO 0.5mM. However, contrary to experiments performed using DETA-NO, the addition of N-acetyl cysteine increased this effect, reaching statistical significance.

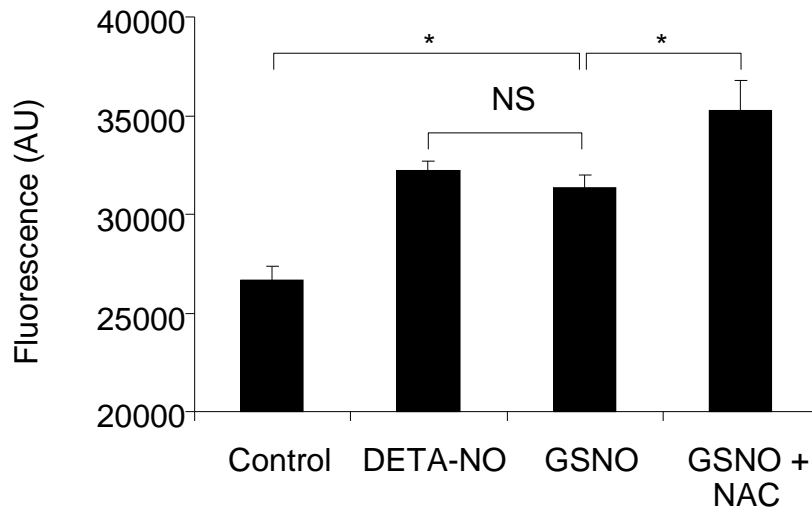


Figure 4.3.1-2: Comparison of the effect of nitric oxide donors and NAC on ROS generation.

The above figure shows the results of 2 separate experiments using 2 populations of HUVEC exposed to DETA-NO 0.5mM, GSNO 1mM or GSNO 1mM with NAC 4mM. Analysis of ROS generation was performed using fluorimetry with the ROS probe H₂DCFDA. Results are expressed as arbitrary units and error bars indicate standard error of the mean. Callipers indicate statistical comparison and asterisks indicate p<0.05 as analysed by t-test. NS = non-significant.

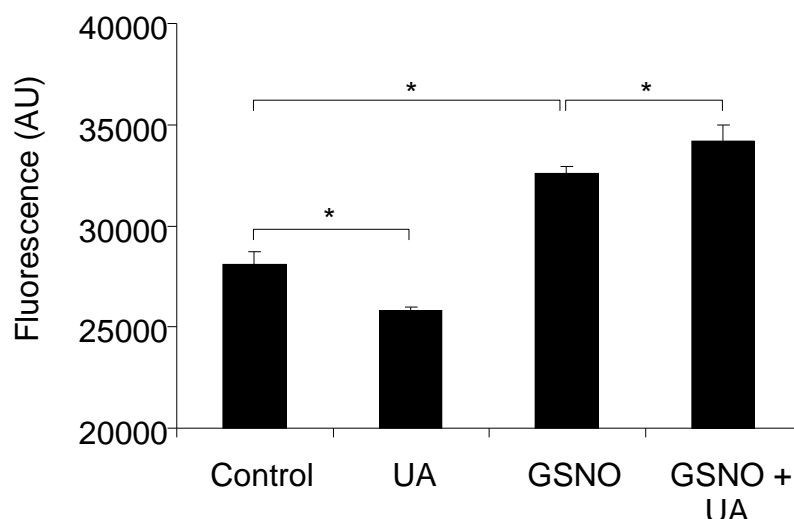


Figure 4.3.1-3: Interaction between GSNO and UA: ROS generation.

The above figure shows the results of a single experiment using HUVEC analysed using 4 wells each. Cells were exposed to uric acid, GSNO 1mM or uric acid and GSNO 1mM and compared to control cells for their ability to generate ROS. ROS was measured by the fluorogenic probe H₂DCFDA and detected using a fluorimeter. Error bars indicate standard error of the mean. Callipers indicate statistical comparison and asterisks indicate occasions where t-test analysis shows $p < 0.05$.

To investigate whether the observed increase in ROS production with GSNO and NAC was due to the presence of a glutathyl-containing antioxidant (NAC), the experiment was repeated using a non-glutathyl-containing antioxidant which was effective at reducing DETA-NO-induced ROS generation. Uric acid interacted with GSNO in a similar manner to NAC, failing to prevent GSNO-induced ROS generation. The experiment was repeated on a single culture of HUVEC with 4 wells per condition. GSNO (1mM) increased ROS production, measured by the fluorogenic probe H₂DCFDA and uric acid was able to decrease the baseline measured ROS production in control cells. However, uric acid was unable to reduce the ROS generated by GSNO and led to a small but statistically significant increase in ROS production by GSNO.

The experiment was repeated with t-BHP as the source of ROS. t-BHP was used at the concentration of 20 μ M in order to achieve the same magnitude of ROS production as seen in 500 μ M DETA-NO. The addition of NAC was enough to reverse the effect of t-BHP on ROS production. In fact, this was enough to reduce measured ROS production to below that seen in control cells.

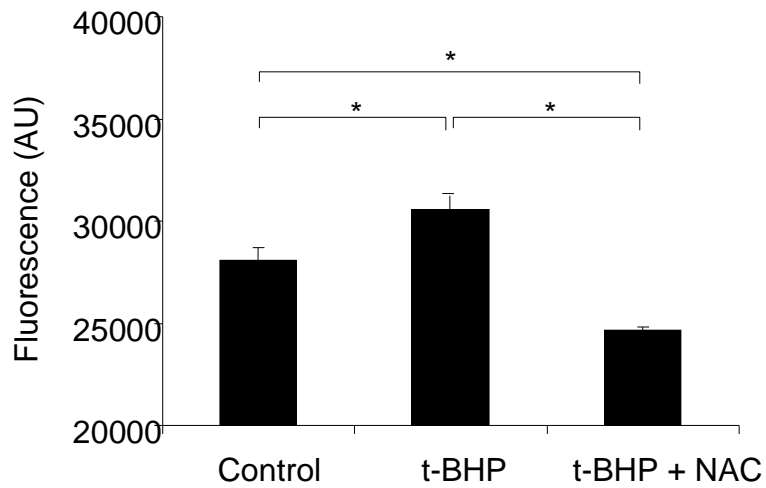


Figure 4.3.1-4: Interaction between t-BHP and NAC: ROS generation.

Assessment of the effect of ROS generation by t-BHP20 μ M and its reversibility by the antioxidant NAC. The experiment was performed on 2 separate occasions using 4 wells per condition and using 2 separate populations of HUVEC. Error bars indicate standard error of the mean. Callipers indicate statistical comparison. Asterisks indicate statistical significance ($p < 0.05$) as analysed by t-test.

I was unable to replicate the increase of ROS generation via eNOS activation with the calcium ionophore A23187. The experiment was repeated in this way to assess whether endothelial cells were capable of producing sufficient nitric oxide to be detected using this model, assessing the physiological relevance of this series of experiments. Data shown are from 2 separate cell populations and each condition was measured in 4 wells.

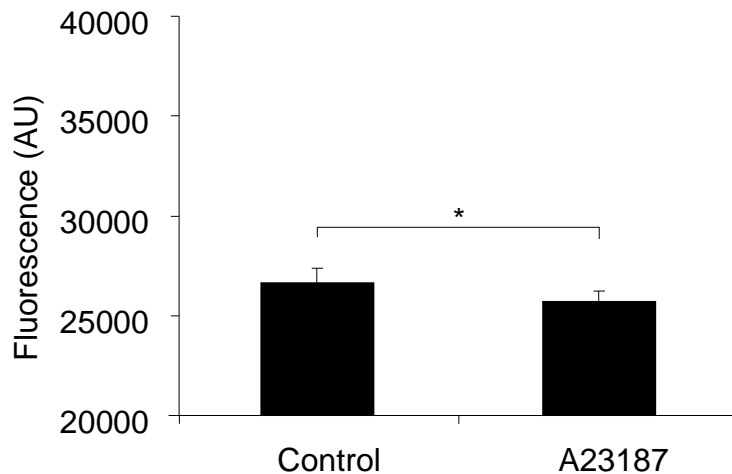


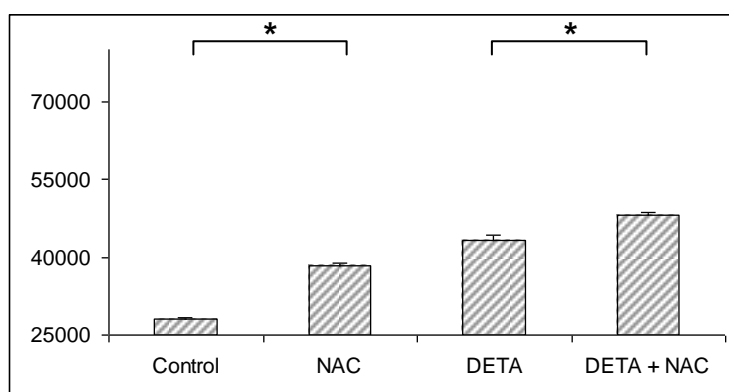
Figure 4.3.1-5: Effect of the calcium ionophore, A23187 on ROS generation by HUVEC.

The above figure shows the result of 2 separate experiments using 2 separate populations of HUVEC to assess the effect of A23187 1 μ M on ROS generation as measured by the fluorogenic probe H₂DCFDA. Each condition was performed in 4 wells. Error bars indicate standard error of the mean. Callipers indicate statistical comparison. Asterisk indicates statistical significance ($p < 0.05$) as analysed by t-test.

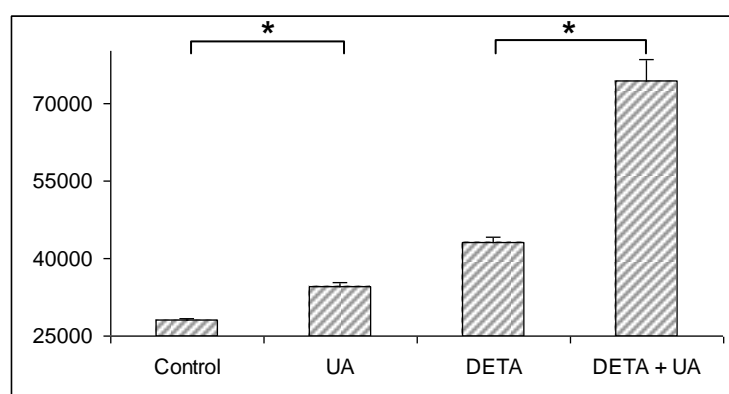
In order to assess the ability of the stressors to oxidize the fluorogenic probe in the extracellular environment, the experiment was repeated by adding the probe to a solution containing the stressors in medium without cells. The wells were not washed to clear the fluorogenic probe, unlike in experiments performed with cells. DETA-NO was able to oxidize the fluorogenic probe, as was NAC and uric acid. Selenomethionine had no effect. Uric acid seemed to have an additive effect on DETA-NO.

This experiment excluded the possibility that the observed reduction of fluorescence after exposure to the fluorogenic probe H₂DCFDA seen in cells treated with NAC and uric acid could be due to probe leaking from the cells or failure of the washing stage to clear the outside of cells of fluorogenic probe prior to adding the various reagents for the experiment.

A



B



C

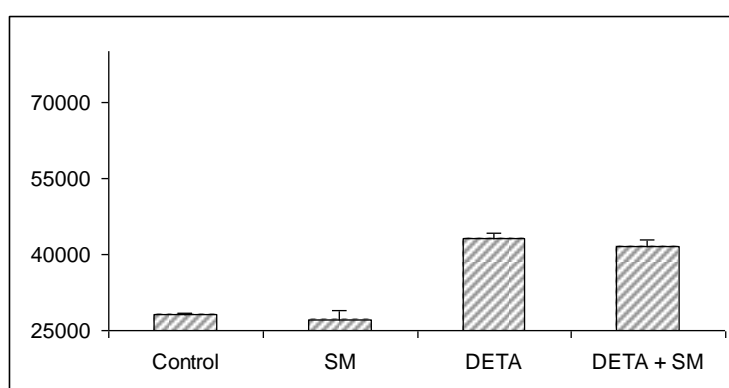


Figure 4.3.1-6: Assessment for interaction between reagents and fluorogenic probe H₂DCFDA in cell-free conditions.

The figures above show the results of a single experiment performed using 4 wells per condition and comparing the ability of the reagents to generate fluorescence in the presence of the fluorogenic probe H₂DCFDA but in the absence of cells. On this occasion, the probe was not washed after pre-incubation, in contrast to experiments performed in the presence of cells. Error bars indicate standard error of the mean. Callipers indicate statistical comparison. Asterisks indicate statistical significance ($p < 0.05$) as analysed by t-test.

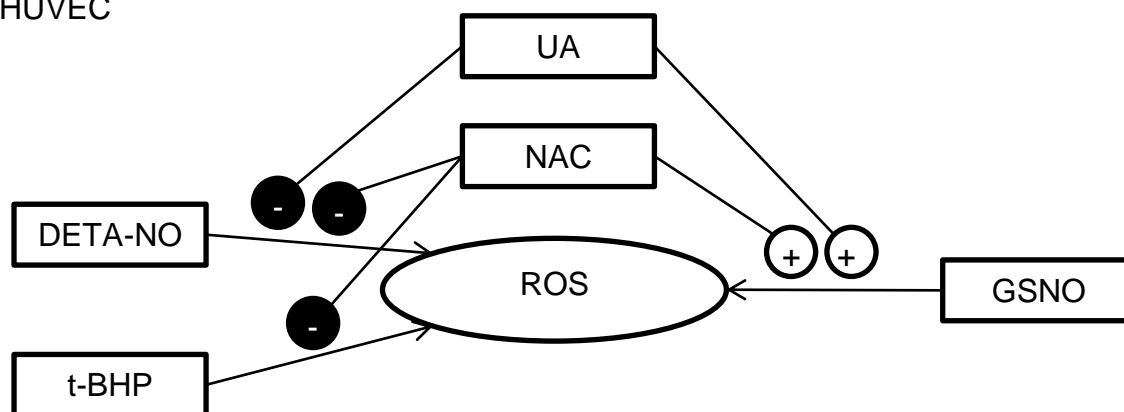
The figures above show the effect of the experimental reagents on the fluorogenic probe in a cell-free environment. There was a significant increase in fluorescence compared to control in all reagents except selenomethionine (SM) (Control vs DETA-NO, $p=0.001$; Control vs NAC, $p<0.001$; Control vs UA, $p<0.001$). The selected antioxidants increased or had no effect on fluorescence generated by DETA-NO (DETA-NO vs DETA-NO plus NAC, $p=0.002$; DETA-NO vs DETA-NO plus uric acid, $p=0.005$; DETA-NO vs DETA-NO plus selenomethionine $p=NS$). All p values calculated using Microsoft Excel students unpaired 2-tailed t-test assuming unequal variance.

Experimental reagents were also assessed for their ability to fluoresce without probe and universally had no effect on fluorescence in this range of light wavelength.

4.4 Conclusion

We started this chapter with the aim to demonstrate the effect of nitric oxide donors and the pro-oxidant tBHP on ROS generation in HUVEC. In concert, we investigated the interaction of these pro-oxidant drugs with antioxidants.

A HUVEC



B Cell-free system

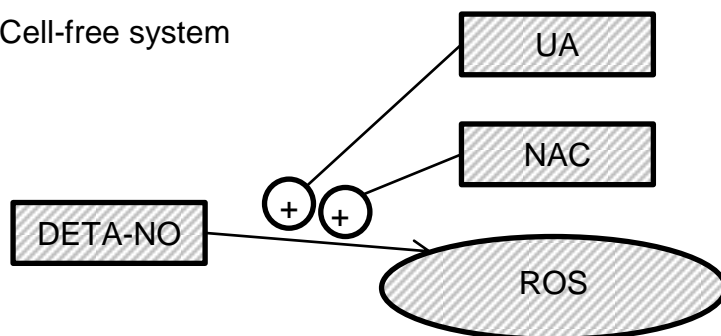


Figure 4.3.1-1: Schematic diagram of experimental results investigating the effect of oxidative and nitrosative stressors on generation of ROS.

H₂DCFDA requires a deacetylation to be activated and this occurs in cells. Therefore, the probe ought to be able to detect intracellular ROS. However, in my cell-free experiment, I saw an increase in fluorescence with DETA-NO. The amount of available H₂DCFDA was much greater in this experimental set-up as there was no washing step and in addition, the interaction between DETA-NO and antioxidants was not consistent with experiments performed in the presence of HUVEC. Therefore it is likely that nitric oxide donors are able to increase ROS production in HUVEC. This can be reversed in the case of DETA-NO by adding antioxidants NAC and UA. However, this is not seen when the nitric oxide donor is GSNO. At the concentration studied, GSNO was able to exert a similar magnitude of oxidation of H₂DCFDA as seen with DETA-NO but this could not be prevented by either NAC or UA.

If nitric oxide was directly interacting with the fluorogenic probe, and NAC and UA were able to prevent this, the GSNO series of experiments raises a question as to whether GSNO interacted with H₂DCFDA via an additional, second mechanism. I had postulated that this may be by generation of the glutathyl radical, explaining why increasing the availability of glutathione by adding NAC would not reduce ROS generation. However, UA was also unable to prevent GSNO increasing ROS generation.

The lack of effect seen with selenomethionine suggests that the increase in ROS generated by DETA-NO was not mediated by peroxynitrite.

Furthermore, NAC was able to reduce non-nitric oxide-induced ROS generation via its interaction with t-BHP. Finally, NAC was not able to reduce the DETA-NO effect on the fluorogenic probe in a cell-free environment.

The attempt to increase nitric oxide production via the addition of the calcium ionophore and eNOS activator, A23187 produced no observable effect and is disappointing when considering if the observed effect of DETA-NO on endothelial cells would be physiologically relevant.

5 The influence of nitric oxide on senescence in human vascular cells

5.1 Introduction

Nitric oxide is a reactive nitrogen species, capable of generating reactive oxygen species and an important signalling molecule in human vascular cells. Reports have suggested that it may have an effect on senescence, or may be generated in phenotypically young endothelial cells and can therefore be associated with or may help maintain endothelial cells in their young phenotype.

However, the cumulative effect of years of exposure to such a molecule which is able to diffuse freely throughout all cell compartments by crossing membranes without the need for permissive channel opening or transporters, may yet be deleterious. Moreover, the role of nitric oxide as a toxic agent in inflammation, a process which when activated is able to generate higher concentrations of nitric oxide, may result in unintended spill-over and damage to healthy tissue.

Finally, nitric oxide donors and nitric oxide itself are used in human medicine as systemic and pulmonary vasodilators and venodilators and thus any potential long-term effects of high doses of nitric oxide on the vasculature are important to elucidate.

5.2 Aims

Given previously published evidence that nitric oxide can exert an effect on cell senescence, I aimed to reproduce this in a reliable manner. Having achieved this, I planned to assess the range of concentrations of nitric oxide associated with changes in cell senescence.

If nitric oxide is able to influence senescence, we will explore the mechanism responsible by looking at pharmacological manipulation of targets of nitric oxide, reducing the effect of nitric oxide in generating reactive oxygen and nitrogen species and by assessing the effect of antioxidants and peroxynitrite scavengers. In addition, we will assess the effect of cold light, a factor known to reduce protein transnitrosation.

Where an effect was observed, multiple methods were used to confirm and to measure senescence. The mechanism by which senescence was achieved or prevented would then be assessed.

5.3 The influence of nitric oxide on senescence

5.3.1 Effect of DETA-NO on HUVEC senescence

We investigated the effect of nitric oxide on HUVEC by treating cells with the nitric oxide donor DETA-NO. This compound generates a steady concentration of nitric oxide which is maintained over a period of several hours. Cells were grown to confluence and then DETA-NO was added to cell culture by daily change of medium during three consecutive days. Cells were disassociated using trypsin/EDTA and were analysed in the Coulter particle analyser for number and diameter. Cells were then replated at the same density and grown for a further 3-4 days in normal medium only. Prior attempts to expose cells to concentrations of nitric oxide during the exponential growth phase led to growth arrest and cells were too sparse for analysis. Cells exposed to 0.01mM or 0.1mM DETA-NO showed no discernible change from control but doses of 0.5mM produced a significant increase in cell diameter.

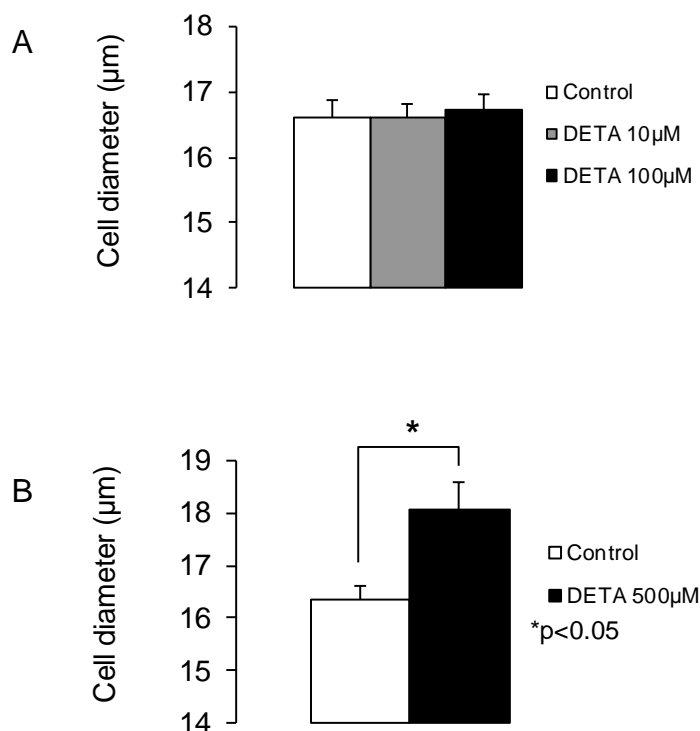


Figure 5.3.1-1: Effect of DETA-NO on cell diameter.

Effect of varying doses of DETA-NO on cell diameter measured by particle analyser. The upper graph (A) is the mean of 5 identical populations of cells and the lower graph (B) is the mean of 4 experiments. Error bars indicate standard error of the mean. Callipers indicate statistical comparison using t-test where the result was statistically-significant ($p < 0.05$).

The experiment was repeated following the same culture protocol and then cells were analysed for total β -galactosidase activity by flow cytometry using the C₁₂FDG fluorogenic probe.

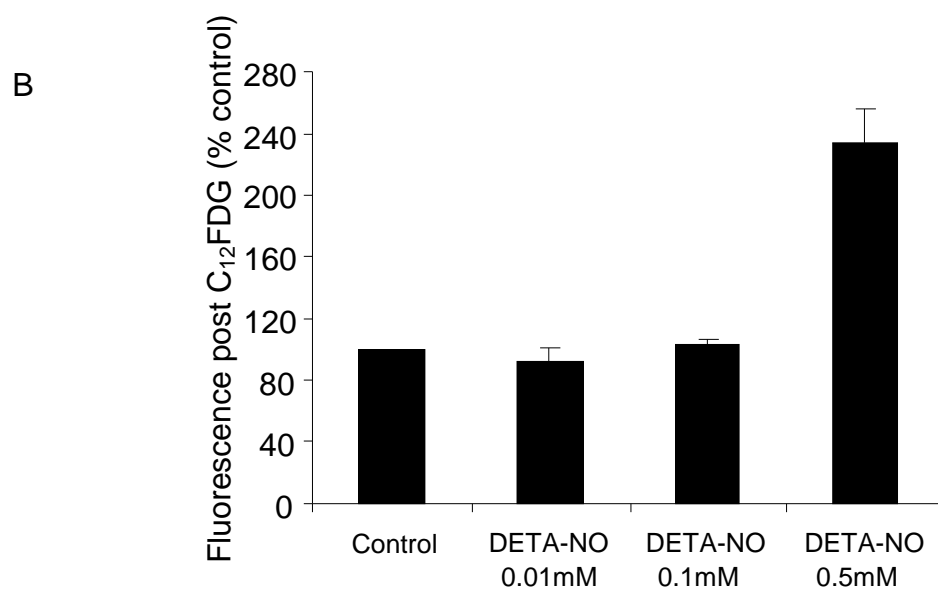
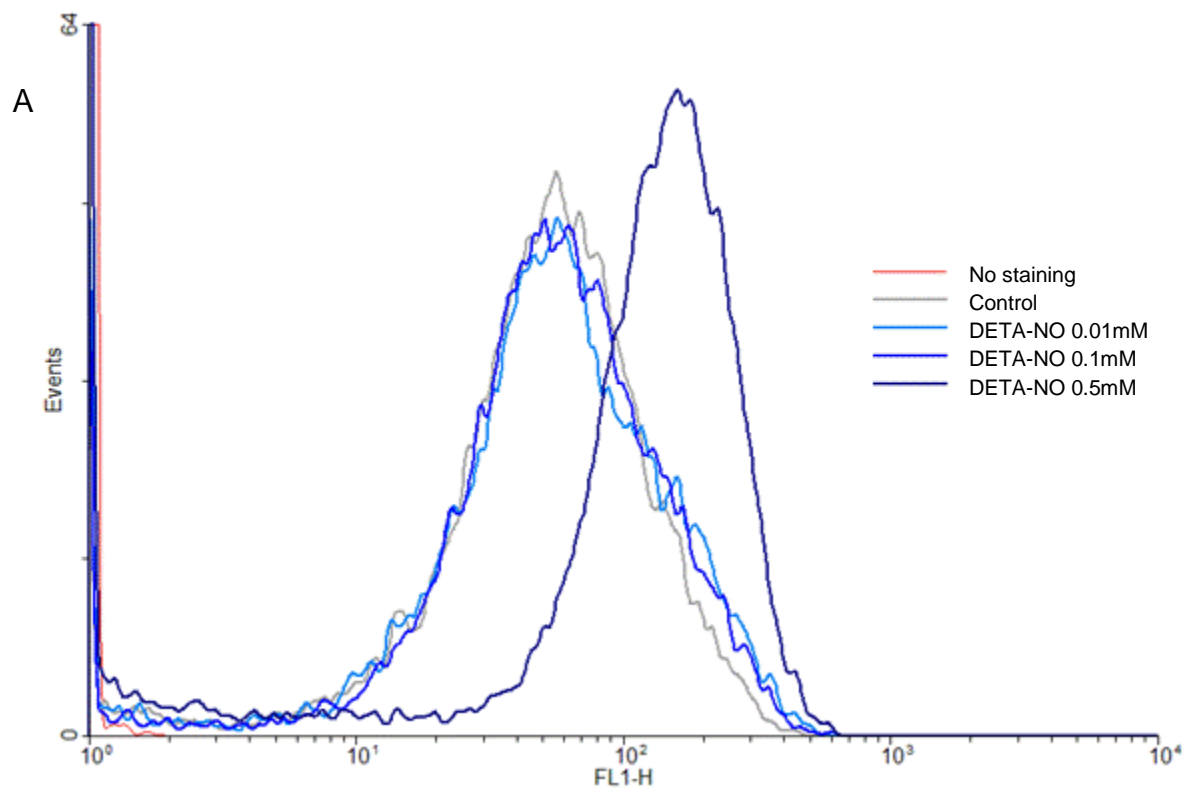


Figure 5.3.1-2: Dose response for the effect of DETA-NO on β -galactosidase activity.

Cells were treated with various concentrations of DETA-NO as indicated in the main text and β -galactosidase activity was measured by flow cytometry. Panel A shows an overlay histogram from a representative experiment. Panel B shows the relative fluorescence expressed as a percentage of the values measured in untreated cells. Results represent the mean \pm SEM of 3 separate experiments

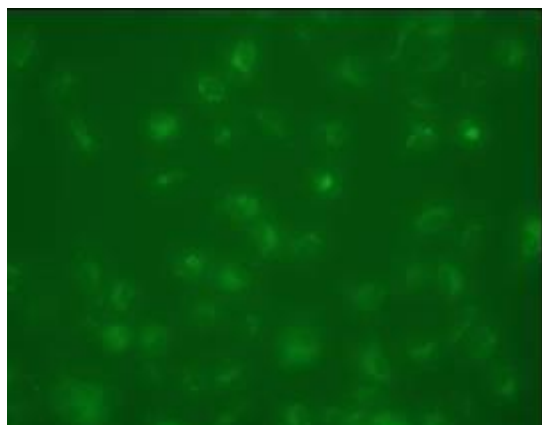
The overlay histogram in panel A (above) shows the un-gated result obtained from a representative experiment. The X-axis is the FL1-H channel which denotes

fluorescence post C_{12} FDG exposure in this case and the Y-axis is related to the number of events counted by the cytometer. There is little difference between the cells in the control group and the cells treated with lower doses of DETA-NO. However, there is a clear shift to the right in cells treated with 0.5mM DETA-NO. The shift in those cells is generalised, rather than there being a new separate sub-population, distinct from the baseline control group. This generalised increase in fluorescence post C_{12} FDG exposure is consistent with either there being a cell phenotype between healthy and senescent or, more likely, that senescence starts with a fundamental change in cellular physiology with irreversible cell cycle arrest, followed by the accumulation of β -galactosidase which increases gradually until a new equilibrium is met. Non-stained samples were performed on each occasion to confirm that the shift was not due to an increase in the intrinsic fluorescence of the cells. Samples were gated to exclude cell debris and analysed using geographic mean. Results were analysed for statistical significance using Microsoft Excel two-tailed t-test assuming unequal variance.

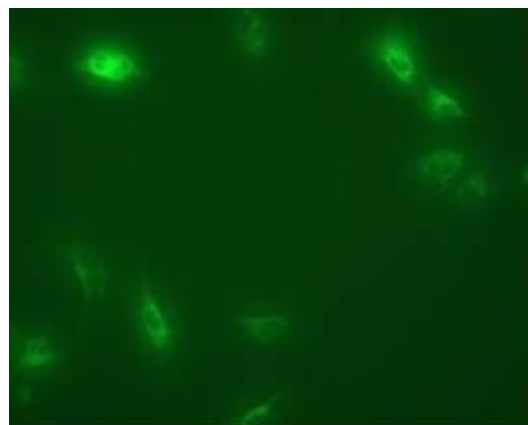
There was no significant decrease in fluorescence post C_{12} FDG exposure between control and DETA-NO 0.01mM or 0.1mM treated cells (mean fluorescence 0.01mM 92% of control, $p=0.21$; 0.1mM 103.6% of control, $p=0.13$, by two sample t-test). There was a large, significant increase in fluorescence post C_{12} FDG exposure between control and DETA-NO 0.5mM treated cells (mean fluorescence 233.6% of control, $p=0.007$).

In a separate experiment using the same technique of exposing cells to DETA-NO 0.5mM, cells were treated with C_{12} FDG and then washed in PBS and photographed. On the following page are fluorescence and light micrographs of HUVEC from the same donor. Cells treated with DETA-NO failed to recover their replicative ability and there was an increased fluorescence intensity of the fluorogenic product of the β -galactosidase reaction with C_{12} FDG. Cells treated with DETA-NO also had a larger diameter, consistent with previous experiments.

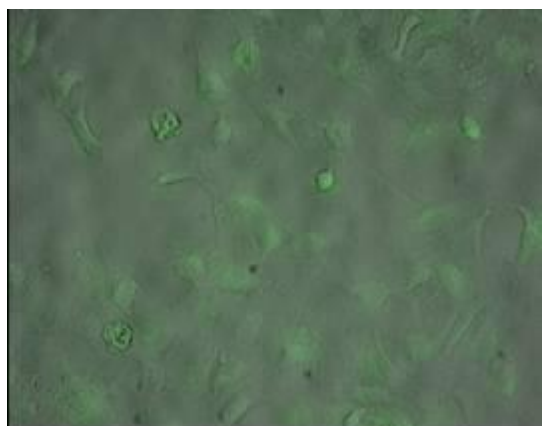
Control



DETA-NO 0.5mM



Control merged images



DETA-NO 0.5mM merged images

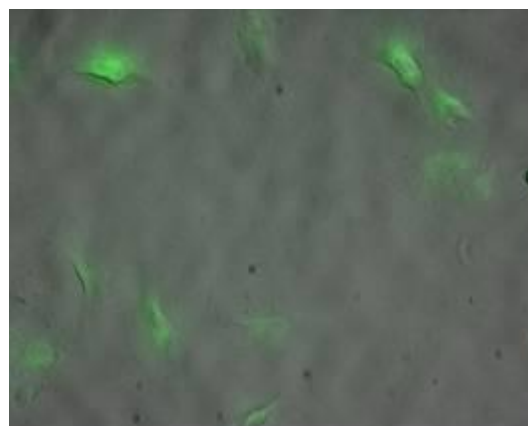


Figure 5.3.1-3: Micrographs of fluorescence post C₁₂FDG exposure: DETA-NO.

Light and fluorescent micrographs of cells stained with C₁₂FDG and later excited with UV light to demonstrate the fluorescent-labelled product of the reaction between C₁₂FDG and β -galactosidase. Both groups of cells were harvested and replated at the same density in normal medium without DETA-NO. Cells were photographed 3 days after replating. Merged pictures are shown for illustration and were created using Photoshop CS. Background was removed from both images using the same adjustment (input 84, 1.00, 255) and the overlaid fluorescent image was adjusted to 50% opacity.

5.3.2 Assessing nitric oxide-mediated HUVEC and HUASMC senescence by senescence-associated β -galactosidase

The photomicrographs below show the effect of nitric oxide donors on the appearance of senescent cells as detected by staining for senescence-associated β -galactosidase. In this case nuclear red staining was used to contrast the blue β -galactosidase staining with a red DNA stain for ease of visualisation.

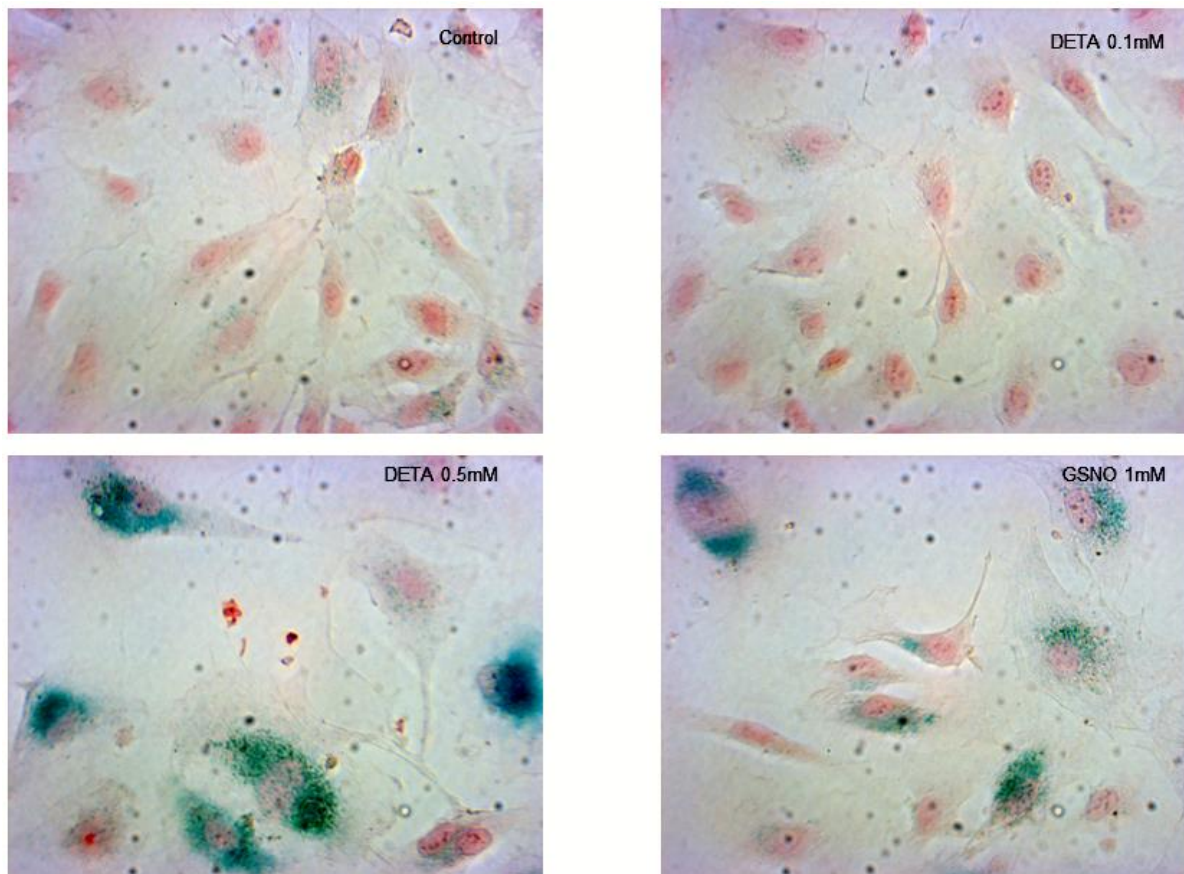


Figure 5.3.2-1: Comparison of the effect of nitric oxide donors on senescence-associated β -galactosidase.

3rd passage HUVEC were exposed to DETA-NO or GSNO on 3 consecutive daily changes of medium, rested for 2 days, then stained for senescence-associated β -galactosidase activity and counterstained with nuclear red solution to identify the nuclei. Photographs were taken under the same magnification and images were processed with the Windows Live Photo Gallery application (Microsoft Corporation) using an auto-adjust filter on all 4 panels simultaneously to ensure the same adjustment.

Consistent with the induction of senescence, cultures treated with high concentrations of nitric oxide donors show the presence of flat, enlarged and intensely blue-stained cells. In contrast cells treated with a low concentration of nitric oxide show a normal morphology and no or faint β -galactosidase staining. The presence of these lightly stained β -galactosidase positive cells may either be stressed or senescent. This illustrates the difficulty in discerning between senescent and non-senescent cells when counting cells by visual inspection.

In order to assess whether the observed effect of nitric oxide donors on senescence-associated β -galactosidase could occur in other cells types, HUASMC were grown from explant and passaged twice before exposure to various doses of DETA-NO on exchange of medium every 2 days and stained after 7 days of this regime followed by microscopic examination.

At the end of the exposure period, cells were stained for senescence-associated β -galactosidase.

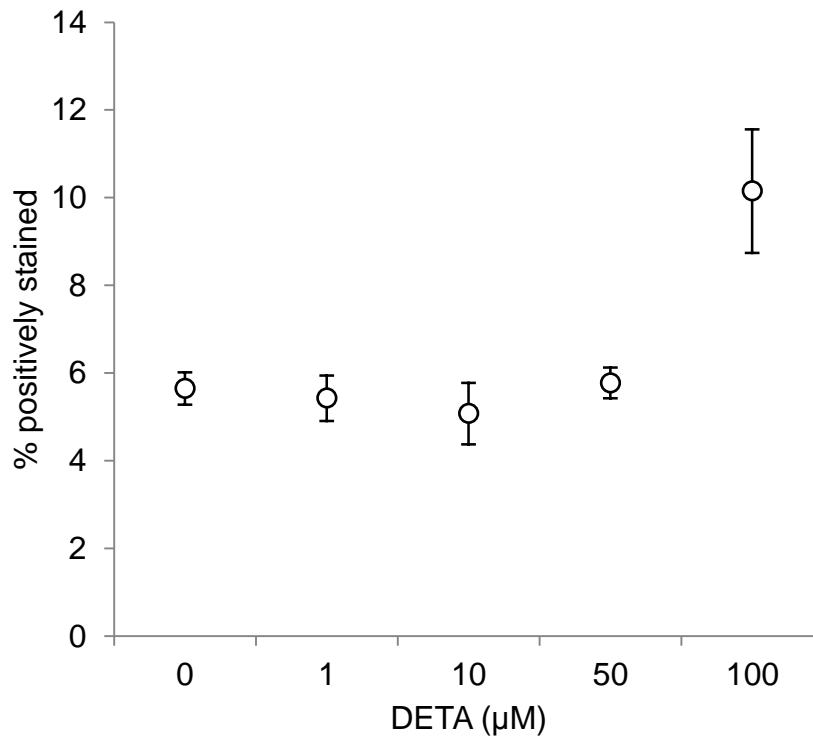


Figure 5.3.2-2: Dose-response for the effect of DETA-NO on the induction of senescence in cultures of HUASMC.

Cells were treated with various concentrations of DETA-NO as indicated in the main text and β -galactosidase activity was measured by cytochemistry using X-gal. Results represent the percentages of positively-stained cells (mean \pm SEM of 4 replicate wells for each concentration of DETA-NO and 8 replicate wells for the control group).

4 separate fields of view were counted using phase contrast light microscopy at 20 x magnification from 4 wells of each condition (except control where 8 wells were used). The figure above shows that at relatively low concentrations (1-50 μ M), DETA-NO did not increase the percentage of senescent cells beyond that present in untreated control cells. In contrast at 0.1mM DETA-NO caused a significant increase in the percentage of senescent cells (10.2 \pm 1.4, $p=0.05$). The small decrease in the percentage of senescent cells seen with 0.01mM DETA-NO was not statistically significant, ($p=0.5$).

Thus it appears that both HUVEC and HUASMC are prone to DETA-NO-induced increases in β -galactosidase activity. There also appears to be a greater sensitivity on the part of HUASMC. As previously discussed in section 1.3.3.4, this may be due to the presence of eNOS in HUVEC protecting against the effect of exogenous nitric oxide.

5.3.3 Senescence vs. apoptosis

The processes of senescence and apoptosis may be linked as they share signalling pathways. We investigated whether cells exposed to DETA-NO may have been preparing to undergo apoptosis via senescence. We added to the flow cytometry

method of assessing β -galactosidase activity by using additional fluorogenic probes for cell membrane markers of apoptosis (Annexin-V) and DNA staining (7-AAD), providing simultaneous assessments of cells for all 3 variables.

Cells were grown to confluence and treated 3 times for 3 consecutive days with DETA-NO 0.5mM in EGM-2 or EGM-2 alone. Following treatment, cells were rested in normal medium for 2 days, trypsinized and replated for final collection 3 days later. Cells were incubated with C_{12} FDG for 4 hours and then trypsinized and further incubated with either the DNA stain 7-AAD or Annexin-V-PE for 15 mins according to the manufacturer's protocol. Samples were placed on ice until analysis with a BD FacsCalibur. Results are shown in the figure below.

	No apoptosis	Early apoptosis	Late apoptosis	Necrosis
7-AAD / Ann V	- / -	- / +	+ / +	+ / -
Control	74%	22.8%	2.2%	1.0%
DETA-NO-treated	70.2%	25.2%	2.4%	2.2%

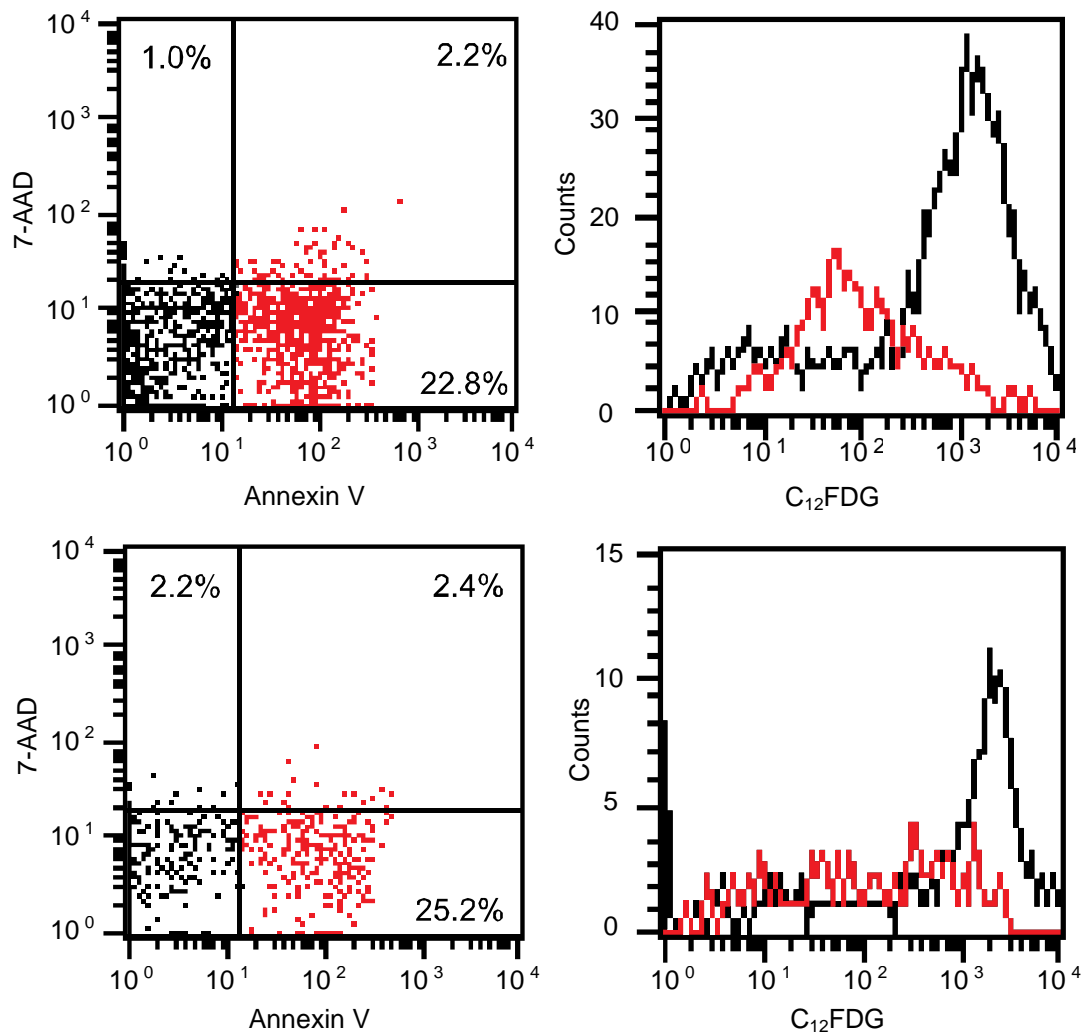


Figure 5.3.3-1: Effect of DETA-NO on senescence and apoptosis.

Cells were treated with DETA-NO as described in the text and then analysed by flow cytometry for simultaneous detection of senescence and apoptosis. C₁₂FDG is detected using the FL-1 channel, PE by FL-2 and 7-AAD by FL-4. Results from a representative experiment depicting the analysis of control cells (top panels) and DETA-NO treated cells (bottom panels) are shown. The dot plots on the left side show the distribution of apoptotic and non-apoptotic cells; quadrant boundaries were set with reference to a parallel unstained sample. The histograms on the right side correspond to the events gated in the respective right (red dots) and left (black dots) quadrants.

The figure on the previous page represents the results of a single pilot experiment to assess whether cells exhibiting a higher activity of β -galactosidase were also undergoing senescence. Red histogram plots represent cells exhibiting high Annexin V fluorescence whereas black plots are Annexin V negative. There is a small overall increase in apoptosis of the cells treated with DETA-NO. However, the cells which have an increased amount of β -galactosidase are less likely to display features of apoptosis. Of particular note, the Annexin V negative population in both cell samples contain all the high fluorescence C_{12} FDG senescent population of cells but fewer apoptotic cells as measured by cell surface Annexin-V.

5.3.4 Assessing nitric oxide-mediated HUVEC senescence by cell cycle protein expression

Cells were grown to confluence and then treated 3 times for 3 consecutive days with DETA-NO in EGM-2 or EGM-2 alone. Following treatment, cells were rested in normal medium for 2 days, trypsinized and replated for final collection 4 days later. Cells were lysed and sonicated and loaded onto SDS-PAGE gel using equal amounts of protein within experiments. Finally, following transfer onto membrane, cells were probed with antibodies against p16^{INK4a}, p21^{WAF} and α tubulin or actin as loading controls.

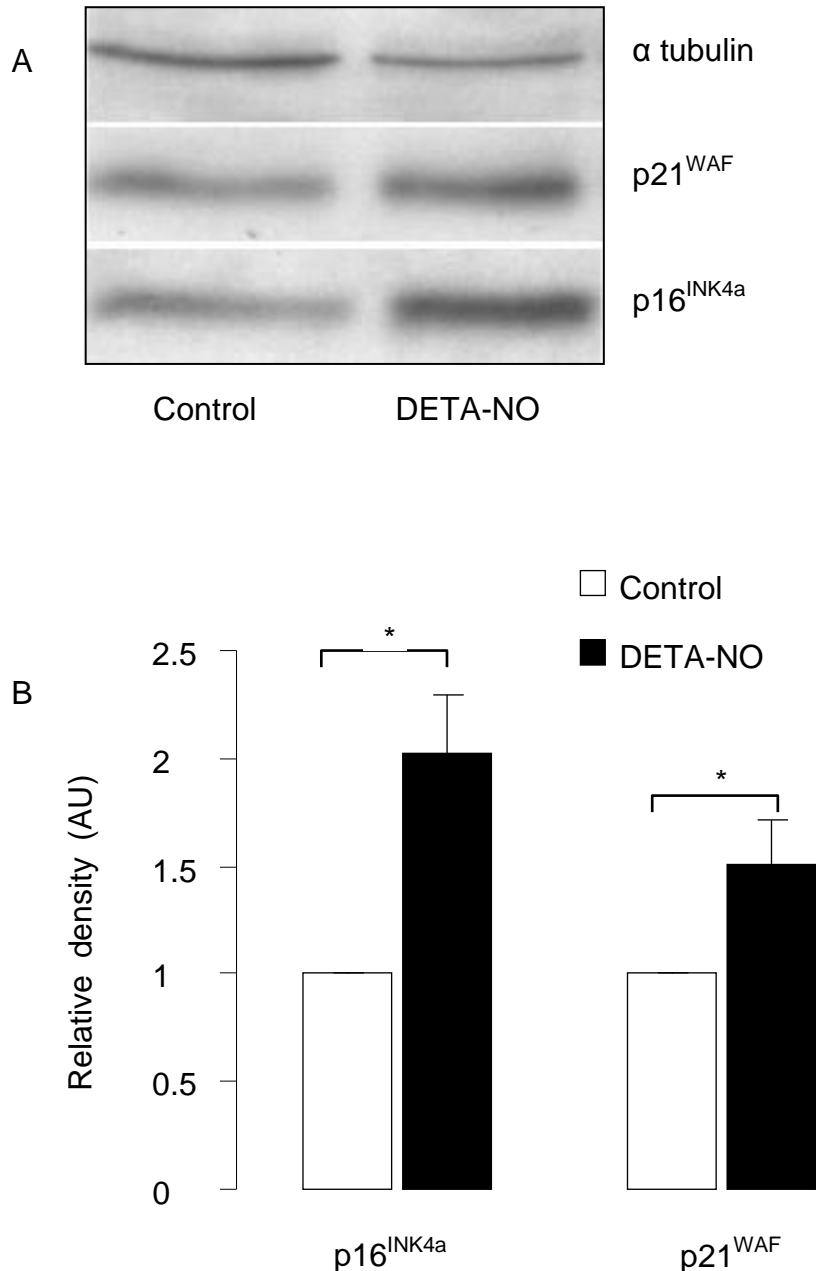


Figure 5.3.4-1: DETA-NO increases the expression of cyclin-dependent kinase inhibitors.

Western blot analysis of p16^{INK4a} and p21^{WAF} protein expression in control and DETA-NO-treated HUVEC. A representative immunoblot is shown on the top panel (A) and densitometric quantification is shown on the bottom panel (B). Results in the bottom panel represent the mean \pm SEM of 4 determinations for p21^{WAF} and 5 determinations for p16^{INK4a}, each from a different donor. Relative protein levels were calculated as the ratio of the intensity of the indicated bands to the intensity of the corresponding tubulin bands which were used as a loading control. Results are shown relative to control.

Densitometry was performed after scanning films from each experiment using AlphaEase software and the area of each band was used for the final calculation. Results confirmed a significant increase in p16^{INK4a} 2 times over control ($p=0.001$ by 2-sample t-test) and of 1.5 times for p21^{WAF} ($p=0.001$ by 2-sample t-test).

5.3.5 Assessing nitric oxide-mediated HUVEC senescence by measuring cell cycle arrest

Senescence is a form of growth arrest but it is not the only form of growth arrest. Our cells were treated in a confluent state. We wished to assess if the cells were simply quiescent or irreversibly in a state of growth arrest. Therefore, in order to assess if the increase in β -galactosidase activity seen in DETA-NO-treated cells represented cell cycle arrest, and not a transient increase in enzymatic activity, we assessed cells for BrDU incorporation after the usual rest period.

Cells were grown to confluence and then treated with DETA-NO as described previously. Following a 2 day rest period, cells were replated and finally harvested after 3 days.

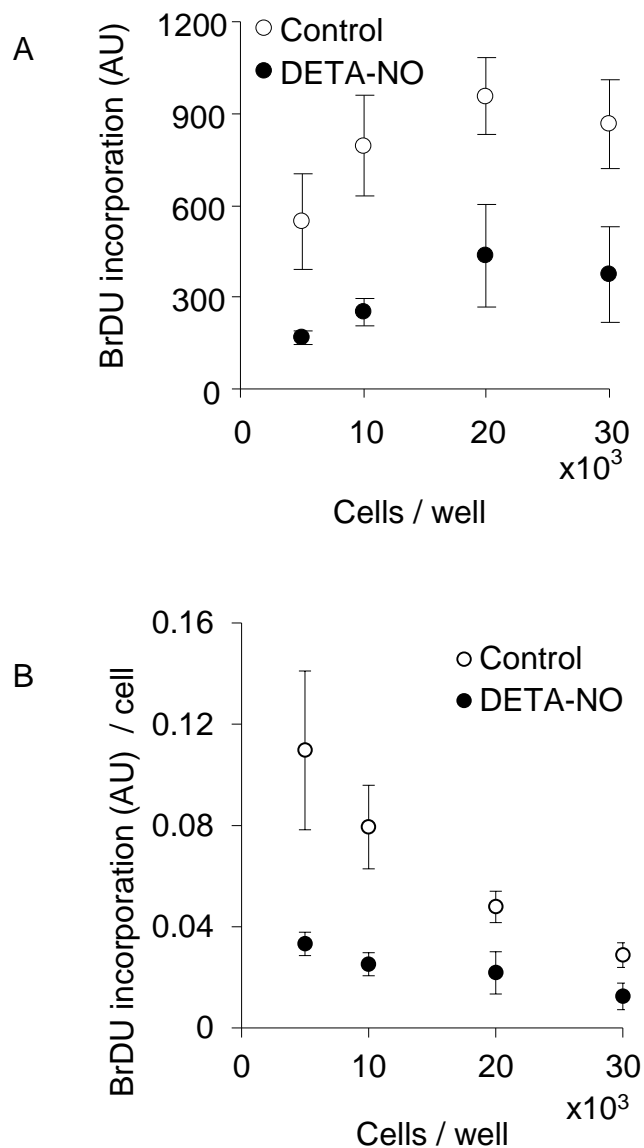


Figure 5.3.5-1: BrDU incorporation by cells exposed to DETA-NO vs. control.

Data were analysed in two forms. The top graph (A) shows total BrDU incorporation per well vs. the original plating density. The lower graph (B) shows the BrDU incorporation per cell vs. original plating density. DETA-NO dose was 0.5mM. Error bars in the upper graph indicate standard error of the mean.

An ELISA-based BrDU incorporation assay was carried out to assess proliferative activity and results are shown above. Cells were counted using the Coulter particle analyser to equalise the number of cells being analysed and several cell densities were used. Cells of same conditions and densities were plated in 4 replicates in a 96 well plate and analysed using a Spectramax plate reader every 5 minutes for 30 minutes in total. The calculations were based on the area under the curve of BrDU-induced colorimetric increase in the reagent.

The lower BrDU incorporation seen at the highest cell density is likely to represent contact inhibition. There is a clear difference in BrDU incorporation in cells previously treated with DETA-NO, when compared to those in the control group. This is despite a remote exposure to DETA-NO as the last exposure was 1 week prior to analysis. Using 10^4 cells per well as a representative result for analysis, average BrDU incorporation was 794.2AU in the control group and 251.7AU in the DETA-NO treated group, $p=0.02$ with 2 tail paired t-test assuming unequal variance. Analysis of the whole sample set by two-factor ANOVA confirmed this, $p=0.0001$.

5.3.6 Coculture of HUVEC with tet-iNOS HEK 293

The effect of high concentrations of nitric oxide released by DETA-NO or GSNO on endothelial cells *in vitro* may of course be of no physiological significance if cells are never exposed to such high concentrations *in vivo*. The hypothesis that this may occur during periods of inflammatory or infective stress and that iNOS-generated nitric oxide concentrations could be sufficient to induce the effects seen *in vitro* was investigated using a co-culture technique with a human embryonic kidney cell line (HEK-293) which was transfected with a tetracycline-inducible iNOS gene sequence. The cell line expressed iNOS in a dose-dependent manner, according to the concentration of tetracycline used to induce iNOS production.¹⁹⁸

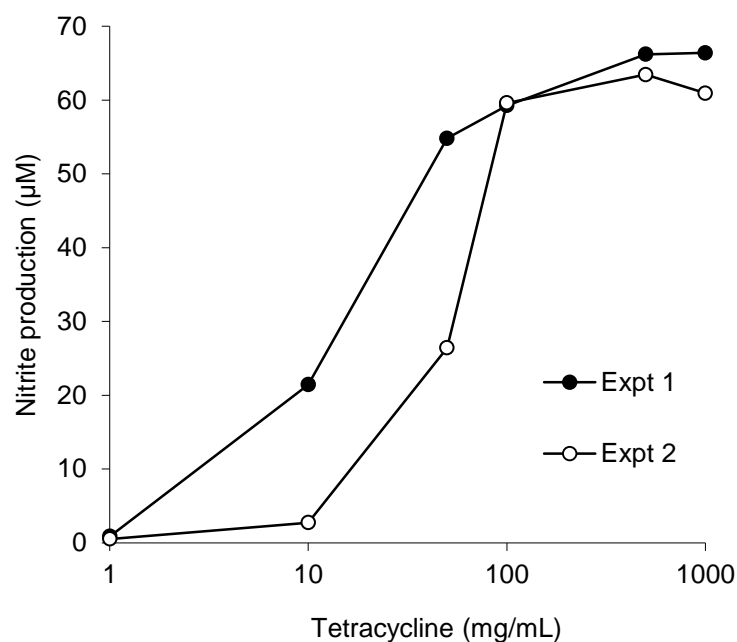


Figure 5.3.6-1: Confirmation of nitric oxide production after tetracycline-induction of iNOS.

Cells were exposed to tetracycline as described. Nitrite was measured by Griess reaction (data courtesy of M. Quintero, WIBR, UCL).

HUVEC were grown in 6 well plates to confluence. iNOS-HEK-293 cells were grown in Transwell inserts in separate 6 well plates. The Transwell has a porous

membrane which is small enough to avoid any cell escape but allows free diffusion of liquids in both directions. iNOS-HEK-293 cells were then induced to express iNOS by exposure to tetracycline and, after washing, were placed in the wells containing HUVEC and left in close contact co-culture for 3 days. Thereafter, medium was changed and the iNOS-HEK-293 Transwells were removed and discarded. Two days later, the HUVEC were replated in T-25 flasks and grown for 3 days before final analysis by flow cytometry.

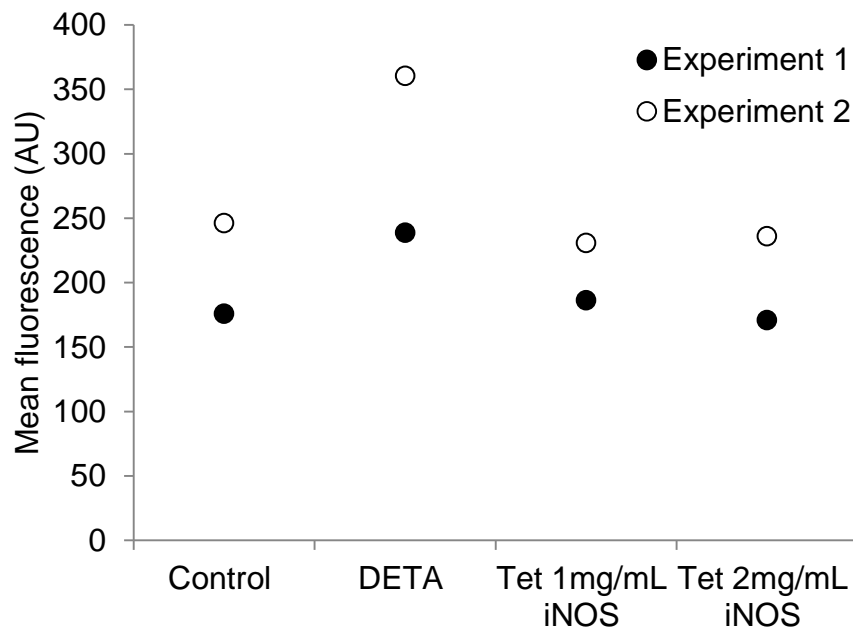


Figure 5.3.6-2: β -galactosidase activity of coculture of HUVEC with iNOS-expressing HEK-293.

Cells were exposed to 0.5mM DETA-NO or to cells induced to express iNOS after washing away the tetracycline inducer. “Tet *x*mg/mL iNOS” denotes the concentration of the dose of tetracycline used to induce iNOS expression in tetracycline-inducible, iNOS expressing HEK-293 cells. HUVEC were analysed for total β -galactosidase activity by flow cytometry. Results represent the 2 separate experiments using 2 separate populations of HUVEC and are shown as arbitrary units of fluorescence post C_{12} FDG exposure.

The figure above shows that as in previous experiments, there was a demonstrable increase in fluorescence (FDG) in the DETA-NO treated groups, but there was no increase in the fluorescent intensity in the tetracycline-induced iNOS HEK-293 exposed HUVEC. Despite the trend to a small decrease in FDG activity, statistical analysis by single-factor ANOVA gave a non-significant result ($p=0.76$).

Thus, this attempt to establish physiological relevance was unsuccessful. This may have been due to the inability provide cell to cell contact, or a sufficient proximity between the cells as may occur *in vivo*.

5.4 Assessing the potential mechanisms of nitric oxide-mediated HUVEC senescence

5.4.1 Soluble guanylate cyclase inhibition

Soluble guanylate cyclase acts as a receptor for nitric oxide and mediates many of its physiological effects. We investigated whether this was the mediator of the nitric oxide senescence effect by antagonizing its action using ODQ during exposure to DETA-NO.

The experiment was performed with a control group and either ODQ 0.3 μ M, DETA-NO 0.5mM or both ODQ and DETA-NO to a HUVEC population to assess the magnitude of soluble guanylate cyclase-mediated effects. Cells were analysed for size using a Coulter particle analyser. The figure below shows that there was a DETA-NO-induced increase in cell diameter even in the presence of ODQ compared to ODQ alone. The effect of DETA-NO was not significantly attenuated by the addition of ODQ to DETA-NO treated cells (two-tailed student's t-test $p=0.113$). There was no significant change in cell diameter induced by ODQ vs. the control group ($p=0.144$).

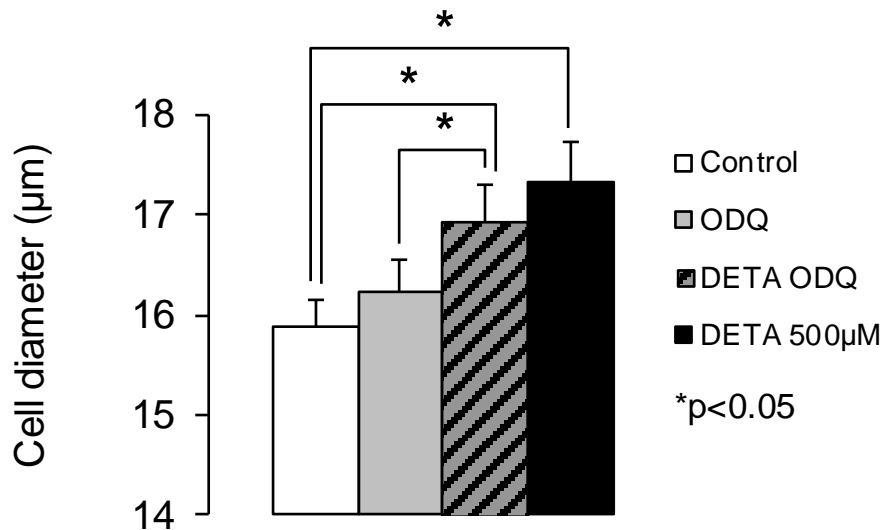


Figure 5.4.1-1: Effect of inhibiting soluble guanylate cyclase on the increase in cell diameter measured by particle analyser seen on exposure of HUVEC to DETA-NO.

Results represent the mean of five separate experiments with 5 separate populations of HUVEC. Cell diameter in µm is shown and error bars indicate standard error of the mean. Callipers indicate statistical comparison using t-test and asterisks indicate $p < 0.05$. ODQ indicates cells exposed to ODQ 0.3µM, DETA-NO dose was 0.5mM and DETA-NO ODQ indicates ODQ 0.3µM and DETA-NO 0.5mM.

Cells were replated for a further 3 days in order to allow exponential growth to be re-established. Cells were then treated with $C_{12}FDG$ and disassociated using trypsin/EDTA and transferred to FACS-compatible polystyrene tubes for FACS analysis. The next page contains a typical example of the results obtained.

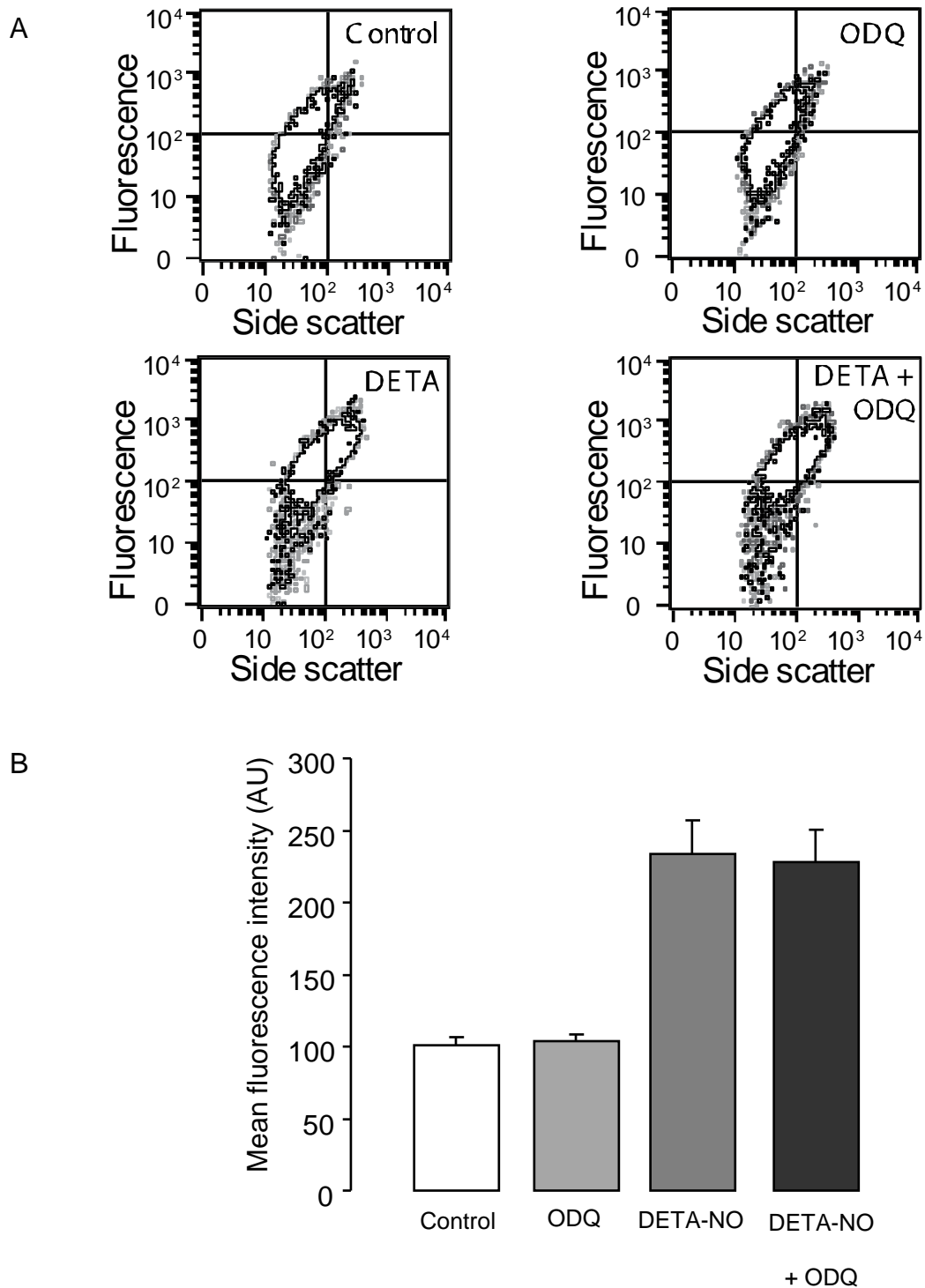


Figure 5.4.1-2: Effect of soluble guanylate cyclase inhibition on the induction of senescence by DETA-NO.

Cells were treated as described in the previous figure and then exposed to C_{12} FDG prior to flow cytometric analysis. Panel A is a representative density plot of fluorescence post C_{12} FDG exposure plotted against side scatter. Panel B shows the mean results of the effect of interventions to prevent the effect of DETA-NO on total β -galactosidase activity. Each experiment was carried out in triplicate on cells from three different donors. DETA-NO dose was 0.5mM, ODQ 0.3 μ M and NAC 4mM. Mean fluorescence intensity is expressed in arbitrary units. Error bars indicate standard error of the mean.

Panel A in the previous page contains density plots which demonstrate analysis of the FL-1 channel vs. side scatter with cells treated with DETA-NO 0.5mM, ODQ 0.3µM, neither or both for 1 week and subsequently replated for 3-4 days. Fluorescence in the figure denotes the FL-1 channel which is used to detect the fluorescent product of the C₁₂FDG interaction with β-galactosidase. Side scatter is a marker of cell size.

In panel B, the cells exhibit a higher overall fluorescence and side scatter. This effect was not significantly affected by ODQ 0.3µM (p=0.93) or ODQ 1.0µM (p=0.21) (Data not shown for ODQ 1.0µM). There was no significant interaction between ODQ and DETA-NO for either dose (p=0.79 for 0.3µM, p=0.6 for 1µM).

5.4.2 Antioxidants and DETA-NO

5.4.2.1 Selenomethionine

Selenomethionine (SM) is a selenium containing amino acid with peroxynitrite-scavenging abilities. The rate constant for selenomethionine interception of peroxynitrite is $2.4 \times 10^3 \text{ M}^{-1}\text{s}^{-1}$, compared to glutathione $5.8 \times 10^2 \text{ M}^{-1}\text{s}^{-1}$ and glutathione peroxidase $8 \times 10^6 \text{ M}^{-1}\text{s}^{-1}$. Peroxynitrite reacts directly with SM. Furthermore, SM can also be substituted for methionine in proteins and this may act as a source of peroxynitrite scavenging. SM reduces oxidation of the probe Dihydrorhodamine-123, a compound which reacts with both reactive nitrogen and oxygen species.^{199;200} SM also confers a protective effect on lung cancer cells exposed to UV radiation by activating the tumour suppressor p53 and specifically activated the DNA repair mechanism mediated by p53 without itself causing DNA damage.²⁰¹ Therefore we investigated the effects of SM on our model.

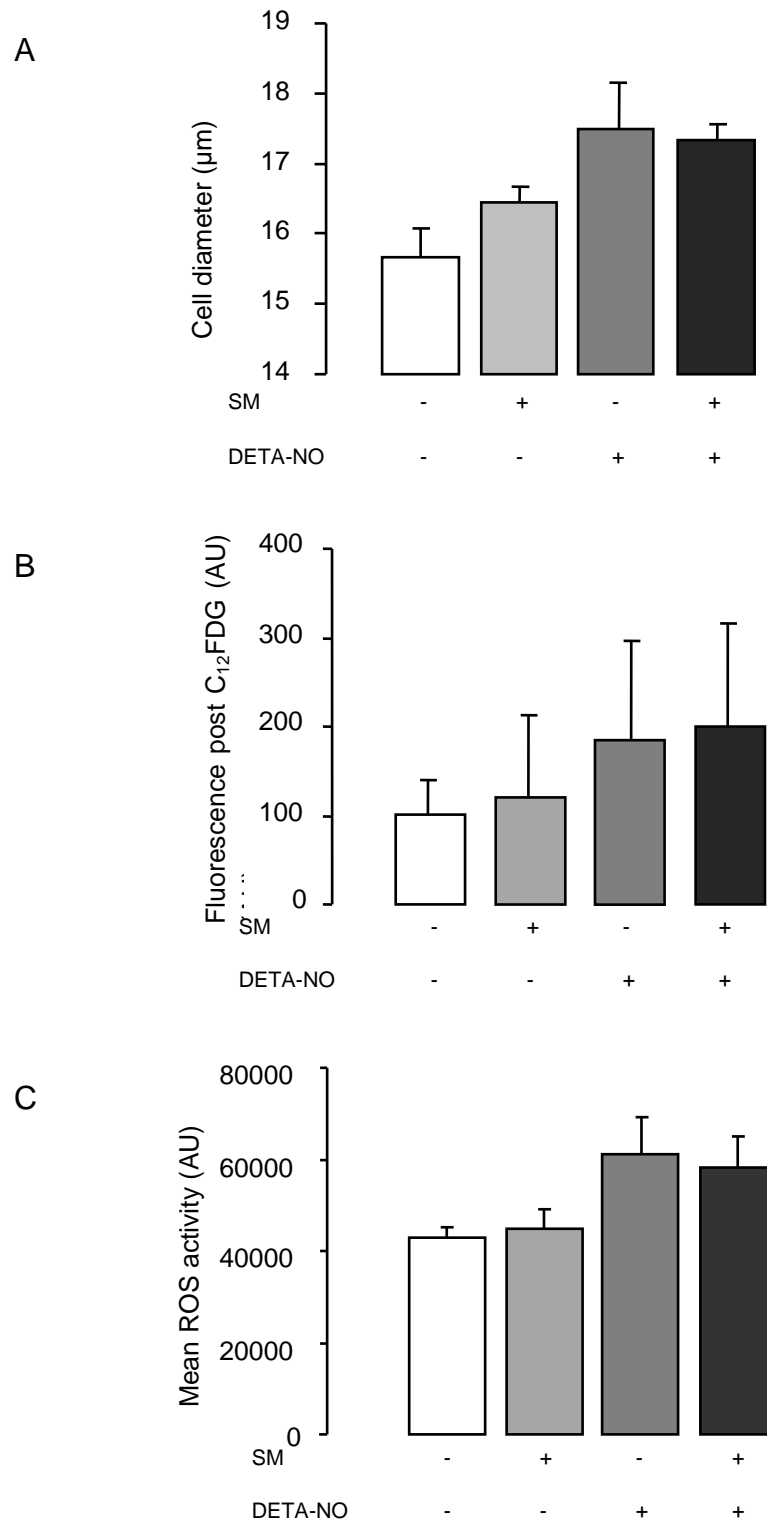


Figure 5.4.2-1: Effect of selenomethionine on the induction of senescence by DETA-NO.

Interaction between selenomethionine and DETA-NO on cell diameter (A), total β -galactosidase activity (B) and ROS activity (C). The ROS data were shown in the previous chapter but are repeated in this figure for comparison. Drug concentrations were: DETA-NO 0.5mM, SM 30 μM . All units are expressed in arbitrary units and error bars indicate standard error of the mean.

The figure above shows the results of experiments to compare cell diameter, β -galactosidase activity and ROS generation in HUVEC exposed to DETA-NO and the

effect of adding selenomethionine 30 μ M to the system. There was a small but statistically insignificant increase in cell diameter in cells treated with SM (16.67 μ m vs. 17.43 μ m, n=3, p=0.49 (2-way ANOVA) and there was no significant interaction between DETA-NO and SM (p=0.3). SM had no significant difference in ROS production either basally or in conjunction with DETA-NO. Moreover, the increase in cell size was not as a consequence of β -galactosidase activity as measured using the C₁₂FDG fluorogenic probe as total β -galactosidase activity was unchanged in both untreated cells and those concurrently treated with DETA-NO.

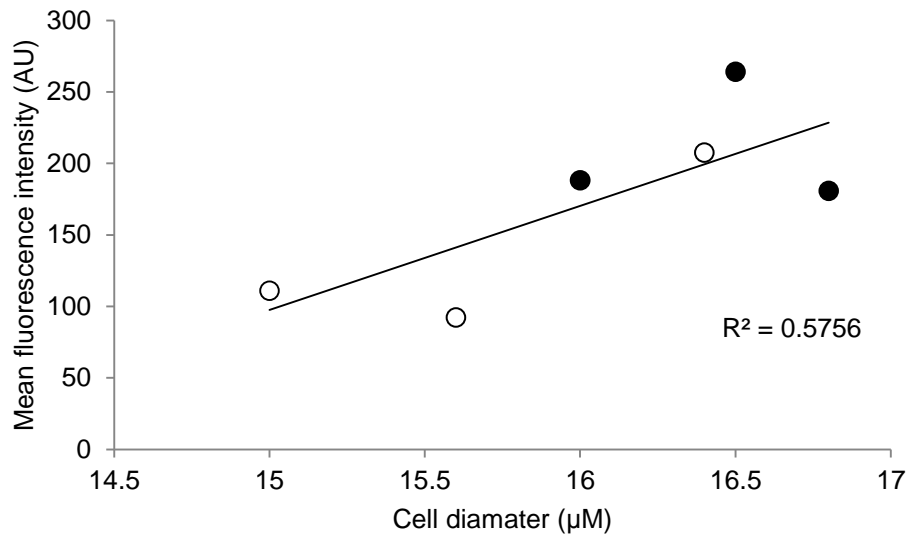


Figure 5.4.2-2: Correlation between cell diameter and total β -galactosidase activity in SM treated cells.

The above figure includes individual data points comparing cell diameter with subsequent total β -galactosidase activity measured by flow cytometry of FDG treated cells. Unfilled circles are from the control group, dark circles are from the group treated with SM 30 μ M. Fluorescence activity is expressed in arbitrary units.

5.4.2.2 Uric acid

Uric acid has a biphasic action on ROS scavenging. At low concentration, it is mainly a peroxynitrite scavenger. At physiological concentrations, it is also a hydroxyl radical scavenger. The above experiment was conducted to investigate the effect of a concentration of uric acid which is in the low normal range for adult humans in health and a concentration known to permit hydroxyl and peroxynitrite scavenging (150mM).

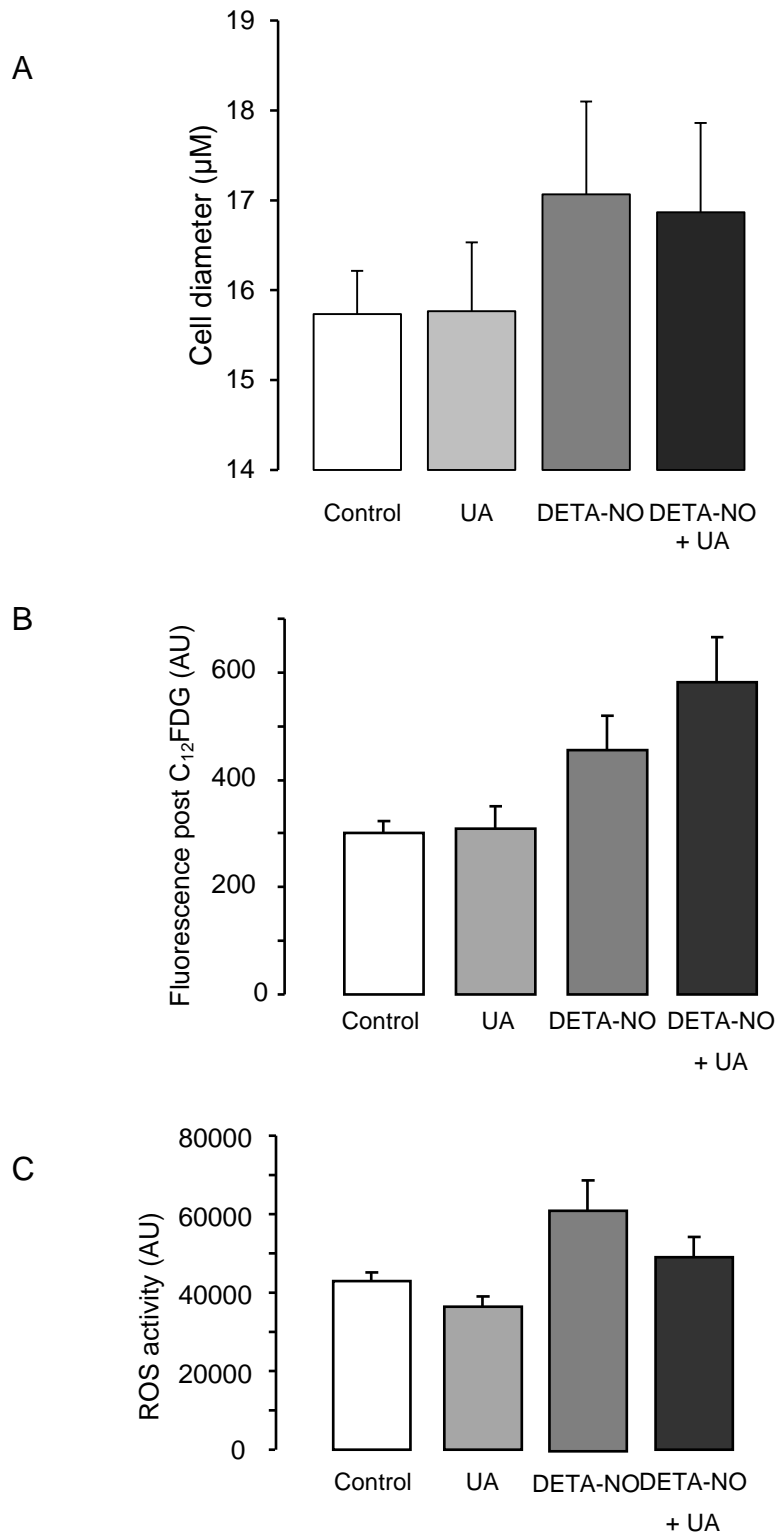


Figure 5.4.2-3: Effect of uric acid on the induction of senescence by DETA-NO.

The ROS data were shown in the previous chapter but are repeated here for comparison. Drug concentrations were DETA-NO 0.5mM and UA 150mM. AU represents arbitrary units and error bars indicate standard error of the mean. (A) shows cell diameter, (B) β -galactosidase activity and (C) ROS activity.

The figure on the previous page shows the results of experiments to compare ROS generation and β -galactosidase activity in HUVEC exposed to DETA-NO and the effect of adding UA to the system. Cells were grown to confluence and treated with DETA-NO 0.5mM, uric acid (UA) 150mM, or UA and DETA-NO. Cells being analysed for ROS activity were incubated with reagents and probe and analysed in situ in 96 well plates. The experiment was repeated 3 times. ROS activity was measured using the H₂DCFDA probe and a Victor automated plate reader. Results were analysed using the Microsoft Excel 2-sample t-test assuming unequal variance and results are for 2-tailed analysis. The results show a modest decrease in ROS activity between control and uric acid-treated cells (Mean fluorescence (AU) control 42945.5 vs. UA 36420.7; p=0.02). Moreover, the DETA-NO treated cells exhibited a marked increase in ROS activity but this was not prevented by the addition of UA (Mean fluorescence (AU) DETA-NO 61147.5 vs. DETA-NO plus UA 49077.8; p=0.08). Comparing control to DETA-NO plus UA, there remained an increase in fluorescence in the DETA-NO plus UA group which did not reach statistical significance (p=0.11).

The experiment was repeated using a longer exposure to reagents for 1 week with changes of medium every 2 days. Cells were rested for 2 further days without reagents and harvested, replated for 3 days without reagents and then analysed using flow cytometry for β -galactosidase activity using the C₁₂FDG fluorogenic probe. Results were analysed using the Microsoft Excel 2-sample t-test assuming unequal variance and results are for 2-tailed analysis. In this case, there was no decrease in fluorescence post C₁₂FDG exposure between control and UA treated cells (mean fluorescence in control cells (AU) 301.4, UA treated cells 308.4, p=0.79). However, there was a marked increase in activity when comparing the DETA-NO-treated cells and those treated with DETA-NO and UA (mean fluorescence DETA-NO treated cells (AU) 456.2, DETA-NO plus UA treated cells 582.4, p=0.02). Therefore in the presence of DETA-NO, uric acid exerts an additive effect on fluorescence post C₁₂FDG exposure, despite reducing the generation of reactive oxygen species when measured by fluorescence after exposure to H₂DCFDA.

As previously stated, this may be because peroxynitrite generation has been effectively countered but that the hydroxyl radical continues to exert an effect which may be more powerful in promoting senescence. Alternatively, DETA-NO and UA may interact to produce a more senescence-inducing compound which is not itself a reactive oxygen species.

This could be investigated by looking into the effect of hydroxyl radical generating compounds on the system and this is described later with experiments involving the exposure of the system to tert-butyl hydrogen peroxide.

However, in conclusion the senescence promoting effect of DETA-NO on our model does not seem to be due to peroxynitrite or a general increase in reactive oxygen species.

5.4.3 DETA-NO and NAC

As discussed in the previous chapter, NAC prevented the generation of ROS in HUVEC exposed to nitric oxide. I therefore investigated whether it had an effect on HUVEC senescence as measured by β -galactosidase.

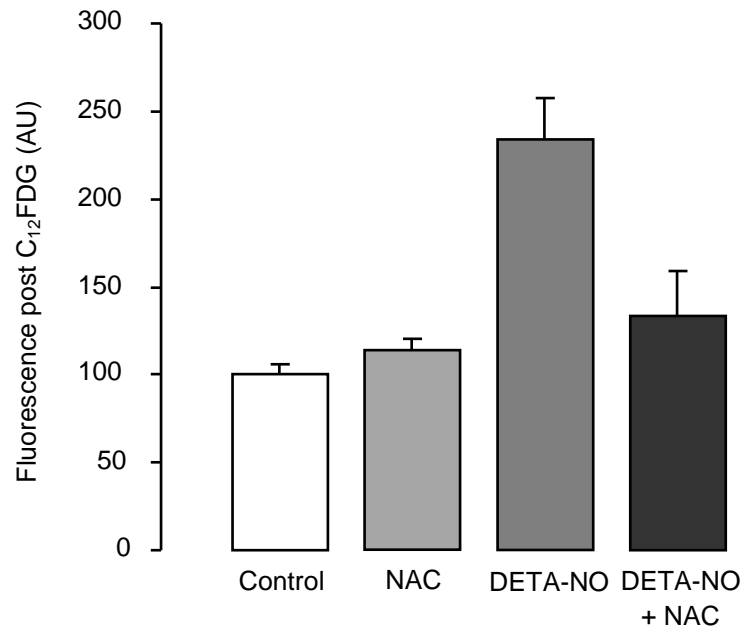


Figure 5.4.3-1: Effect of NAC on the induction of senescence by DETA-NO.

Results represent the mean of 3 experiments assessing HUVEC β -galactosidase activity by flow cytometry. The doses of reagents were DETA-NO 0.5mM, NAC 4mM. Geographical mean fluorescent intensity was calculated after gating to exclude cell debris. Error bars represent standard error of the mean.

HUVEC were grown to confluence and then exposed to DETA-NO 0.5mM, NAC 4mM or both on 3 consecutive days with change of medium. Thereafter, reagents were removed by replacing with medium for 2 days' rest. Cells were replated at 7500 cells/cm² and finally harvested for analysis using the fluorogenic probe C₁₂FDG and flow cytometry to assess β -galactosidase activity. As before, there was a large increase in fluorescence post C₁₂FDG exposure in the group of cells treated with DETA-NO. However, in contrast to previous experiments, NAC was effective in abolishing this effect. Furthermore, NAC alone was not able to reduce fluorescence post C₁₂FDG exposure lower than that seen in control cells.

5.4.4 Nitric oxide release from DETA-NO with NAC

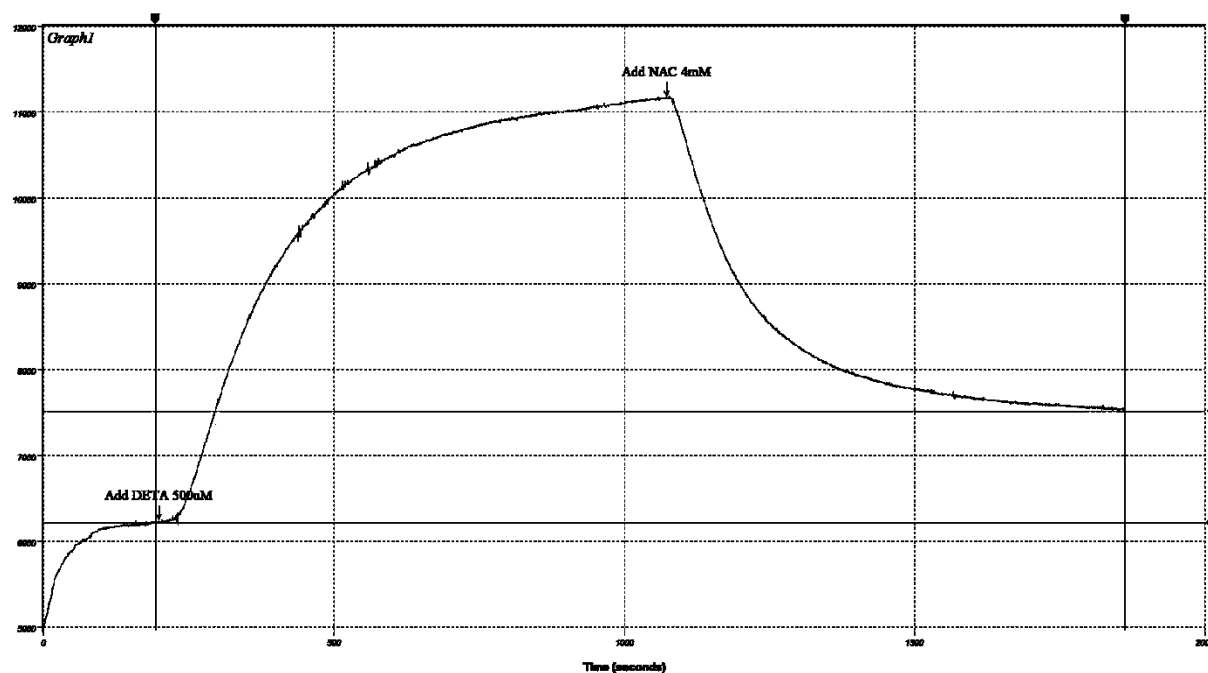


Figure 5.4.4-1: Effect of NAC on the generation of nitric oxide from DETA-NO.

Digital output of nitric oxide electrode measurement of nitric oxide generated by DETA-NO 0.5mM, before and after addition of NAC 4mM. y-axis represents nitric oxide concentration (nM).

In order to assess the direct chemical effect of NAC on DETA-NO in a cell-free environment, DETA-NO was added to a buffer solution and allowed to approach equilibrium, while measuring nitric oxide. After nearing plateau, NAC 4mM was added and there was an immediate drop in the measured nitric oxide concentration.

One possibility as to this observed drop was that nitric oxide release was countered by NAC by creating a nitrosothiol adduct. Therefore the cell based experiment was repeated with GSNO.

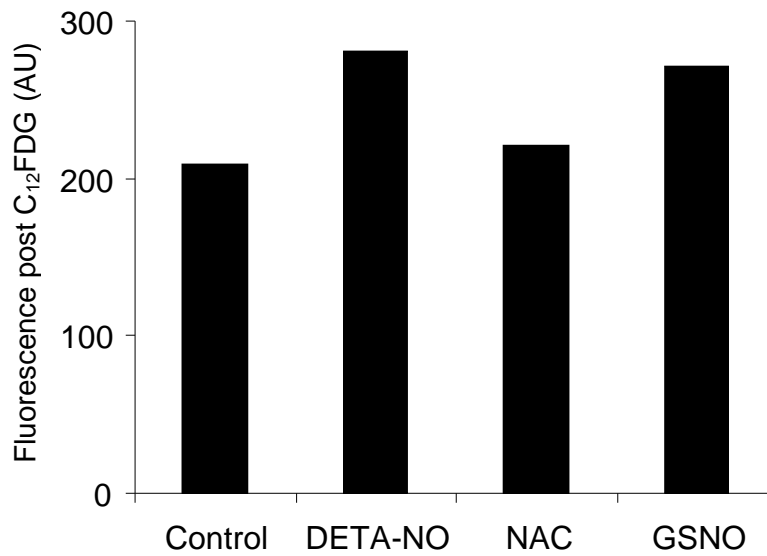


Figure 5.4.4-2: Comparison between the effects of DETA-NO and GSNO on the induction of senescence: GSNO, DETA-NO and NAC.

The graph shows the result of a single experiment carried out on HUVEC to assess the effect of GSNO as the nitric oxide donor on total β -galactosidase activity. Concentrations were GSNO 1mM, DETA-NO 0.5mM, NAC 4mM. Y-axis values represent arbitrary units of geographical mean fluorescence of FDG.

GSNO was also seen to increase the level of fluorescence post C₁₂FDG exposure, in a similar fashion to DETA-NO. Thus NAC reduces the available nitric oxide from DETA-NO and it is likely, given the effects seen with GSNO, that if this is due to the formation of intermediate nitrosothiols in the cell medium, that they do not themselves exert any influence on fluorescence post C₁₂FDG exposure. It is also likely that NAC is not exerting an intracellular effect but rather is preventing the senescence-inducing concentration of nitric oxide from being reached.

5.4.5 Cold light with DETA-NO

In order to assess whether the effect of DETA-NO on HUVEC β -galactosidase activity was due to protein transnitrosation, the experiment was repeated with cells exposed to DETA-NO and/or exposure to cold light.

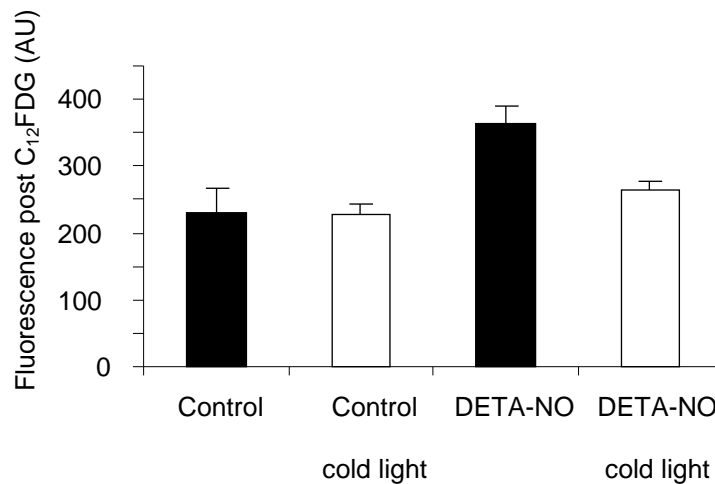


Figure 5.4.5-1: Effect of cold light on the induction of senescence by DETA-NO.

The figure represents data from 3 separate experiments carried out on different populations of HUVEC. Y-axis values represent arbitrary units of geographic mean fluorescence after exposure to FDG. Empty bars indicate cold light-treated cells. Error bars indicate standard error of the mean.

HUVEC were grown in EGM-2 to confluence in T-25 flasks. Thereafter, flasks were covered with aluminium foil which had its inner surface coated with black marker ink to absorb light. The outer surface was left clean in order to reflect light and reduce any conductive heat gain. Flasks containing cells in the light treatment regime were not covered. The incubator outer door was left open and covered with aluminium foil, except for a window to allow the concentrated cold light to enter. A cold light source was used to avoid heating the cells. Flasks were placed in a box lined with aluminium foil to maximise reflection. A cold light source was then placed at the windowed inner door of the incubator and, using a mains electricity timer, was programmed to deliver the light treatment for 60 minute periods twice daily at 6 hourly intervals. The light intensity emitted by the source was approximately 8Mlx. Medium was changed daily for 3 days, along with reagents (DETA-NO). After this period, cells were rested for 2 days and replated at 7500 cells/cm² for 3 days, before harvest and analysis for C₁₂FDG using flow cytometry and Western blotting. Initial attempts to replate immediately led to a high rate of cell death.

There was no difference between control cells exposed to light or kept in dark conditions. There was a significant increase in fluorescence post C₁₂FDG exposure in the DETA-NO treated group when compared to control, light-treated control and light-treated DETA-NO exposed cells. Mean fluorescence of control was 230.2, light treated control was 227.9, DETA-NO_{dark} was 364.1 and DETA-NO_{light} was 264.3. Paired t-test (2-tail assuming unequal variances) were performed on control_{dark} vs. control_{light}, p=0.98; control vs. DETA-NO_{dark}, p=0.004; DETA-NO_{dark} vs. DETA-NO_{light}, p=0.006.

While GSNO and sodium nitroprusside are both known to be photolabile, this property has not been described in DETA-NO.

Light therefore is able to prevent and reverse DETA-NO-induced increases in fluorescence post C_{12} FDG exposure in this model of stress-induced senescence. The mechanism may be a direct effect on the cells, but no effect was seen in the control group. Secondly, there may be a nitric oxide-quenching effect, preventing the concentration of nitric oxide from increasing as it is released from DETA-NO. However, this has not been reported in the literature.

Nitric oxide concentrations have been measured to increase when cells exposed to angiotensin II stress are then treated with agents (for example, N-acetyl cysteine) which cleave the cysteine nitroso bonds to denitrosate transnitrosated proteins.¹²¹ Therefore, a feasible explanation is that transnitrosation of a protein intimately associated with the senescence process promotes senescence and that, when it is exposed to a cold light source, the de-nitrosation of this molecule is able to abort the senescence process.

In order to assess whether transnitrosation was responsible for the observed increase in senescence of cells exposed to DETA-NO, a modified biotin switch technique was used to assess general protein transnitrosation.^{202;203} Cells were treated with DETA-NO and exposed to cold light in the same way as described above.

Thereafter, the cells were lysed and exposed to the metal chelator neocuproine in order to facilitate the later reduction phase by ascorbic acid (which is inhibited by transition metal-catalysed reactions). Any free thiol/cysteine residues were then blocked using methyl methanethiosulfonate (MMTS). Thus all thiol residues were presumed to be either transnitrosated or irreversibly blocked by MMTS. Lysates were then exposed to the reducing agent, ascorbic acid. This would have the effect of detransnitrosating the previously transnitrosated thiol residues and primed them for labelling with a biotin-labelled reactive disulphide which readily reacts with free thiol residues biotin-hexyl-pyridyldithiopropionamide (biotin-HPDP). The final stages involved protein assays using the Bradford method, to allow an even protein loading and finally protein electrophoresis and staining with an avidin-labelled peroxidase.

Experiments were run with non-labelled samples and non-reduced samples in order to compare with the fully reduced and labelled lysates. The comparative difference between reduced and non-reduced lysate staining would be the degree to which cell proteins were originally transnitrosated.

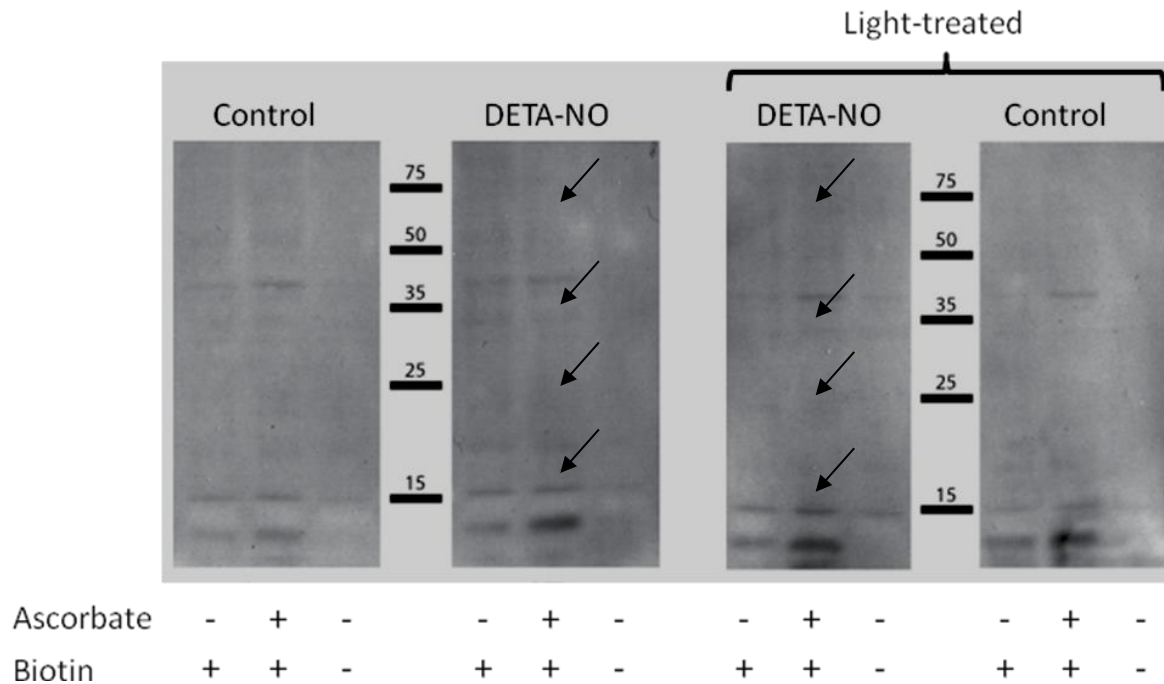


Figure 5.4.5-2: Identification of transnitrosated proteins by the biotin switch method.

Digital photograph of a film of a biotin switch experiment. Left-hand lanes indicate non-specific labelling by biotin. Central lanes are where, after reduction by ascorbate, the biotin labelling indicates transnitrosated proteins. The horizontal bars indicate the position of molecular weight markers with the respective sizes expressed in kDa.

All groups in the experiment exhibited an increase in labelling between the non-reduced (Biotin) and reduced (Biotin plus ascorbate) samples, indicating a degree of transnitrosation at baseline in all groups. However, the degree of transnitrosation was not clearly different between the DETA-NO-treated sample and the DETA-NO and cold light-treated sample. If anything, there seemed to be a greater increase in staining between biotin and biotin plus ascorbic acid groups in the light treated samples with or without DETA-NO than in the groups treated in dark conditions. This is directly contradictory to the idea that generalised transnitrosation is involved in the senescence process. However, the technique supports the assumption that there is little in the way of nitric oxide quenching by light as transnitrosation appears to occur in all groups. Furthermore, this method only shows a general view of transnitrosation and cannot discern the degree to which any protein involved in the senescence signalling process has been affected specifically by transnitrosation.

5.4.6 Transnitrosation band analysis

We performed a further analysis of the gel. Using Alphaease software, we were able to select the mid portions of the bands and analyse the density digitally. This was combined by using the molecular weight markers to create a formula to calculate the molecular weight of each band. We then subtracted the difference in intensity seen in the ascorbic acid group from the ascorbic acid and biotin-labelled cysteine residue

group to arrive at a graph demonstrating the maximum differences between non-specific labelling and labelling due to transnitrosation.

The figure below shows the results of that calculation. Looking at the biggest peaks of difference between transnitrosated and non-transnitrosated proteins, where bands were found in all 4 conditions, there were 4 bands. The predicted molecular weights of these proteins were 16.2kDa, 24.4kDa, 33kDa and 64.4kDa. Two proteins of this molecular weight have already been mentioned in the introduction of this manuscript – p65 and p66^{shc}.

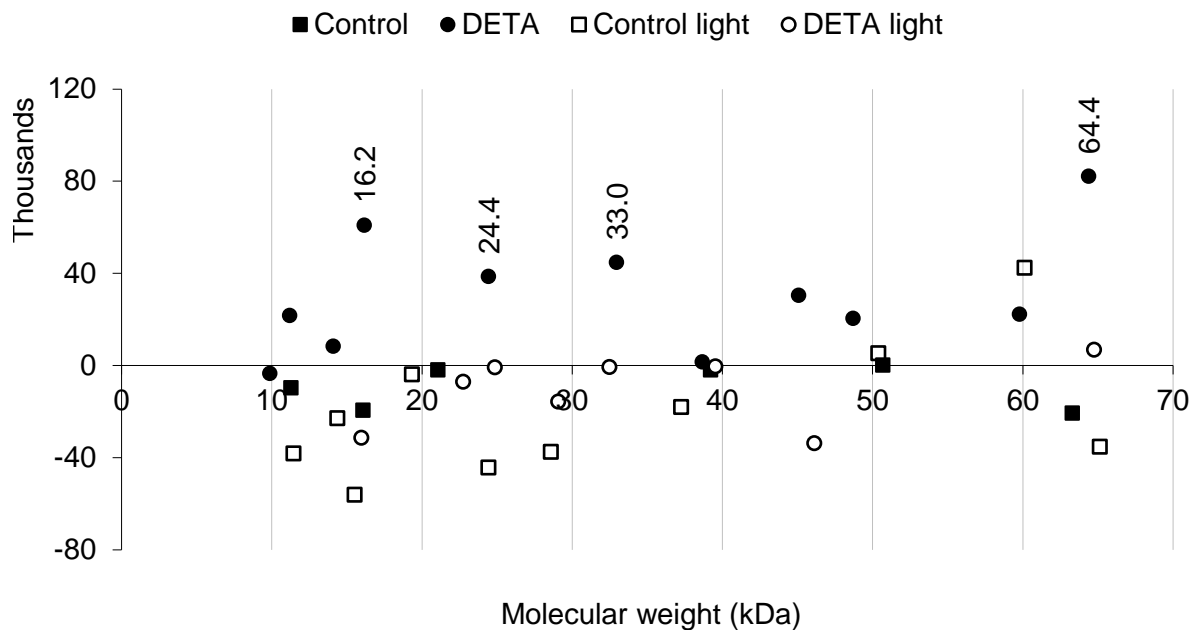


Figure 5.4.6-1: Specific band analysis of biotin switch.

The above graph shows the result of band analysis of the experiment to assess protein transnitrosation. Unfilled symbols indicate data from cells exposed to light, circles indicate cells exposed to DETA-NO 0.5mM. Data are expressed in thousands of arbitrary units which are calculated by subtracting band intensity from cells without biotin labelling from those which were labelled in this way.

Studies of transnitrosation of p65, in the context of inducing iNOS by exposing cells to lipopolysaccharide have shown increases in transnitrosation of NF- κ B on the p65 subunit being associated with a reduction in NF- κ B function.^{204;205}

No such data was found for p16^{INK4a}. The reason for its increase in apparent transnitrosation as detected by this method is not clear. This may be a consequence of an increase in protein expression with consequential increases in non-specific staining. This also raises the possibility that p65 is similarly increased, although the fact that it is known to be transnitrosated, and that this transnitrosation leads to a decrease in function remains interesting. This experiment was repeated several times but technical difficulties with the assay made interpretation difficult. The above discussion should therefore be interpreted in light of this. Since the experimental work was carried out, newer methods of detecting protein transnitrosation have been developed^{204;205}. These hypotheses may therefore be confirmed using a more reliable method in the future.

5.5 Conclusion

We have shown that nitric oxide, at concentrations in the high end of the range which can be seen *in vivo*, causes senescence in vascular cells. This was demonstrated in several ways in order to be certain that this was indeed senescence. Histological staining for senescence-associated β -galactosidase, flow cytometric analysis of β -galactosidase activity, cell proliferation studies and western analysis of cell cycle proteins were all consistent with this conclusion. Cells which demonstrated higher β -galactosidase activity did not appear to be undergoing apoptosis and there were fewer apoptotic cells in the HUVEC exposed to DETA-NO. It is possible that a proportion of cells exposed to DETA-NO in our model apoptose before analysis (i.e. during the exposure to DETA-NO). Furthermore, this may mean that cells which are subsequently analysed have been selected for resistance to apoptosis. This is consistent with previous groups' observations that senescent cells are resistant to apoptosis (see Introduction).

As further evidence of the influence of DETA-NO on senescence, our group previously investigated its effect on telomerase activity in HUVEC.

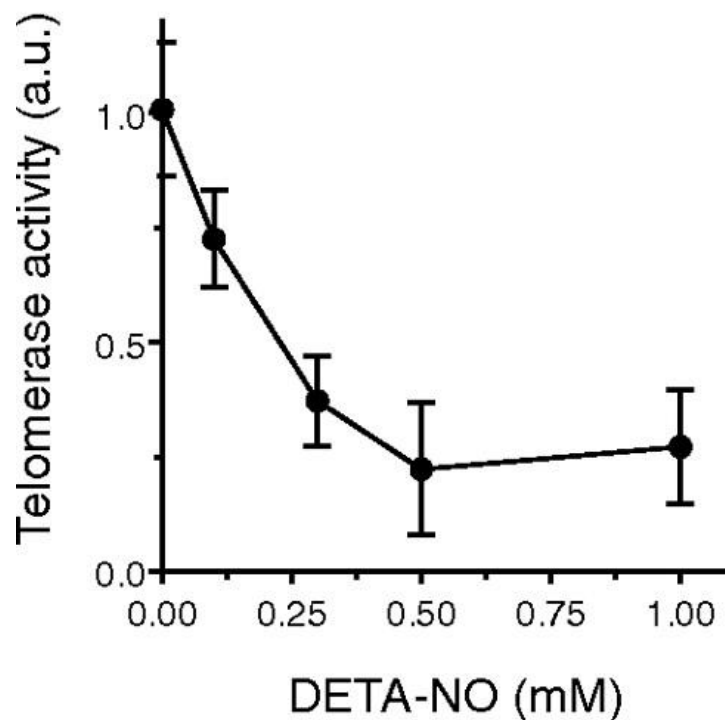


Figure 5.5-1: Effect of high doses of exogenously added nitric oxide on telomerase activity.

The above chart demonstrates previous work by our group. HUVEC were treated with DETA-NO for 24 h prior to measurement of telomerase activity.²⁰⁶

The use of two nitric oxide donors to achieve the high concentration of nitric oxide suggests that the effect was not due to DETA-NO, but rather the nitric oxide released as a consequence of its liberation from DETA-NO. The effect seen with DETA-NO

did not seem to be due to a disturbance in the equilibrium of glutathione products as there was no demonstrable difference in the effect when we used GSNO as the nitric oxide donor.

The pro-senescent effect of nitric oxide on HUVEC was also seen in vascular smooth muscle cells harvested from human umbilical cords and rat aortic smooth muscle cells, suggesting this is an effect which may be seen throughout the vessel walls of both humans and rats.

If anything, smooth muscle cells appeared to be more sensitive to the effects of nitric oxide as increases in senescence were seen with lower doses of nitric oxide donor, compared to HUVEC. Again this increases the possibility that this is a physiologically-relevant phenomenon.

We were surprised to see the rapid depletion of nitric oxide when NAC was added to DETA-NO in solution. Clearly, this could easily explain the reduction in reactive oxygen species generation and senescence seen in cells treated with both DETA-NO and NAC. The mechanism for the reduction was not immediately clear but was not accounted for by pH or temperature as subsequent experiments were conducted after re-measuring pH and there was no change seen in the temperature of the reaction mix during the nitric oxide electrode experiment.

With regard to the decreases in senescence seen by other groups who have looked at lower ranges of nitric oxide concentration, we saw no significant effect in reducing total β -galactosidase activity at the lowest concentration of DETA-NO tested. This may reflect the fact that our system was not sensitive enough to detect what could be a significant difference in cells treated at those concentrations. However, we chose to follow the novel and apparently more significant effect of large increases in senescent cells exposed to the higher sub-lethal concentrations of nitric oxide.

This investigation showed us that all features of senescence were seen in those cells exposed to sub-lethal doses of nitric oxide. This effect was remarkable in its magnitude, with cells showing a reduction in DNA synthesis of more than 50%.

Our assumption that high ranges of iNOS could generate similar concentrations of nitric oxide and that these concentrations could lead to senescence were tested with the co-culture experiments with tet-iNOS HEK-293 cells grown in close proximity to HUVEC, without being in contact. In retrospect, the lack of effect may simply have been a limitation of keeping cells apart and need not necessarily mean that cells maximally expressing iNOS cannot generate sufficient nitric oxide. A rapid consumption of nitric oxide could have accounted for the lack of effect as the molecule crossed the layer of medium before reaching the HUVEC. This situation would not occur *in vivo*.

Regarding the potential mechanism for nitric oxide-induced senescence, we used ODQ to inhibit soluble guanylate cyclase and this had no ability to reduce or prevent

the effect of DETA-NO on senescence. Similarly, antioxidants were ineffective and uric acid was positively deleterious. Despite being the most efficient compound with regard to its ability to prevent the oxidation of H₂DCFDA, it appeared to increase our cells' tendency to senesce. Thus the mechanism of nitric oxide induced senescence was unlikely to be simply due to increasing oxidant species. Uric acid's additive effect on DETA-NO-induced senescence may have been due to reactive intermediates generated by the reaction between nitric oxide and uric acid, as discussed in the introduction. These may not all react with H₂DCFDA in our system of detection of ROS.

Finally, the effect of cold light was interesting in that it was able to completely prevent nitric oxide-induced increases in β -galactosidase activity. This was despite the fact that light was delivered in pulses of 1 hour each, while DETA-NO tends to release nitric oxide constantly throughout. DETA-NO is not known to be unstable in light but a potential explanation of our finding is that it is rapidly degraded when exposed to high intensity cold light and therefore not able to exert the pro-senescent effect. Other nitric oxide donors, for example, GSNO and sodium nitroprusside are well known to be light sensitive.²⁰⁷ When exposed to light, they rapidly release nitric oxide and this would therefore have the effect of increasing nitric oxide concentrations while preventing its transnitrosating effect on protein targets. In fact, the property of light sensitivity of GSNO was used in my work to assess whether senescence induced by DETA-NO was due to transnitrosation of similar cysteine residues.

The biotin switch method was at first glance disappointing with no real discernible difference in protein transnitrosation. However the further analysis offered by comparing patterns of transnitrosation was potentially revealing in that some proteins appeared to have increased density specifically in the DETA-NO treated groups.

Unfortunately, we were not able to formally identify these but the potential that p16^{INK4a} could be transnitrosated is interesting and the finding of a band which could represent p65 appears to offer a plausible mechanism for our finding, suggesting it could be involved in the process of either defending cells against senescence or defending them against apoptosis, only for them to senesce.

Protein p65 is a subunit of NF- κ B, a key transcription factor known to coordinate cellular responses to stress. In addition to this, it has been thought to be subject to transnitrosation at site cysteine 38, (Uni-Prot database) a post-translational modification which causes a decrease in activity of morphologically similar proteins.

GPS-SNO 1.0 is an online program which predicts likely transnitrosation sites according to the protein sequence, its predicted structure and known transnitrosation sites on similar molecules. Using GPS-SNO 1.0, p66^{shc} also has a likelihood of being transnitrosated, even using a medium threshold to search for transnitrosation sites at the cysteine on position 197. The likelihood score was 21.6 for cys-197 and 2.4 for

cys-38 (below the arbitrary “low threshold”). Sensitivity for sequences predicted above the low threshold for transnitrosation is 53.57%, specificity 80.14%, accuracy 75.8%.¹¹⁷

In addition, there was a band at 16.2kDa, a candidate to be p16^{INK4a}. Similar analysis using GPS-SNO 1.0 gave a candidate cysteine residue at position 72 with a likelihood score of 0.22, placing it below the low threshold of likelihood as a transnitrosation site.

While of interest, these findings would need to be clarified with further experiments to specifically look to identify the protein bands described.

6 Metabolic stress and senescence

6.1 Introduction

Autophagy and related disorders of this process may play a part in the accumulation of lysosomes measured by the various β -galactosidase assays we have used in previous chapters. Therefore, we chose to assess whether this process could be manipulated pharmacologically in such a way that an effect on senescence would be observed.

6.1.1 Bafilomycin A1

Bafilomycin A1 acts to prevent autophagy by reducing lysosomal function. Bafilomycin A1 inhibits the lysosomal proton pump which reduces the ability of lysosomes to acidify their interiors via the vacuolar H^+ -ATPase.²⁰⁸ This, perhaps by a similar mechanism, allows the accumulation of acidic vacuoles within cells and prevents the degradation of long-lived proteins, the fusion of lysosomes and acidic vacuoles into autophagolysosomes and autophagy in cell lines.²⁰⁹ We exploited this property to investigate the phenomenon of increasing lysosomal size and its relationship with senescence and to help ascertain if impairment of protein degradation and mitochondrial cycling is causally linked to replicative senescence.

6.1.2 Rapamycin

Rapamycin inhibits the mammalian target of rapamycin (mTOR) and as such is able to increase autophagy activity and this in turn should lead to a decrease in lysosomal accumulation due to more efficient turnover of damaged proteins and organelles.

mTOR is a downstream target of PI3K and Akt, which regulate survival pathways. As discussed previously, Akt activation can be induced by nitric oxide. Nitric oxide activation of Akt may lead to reduced protein cycling by reducing protein synthesis and reducing cell proliferation rates. If proteins are not being cycled, there may be an increased chance of oxidative or nitrosative damage. We postulated this advances the possibility of protein aging which may in turn act as a signal for senescence. This may be most important in mitochondria which are responsible for signalling for many routes to apoptosis. Therefore, rapamycin offers another angle to investigate the phenomenon of nitric oxide-induced senescence by looking at the potential for Akt survival signalling being part of the route to nitric oxide-induced senescence.

The use of rapamycin in the vasculature is widespread since the advent of drug-eluting stents for coronary artery disease. In addition, rapamycin had an established role as an immunosuppressant in transplant medicine. Studies have investigated its effects on cell proliferation and survival and have shown it to reduce lung microvascular endothelial cells' ability to survive a hyperoxic insult.²¹⁰ In addition, rapamycin has been shown to have an anti-proliferative effect on vascular smooth

muscle cells subjected to balloon injury, again via an effect on the PI3K/Akt cascade.²¹¹

6.1.3 AMP kinase

AMPK activity has been shown to increase with advancing organismal age in response to hypoxic stress.¹⁶⁴ AMPK itself is activated by the tumour suppressor gene LKB1 and this is also responsive to the effects of the AMP analogue AICAR. LKB1 activation confers an anti-apoptotic effect and we initially postulated this could in turn lead to senescence.¹⁶⁵ As many cell stressors appear to be both pro-apoptotic and pro-senescent, we postulated that cell stress-response pathways may be activated by such a stress and that they may be forced to choose between apoptosis or senescence. Cell stress-response pathways may thereby involve an anti-apoptotic pathway which is pro-senescent. AICAR is an AMP analogue which activates AMP kinase in a similar fashion to the increase in AMP:ATP ratio. Thus it simulates the effect of ATP depletion and therefore, bioenergetic stress in a cell. AMP kinase has a wide range of proven and putative effects in its ability to modulate the metabolism of the cell, changing it from a synthetic unit to a catalytic unit and conferring an improved anti-oxidant defence mechanism. This may be a means of energy-conservation in a time of relative scarcity (see Introduction).

We chose to investigate its effect on senescence and its potential role in signalling for senescence, given that at high concentrations nitric oxide may cause bioenergetic stress by inhibiting mitochondrial respiration and consequently leading to an increase in the AMP:ATP ratio.²¹²

Other stimulators of AMPK include the oral hypoglycaemic drug metformin. The method by which metformin activates AMP kinase may involve inhibition of the electron transport chain complex 1 and thereby increase the AMP:ATP ratio but it has been thought to be independent of LKB1 and may therefore help to discriminate between two mechanisms of AMPK activation.

There is also relevance in investigating AMP kinase activation specifically in endothelial cells as there is variability in the forms of AMP kinase present in various cell types. The $\alpha 1$ subunit is expressed in endothelial cells and both $\alpha 1$ and $\alpha 2$ subunits are expressed in liver, cardiomyocytes, and skeletal muscle. The $\alpha 2$ subunit is more responsive to bioenergetic stress than the $\alpha 1$ subunit.¹⁷²

6.2 Mimicking lysosomal dysfunction

6.2.1 Effect of lysosomal proton pump inhibitor, bafilomycin A1 on HUVEC senescence

6.2.1.1 Effect of bafilomycin A1 on HUVEC cell diameter

Bafilomycin A1 is poorly soluble in water and was therefore dissolved in dimethyl sulfoxide at a relative concentration of 0.01% per 1nM bafilomycin A1.

In order to test the effect of bafilomycin A1 on senescence, cells were seeded at 3500 cells/cm² and fed 3 times per week with or without the addition of bafilomycin A1. As cells approached 80% confluence, the experiment was terminated by trypsinization for counting and size measurement using a Coulter Multisizer Z2 Particle analyser. These experiments revealed a modest but statistically-significant increase in cell diameter in a dose-related fashion. The relationship between cell size and dose of bafilomycin A1 is shown below.

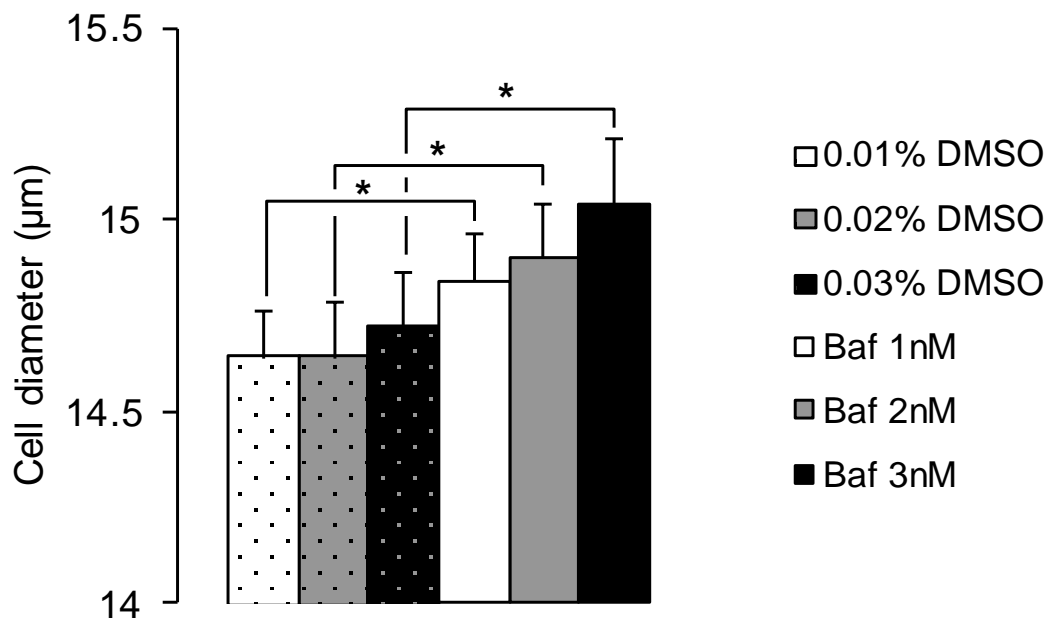


Figure 6.2.1-1: Dose response for the effect of bafilomycin A1 on cell diameter of HUVEC.

The figure represents the mean cell diameters of 5 separate experiments using HUVEC from 5 separate populations. Cells were exposed to varying concentrations of bafilomycin A1 in its solvent, DMSO (1nM in 0.01% DMSO, 2nM in 0.02% DMSO or 3nM in 0.03% DMSO), or solvent alone. Error bars represent standard error of the mean. Callipers show the comparison of the cells exposed to the same concentration of the solvent DMSO with or without the corresponding concentration of bafilomycin A1. T-test * p<0.05

The dose-response curve demonstrated no significant difference between doses of DMSO or between doses of bafilomycin A1. However, comparing bafilomycin doses

with the equivalent dose of DMSO, all doses were associated with a significant increase in cell diameter.

6.2.1.2 Effect of bafilomycin A1 on HUVEC cell proliferation

To assess the effect of bafilomycin A1 on HUVEC cell proliferation, cells were seeded at 3500 cells/cm² and fed 3 times per week. Once the fastest proliferating cells reached ~80% confluence, the experiment was terminated by trypsinization for counting and size measurement using a Coulter Multisizer Z2 Particle analyser. The relationship between cell proliferation and dose of bafilomycin A1 is shown below.

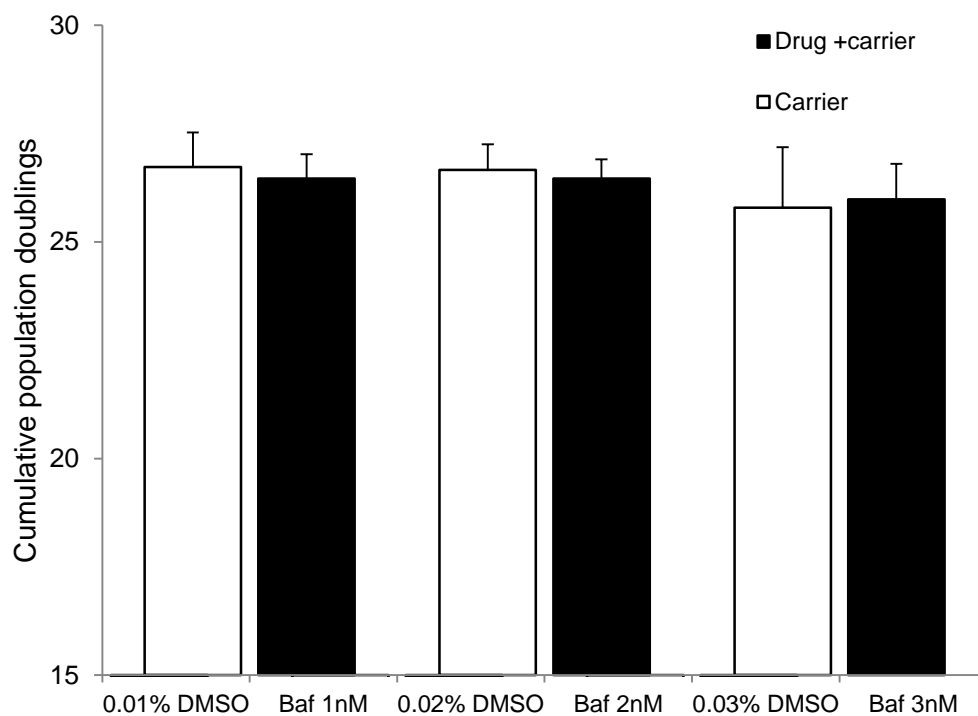


Figure 6.2.1-2: Effect of bafilomycin A1 or carrier on population doubling per passage HUVEC.

Effect of exposure to bafilomycin A1 or carrier (DMSO) on population doubling per passage is shown above. Cells were counted at the same time on trypsinization using a Coulter Particle analyser. The experiment was repeated on 3 separate occasions using different populations of HUVEC. Error bars indicate standard error of the mean.

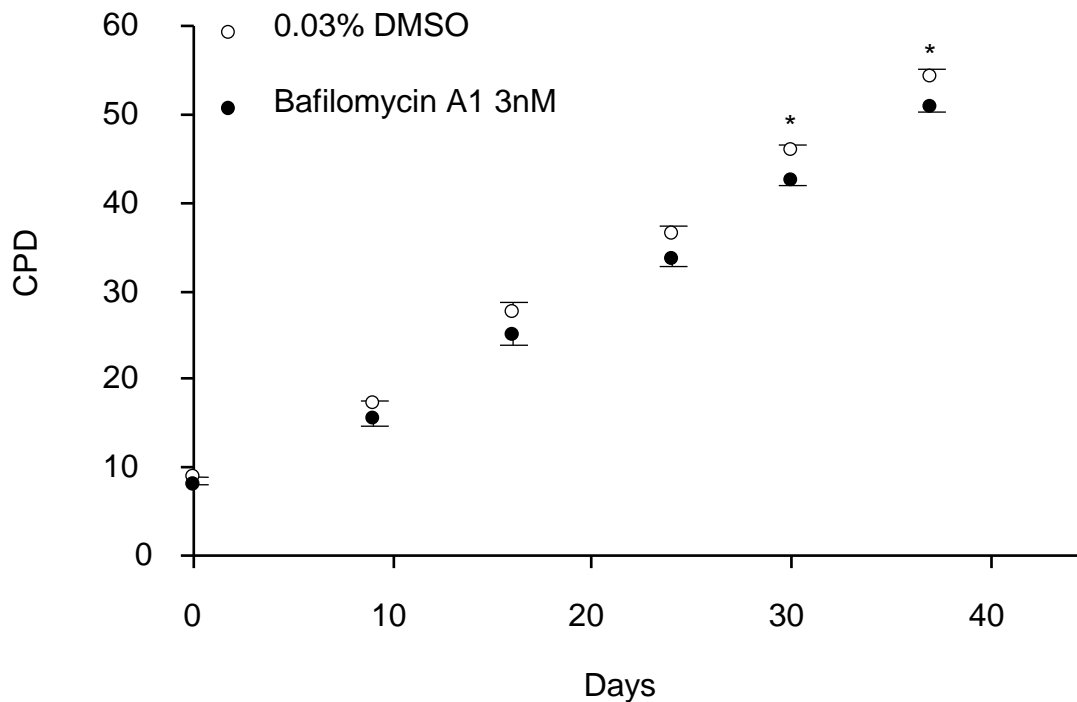


Figure 6.2.1-3: Effect of bafilomycin A1 on cumulative population doubling in HUVEC.

The above figure shows the results of a single experiment comparing longer exposure to bafilomycin A1 in carrier or carrier only. Time indicates time since first seeding. Cells were counted using the Coulter Particle analyser using 3 samples from the same well. Error bars indicate 95% confidence interval and asterisks indicate the points where there was a statistically different number of cumulative population doublings between the cell groups.

Small differences were noted in the rate of proliferation and in one extended experiment, these reached statistical significance. However, the overall picture was of no difference in proliferation.

The experiment was extended for 5 passages to assess whether there would be a cumulative effect on population doubling. The final 2 passages began to show a significant difference in population doublings between cells treated with bafilomycin A1 3nM and those exposed to carrier only (DMSO 0.03%).

6.2.1.3 Effect of bafilomycin A1 on HUVEC senescence-associated β -galactosidase

HUVEC were grown as before and were then fixed and stained for senescence-associated β -galactosidase.

Wells stained for senescence-associated β -galactosidase were counted using a graticule and 4 random samples within each well was counted to a total cell count of at least 200. Positive cells were then counted and were compared to the corresponding control. In the case of senescence-associated β -galactosidase experiments, 2 independent samples were counted 4 times each.

The results shown below indicate a striking reduction in the rates of positively-stained cells for cells treated with bafilomycin A1. Positively stained cells in the treated wells appeared to have been stained much less avidly. Importantly, there was no significant difference in senescence-associated β -galactosidase staining between the various concentrations of DMSO but there was a dose response relationship between the doses of bafilomycin A1, even when the corresponding concentration of DMSO was used as an internal control.

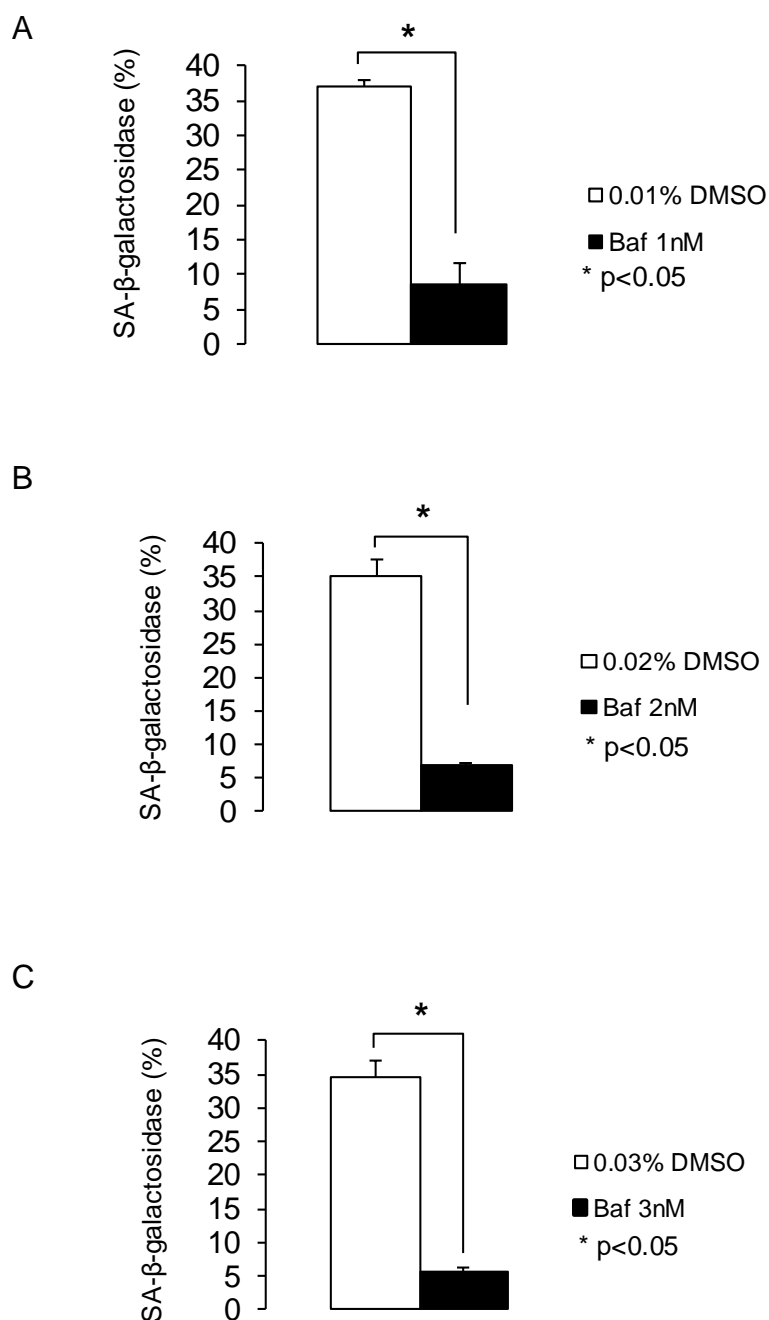


Figure 6.2.1-4: Bafilomycin A1 and DMSO dose response of HUVEC: senescence-associated β-galactosidase.

Graphs are grouped by bafilomycin A1 dose and equivalent carrier concentration. Senescence-associated β-galactosidase (%) represents percentage of cells positively-stained for senescence-associated β-galactosidase. Error bars denote standard error of the mean and callipers denote statistical comparisons. *p<0.05. (A) shows bafilomycin 1nM, (B) 2nM, (C) 3nM.

The above 3 graphs show the results of senescence-associated β-galactosidase staining experiments with comparisons between cells exposed to bafilomycin A1 or

the solvent DMSO. DMSO was used to dissolve bafilomycin A1 and, as it exerts a weak antioxidant effect, the control population of cells was exposed to the same concentration of DMSO as was contained in the bafilomycin A1 mixture. At each dose, there was a marked decrease in cells which stained positive for senescence-associated β -galactosidase.

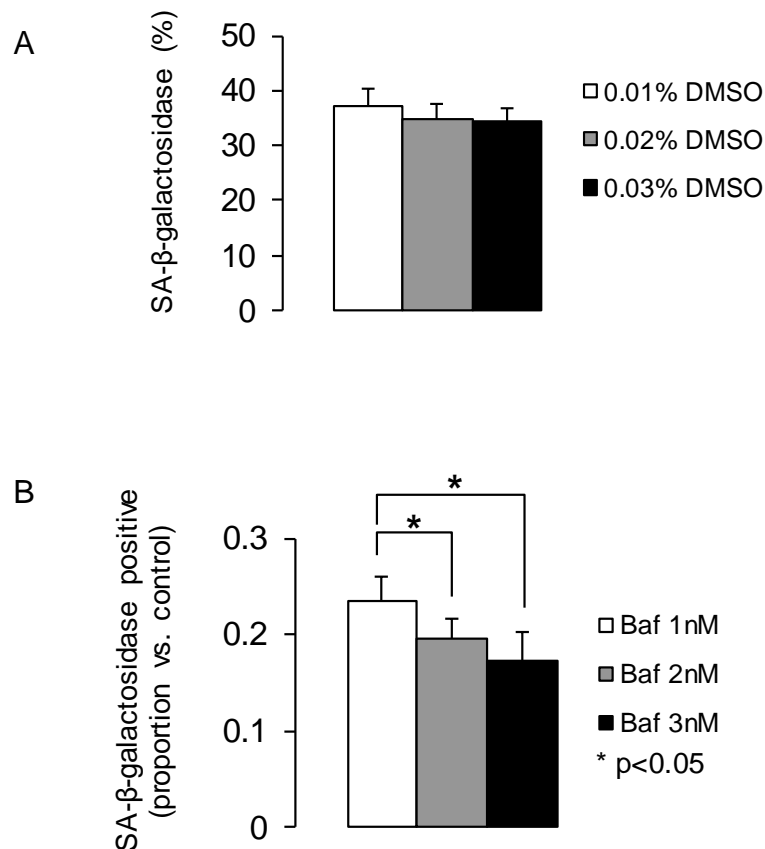


Figure 6.2.1-5: Bafilomycin A1 and DMSO dose response of HUVEC: senescence-associated β -galactosidase.

Graphs are grouped by carrier solvent (DMSO) alone (A) or by bafilomycin A1 dose (B). Senescence-associated β -galactosidase (%) represents percentage of cells positively-stained for senescence-associated β -galactosidase. Senescence-associated β -galactosidase positive (proportion vs. control) represents ratio of positive cells in bafilomycin A1 treated cells : positive cells in corresponding dose of carrier. Error bars denote standard error of the mean and callipers denote statistical comparisons. *p<0.05.

The same data are shown as above, but in this case, comparisons are between doses of solvent and doses of bafilomycin A1. There were no statistically significant interactions between doses of DMSO solvent. However, bafilomycin A1 exerted a dose-dependent reduction in senescence-associated β -galactosidase activity.

6.2.1.4 Effect of bafilomycin A1 on HUVEC total β -galactosidase activity as measured by flow cytometry

Therefore, in the case of bafilomycin A1, there is a dose related increase in cell diameter but a decrease in senescence-associated β -galactosidase staining.

Further investigation into the total amount of β -galactosidase activity by flow cytometry was performed to assess if bafilomycin A1 truly reduces β -galactosidase activity and therefore separates the relationship between β -galactosidase, cell size and senescence.

Cells were grown to confluence and treated with bafilomycin A1 3nM for 3 consecutive days. They were then rested for 3 days in normal medium. Cells were replated at 5000 cells/cm² and then analysed for total β -galactosidase activity measuring C₁₂FDG metabolism by β -galactosidase to fluorescein by flow cytometry. There was no significant difference in total β -galactosidase activity.

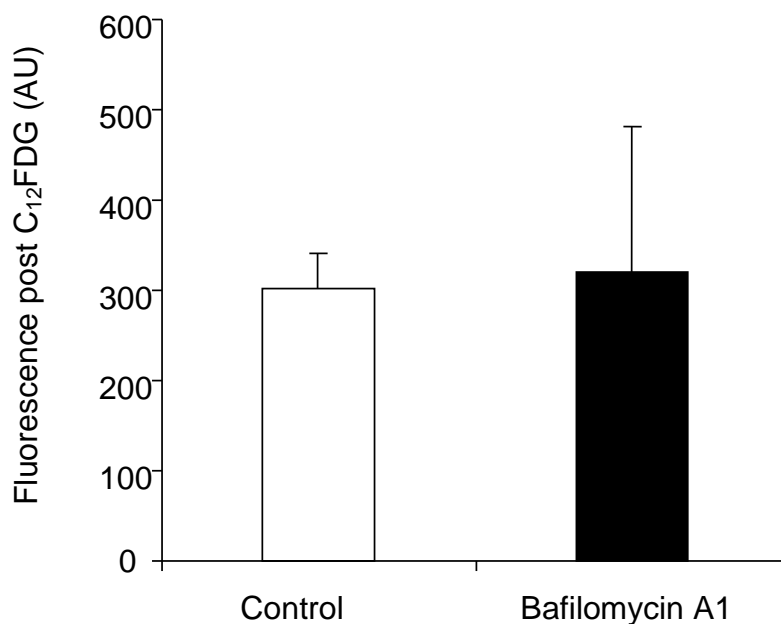


Figure 6.2.1-6: Effect of bafilomycin A1 on HUVEC β -galactosidase activity.

Result of 3 separate experiments on 3 separate populations of HUVEC. Columns indicate the mean of mean fluorescence intensity post C₁₂FDG exposure; error bars indicate standard error of the mean (SEM).

The flow cytometry results contrasted markedly with those seen in the standard histological staining method for measuring senescence-associated β -galactosidase. This clearly posed the question as to the effect of bafilomycin A1 on the staining technique itself. It is quite possible that the relative alkalisation of lysosomes by bafilomycin A1 inhibits the reaction at pH6 to such an extent that not enough

coloured product is made to be detectable in the histological stain, it may affect the dye itself or there may be a direct interaction between bafilomycin A1 and β -galactosidase.

However, in this case, it seems that the fluorescent product visualized by flow cytometry provides a more sensitive measure as it is likely that bafilomycin A1, as a known inhibitor of autophagy is unlikely to be able to reduce lysosomal mass and therefore β -galactosidase activity, processes which have previously been shown to correlate.^{10;213}

6.2.2 mTOR inhibition

As rapamycin has previously been shown to demonstrate anti-proliferative effects, I elected not to investigate senescence by assessing proliferation.

I therefore investigated the effect of rapamycin on cell diameter and on total β -galactosidase activity as measured by flow cytometry. Inhibiting mTOR ought to encourage autophagy and thereby may retard senescence by preventing accumulation of damaged mitochondria.

Analysis of cell diameter was first carried out in the context of a dose response curve on a single population of HUVEC and then repeated on 4 further populations of HUVEC.

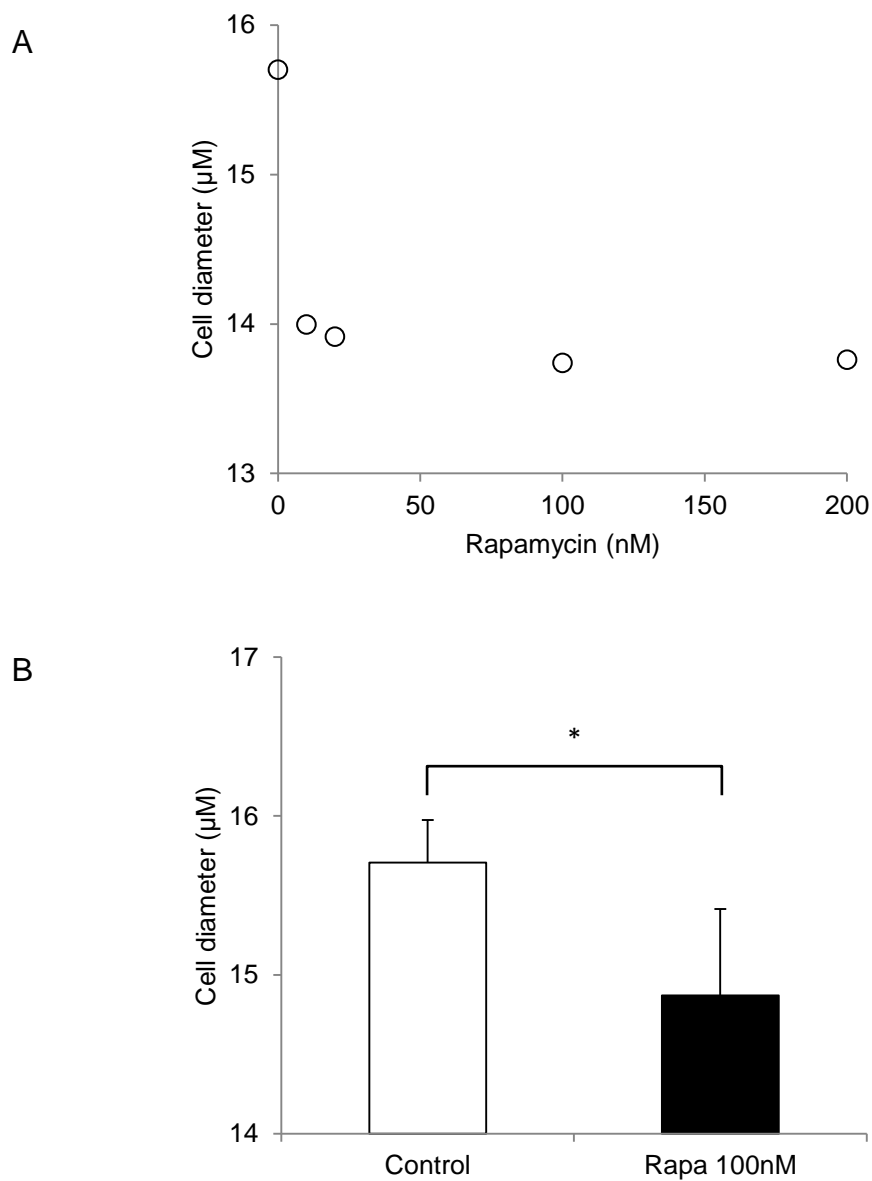


Figure 6.2.2-1: Effect of rapamycin on HUVEC cell diameter.

Upper panel (A) shows a dose response curve of the effect of rapamycin on cell diameter at differing doses on a single population of HUVEC. Lower panel (B) shows a comparison of HUVEC cell diameter in control cells vs those exposed to rapamycin 100nM (n=5, error bars indicate SEM, asterisk indicates $p < 0.05$).

Cell diameter decreased in the presence of all doses of rapamycin (10nM, 20nM, 100nM and 200nM). The experiment was repeated on 5 separate populations of cells exposed to rapamycin 100nM. Analysis revealed a statistically significant decrease in cell diameter (control $15.7\mu\text{M}$ vs rapamycin 100nM $14.9\mu\text{M}$, $p=0.04$).

I repeated the experiment using HUVEC and growing them in the presence of rapamycin 100nM using 3 separate populations of cells, such that they were exposed to rapamycin with each change of medium for 7 days. At the end of the week, cells were harvested and replated without drug treatment for 3 days, before being harvested for analysis by flow cytometry.

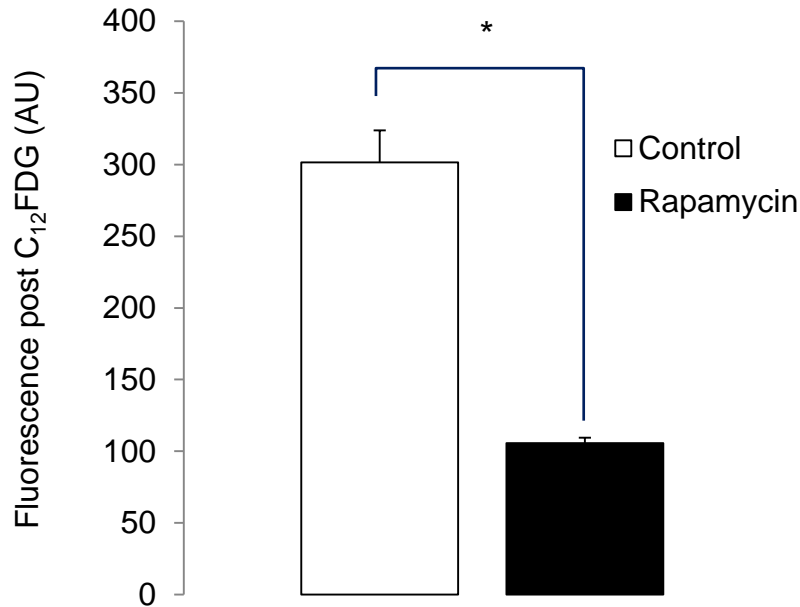


Figure 6.2.2-2: Effect of rapamycin on HUVEC β -galactosidase activity.

Result of 3 separate experiments using 5th passage HUVEC. Columns indicate mean fluorescence post exposure to C₁₂FDG, measured by flow cytometry. Error bars indicate standard error of the mean. *p<0.001

The results of the experiment revealed that, whereas control cells had a mean fluorescence post C₁₂FDG exposure of 301.43 arbitrary units, SEM 22.36; mean fluorescence post C₁₂FDG exposure for rapamycin treated cells was 105.6 arbitrary units, SEM 3.9. When analysed by two-tailed t-test, p= 0.00006.

Rapamycin therefore has a large effect on reducing β -galactosidase activity as measured by flow cytometry, despite being anti-proliferative.

6.3 AMP kinase activation

6.3.1 Effect of AMP kinase activator, AICAR on HUVEC senescence and its interaction with DETA-NO

In order to investigate the effect of AMP kinase activation, I performed experiments to assess the effect of AICAR on cell diameter, cell proliferation and β -galactosidase activity.

Cells from passages 3-5 were grown in the presence of AICAR to assess the effect of the drug on cell size and were analysed using the Coulter Multisizer particle analyser. Cells were grown in 6 well plates with an initial seeding density of 2500 cells/cm² and medium was changed 3 times per week. On each change of medium, AICAR was added. As the fastest growing cells approached 80% confluence, all cells were harvested and counted using the Coulter particle analyser.

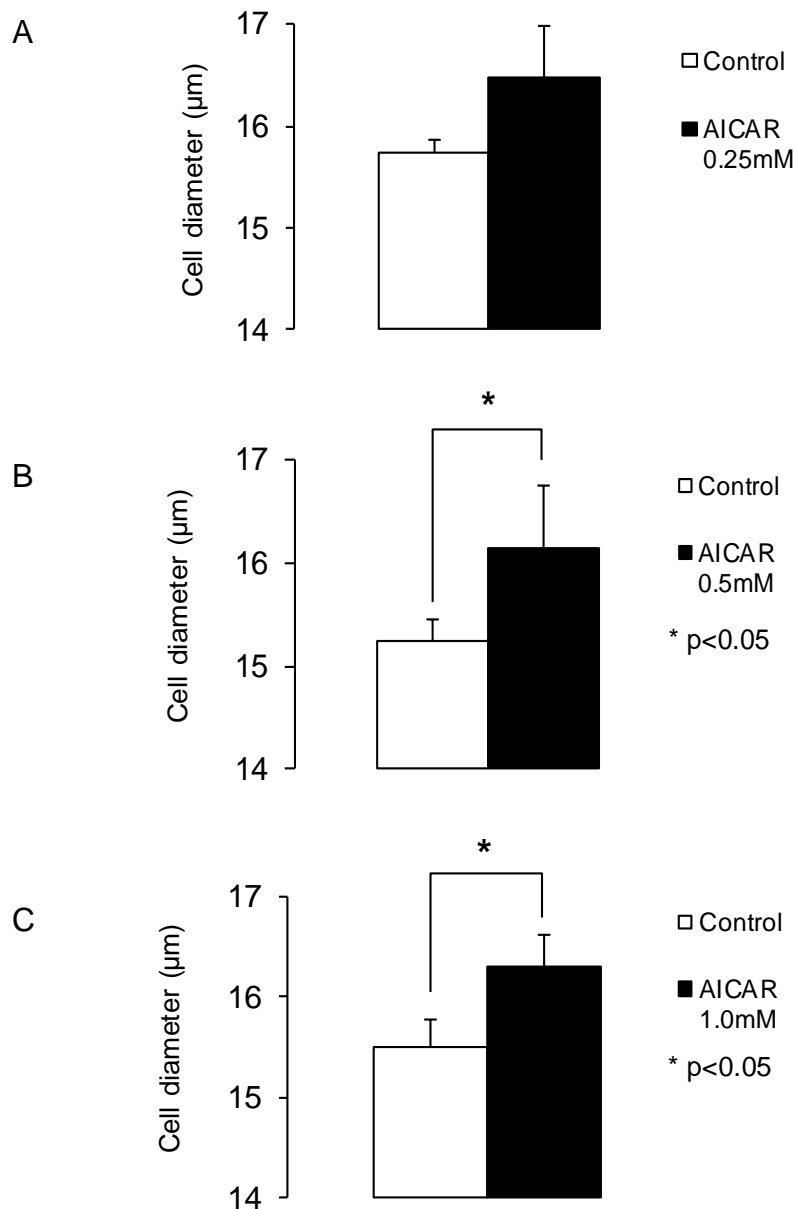


Figure 6.3.1-1: Effect of AICAR on HUVEC cell diameter: dose response.

The above three graphs display the effects of varying concentrations of AICAR on cell diameter (0.25mM (A), 0.5mM (B), 1mM (C)), versus control conditions. Error bars indicate standard error of the mean and callipers with asterisks indicate statistical significance when measured by t-test.

Cell diameter was measured using the Coulter Particle Analyser and experiments were repeated using 3, 4 and 7 different populations of HUVEC in the case of AICAR 0.25mM, 0.5mM and 1mM respectively. AICAR, at a variety of doses, increases cell size suggestive of an effect on senescence.

The graphs below demonstrate the effect of AICAR on population doubling and population doubling rate over the course of 6 passages.

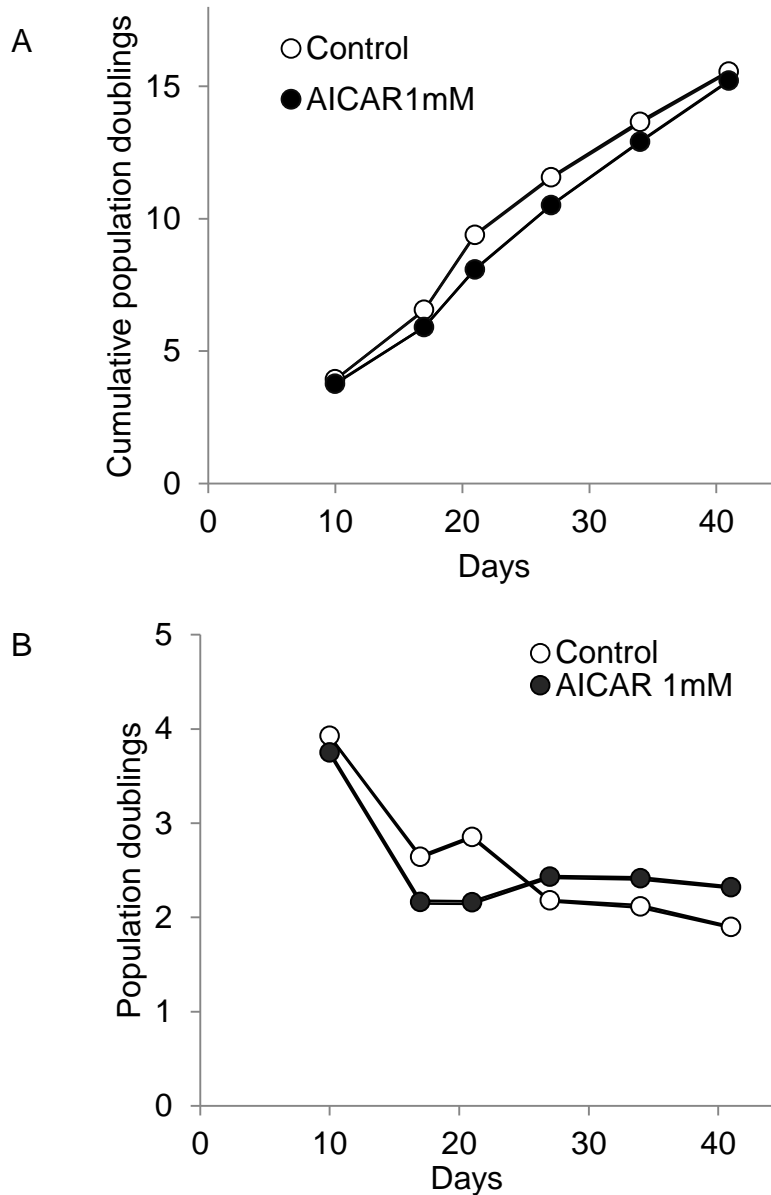


Figure 6.3.1-2: Effect of AICAR on proliferation of HUVEC.

The figures show the same data expressed in different ways. The top graph (A) shows cumulative population doubling of HUVEC exposed to AICAR 1mM, the bottom graph (B) shows population doubling per passage of the same cells. The time indicates the number of days since initial seeding. Each count was in triplicate and an average of each measurement was used to calculate population doubling. Lines connecting markers indicate SEM.

There was a modest but significant difference in cumulative population doubling between control and treatment groups and this in turn suggested that AICAR may cause cell cycle arrest in stress-induced senescence manner (ANOVA $p=0.005$).

Further evidence for an effect of AICAR on senescence was obtained using flow cytometric analysis of cell forward scatter, cell side scatter and fluorescence intensity of C_{12} fluorescein, a product of the reaction between β galactosidase and C_{12} FDG.

Cells were grown to confluence in T-75 flasks in EGM-2 growth medium. Medium was changed daily and AICAR 0.25mM was added daily for 3 days. Medium was then changed and cells were passaged 48 hours later. Cells were replated at 5000 cells/cm² on 60mm diameter plates and grown for a further 3 days. Cells were then exposed to C₁₂FDG for 4 hours and washed twice with PBS. Samples were harvested using trypsin and placed on ice until flow cytometric analysis.

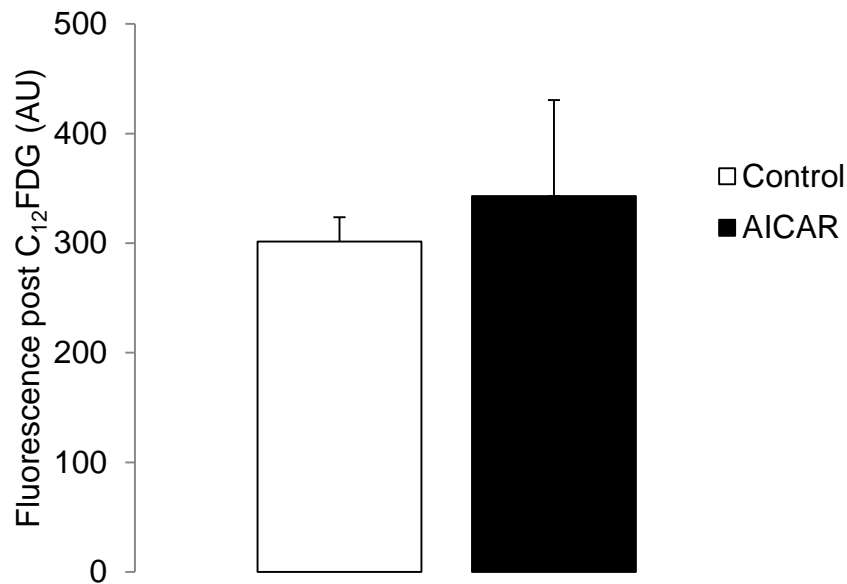


Figure 6.3.1-3: Effect of AICAR on β -galactosidase activity by flow cytometry.

Results of flow cytometric analysis of β -galactosidase activity using the fluorescent probe C₁₂FDG. Experiments were performed using 3 different cell populations. Error bars indicate standard error of the mean fluorescence activity in HUVEC with and without exposure to AICAR 0.25mM (shaded column).

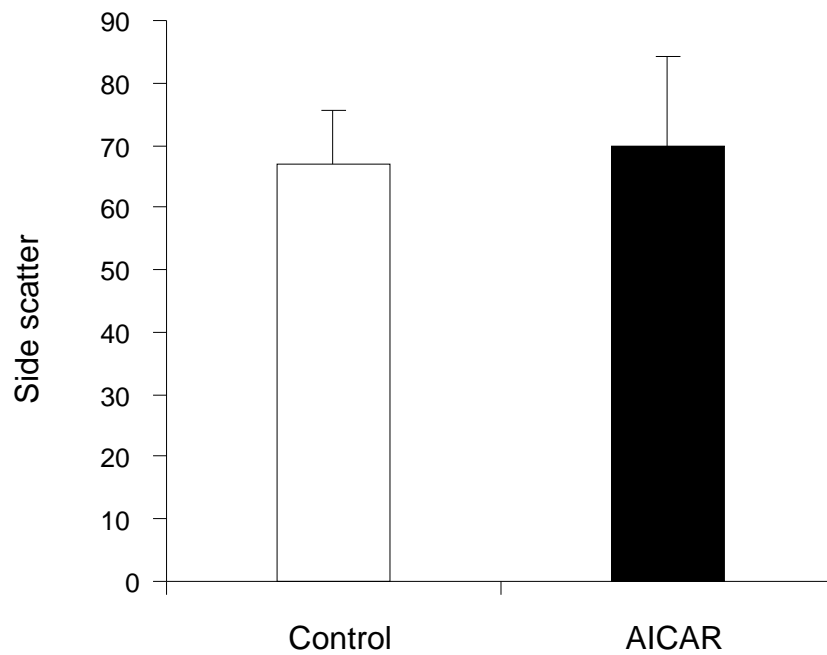


Figure 6.3.1-4: Effect of AICAR on side scatter of HUVEC.

Figure shows flow cytometry analysis of the side scatter of cells with or without exposure to AICAR 0.25mM. Error bars indicate standard error. Experiments were performed using 3 different cell populations of HUVEC.

The effect of AICAR on our model of nitric oxide-induced HUVEC senescence was analysed by the flow cytometric technique. Using the same method as described above, cells were exposed to AICAR, DETA-NO or both and then analysed.

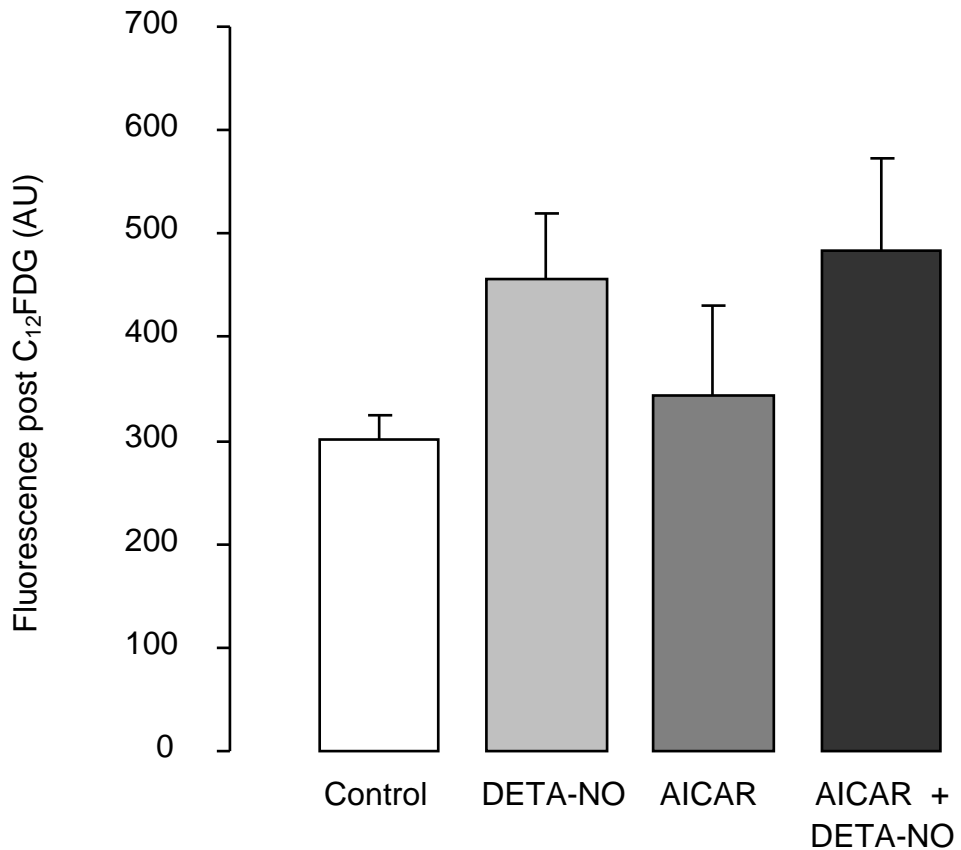


Figure 6.3.1-5: Interaction between AICAR and DETA-NO on HUVEC β -galactosidase activity.

Results of 3 separate experiments involving separate populations of HUVEC. Cells were exposed to DETA-NO 0.5mM, AICAR 0.25mM or both reagents and were then analysed for β -galactosidase activity by flow cytometry. Results were mean fluorescence intensity and error bars denote standard error of the mean.

After repeating the experiment 3 times, it became evident that AICAR did not prevent DETA-NO-induced senescence as measured by β -galactosidase activity. The only significant differences between conditions were those comparing cells exposed to DETA-NO to those not exposed to DETA-NO. Results of mean fluorescence activity as expressed in arbitrary units were as follows: Control 301.4, SEM 22.4; DETA-NO 456.2, SEM 64.2; AICAR 342.9, SEM 87.6; AICAR and DETA-NO 483.7, SEM 88.5. t-tests: Control vs. AICAR $p=0.42$, DETA-NO vs. AICAR and DETA-NO $p=0.62$.

The effect of AICAR on the generation of reactive oxygen species within the cell was also assessed. The hypothesis was that an increase of ROS oxidizes proteins which are recognized by phagosomes. These irreversibly damaged proteins are normally cleared by lysosomes but this mechanism could be overwhelmed in senescence and that this leads to an increase in lysosomal mass. This could be the mechanism by which nitric oxide leads to senescence as it is known to indirectly increase the generation of superoxide. The effect of AMP kinase activation as a coordinator of a response to bioenergetic stress includes blocking further anabolic processes such as

DNA and protein synthesis. It also promotes catabolic processes and therefore could lead to an increase in ROS production by increasing aerobic respiration and indirectly increasing mitochondrial superoxide production. This combination of blocking protein synthesis and increasing superoxide could lead to an excessive accumulation of oxidized protein.

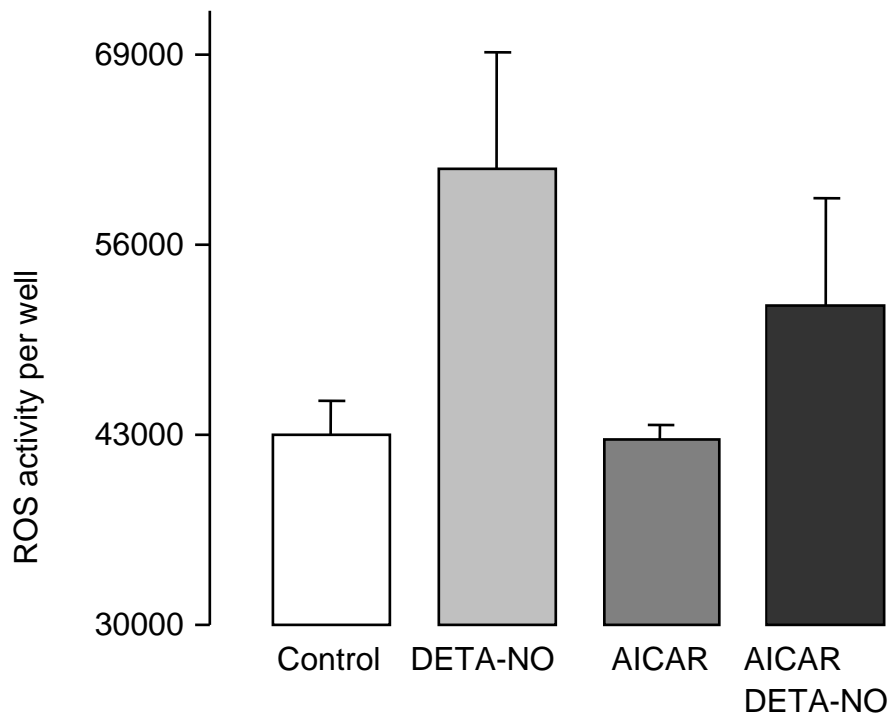


Figure 6.3.1-6: Interaction between DETA-NO and AICAR: flow cytometric analysis of ROS.

Results of mean of 3 separate experiments involving separate populations of HUVEC. Cells were exposed to DETA-NO 0.5mM, AICAR 0.25mM or both reagents and were then analysed for their ability to generate ROS as detected by exposure to H₂DCFDA. Results were mean fluorescence and error bars denote standard error of the mean.

We investigated ROS production in HUVEC using H₂DCFDA fluorometric analysis which detects ROS species. AICAR at a dose of 0.25mM was not shown to have an effect on ROS generation, but was able to prevent DETA-NO-induced increases in ROS generation. This interaction was not significant on ANOVA. Direct comparison of DETA-NO alone and AICAR with DETA-NO by t-test was also non-significant. Average ROS activity as measured by H₂DCFDA by fluorimetry was as follows: control 4.29 x 10³, SEM 2.36 x 10³; DETA-NO 61.1 x 10³, SEM 8.0 x 10³; AICAR 42.7 x 10³, SEM 9.9 x 10³; AICAR and DETA-NO 51.8 x 10³, SEM 7.3 x 10³; t-test of DETA-NO vs. DETA-NO and AICAR p=0.07.

As previously reported, AMP kinase can also activate protective responses to oxidative stress and this may explain our results with respect to the effect on reactive oxygen species generation as detected by the fluorogenic probe H₂DCFDA.

However, the protection afforded by activating AMP kinase in this way was unable to translate to an effect to prevent the senescence seen when exposing cells to DETA-NO 0.5mM.

In our model, AMP kinase activation – in contrast to work from other groups was unable to exert an effect on senescence.(See Introduction).

6.3.2 Assessing the effect of AMP kinase activation on human umbilical artery smooth muscle cells by senescence-associated β -galactosidase staining

The effect of AICAR 0.25mM on senescence-associated β -galactosidase was assessed. Cells were initially explanted from human umbilical cord and passaged 3 times before exposure to AICAR 0.25mM for 1 week. At the end of the exposure period, cells were stained for senescence-associated β -galactosidase and counted using phase contrast light microscopy at 20 x magnification.

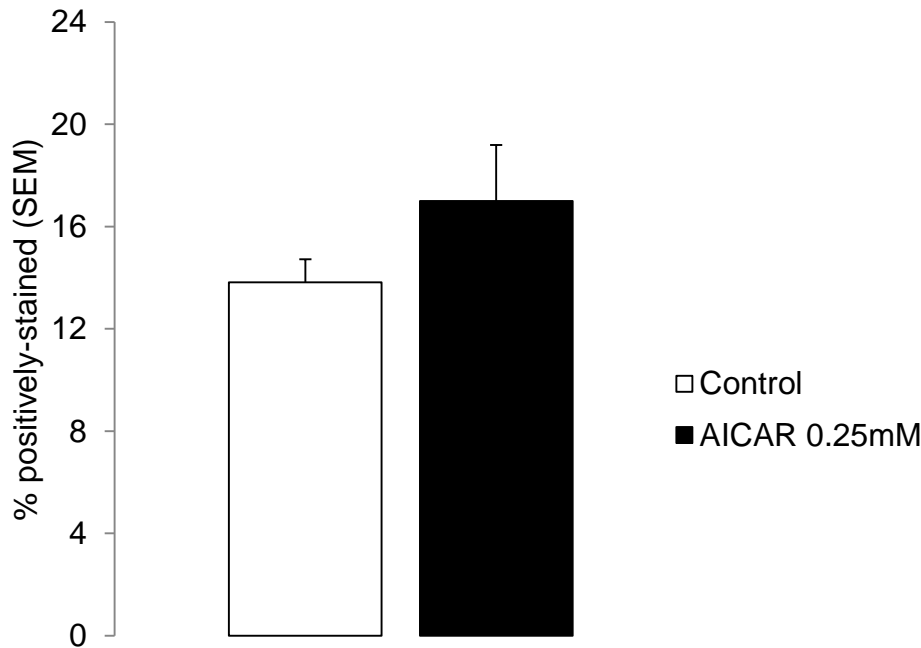


Figure 6.3.2-1 Effect of AICAR on HUASMC: senescence-associated β -galactosidase.

Result from a single sample of HUASMC at 3rd passage exposed to AICAR 0.25mM vs. control. Each condition was repeated in 4 individual wells and results are mean percentage of counted positively stained cells for senescence-associated β -galactosidase vs. total cells counted. Error bars indicate standard error of the mean.

4 separate fields of view were counted from 4 wells of each condition. Control cells demonstrated positive staining in a mean of 13.8%, SEM 0.9 and cells exposed to AICAR 0.25mM 17.0%, SEM 2.2. Statistical comparison using two-tailed t-test assuming unequal variance gave $p=0.25$.

Therefore there was a non-statistically significant increase in senescence-associated β -galactosidase in smooth muscle cells exposed to AICAR 0.25mM.

6.3.3 Effect of metformin on HUVEC proliferation and senescence

Metformin activates AMP kinase in a manner independent of LKB1. Thus metformin complements AICAR as a means of assessing the senescence pathway via AMPK to ascertain if LKB1 is essential in the senescence pathway.

Cells were grown in the presence of a variety of drug concentrations for the one week with 3 changes of medium and drug in EGM-2 medium. At 80% confluence, cells were passaged in the normal fashion and counted and measured using the Coulter Particle Analyser.

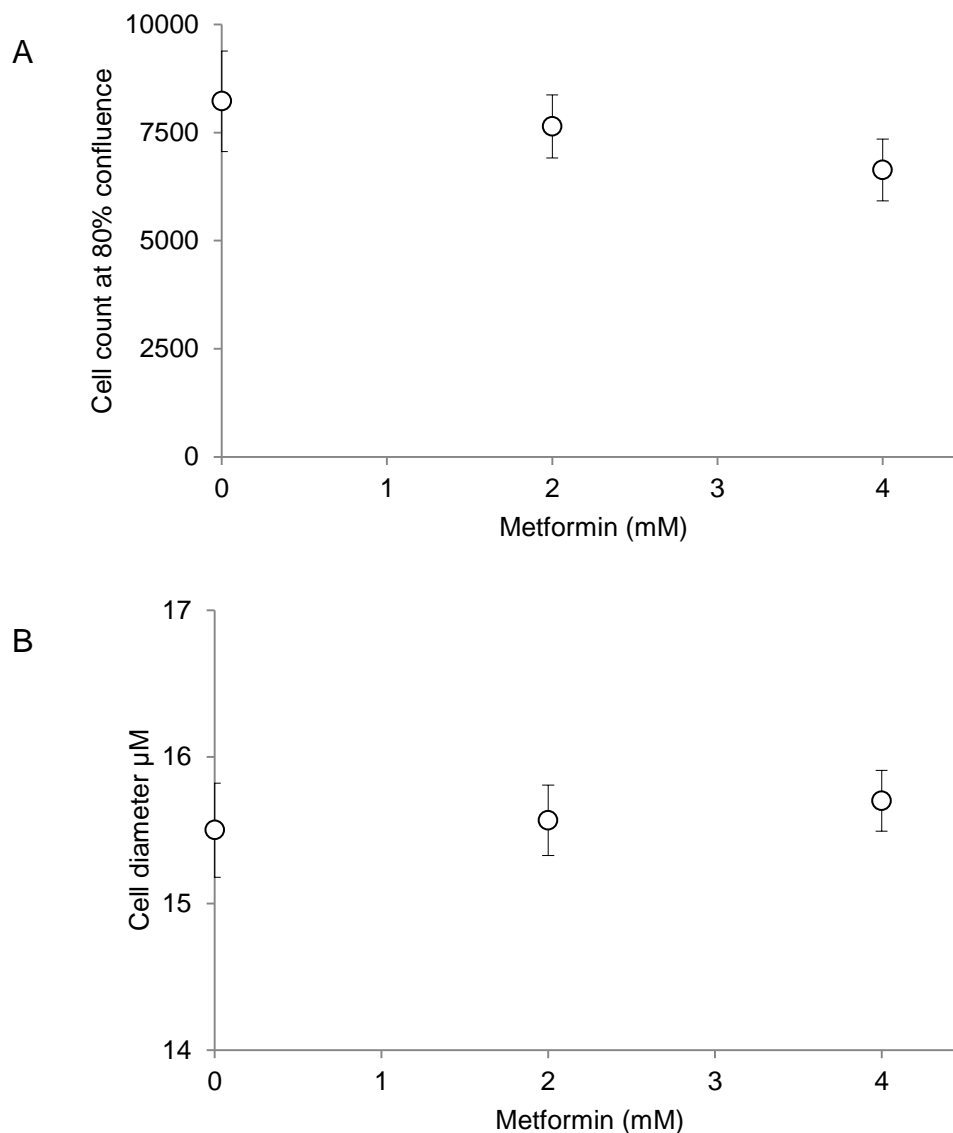


Figure 6.3.3-1: Dose response for the effect of metformin on HUVEC diameter and count.

Effect of various doses of metformin on cell counts at harvest and cell diameter as measured by Coulter particle analyser. The top graph (A) displays the cell count per mL in wells harvested by trypsinization when the most rapidly-replicating well reached 80% confluence. Lower panel (B) represents the cell diameter at harvest. Error bars indicate standard error. n=3.

A similar dose-dependent trend was observed to that seen in AICAR. Cell proliferation was maintained ($p=0.31$ by ANOVA) and cell size exhibited a non-significant increase ($p=0.17$ by ANOVA). This in turn could suggest that LKB1 activation is not necessary for initiation of the senescent phenotypical change. Parallel to this experiment, cells were also stained for senescence-associated β -galactosidase using the standard histological method. In order to achieve an increased sample size, cells were grown in 6 well plates with 4 wells per condition. The total number of cells in a field of view were counted using phased light microscopy. Cells stained blue for senescence-associated β -galactosidase were then counted and used to calculate a percentage of positively-stained cells. Data were analysed using Microsoft Excel with a single condition ANOVA.

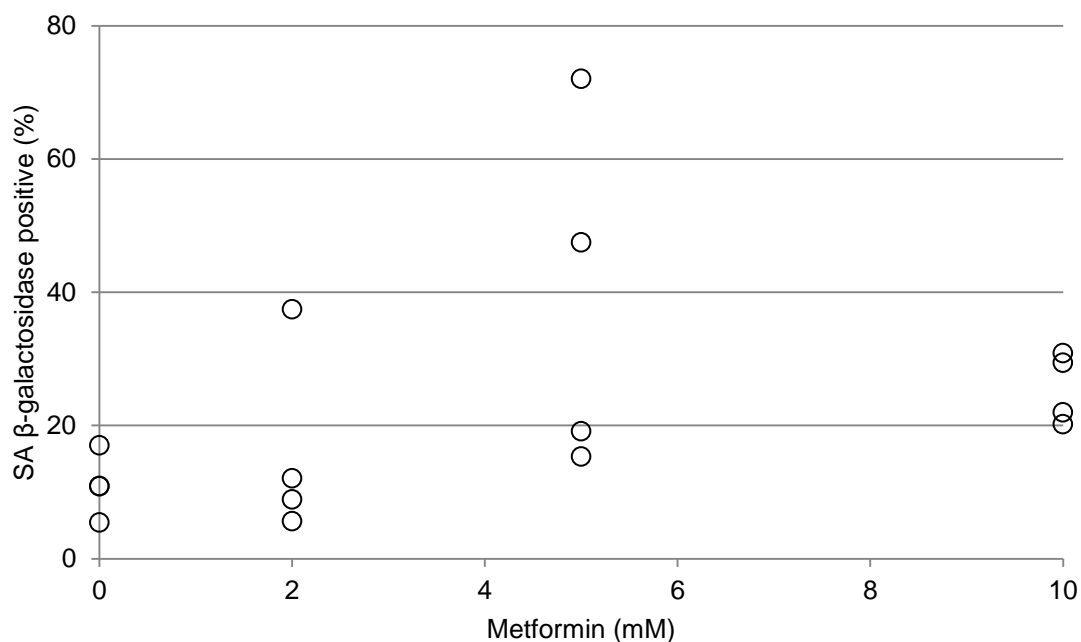


Figure 6.3.3-2: Effect of metformin on HUVEC senescence: senescence-associated β -galactosidase.

Results of an experiment with increasing doses of metformin and its effect on a population of HUVEC. The data shown are individual counts from wells stained with senescence-associated β -galactosidase.

Results were as follows; control cells mean 11.05, SEM 2.37; metformin 2mM mean 16.01, SEM 7.27; metformin 5mM mean 38.49, SEM 13.29; metformin 10mM mean 25.6, SEM 2.66. ANOVA $p=0.117$.

Cells from 3 separate donors were further analysed using flow cytometric quantification of β -galactosidase activity using the fluorogenic probe, C_{12} FDG. Cells were grown to confluence and then exposed to metformin 10mM at each daily change of medium for 3 days. Cells were harvested and analysed by flow cytometry.

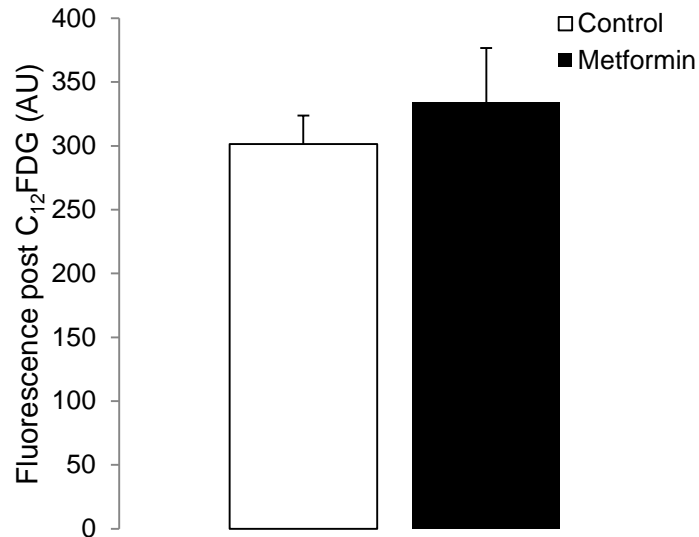


Figure 6.3.3-3: HUVEC senescence and metformin: flow cytometric analysis of β -galactosidase activity.

Results of 3 separate experiments assessing the effect of metformin on β -galactosidase activity as measured by flow cytometry. Columns indicate the mean results of mean fluorescence intensity and error bars indicate standard error of the mean.

Mean fluorescent activity in control cells was 301.43 arbitrary units, SEM 22.36 and for metformin 10mM was 334.2 arbitrary units, SEM 42.3. Analysis by two-tailed t-test revealed a lack of statistical significance, $p=0.23$.

6.3.4 Effect of metformin on HUASMC senescence

The experiment also performed in HUASMC using metformin at 1mM and 2mM dosages.

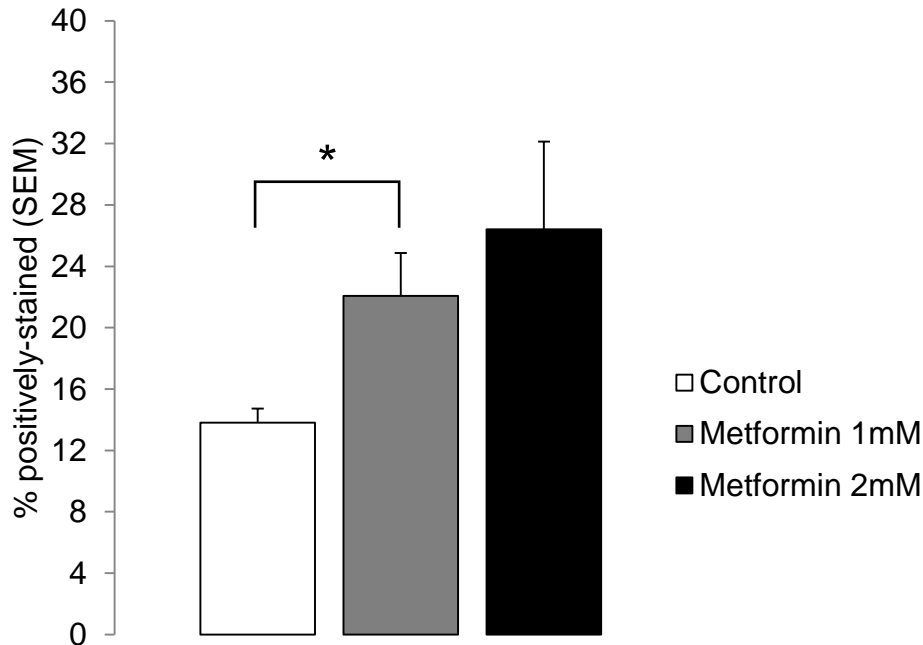


Figure 6.3.4-1: Effect of metformin on HUASMC: senescence-associated β -galactosidase.

Result from a single sample of HUASMC at 3rd passage exposed to metformin 1mM or 2mM vs. control. Each condition was repeated in 4 individual wells and results are mean percentage of counted positively stained cells for senescence-associated β -galactosidase vs. total cells counted. Error bars indicate standard error of the mean. Callipers indicate statistical comparison using a two-tailed t-test assuming unequal variance and asterisks indicate $p < 0.05$.

Results indicate a dose-related increase in senescence-associated β -galactosidase activity in cells exposed to metformin. As before, control cells demonstrated positive staining in a mean of 13.8%, SEM 0.9, metformin 1mM 22.1%, SEM 2.8; metformin 2mM 26.4, SEM 5.7. Two-tailed t-tests assuming unequal variance performed comparing each individual dose of metformin to control showed significant differences; control vs. metformin 1mM $p = 0.04$, control vs. metformin 2mM $p = 0.12$. However, a single factor ANOVA comparing all conditions was not significant $p = 0.10$.

6.4 Conclusion

In this chapter, I attempt to assess the influence of drugs which are able to manipulate autophagy and mobilise cellular defences against oxidative stress, rather than simply being antioxidants themselves.

In HUVEC, none of the treatments were seen to promote senescence as measured either by cell proliferation rates or β -galactosidase activity. Meanwhile, cells exposed to AICAR, bafilomycin A1 and metformin each demonstrated an increase in cell mass. There was, however, a small effect in promoting senescence in HUASMC by metformin. As previously discussed, this may be a consequence of the differing AMP kinase subunits present in HUASMC vs. HUVEC.

As an inhibitor of autophagy, we expected bafilomycin A1 could lead to cellular vulnerability to senescence, rather than to reduce it. β -galactosidase assays were performed using both the standard histochemical senescence-associated β -galactosidase assay and by flow cytometry using C_{12} FDG. The effect demonstrated by bafilomycin A1 was interesting in that there were discrepancies between methods. Using the histochemical technique to look for senescence-associated β -galactosidase, I observed a marked reduction in staining. However, this technique relies on a visual inspection of cells under light microscopy. There is an element of judgement when counting cells and weaker staining may account for the discrepancy between the number of cells staining positive for senescence-associated β -galactosidase and the lack of difference seen in the other methods used to assess β -galactosidase activity. Furthermore, the senescence-associated β -galactosidase assay relies upon an excess of β -galactosidase enzyme activity in senescent cells to overcome the fact that the stain is performed at a relatively-alkaline pH. Excessive pre-alkalinisation caused by bafilomycin A1 may therefore affect the assay by further reducing β -galactosidase activity beyond a threshold where it can be seen to alter X-gal. However, this is an effect one may expect to affect the flow cytometric method in a similar fashion.

Other techniques were more consistent with bafilomycin A1 exerting no effect on senescence. The increase in cell mass seen with bafilomycin A1 and the small reduction in proliferation rate seemed most consistent with the flow cytometric assay results, demonstrating no difference in β -galactosidase activity.

Rapamycin, in contrast, demonstrated a large reduction in β -galactosidase, despite being a known anti-proliferative agent. Rapamycin is also able to inhibit autophagy and therefore the reduction in β -galactosidase activity is unexpected. It may be that there is a direct interference with the assay, rather than this being a physiologically significant function. It is possible that the fluorogenic substrate for β -galactosidase, C_{12} FDG, is unable to enter the lysosome when autophagy is being inhibited. Unfortunately, we did not have time to assess the effect this had on proliferation in our model and also to assess whether other markers of senescence were increased.

The results from this chapter are consistent with the hypothesis that AMP kinase activation by AICAR mobilises cellular defences against oxidative stress. This was demonstrated by a small decrease in ROS generation by cells exposed to DETA-NO and AICAR. However, this did not lead to a decrease in β -galactosidase activity in HUVEC. The small effect in HUASMC merits further investigation. Again, this is consistent with results from earlier in this document showing no effect on the ability of DETA-NO to cause cellular senescence with concurrent exposure to antioxidants, even when they are able to reduce ROS generation.

7 Conclusions and discussion

We have investigated several known methods of detecting senescence in order to find a method which is capable of detecting cellular senescence at an early stage. Having looked at all of the methods, I found that the flow cytometric detection of total β -galactosidase activity offered the most promise for ease of use and sensitivity.

I used this as the starting point for my investigation into the effects of various pharmacological manipulations of vascular cells and the consequences with regard to senescence. Of the other means of assessing β -galactosidase activity, the histochemical staining of senescence-associated β -galactosidase relied on a degree of subjectivity when counting cells by eye and could be subject to bias. In addition, the staining technique required cell fixation and several washing steps, some of which could strip cells from the plate. One could not be certain that this would not preferentially select healthy or senescent cells, and as such could under- or over-estimate an effect on senescence.

It was interesting to observe the comparison between flow cytometric analysis of β -galactosidase activity and senescence-associated β -galactosidase staining when looking at cells exposed to bafilomycin A1. In this series of experiments, an apparent large reduction in staining for senescence-associated β -galactosidase was not repeated on flow cytometric analysis of β -galactosidase activity, which showed no difference in control groups and those treated with bafilomycin A1. As discussed earlier, this discrepancy could simply be explained by an interaction between the action of bafilomycin A1 and the X-gal histochemical assay. Certainly, from other groups' data on autophagy and aging, we would have expected to observe either an increase in senescence or no effect.^{151;153-155} Further work using other techniques to detect senescence such as the expression of cell cycle protein p16^{INK4a} will help to investigate whether bafilomycin A1 has an effect on senescence.

Assessing total β -galactosidase activity by MUG fluorescence in cell lysates seemed to lack sensitivity and would be unable to reveal if some cells senesced in a population and others remained healthy. Furthermore, the measurements made to correct for the amount of protein analysed could be a source of error and some of the protein could have been extracellular. As senescent cells are larger, correcting for β -galactosidase activity per cell would have been useful and is not possible in cell lysates.

Our analysis of Annexin-V binding as a marker for apoptosis with co-staining for β -galactosidase revealed that cells which express an increase in β -galactosidase activity are not also undergoing senescence. This is consistent with previous observations that senescent cells are resistant to apoptosis.⁵⁵

Choosing a main cell type to work with for our model, we tried to harvest cells in an environment of low stress and chose initially to try obtaining explanted HUASMC. However, as our explanted HUASMC were harvested with variable efficiency and

senesced after a relatively low number of population doublings, they were not a good cell type to look at if one wished to separate out replicative senescence from stress-induced senescence.

Despite this, the main positive finding in this investigation was that vascular cells senesce on exposure to nitric oxide donors and this was universal across the cell types analysed.

Western blotting for the senescence-associated proteins p16^{INK4a} and p21^{WAF} was used to confirm that cell populations which had indications of senescence with increased β -galactosidase activity had all of the features of senescent cells. Again, analysis of cells in this way suffers from being based on cell lysates, rather than analysing whole cells individually. However, it is an analysis of the machinery of senescence and is therefore a more direct measure. It would have been interesting to perform further experiments on fixed cells with immunofluorescence or in situ hybridization to confirm that cells either expressed some or none of these proteins, because with our other method, it was clear that all cells have β -galactosidase activity but senescent cells have more.

Although not necessarily a measure of senescence, the loss of replicative capacity observed from analysing BrDU incorporation in senescent cells was required as a confirmation that cells would not regain their proliferative capacity after the stressors had been removed. Analysing the cell populations at different cell seeding densities also revealed the effect of contact inhibition in endothelial cells grown in monolayer. The first point to note is that these cells had previously been confluent in culture during exposure to the various agents used to stress the cells or protect them from senescence; however they were able to immediately regain their proliferative ability. The second point to note is that irrespective of cell density, the peak proliferative capacity in cells exposed to DETA-NO was markedly decreased, consistent with the idea that this treatment did induce senescence.

The choice of working with endothelial cells in a confluent monolayer was forced upon us as cells grown exponentially in culture would either stop growing on first exposure to nitric oxide or die when exposed to higher concentrations. While I cannot exclude that a proportion of cells did senesce as a consequence of being grown in a confluent manner, this did not appear to be a large effect as cells recovered replicative capacity on replating. Furthermore, this effect was controlled for in both treatment and control groups.

We did not investigate the effect of telomerase or telomere length in our model as other groups have previously done so.

Our search for a reason as to why cells exposed to nitric oxide senesced and also into the mechanism took us into an area which was already of interest for being one of the main theories of aging, the free radical theory of aging. I had hoped to use t-BHP as a positive comparator in our model of senescence, but I was unable to

demonstrate an effect on senescence from any concentration of t-BHP. This was in contrast to work from other groups in the area. One possibility is that cells which are confluent have far superior defences against oxidative stress. Another is that the ascorbic acid in our culture medium had sufficient antioxidant activity to counter the effect of hydrogen peroxide.

In either event, we were able to demonstrate an increase in ROS generation in cells exposed to t-BHP and this had a linear relationship to the concentration of t-BHP added to the cell culture medium. Moreover, we were able to calculate which concentration of t-BHP would replicate the same amount of ROS generation as measured by the probe, H₂DCFDA by exposing cells to DETA-NO at the senescence-generating concentration. In these experiments, it was clear that t-BHP had no effect on promoting senescence in our model. While it is possible that t-BHP may cause senescence without increasing total β-galactosidase activity, we feel this is unlikely as Touissant measured senescence by senescence-associated β-galactosidase staining.⁴⁶ The lack of effect of t-BHP was contrary to the effect seen with DETA-NO, despite identical levels of ROS generation. This led us to conclude that DETA-NO does not induce senescence purely by increasing ROS.

Despite the concept that H₂DCFDA is activated by de-acetylation within cells and is therefore an intracellular probe for ROS, we saw an effect in a cell-free environment when the probe was exposed to the oxidative reagents. As discussed earlier, this effect was in the presence of a much higher concentration of H₂DCFDA as there was no washing stage. In addition, the interaction between oxidants and antioxidants was different. Lastly, the effect was controlled for using control populations of cells. Clearly this is a significant limitation to measuring ROS in this way using fluorimetry.

As further confirmation, we were able to investigate a variety of antioxidants in the DETA-NO-induced senescence model. First we looked at their effectiveness in preventing the increase in ROS generation and then at their effect on total β-galactosidase activity. Uric acid and NAC were effective antioxidants in cells exposed to DETA-NO. NAC was also effective in cells exposed to t-BHP. However, uric acid and NAC increased ROS generation in the cells exposed to GSNO. In contrast, selenomethionine was ineffective in preventing ROS generation by DETA-NO.

	Cellular ROS	Cell-free ROS	Senescence
DETA-NO	+	+	+
DETA-NO + NAC	Prevents	++	Prevents
DETA-NO + UA	Prevents	++	+
GSNO	+	+	+
GSNO + NAC	++		

Figure 7-1: Summary of ROS and senescence data.

Despite uric acid being an effective antioxidant in cells exposed to DETA-NO, it caused an increase in β -galactosidase activity in HUVEC exposed to DETA-NO. As expected, selenomethionine had no effect in either direction. However, NAC was able to completely abolish the DETA-NO effect on HUVEC senescence. The effect may be due to a genuine decrease in ROS generation within cells or due to replenishment of cellular reduced glutathione by NAC. However, results from the NO electrode measurement of NO generated by DETA-NO with subsequent addition of NAC showed that the likeliest explanation of the effect of NAC is that it almost completely quenches nitric oxide as it is being released by DETA-NO. This raised the possibility that a nitrosothiol substance formed in the reaction between NAC and DETA-NO may be protective against senescence. As a way of investigating this possibility, we used the nitrosothiol NO donor GSNO. This also promoted senescence in a similar fashion to DETA-NO. Thus nitrosothiols are less likely to explain the protective effect of NAC against NO induced senescence.

The effect of DETA-NO was not prevented by inhibiting soluble guanylate cyclase activity. Although the effect of ODQ was not directly measured by cGMP assay as part of our investigation, Heller et al had previously done so.²¹⁴ The absence of any effect at any concentration of ODQ therefore made soluble guanylate cyclase an unlikely target for the pathway to senescence.

Protein transnitrosation seemed a possible general mechanism after our experiment using cold light on cells exposed to DETA-NO. The complete reversal of nitric oxide-induced increases in β -galactosidase activity in cells exposed to pulses of cold light was further investigated by looking at protein transnitrosation by using the biotin switch method. We used cell lysates for this method. Therefore the whole proteome was analysed. While we did not detect general increases in protein transnitrosation, this method also offers a means of comparing differences in bands representing proteins which could be specific targets for transnitrosation. Band analysis revealed peaks of difference in non-specific labelling and nitrosylated proteins at a predicted molecular weight of 16.4kDa and 64.4kDa. As previously discussed, p16^{INK4a} was present in increased levels in NO-induced senescent cells. Also, p65 and p66^{shc} are potential signalling molecules for the stress response by NF- κ B and protein kinase C- β -mediated signalling, a pathway seen to be increasingly active in elderly humans.

We would like to further investigate if either pathway were responsible for the observed effect of nitric oxide on vascular cell senescence.

Regarding the physiological relevance to nitric oxide-induced senescence, we looked at endogenous NO generation. We induced maximal eNOS-induced release of NO with A23187 but this had no measurable effect on β -galactosidase activity (or ROS generation). We also looked at the effect of inducing iNOS-generated NO by using the tet-iNOS HEK 293 cell line and growing in the same medium as HUVEC in Transwells. Again, this did not have a measureable effect on β -galactosidase activity. Thus we were unable to demonstrate that endogenously generated NO

causes senescence. In both conditions, I assume that the local nitric oxide concentration was too low. However, in the case of eNOS, a lack of uncoupling of eNOS may be relevant. In the tetracycline-inducible iNOS experiments, the relatively great distance between cells generating nitric oxide and the HUVEC being analysed may have prevented sufficient concentrations of nitric oxide.

AICAR and metformin both activate AMP kinase, a central protective pathway against metabolic and oxidative stress. Interestingly, we were unable to demonstrate an effect of either molecule on senescence of HUVEC. However, HUASMC demonstrated an increase in senescence-associated β -galactosidase activity when exposed to either AICAR or metformin. This sensitivity may be explained by the presence of the $\alpha 2$ subunit of AMP kinase seen in smooth muscle cells and would support the theory that AMP kinase may act to prevent excessive apoptosis by encouraging some cells to senesce in the presence of bioenergetic stress.

AMP kinase activation in HUVEC may not have led to senescence but we did demonstrate a small reduction in ROS generation in cells exposed to DETA-NO when they were also exposed to AICAR. However, AICAR was unable to prevent DETA-NO induced HUVEC senescence. This was consistent with our observation that oxidative stress was not a key factor in generating senescence. However, it also suggested that means to stimulate autophagy would not prevent NO-induced senescence in HUVEC.

8 Future work

Following on directly from my work, investigation into the role of NF- κ B in signalling stress-induced senescence would be warranted, as would p66^{shc}. Sen et al have subsequently investigated the role of the C-38 cysteine on the p65 subunit of NF- κ B and specifically at post-translational modification by either sulfhydration or transnitrosation.²¹⁵ Both the modifications were seen in primary macrophages exposed to TNF- α but they occurred in sequence, with sulfhydration occurring first. Transnitrosation would inactivate p65, an effect which promoted apoptosis and could be replicated by exposing the cells to GSNO 0.5mM.

There is a need to relate our findings to the *in vivo* situation, especially given the uncertainty regarding the range of concentrations of NO which cells are able to generate. One arena to investigate would be a sepsis model. Firstly, one would compare healthy vascular cells to those from survivors of severe sepsis. However, a prospective study would be interesting to assess the effect of administering nitric oxide donors. There are already a population of patients who have been exposed to chronic increases in nitric oxide donors, namely those taking oral nitrates to control angina, a common first-line treatment available for decades. These drugs are known to confer short-term symptomatic improvement by vasodilation of narrowed arteries, but despite this have no effect on improving mortality.

On a separate course, wortmanin (WM) is a specific inhibitor of PI3KF which mediates the effects of Akt on eNOS phosphorylation and has been shown to be effective in preventing high-glucose-mediated apoptosis in HUVEC at a dose of 100nM and may therefore be used to investigate the role of the Akt pathway.²¹⁶ The MEK pathway may be investigated using the U0126 (MEK inhibitor) which has been shown to nullify pro-apoptotic effects of nitric oxide on macrophages.²¹⁷ Inhibition of the electron transport chain by compounds such as rotenone or myxothiazol may experimentally mimic nitric oxide's role in this respect and can be exploited to assess the effect of bioenergetic stress on senescence.

Notch signalling is intimately involved with developmental processes and vascular formation. However, Notch signalling also appears to be involved with the development of senescence. Notch activated cells demonstrate a reduced ability to proliferate, cells enlarge and flatten and they express increased positive staining for senescence associated β -galactosidase. Moreover, they express increased levels of p16^{INK4a} and p53.²¹⁸

Notch activation also reduces the ability of the endothelium to form a barrier, increasing permeability with falling levels of β -catenin and cadherin. β -catenin and VE-cadherin were located away from the cell membrane and cell-cell junctions were not seen. The mechanism for these actions was shown to involve RhoA, rather than more traditional Notch targets. However, two distinct pathways were seen. The loss of barrier function was blocked by inhibition of RhoA kinase without affecting senescence.

The pathway involved in Notch mediated senescence involved MAP kinase, ERK and Akt phosphorylation and could be blocked by inhibition of MAP kinase kinase using the inhibitor U0126. Therefore RhoA causes senescence and an increase in endothelial cell permeability by separate mechanisms. Exploring the downstream targets of RhoA may therefore aid understanding of the bioenergetic stress-induced senescence process.

MicroRNAs are short sections of RNA which do not code but regulate gene expression of 30% of genes by interfering with mRNA encoded by these genes. They tend to be around 20 nucleotides long and are endogenous and conserved between individuals and species. They are thought therefore to play an important role in cellular regulation and some are specifically associated with the senescent endothelial phenotype. We did not investigate their role in signalling for senescence in our model.

MicroRNA-217 has been shown to positively correlate with senescence in endothelial cells, such that overexpression leads to senescence and inhibition prevents it. Putative targets have been investigated and SIRT1 has been found to be a candidate. Menghini et al²¹⁹ were able to use computer-modelled predictions of interactions of MiRNA-217 and SIRT1 to guide their study into the effect MiRNA-217 on HUVEC, human aortic endothelial cells and human coronary artery endothelial cells. The above findings were obtained using transfection techniques to insert MiRNA-217 into infected cells and anti-sense MiRNA-217 to reduce expression. In addition, MiRNA-217 negatively modulates eNOS activity by enhancing acetylation and therefore reducing function. This was seen *in vitro* and also in histological specimens of human atherosclerotic plaques.

MiRNA-200c is also associated with senescence in HUVEC *in vitro* studies. More specifically, it is involved in the process of oxidative stress-induced senescence seen when hydrogen peroxide is used as a stressor and also in mouse skeletal muscle cells exposed to ischaemia reperfusion injury. Inhibition of MiRNA-200c in cells exposed to hydrogen peroxide prevented senescence as a protective response. Furthermore, cells which were exposed to hydrogen peroxide tended to garner their response to stress via increasing p53 and pRb dephosphorylation.²²⁰

The Forkhead transcription factors are well-conserved across species and are associated with increased longevity, stress response and in particular, protection against the effects of ROS generation or oxidative stress and are involved with regulation of the cell cycle. They have been shown to interact with SIRT1 in situations of oxidative stress and are able to increase expression of Mn superoxide dismutase and catalase.^{221;222} Therefore they may have a role in our senescence model.

Reference List

- (1) HAYFLICK L, MOORHEAD PS. The serial cultivation of human diploid cell strains. *Exp Cell Res* 1961; 25:585-621.
- (2) Cristofalo VJ, Pignolo RJ. Replicative senescence of human fibroblast-like cells in culture. *Physiol Rev* 1993; 73(3):617-638.
- (3) Matthews C, Gorenne I, Scott S, Figg N, Kirkpatrick P, Ritchie A et al. Vascular smooth muscle cells undergo telomere-based senescence in human atherosclerosis: effects of telomerase and oxidative stress. *Circ Res* 2006; 99(2):156-164.
- (4) Chen YL, Jan KM, Lin HS, Chien S. Relationship between endothelial cell turnover and permeability to horseradish peroxidase. *Atherosclerosis* 1997; 133(1):7-14.
- (5) Caplan BA, Schwartz CJ. Increased endothelial cell turnover in areas of in vivo Evans Blue uptake in the pig aorta. *Atherosclerosis* 1973; 17(3):401-417.
- (6) Ku DN, Giddens DP, Zarins CK, Glagov S. Pulsatile flow and atherosclerosis in the human carotid bifurcation. Positive correlation between plaque location and low oscillating shear stress. *Arteriosclerosis* 1985; 5(3):293-302.
- (7) Rodier F, Campisi J. Four faces of cellular senescence. *J Cell Biol* 2011; 192(4):547-556.
- (8) Dimri GP, Lee X, Basile G, Acosta M, Scott G, Roskelley C et al. A biomarker that identifies senescent human cells in culture and in aging skin in vivo. *Proc Natl Acad Sci U S A* 1995; 92(20):9363-9367.

- (9) van der LB, Fenton MJ, Erusalimsky JD. Cytochemical detection of a senescence-associated beta-galactosidase in endothelial and smooth muscle cells from human and rabbit blood vessels. *Exp Cell Res* 1998; 241(2):309-315.
- (10) Kurz DJ, Decary S, Hong Y, Erusalimsky JD. Senescence-associated (beta)-galactosidase reflects an increase in lysosomal mass during replicative ageing of human endothelial cells. *J Cell Sci* 2000; 113 (Pt 20):3613-3622.
- (11) Lee BY, Han JA, Im JS, Morrone A, Johung K, Goodwin EC et al. Senescence-associated beta-galactosidase is lysosomal beta-galactosidase. *Aging Cell* 2006; 5(2):187-195.
- (12) Palm W, de LT. How shelterin protects mammalian telomeres. *Annu Rev Genet* 2008; 42:301-334.
- (13) Longhese MP, Bonetti D, Manfrini N, Clerici M. Mechanisms and regulation of DNA end resection. *EMBO J* 2010; 29(17):2864-2874.
- (14) Counter CM, Avilion AA, LeFeuvre CE, Stewart NG, Greider CW, Harley CB et al. Telomere shortening associated with chromosome instability is arrested in immortal cells which express telomerase activity. *EMBO J* 1992; 11(5):1921-1929.
- (15) Shay JW, Van Der Haegen BA, Ying Y, Wright WE. The frequency of immortalization of human fibroblasts and mammary epithelial cells transfected with SV40 large T-antigen. *Exp Cell Res* 1993; 209(1):45-52.
- (16) Counter CM, Botelho FM, Wang P, Harley CB, Bacchetti S. Stabilization of short telomeres and telomerase activity accompany immortalization of Epstein-Barr virus-transformed human B lymphocytes. *J Virol* 1994; 68(5):3410-3414.
- (17) Kim NW, Piatyszek MA, Prowse KR, Harley CB, West MD, Ho PL et al. Specific association of human telomerase activity with immortal cells and cancer. *Science* 1994; 266(5193):2011-2015.
- (18) Klingelhutz AJ, Foster SA, McDougall JK. Telomerase activation by the E6 gene product of human papillomavirus type 16. *Nature* 1996; 380(6569):79-82.

- (19) Greider CW, Blackburn EH. A telomeric sequence in the RNA of Tetrahymena telomerase required for telomere repeat synthesis. *Nature* 1989; 337(6205):331-337.
- (20) Blackburn EH, Greider CW, Henderson E, Lee MS, Shampay J, Shippen-Lentz D. Recognition and elongation of telomeres by telomerase. *Genome* 1989; 31(2):553-560.
- (21) Greider CW, Blackburn EH. The telomere terminal transferase of Tetrahymena is a ribonucleoprotein enzyme with two kinds of primer specificity. *Cell* 1987; 51(6):887-898.
- (22) Greider CW, Blackburn EH. Identification of a specific telomere terminal transferase activity in Tetrahymena extracts. *Cell* 1985; 43(2 Pt 1):405-413.
- (23) Lundblad V, Szostak JW. A mutant with a defect in telomere elongation leads to senescence in yeast. *Cell* 1989; 57(4):633-643.
- (24) Shampay J, Szostak JW, Blackburn EH. DNA sequences of telomeres maintained in yeast. *Nature* 1984; 310(5973):154-157.
- (25) Ramirez RD, Morales CP, Herbert BS, Rohde JM, Passons C, Shay JW et al. Putative telomere-independent mechanisms of replicative aging reflect inadequate growth conditions. *Genes Dev* 2001; 15(4):398-403.
- (26) Minamino T, Yoshida T, Tateno K, Miyauchi H, Zou Y, Toko H et al. Ras induces vascular smooth muscle cell senescence and inflammation in human atherosclerosis. *Circulation* 2003; 108(18):2264-2269.
- (27) Capper R, Britt-Compton B, Tankimanova M, Rowson J, Letsolo B, Man S et al. The nature of telomere fusion and a definition of the critical telomere length in human cells. *Genes Dev* 2007; 21(19):2495-2508.
- (28) Greider CW, Blackburn EH. Identification of a specific telomere terminal transferase activity in Tetrahymena extracts. *Cell* 1985; 43(2 Pt 1):405-413.
- (29) van SB, Smogorzewska A, de LT. TRF2 protects human telomeres from end-to-end fusions. *Cell* 1998; 92(3):401-413.
- (30) van SB, de LT. Control of telomere length by the human telomeric protein TRF1. *Nature* 1997; 385(6618):740-743.

- (31) Campisi J. Cancer, aging and cellular senescence. *In Vivo* 2000; 14(1):183-188.
- (32) Collado M, Gil J, Efeyan A, Guerra C, Schuhmacher AJ, Barradas M et al. Tumour biology: senescence in premalignant tumours. *Nature* 2005; 436(7051):642.
- (33) Holliday R. Cancer and cell senescence. *Nature* 1983; 306(5945):742.
- (34) Mathon NF, Lloyd AC. CELL SENESENCE AND CANCER. *Nat Rev Cancer* 2001; 1(3):203-213.
- (35) Minamino T, Yoshida T, Tateno K, Miyauchi H, Zou Y, Toko H et al. Ras induces vascular smooth muscle cell senescence and inflammation in human atherosclerosis. *Circulation* 2003; 108(18):2264-2269.
- (36) Spyridopoulos I, Isner JM, Losordo DW. Oncogenic ras induces premature senescence in endothelial cells: role of p21(Cip1/Waf1). *Basic Res Cardiol* 2002; 97(2):117-124.
- (37) Matthews C, Gorenne I, Scott S, Figg N, Kirkpatrick P, Ritchie A et al. Vascular smooth muscle cells undergo telomere-based senescence in human atherosclerosis: effects of telomerase and oxidative stress. *Circ Res* 2006; 99(2):156-164.
- (38) Minamino T, Miyauchi H, Yoshida T, Ishida Y, Yoshida H, Komuro I. Endothelial cell senescence in human atherosclerosis: role of telomere in endothelial dysfunction. *Circulation* 2002; 105(13):1541-1544.
- (39) Brookes S, Rowe J, Gutierrez Del AA, Bond J, Peters G. Contribution of p16(INK4a) to replicative senescence of human fibroblasts. *Exp Cell Res* 2004; 298(2):549-559.
- (40) Campisi J. Cellular senescence and apoptosis: how cellular responses might influence aging phenotypes. *Exp Gerontol* 2003; 38(1-2):5-11.
- (41) Shelton DN, Chang E, Whittier PS, Choi D, Funk WD. Microarray analysis of replicative senescence. *Curr Biol* 1999; 9(17):939-945.
- (42) Beausejour CM, Krtolica A, Galimi F, Narita M, Lowe SW, Yaswen P et al. Reversal of human cellular senescence: roles of the p53 and p16 pathways. *EMBO J* 2003; 22(16):4212-4222.

- (43) Narita M, Nunez S, Heard E, Narita M, Lin AW, Hearn SA et al. Rb-mediated heterochromatin formation and silencing of E2F target genes during cellular senescence. *Cell* 2003; 113(6):703-716.
- (44) Narita M, Narita M, Krizhanovsky V, Nunez S, Chicas A, Hearn SA et al. A novel role for high-mobility group a proteins in cellular senescence and heterochromatin formation. *Cell* 2006; 126(3):503-514.
- (45) Zhang R, Chen W, Adams PD. Molecular dissection of formation of senescence-associated heterochromatin foci. *Mol Cell Biol* 2007; 27(6):2343-2358.
- (46) Fripiat C, Chen QM, Zdanov S, Magalhaes JP, Remacle J, Toussaint O. Subcytotoxic H₂O₂ stress triggers a release of transforming growth factor-beta 1, which induces biomarkers of cellular senescence of human diploid fibroblasts. *J Biol Chem* 2001; 276(4):2531-2537.
- (47) Blanco FJ, Grande MT, Langa C, Oujo B, Velasco S, Rodriguez-Barbero A et al. S-endoglin expression is induced in senescent endothelial cells and contributes to vascular pathology. *Circ Res* 2008; 103(12):1383-1392.
- (48) Hasegawa Y, Saito T, Ogihara T, Ishigaki Y, Yamada T, Imai J et al. Blockade of the nuclear factor-kappaB pathway in the endothelium prevents insulin resistance and prolongs life spans. *Circulation* 2012; 125(9):1122-1133.
- (49) Liu F, Wu S, Ren H, Gu J. Klotho suppresses RIG-I-mediated senescence-associated inflammation. *Nat Cell Biol* 2011; 13(3):254-262.
- (50) Wang Y, Kuro-o M, Sun Z. Klotho gene delivery suppresses Nox2 expression and attenuates oxidative stress in rat aortic smooth muscle cells via the cAMP-PKA pathway. *Aging Cell* 2012; 11(3):410-417.
- (51) Zhan H, Suzuki T, Aizawa K, Miyagawa K, Nagai R. Ataxia telangiectasia mutated (ATM)-mediated DNA damage response in oxidative stress-induced vascular endothelial cell senescence. *J Biol Chem* 2010; 285(38):29662-29670.
- (52) Bartkova J, Horejsi Z, Koed K, Kramer A, Tort F, Zieger K et al. DNA damage response as a candidate anti-cancer barrier in early human tumorigenesis. *Nature* 2005; 434(7035):864-870.

- (53) Bencokova Z, Kaufmann MR, Pires IM, Lecane PS, Giaccia AJ, Hammond EM. ATM activation and signaling under hypoxic conditions. *Mol Cell Biol* 2009; 29(2):526-537.
- (54) Mun GI, Boo YC. Identification of CD44 as a senescence-induced cell adhesion gene responsible for the enhanced monocyte recruitment to senescent endothelial cells. *Am J Physiol Heart Circ Physiol* 2010; 298(6):H2102-H2111.
- (55) Coleman PR, Hahn CN, Grimshaw M, Lu Y, Li X, Brautigan PJ et al. Stress-induced premature senescence mediated by a novel gene, SENEX, results in an anti-inflammatory phenotype in endothelial cells. *Blood* 2010; 116(19):4016-4024.
- (56) Sarkar R, Gordon D, Stanley JC, Webb RC. Cell cycle effects of nitric oxide on vascular smooth muscle cells. *Am J Physiol* 1997; 272(4 Pt 2):H1810-H1818.
- (57) Villalobo A. Nitric oxide and cell proliferation. *FEBS Journal* 2006; 273(11):2329-2344.
- (58) Severino J, Allen RG, Balin S, Balin A, Cristofalo VJ. Is beta-galactosidase staining a marker of senescence in vitro and in vivo? *Exp Cell Res* 2000; 257(1):162-171.
- (59) Forstermann U, Sessa WC. Nitric oxide synthases: regulation and function. *Eur Heart J* 2012; 33(7):829-837d.
- (60) Han Z, Chen YR, Jones CI, Meenakshisundaram G, Zweier JL, Alevriadou BR. Shear-Induced Reactive Nitrogen Species Inhibit Mitochondrial Respiratory Complex Activities in Cultured Vascular Endothelial Cells. *Am J Physiol Cell Physiol* 2006.
- (61) Sun D, Huang A, Yan EH, Wu Z, Yan C, Kaminski PM et al. Reduced release of nitric oxide to shear stress in mesenteric arteries of aged rats. *Am J Physiol Heart Circ Physiol* 2004; 286(6):H2249-H2256.
- (62) Vasa M, Breitschopf K, Zeiher AM, Dimmeler S. Nitric oxide activates telomerase and delays endothelial cell senescence. *Circ Res* 2000; 87(7):540-542.

- (63) Hayashi T, Matsui-Hirai H, Miyazaki-Akita A, Fukatsu A, Funami J, Ding QF et al. Endothelial cellular senescence is inhibited by nitric oxide: implications in atherosclerosis associated with menopause and diabetes. *Proc Natl Acad Sci U S A* 2006; 103(45):17018-17023.
- (64) Levine DZ, Iacovitti M. Real-time measurement of kidney tubule fluid nitric oxide concentrations in early diabetes: disparate changes in different rodent models. *Nitric Oxide* 2006; 15(1):87-92.
- (65) Malinski T. Understanding nitric oxide physiology in the heart: a nanomedical approach. *Am J Cardiol* 2005; 96(7B):13i-24i.
- (66) Hrabie JA, Keefer LK. Chemistry of the nitric oxide-releasing diazeniumdiolate ("nitrosohydroxylamine") functional group and its oxygen-substituted derivatives. *Chem Rev* 2002; 102(4):1135-1154.
- (67) Mun GI, Lee SJ, An SM, Kim IK, Boo YC. Differential gene expression in young and senescent endothelial cells under static and laminar shear stress conditions. *Free Radic Biol Med* 2009; 47(3):291-299.
- (68) Ku DN, Giddens DP, Zarins CK, Glagov S. Pulsatile flow and atherosclerosis in the human carotid bifurcation. Positive correlation between plaque location and low oscillating shear stress. *Arteriosclerosis* 1985; 5(3):293-302.
- (69) Burrig KF. The endothelium of advanced arteriosclerotic plaques in humans. *Arterioscler Thromb* 1991; 11(6):1678-1689.
- (70) van der LB, Bachschmid M, Labugger R, Schildknecht S, Kilo J, Hahn R et al. Expression and activity patterns of nitric oxide synthases and antioxidant enzymes reveal a substantial heterogeneity between cardiac and vascular aging in the rat. *Biogerontology* 2005; 6(5):325-334.
- (71) Chen J, Brodsky SV, Goligorsky DM, Hampel DJ, Li H, Gross SS et al. Glycated collagen I induces premature senescence-like phenotypic changes in endothelial cells. *Circ Res* 2002; 90(12):1290-1298.
- (72) Martin W, Furchgott RF, Villani GM, Jothianandan D. Depression of contractile responses in rat aorta by spontaneously released endothelium-derived relaxing factor. *J Pharmacol Exp Ther* 1986; 237(2):529-538.
- (73) Kelm M, Feelisch M, Spahr R, Piper HM, Noack E, Schrader J. Quantitative and kinetic characterization of nitric oxide and EDRF released from cultured endothelial cells. *Biochem Biophys Res Commun* 1988; 154(1):236-244.

- (74) Delikouras A, Hayes M, Malde P, Lechler RI, Dorling A. Nitric oxide-mediated expression of Bcl-2 and Bcl-xl and protection from tumor necrosis factor-alpha-mediated apoptosis in porcine endothelial cells after exposure to low concentrations of xenoreactive natural antibody. *Transplantation* 2001; 71(5):599-605.
- (75) Ho FM, Liu SH, Liao CS, Huang PJ, Shiah SG, Lin-Shiau SY. Nitric oxide prevents apoptosis of human endothelial cells from high glucose exposure during early stage. *J Cell Biochem* 1999; 75(2):258-263.
- (76) Rossig L, Haendeler J, Hermann C, Malchow P, Urbich C, Zeiher AM et al. Nitric oxide down-regulates MKP-3 mRNA levels: involvement in endothelial cell protection from apoptosis. *J Biol Chem* 2000; 275(33):25502-25507.
- (77) Mattiussi S, Turrini P, Testolin L, Martelli F, Zaccagnini G, Mangoni A et al. p21(Waf1/Cip1/Sdi1) mediates shear stress-dependent antiapoptotic function. *Cardiovasc Res* 2004; 61(4):693-704.
- (78) Matsushita H, Chang E, Glassford AJ, Cooke JP, Chiu CP, Tsao PS. eNOS activity is reduced in senescent human endothelial cells: Preservation by hTERT immortalization. *Circ Res* 2001; 89(9):793-798.
- (79) Hayashi T, Sumi D, Juliet PA, Matsui-Hirai H, Sai-Tanaka Y, Kano H et al. Gene transfer of endothelial NO synthase, but not eNOS plus inducible NOS, regressed atherosclerosis in rabbits. *Cardiovasc Res* 2004; 61(2):339-351.
- (80) Chou TC, Yen MH, Li CY, Ding YA. Alterations of nitric oxide synthase expression with aging and hypertension in rats. *Hypertension* 1998; 31(2):643-648.
- (81) Vaziri ND, Wang XQ, Ni ZN, Kivlighn S, Shahinfar S. Effects of aging and AT-1 receptor blockade on NO synthase expression and renal function in SHR. *Biochim Biophys Acta* 2002; 1592(2):153-161.
- (82) Tanabe T, Maeda S, Miyauchi T, Iemitsu M, Takanashi M, Irukayama-Tomobe Y et al. Exercise training improves ageing-induced decrease in eNOS expression of the aorta. *Acta Physiol Scand* 2003; 178(1):3-10.
- (83) Cauwels A, Janssen B, Buys E, Sips P, Brouckaert P. Anaphylactic shock depends on PI3K and eNOS-derived NO. *J Clin Invest* 2006; 116(8):2244-2251.

- (84) Zhang J, Jin B, Li L, Block ER, Patel JM. Nitric oxide-induced persistent inhibition and nitrosylation of active site cysteine residues of mitochondrial cytochrome-c oxidase in lung endothelial cells. *Am J Physiol Cell Physiol* 2005; 288(4):C840-C849.
- (85) Guikema B, Lu Q, Jourd'heuil D. Chemical considerations and biological selectivity of protein nitrosation: implications for NO-mediated signal transduction. *Antioxid Redox Signal* 2005; 7(5-6):593-606.
- (86) Burwell LS, Nadtochiy SM, Tompkins AJ, Young S, Brookes PS. Direct evidence for S-nitrosation of mitochondrial complex I. *Biochem J* 2006; 394(Pt 3):627-634.
- (87) Martinez-Ruiz A, Lamas S. S-nitrosylation: a potential new paradigm in signal transduction. *Cardiovasc Res* 2004; 62(1):43-52.
- (88) Erwin PA, Lin AJ, Golan DE, Michel T. Receptor-regulated dynamic S-nitrosylation of endothelial nitric-oxide synthase in vascular endothelial cells. *J Biol Chem* 2005; 280(20):19888-19894.
- (89) Hess DT, Matsumoto A, Kim SO, Marshall HE, Stamler JS. Protein S-nitrosylation: purview and parameters. *Nat Rev Mol Cell Biol* 2005; 6(2):150-166.
- (90) Santhanam L, Lim HK, Lim HK, Miriel V, Brown T, Patel M et al. Inducible NO synthase dependent S-nitrosylation and activation of arginase1 contribute to age-related endothelial dysfunction. *Circ Res* 2007; 101(7):692-702.
- (91) Kim CO, Huh AJ, Han SH, Kim JM. Analysis of cellular senescence induced by lipopolysaccharide in pulmonary alveolar epithelial cells. *Arch Gerontol Geriatr* 2012; 54(2):e35-e41.
- (92) Goettsch W, Lattmann T, Amann K, Szibor M, Morawietz H, Munter K et al. Increased expression of endothelin-1 and inducible nitric oxide synthase isoform II in aging arteries in vivo: implications for atherosclerosis. *Biochem Biophys Res Commun* 2001; 280(3):908-913.
- (93) Fukagawa NK, Li M, Timblin CR, Mossman BT. Modulation of cell injury and survival by high glucose and advancing age. *Free Radic Biol Med* 2001; 31(12):1560-1569.
- (94) Lavnikova N, Laskin DL. Unique patterns of regulation of nitric oxide production in fibroblasts. *J Leukoc Biol* 1995; 58(4):451-458.

- (95) Chen LC, Pace JL, Russell SW, Morrison DC. Altered regulation of inducible nitric oxide synthase expression in macrophages from senescent mice. *Infect Immun* 1996; 64(10):4288-4298.
- (96) Cernadas MR, Sanchez de ML, Garcia-Duran M, Gonzalez-Fernandez F, Millas I, Monton M et al. Expression of constitutive and inducible nitric oxide synthases in the vascular wall of young and aging rats. *Circ Res* 1998; 83(3):279-286.
- (97) Francia P, delli GC, Bachschmid M, Martin-Padura I, Savoia C, Migliaccio E et al. Deletion of p66shc gene protects against age-related endothelial dysfunction. *Circulation* 2004; 110(18):2889-2895.
- (98) Zhou S, Chen HZ, Wan YZ, Zhang QJ, Wei YS, Huang S et al. Repression of P66Shc expression by SIRT1 contributes to the prevention of hyperglycemia-induced endothelial dysfunction. *Circ Res* 2011; 109(6):639-648.
- (99) Pandolfi S, Bonafe M, Di TL, Tiberi L, Salvioli S, Monti D et al. p66(shc) is highly expressed in fibroblasts from centenarians. *Mech Ageing Dev* 2005; 126(8):839-844.
- (100) Li D, Qu Y, Tao L, Liu H, Hu A, Gao F et al. Inhibition of iNOS protects the aging heart against beta-adrenergic receptor stimulation-induced cardiac dysfunction and myocardial ischemic injury. *J Surg Res* 2006; 131(1):64-72.
- (101) Jugdutt BI, Palaniyappan A, Uwiera RR, Idikio H. Role of healing-specific-matricellular proteins and matrix metalloproteinases in age-related enhanced early remodeling after reperfused STEMI in dogs. *Mol Cell Biochem* 2009; 322(1-2):25-36.
- (102) Marchand A, Atassi F, Gaaya A, Leprince P, Le FC, Soubrier F et al. The Wnt/beta-catenin pathway is activated during advanced arterial aging in humans. *Aging Cell* 2011; 10(2):220-232.
- (103) Yonemasu K, Kitajima H, Tanabe S, Ochi T, Shinkai H. Effect of age on C1q and C3 levels in human serum and their presence in colostrum. *Immunology* 1978; 35(3):523-530.
- (104) Naito AT, Sumida T, Nomura S, Liu ML, Higo T, Nakagawa A et al. Complement c1q activates canonical wnt signaling and promotes aging-related phenotypes. *Cell* 2012; 149(6):1298-1313.

- (105) Borutaite V, Matthias A, Harris H, Moncada S, Brown GC. Reversible inhibition of cellular respiration by nitric oxide in vascular inflammation. *Am J Physiol Heart Circ Physiol* 2001; 281(6):H2256-H2260.
- (106) Xu W, Charles IG, Moncada S. Nitric oxide: orchestrating hypoxia regulation through mitochondrial respiration and the endoplasmic reticulum stress response. *Cell Res* 2005; 15(1):63-65.
- (107) An HJ, Maeng O, Kang KH, Lee JO, Kim YS, Paik SG et al. Activation of RAS upregulates pro-apoptotic BNIP3 in nitric oxide-induced cell death. *Journal of Biological Chemistry* 2006;M605819200.
- (108) Heller R, Polack T, Grabner R, Till U. Nitric oxide inhibits proliferation of human endothelial cells via a mechanism independent of cGMP. *Atherosclerosis* 1999; 144(1):49-57.
- (109) Erwin PA, Mitchell DA, Sartoretto J, Marletta MA, Michel T. Subcellular targeting and differential S-nitrosylation of endothelial nitric-oxide synthase. *J Biol Chem* 2006; 281(1):151-157.
- (110) van der Loo B, Labugger R, Skepper JN, Bachschmid M, Kilo J, Powell JM et al. Enhanced peroxynitrite formation is associated with vascular aging. *J Exp Med* 2000; 192(12):1731-1744.
- (111) Riobo NA, Clementi E, Melani M, Boveris A, Cadenas E, Moncada S et al. Nitric oxide inhibits mitochondrial NADH:ubiquinone reductase activity through peroxynitrite formation. *Biochem J* 2001; 359(Pt 1):139-145.
- (112) Lener B, Koziel R, Pircher H, Hutter E, Greussing R, Herndler-Brandstetter D et al. The NADPH oxidase Nox4 restricts the replicative lifespan of human endothelial cells. *Biochem J* 2009; 423(3):363-374.
- (113) Borniquel S, Valle I, Cadenas S, Lamas S, Monsalve M. Nitric oxide regulates mitochondrial oxidative stress protection via the transcriptional coactivator PGC-1alpha. *FASEB J* 2006; 20(11):1889-1891.
- (114) Godecke A, Schrader J, Reinartz M. Nitric oxide-mediated protein modification in cardiovascular physiology and pathology. *Proteomics Clin Appl* 2008; 2(6):811-822.
- (115) Gow AJ, Farkouh CR, Munson DA, Posencheg MA, Ischiropoulos H. Biological significance of nitric oxide-mediated protein modifications. *Am J Physiol Lung Cell Mol Physiol* 2004; 287(2):L262-L268.

- (116) Banci L, Bertini I, Ciofi-Baffoni S, Kozyreva T, Zovo K, Palumaa P. Affinity gradients drive copper to cellular destinations. *Nature* 2010; 465(7298):645-648.
- (117) Xue Y, Liu Z, Gao X, Jin C, Wen L, Yao X et al. GPS-SNO: computational prediction of protein S-nitrosylation sites with a modified GPS algorithm. *PLoS One* 2010; 5(6):e11290.
- (118) van der Loo B, Labugger R, Skepper JN, Bachschmid M, Kilo J, Powell JM et al. Enhanced peroxynitrite formation is associated with vascular aging. *J Exp Med* 2000; 192(12):1731-1744.
- (119) MacMillan-Crow LA, Crow JP, Kerby JD, Beckman JS, Thompson JA. Nitration and inactivation of manganese superoxide dismutase in chronic rejection of human renal allografts. *Proc Natl Acad Sci U S A* 1996; 93(21):11853-11858.
- (120) Shishehbor MH, Aviles RJ, Brennan ML, Fu X, Goormastic M, Pearce GL et al. Association of nitrotyrosine levels with cardiovascular disease and modulation by statin therapy. *JAMA* 2003; 289(13):1675-1680.
- (121) Sarr M, Chataigneau M, Etienne-Selloum N, Diallo AS, Schott C, Geffard M et al. Targeted and persistent effects of NO mediated by S-nitrosation of tissue thiols in arteries with endothelial dysfunction. *Nitric Oxide* 2007; 17(1):1-9.
- (122) Bajt ML, Knight TR, Lemasters JJ, Jaeschke H. Acetaminophen-induced oxidant stress and cell injury in cultured mouse hepatocytes: protection by N-acetyl cysteine. *Toxicol Sci* 2004; 80(2):343-349.
- (123) Majano PL, Medina J, Zubia I, Sunyer L, Lara-Pezzi E, Maldonado-Rodriguez A et al. N-Acetyl-cysteine modulates inducible nitric oxide synthase gene expression in human hepatocytes. *J Hepatol* 2004; 40(4):632-637.
- (124) Jiang B, Haverty M, Brecher P. N-acetyl-L-cysteine enhances interleukin-1beta-induced nitric oxide synthase expression. *Hypertension* 1999; 34(4 Pt 1):574-579.
- (125) Vasa M, Breitschopf K, Zeiher AM, Dimmeler S. Nitric oxide activates telomerase and delays endothelial cell senescence. *Circ Res* 2000; 87(7):540-542.

- (126) Assmus B, Urbich C, Aicher A, Hofmann WK, Haendeler J, Rossig L et al. HMG-CoA reductase inhibitors reduce senescence and increase proliferation of endothelial progenitor cells via regulation of cell cycle regulatory genes. *Circ Res* 2003; 92(9):1049-1055.
- (127) Breitschopf K, Zeiher AM, Dimmeler S. Pro-atherogenic factors induce telomerase inactivation in endothelial cells through an Akt-dependent mechanism. *FEBS Lett* 2001; 493(1):21-25.
- (128) Chuang CC, Shiesh SC, Chi CH, Tu YF, Hor LI, Shieh CC et al. Serum total antioxidant capacity reflects severity of illness in patients with severe sepsis. *Crit Care* 2006; 10(1):R36.
- (129) Floriano-Sanchez E, Villanueva C, Medina-Campos ON, Rocha D, Sanchez-Gonzalez DJ, Cardenas-Rodriguez N et al. Nordihydroguaiaretic acid is a potent in vitro scavenger of peroxynitrite, singlet oxygen, hydroxyl radical, superoxide anion and hypochlorous acid and prevents in vivo ozone-induced tyrosine nitration in lungs. *Free Radic Res* 2006; 40(5):523-533.
- (130) Walford GA, Moussignac RL, Scribner AW, Loscalzo J, Leopold JA. Hypoxia potentiates nitric oxide-mediated apoptosis in endothelial cells via peroxynitrite-induced activation of mitochondria-dependent and -independent pathways. *J Biol Chem* 2004; 279(6):4425-4432.
- (131) Kang DH, Park SK, Lee IK, Johnson RJ. Uric acid-induced C-reactive protein expression: implication on cell proliferation and nitric oxide production of human vascular cells. *J Am Soc Nephrol* 2005; 16(12):3553-3562.
- (132) Ames BN, Cathcart R, Schwiers E, Hochstein P. Uric acid provides an antioxidant defense in humans against oxidant- and radical-caused aging and cancer: a hypothesis. *Proc Natl Acad Sci U S A* 1981; 78(11):6858-6862.
- (133) Kand'ar R, Zakova P, Muzakova V. Monitoring of antioxidant properties of uric acid in humans for a consideration measuring of levels of allantoin in plasma by liquid chromatography. *Clin Chim Acta* 2006; 365(1-2):249-256.
- (134) Gersch C, Palii SP, Kim KM, Angerhofer A, Johnson RJ, Henderson GN. Inactivation of nitric oxide by uric acid. *Nucleosides Nucleotides Nucleic Acids* 2008; 27(8):967-978.
- (135) Suzuki T. Nitrosation of uric acid induced by nitric oxide under aerobic conditions. *Nitric Oxide* 2007; 16(2):266-273.

- (136) Skinner KA, White CR, Patel R, Tan S, Barnes S, Kirk M et al. Nitrosation of uric acid by peroxynitrite. Formation of a vasoactive nitric oxide donor. *J Biol Chem* 1998; 273(38):24491-24497.
- (137) Squadrito GL, Cueto R, Splenser AE, Valavanidis A, Zhang H, Uppu RM et al. Reaction of uric acid with peroxynitrite and implications for the mechanism of neuroprotection by uric acid. *Arch Biochem Biophys* 2000; 376(2):333-337.
- (138) Teng RJ, Ye YZ, Parks DA, Beckman JS. Urate produced during hypoxia protects heart proteins from peroxynitrite-mediated protein nitration. *Free Radic Biol Med* 2002; 33(9):1243-1249.
- (139) Ruggiero C, Cherubini A, Ble A, Bos AJ, Maggio M, Dixit VD et al. Uric acid and inflammatory markers. *Eur Heart J* 2006; 27(10):1174-1181.
- (140) Ferrucci L, Corsi A, Lauretani F, Bandinelli S, Bartali B, Taub DD et al. The origins of age-related proinflammatory state. *Blood* 2005; 105(6):2294-2299.
- (141) Corry DB, Eslami P, Yamamoto K, Nyby MD, Makino H, Tuck ML. Uric acid stimulates vascular smooth muscle cell proliferation and oxidative stress via the vascular renin-angiotensin system. *J Hypertens* 2008; 26(2):269-275.
- (142) Noman A, Ang DS, Ogston S, Lang CC, Struthers AD. Effect of high-dose allopurinol on exercise in patients with chronic stable angina: a randomised, placebo controlled crossover trial. *Lancet* 2010; 375(9732):2161-2167.
- (143) Briviba K, Roussyn I, Sharov VS, Sies H. Attenuation of oxidation and nitration reactions of peroxynitrite by selenomethionine, selenocystine and ebselen. *Biochem J* 1996; 319 (Pt 1):13-15.
- (144) Nyman DW, Suzanne SM, Kopplin MJ, Dalkin BL, Nagle RB, Jay GA. Selenium and selenomethionine levels in prostate cancer patients. *Cancer Detect Prev* 2004; 28(1):8-16.
- (145) Ravikumar B, Sarkar S, Davies JE, Futter M, Garcia-Arencibia M, Green-Thompson ZW et al. Regulation of mammalian autophagy in physiology and pathophysiology. *Physiol Rev* 2010; 90(4):1383-1435.
- (146) Hundeshagen P, Hamacher-Brady A, Eils R, Brady NR. Concurrent detection of autolysosome formation and lysosomal degradation by flow cytometry in a high-content screen for inducers of autophagy. *BMC Biol* 2011; 9:38.

- (147) Egan DF, Shackelford DB, Mihaylova MM, Gelino S, Kohnz RA, Mair W et al. Phosphorylation of ULK1 (hATG1) by AMP-activated protein kinase connects energy sensing to mitophagy. *Science* 2011; 331(6016):456-461.
- (148) de Kreutzenberg SV, Ceolotto G, Papparella I, Bortoluzzi A, Semplicini A, Dalla MC et al. Downregulation of the longevity-associated protein sirtuin 1 in insulin resistance and metabolic syndrome: potential biochemical mechanisms. *Diabetes* 2010; 59(4):1006-1015.
- (149) Fleming A, Noda T, Yoshimori T, Rubinsztein DC. Chemical modulators of autophagy as biological probes and potential therapeutics. *Nat Chem Biol* 2011; 7(1):9-17.
- (150) Tasdemir E, Maiuri MC, Galluzzi L, Vitale I, Djavaheri-Mergny M, D'Amelio M et al. Regulation of autophagy by cytoplasmic p53. *Nat Cell Biol* 2008; 10(6):676-687.
- (151) Toth ML, Sigmund T, Borsos E, Barna J, Erdelyi P, Takacs-Vellai K et al. Longevity pathways converge on autophagy genes to regulate life span in *Caenorhabditis elegans*. *Autophagy* 2008; 4(3):330-338.
- (152) Gottlieb RA, Mentzer RM. Autophagy during cardiac stress: joys and frustrations of autophagy. *Annu Rev Physiol* 2010; 72:45-59.
- (153) Alimonti A, Nardella C, Chen Z, Clohessy JG, Carracedo A, Trotman LC et al. A novel type of cellular senescence that can be enhanced in mouse models and human tumor xenografts to suppress prostate tumorigenesis. *J Clin Invest* 2010; 120(3):681-693.
- (154) Tasdemir E, Maiuri MC, Galluzzi L, Vitale I, Djavaheri-Mergny M, D'Amelio M et al. Regulation of autophagy by cytoplasmic p53. *Nat Cell Biol* 2008; 10(6):676-687.
- (155) Blagosklonny MV. Aging-suppressants: cellular senescence (hyperactivation) and its pharmacologic deceleration. *Cell Cycle* 2009; 8(12):1883-1887.
- (156) Maj MC, Tkachyova I, Patel P, Addis JB, Mackay N, Levandovskiy V et al. Oxidative stress alters the regulatory control of p66Shc and Akt in PINK1 deficient cells. *Biochem Biophys Res Commun* 2010; 399(3):331-335.
- (157) Egan DF, Shackelford DB, Mihaylova MM, Gelino S, Kohnz RA, Mair W et al. Phosphorylation of ULK1 (hATG1) by AMP-activated protein kinase connects energy sensing to mitophagy. *Science* 2011; 331(6016):456-461.

- (158) Kim J, Kundu M, Viollet B, Guan KL. AMPK and mTOR regulate autophagy through direct phosphorylation of Ulk1. *Nat Cell Biol* 2011; 13(2):132-141.
- (159) Canto C, Jiang LQ, Deshmukh AS, Matakai C, Coste A, Lagouge M et al. Interdependence of AMPK and SIRT1 for metabolic adaptation to fasting and exercise in skeletal muscle. *Cell Metab* 2010; 11(3):213-219.
- (160) Melendez A, Talloczy Z, Seaman M, Eskelinen EL, Hall DH, Levine B. Autophagy genes are essential for dauer development and life-span extension in *C. elegans*. *Science* 2003; 301(5638):1387-1391.
- (161) Woods A, Cheung PCF, Smith FC, Davison MD, Scott J, Beri RK et al. Characterization of AMP-activated Protein Kinase and Subunits. *Journal of Biological Chemistry* 1996; 271(17):10282-10290.
- (162) Hawley SA, Davison M, Woods A, Davies SP, Beri RK, Carling D et al. Characterization of the AMP-activated protein kinase from rat liver and identification of threonine 172 as the major site at which it phosphorylates AMP-activated protein kinase. *J Biol Chem* 1996; 271(44):27879-27887.
- (163) Hawley SA, Ross FA, Chevtzoff C, Green KA, Evans A, Fogarty S et al. Use of cells expressing gamma subunit variants to identify diverse mechanisms of AMPK activation. *Cell Metab* 2010; 11(6):554-565.
- (164) Gonzalez AA, Kumar R, Mulligan JD, Davis AJ, Saupe KW. Effects of aging on cardiac and skeletal muscle AMPK activity: basal activity, allosteric activation, and response to in vivo hypoxemia in mice. *Am J Physiol Regul Integr Comp Physiol* 2004; 287(5):R1270-R1275.
- (165) Shaw RJ, Kosmatka M, Bardeesy N, Hurley RL, Witters LA, DePinho RA et al. Inaugural Article: The tumor suppressor LKB1 kinase directly activates AMP-activated kinase and regulates apoptosis in response to energy stress. *PNAS* 2004; 101(10):3329-3335.
- (166) Zu Y, Liu L, Lee MY, Xu C, Liang Y, Man RY et al. SIRT1 promotes proliferation and prevents senescence through targeting LKB1 in primary porcine aortic endothelial cells. *Circ Res* 2010; 106(8):1384-1393.
- (167) Morrow VA, Fougelle F, Connell JM, Petrie JR, Gould GW, Salt IP. Direct activation of AMP-activated protein kinase stimulates nitric-oxide synthesis in human aortic endothelial cells. *J Biol Chem* 2003; 278(34):31629-31639.

- (168) Schulz E, Dopheide J, Schuhmacher S, Thomas SR, Chen K, Daiber A et al. Suppression of the JNK pathway by induction of a metabolic stress response prevents vascular injury and dysfunction. *Circulation* 2008; 118(13):1347-1357.
- (169) Nagata D, Takeda R, Sata M, Satonaka H, Suzuki E, Nagano T et al. AMP-activated protein kinase inhibits angiotensin II-stimulated vascular smooth muscle cell proliferation. *Circulation* 2004; 110(4):444-451.
- (170) El-Mir MY, Nogueira V, Fontaine E, Averet N, Rigoulet M, Leverve X. Dimethylbiguanide inhibits cell respiration via an indirect effect targeted on the respiratory chain complex I. *J Biol Chem* 2000; 275(1):223-228.
- (171) Kroller-Schon S, Jansen T, Hauptmann F, Schuler A, Heeren T, Hausding M et al. alpha1AMP-Activated Protein Kinase Mediates Vascular Protective Effects of Exercise. *Arterioscler Thromb Vasc Biol* 2012; 32(7):1632-1641.
- (172) Quintero M, Colombo SL, Godfrey A, Moncada S. Mitochondria as signaling organelles in the vascular endothelium. *Proc Natl Acad Sci U S A* 2006; 103(14):5379-5384.
- (173) Sohn JJ, Schetter AJ, Yfantis HG, Ridnour LA, Horikawa I, Khan MA et al. Macrophages, nitric oxide and microRNAs are associated with DNA damage response pathway and senescence in inflammatory bowel disease. *PLoS One* 2012; 7(9):e44156.
- (174) Mathe E, Nguyen GH, Funamizu N, He P, Moake M, Croce CM et al. Inflammation regulates microRNA expression in cooperation with p53 and nitric oxide. *Int J Cancer* 2012; 131(3):760-765.
- (175) Bargaje R, Gupta S, Sarkeshik A, Park R, Xu T, Sarkar M et al. Identification of novel targets for miR-29a using miRNA proteomics. *PLoS One* 2012; 7(8):e43243.
- (176) Ropelle ER, Pauli JR, Cintra DE, da Silva AS, De Souza CT, Guadagnini D et al. Targeted disruption of inducible nitric oxide synthase protects against aging, S-nitrosation, and insulin resistance in muscle of male mice. *Diabetes* 2013; 62(2):466-470.
- (177) Balchin D, Wallace L, Dirr HW. S-nitrosation of glutathione transferase p1-1 is controlled by the conformation of a dynamic active site helix. *J Biol Chem* 2013; 288(21):14973-14984.

- (178) Crassous PA, Couloubaly S, Huang C, Zhou Z, Baskaran P, Kim DD et al. Soluble guanylyl cyclase is a target of angiotensin II-induced nitrosative stress in a hypertensive rat model. *Am J Physiol Heart Circ Physiol* 2012; 303(5):H597-H604.
- (179) Jandu SK, Webb AK, Pak A, Sevinc B, Nyhan D, Belkin AM et al. Nitric oxide regulates tissue transglutaminase localization and function in the vasculature. *Amino Acids* 2013; 44(1):261-269.
- (180) Wanschel AC, Caceres VM, Moretti AI, Bruni-Cardoso A, de Carvalho HF, de Souza HP et al. Cardioprotective mechanism of S-nitroso-N-acetylcysteine via S-nitrosated betadrenoceptor-2 in the LDLr^{-/-} mice. *Nitric Oxide* 2013.
- (181) Baker DJ, Wijshake T, Tchkonja T, LeBrasseur NK, Childs BG, van de Sluis B et al. Clearance of p16Ink4a-positive senescent cells delays ageing-associated disorders. *Nature* 2011; 479(7372):232-236.
- (182) Smith PK, Krohn RI, Hermanson GT, Mallia AK, Gartner FH, Provenzano MD et al. Measurement of protein using bicinchoninic acid. *Anal Biochem* 1985; 150(1):76-85.
- (183) Bradford MM. A rapid and sensitive method for the quantitation of microgram quantities of protein utilizing the principle of protein-dye binding. *Anal Biochem* 1976; 72:248-254.
- (184) Keller A, Mohamed A, Droese S, Brandt U, Fleming I, Brandes RP. Analysis of dichlorodihydrofluorescein and dihydrocalcein as probes for the detection of intracellular reactive oxygen species. *Free Radic Res* 2004; 38(12):1257-1267.
- (185) Crow JP. Dichlorodihydrofluorescein and dihydrorhodamine 123 are sensitive indicators of peroxynitrite in vitro: implications for intracellular measurement of reactive nitrogen and oxygen species. *Nitric Oxide* 1997; 1(2):145-157.
- (186) LeBel CP, Ischiropoulos H, Bondy SC. Evaluation of the probe 2',7'-dichlorofluorescein as an indicator of reactive oxygen species formation and oxidative stress. *Chem Res Toxicol* 1992; 5(2):227-231.
- (187) Hempel SL, Buettner GR, O'Malley YQ, Wessels DA, Flaherty DM. Dihydrofluorescein diacetate is superior for detecting intracellular oxidants: comparison with 2',7'-dichlorodihydrofluorescein diacetate, 5-(and 6)-carboxy-2',7'-dichlorodihydrofluorescein diacetate, and dihydrorhodamine 123. *Free Radic Biol Med* 1999; 27(1-2):146-159.

- (188) Jaffrey SR, Snyder SH. The biotin switch method for the detection of S-nitrosylated proteins. *Sci STKE* 2001; 2001(86):11.
- (189) Mateo J, Garcia-Lecea M, Cadenas S, Hernandez C, Moncada S. Regulation of hypoxia-inducible factor-1alpha by nitric oxide through mitochondria-dependent and -independent pathways. *Biochem J* 2003; 376(Pt 2):537-544.
- (190) Wang E. Senescent human fibroblasts resist programmed cell death, and failure to suppress bcl2 is involved. *Cancer Res* 1995; 55(11):2284-2292.
- (191) Bennett MR, Macdonald K, Chan SW, Boyle JJ, Weissberg PL. Cooperative interactions between RB and p53 regulate cell proliferation, cell senescence, and apoptosis in human vascular smooth muscle cells from atherosclerotic plaques. *Circ Res* 1998; 82(6):704-712.
- (192) Kramer DL, Chang BD, Chen Y, Diegelman P, Alm K, Black AR et al. Polyamine depletion in human melanoma cells leads to G1 arrest associated with induction of p21WAF1/CIP1/SDI1, changes in the expression of p21-regulated genes, and a senescence-like phenotype. *Cancer Res* 2001; 61(21):7754-7762.
- (193) Wagner M, Hampel B, Bernhard D, Hala M, Zwerschke W, Jansen-Durr P. Replicative senescence of human endothelial cells in vitro involves G1 arrest, polyploidization and senescence-associated apoptosis. *Exp Gerontol* 2001; 36(8):1327-1347.
- (194) Afshari CA, Vojta PJ, Annab LA, Futreal PA, Willard TB, Barrett JC. Investigation of the role of G1/S cell cycle mediators in cellular senescence. *Exp Cell Res* 1993; 209(2):231-237.
- (195) Kim HJ, Lee SI, Lee DH, Smith D, Jo H, Schellhorn HE et al. Ascorbic acid synthesis due to L-gulonolactone oxidase expression enhances NO production in endothelial cells. *Biochem Biophys Res Commun* 2006; 345(4):1657-1662.
- (196) Brovkovich V, Stolarczyk E, Oman J, Tomboulis P, Malinski T. Direct electrochemical measurement of nitric oxide in vascular endothelium. *J Pharm Biomed Anal* 1999; 19(1-2):135-143.
- (197) Bayraktutan U. Effects of angiotensin II on nitric oxide generation in growing and resting rat aortic endothelial cells. *J Hypertens* 2003; 21(11):2093-2101.

- (198) Rodriguez-Juarez F, Aguirre E, Cadenas S. Relative sensitivity of soluble guanylate cyclase and mitochondrial respiration to endogenous nitric oxide at physiological oxygen concentration. *Biochem J* 2007; 405(2):223-231.
- (199) Sies H, Arteel GE. Interaction of peroxynitrite with selenoproteins and glutathione peroxidase mimics. *Free Radic Biol Med* 2000; 28(10):1451-1455.
- (200) Epe B, Ballmaier D, Roussyn I, Briviba K, Sies H. DNA damage by peroxynitrite characterized with DNA repair enzymes. *Nucleic Acids Res* 1996; 24(21):4105-4110.
- (201) Seo YR, Kelley MR, Smith ML. Selenomethionine regulation of p53 by a ref1-dependent redox mechanism. *Proc Natl Acad Sci U S A* 2002; 99(22):14548-14553.
- (202) Forrester MT, Thompson JW, Foster MW, Nogueira L, Moseley MA, Stamler JS. Proteomic analysis of S-nitrosylation and denitrosylation by resin-assisted capture. *Nat Biotechnol* 2009; 27(6):557-559.
- (203) Jaffrey SR, Snyder SH. The biotin switch method for the detection of S-nitrosylated proteins. *Sci STKE* 2001; 2001(86):11.
- (204) Kelleher ZT, Potts EN, Brahmajothi MV, Foster MW, Auten RL, Foster WM et al. NOS2 regulation of LPS-induced airway inflammation via S-nitrosylation of NF- κ B p65. *Am J Physiol Lung Cell Mol Physiol* 2011; 301(3):L327-L333.
- (205) Kelleher ZT, Matsumoto A, Stamler JS, Marshall HE. NOS2 regulation of NF-kappaB by S-nitrosylation of p65. *J Biol Chem* 2007; 282(42):30667-30672.
- (206) Erusalimsky JD, Skene C. Mechanisms of endothelial senescence. *Exp Physiol* 2009; 94(3):299-304.
- (207) Miller MR, Megson IL. Recent developments in nitric oxide donor drugs. *Br J Pharmacol* 2007; 151(3):305-321.
- (208) Yoshimori T, Yamamoto A, Moriyama Y, Futai M, Tashiro Y. Bafilomycin A1, a specific inhibitor of vacuolar-type H(+)-ATPase, inhibits acidification and protein degradation in lysosomes of cultured cells. *Journal of Biological Chemistry* 1991; 266(26):17707-17712.

- (209) Boya P, Gonzalez-Polo RA, Casares N, Perfettini JL, Dessen P, Larochette N et al. Inhibition of Macroautophagy Triggers Apoptosis. *Mol Cell Biol* 2005; 25(3):1025-1040.
- (210) Ahmad S, Ahmad A, Ghosh M, Leslie CC, White CW. Extracellular ATP-mediated signaling for survival in hyperoxia-induced oxidative stress. *J Biol Chem* 2004; 279(16):16317-16325.
- (211) Braun-Dullaeus RC, Mann MJ, Seay U, Zhang L, von Der Leyen HE, Morris RE et al. Cell cycle protein expression in vascular smooth muscle cells in vitro and in vivo is regulated through phosphatidylinositol 3-kinase and mammalian target of rapamycin. *Arterioscler Thromb Vasc Biol* 2001; 21(7):1152-1158.
- (212) Moncada S, Erusalimsky JD. Does nitric oxide modulate mitochondrial energy generation and apoptosis? *Nat Rev Mol Cell Biol* 2002; 3(3):214-220.
- (213) Hundeshagen P, Hamacher-Brady A, Eils R, Brady NR. Concurrent detection of autolysosome formation and lysosomal degradation by flow cytometry in a high-content screen for inducers of autophagy. *BMC Biol* 2011; 9:38.
- (214) Heller R, Polack T, Grabner R, Till U. Nitric oxide inhibits proliferation of human endothelial cells via a mechanism independent of cGMP. *Atherosclerosis* 1999; 144(1):49-57.
- (215) Sen N, Paul BD, Gadalla MM, Mustafa AK, Sen T, Xu R et al. Hydrogen sulfide-linked sulfhydration of NF-kappaB mediates its antiapoptotic actions. *Mol Cell* 2012; 45(1):13-24.
- (216) Sheu ML, Ho FM, Yang RS, Chao KF, Lin WW, Lin-Shiau SY et al. High Glucose Induces Human Endothelial Cell Apoptosis Through a Phosphoinositide 3-Kinase-Regulated Cyclooxygenase-2 Pathway. *Arterioscler Thromb Vasc Biol* 2005; 25(3):539-545.
- (217) An HJ, Maeng O, Kang KH, Lee JO, Kim YS, Paik SG et al. Activation of Ras up-regulates pro-apoptotic BNIP3 in nitric oxide-induced cell death. *J Biol Chem* 2006; 281(45):33939-33948.
- (218) Venkatesh D, Fredette N, Rostama B, Tang Y, Vary CP, Liaw L et al. RhoA-mediated signaling in Notch-induced senescence-like growth arrest and endothelial barrier dysfunction. *Arterioscler Thromb Vasc Biol* 2011; 31(4):876-882.

- (219) Menghini R, Casagrande V, Cardellini M, Martelli E, Terrinoni A, Amati F et al. MicroRNA 217 modulates endothelial cell senescence via silent information regulator 1. *Circulation* 2009; 120(15):1524-1532.
- (220) Magenta A, Cencioni C, Fasanaro P, Zaccagnini G, Greco S, Sarra-Ferraris G et al. miR-200c is upregulated by oxidative stress and induces endothelial cell apoptosis and senescence via ZEB1 inhibition. *Cell Death Differ* 2011; 18(10):1628-1639.
- (221) Kops GJ, de Ruiter ND, De Vries-Smits AM, Powell DR, Bos JL, Burgering BM. Direct control of the Forkhead transcription factor AFX by protein kinase B. *Nature* 1999; 398(6728):630-634.
- (222) Nemoto S, Finkel T. Redox regulation of forkhead proteins through a p66shc-dependent signaling pathway. *Science* 2002; 295(5564):2450-2452.